KWAME NKRUMAH UNIVERSITY OF SCIENCE & TECHNOLOGY,

KUMASI, GHANA

Development of Controlled Release Intramuscular Artemether-Loaded Poly (lactic co-glycolic acid) (PLGA) Microspheres for Treatment of Severe Malaria in Children

by

Mariam El Boakye-Gyasi (B. Pharm (Hons), MPhil. Pharmaceutics)

A Thesis submitted to the Department of Pharmaceutics,
Faculty of Pharmacy and Pharmaceutical Sciences, College of Health Sciences
in partial fulfilment of the requirements for the degree of

DOCTOR OF PHILOSOPHY

APRIL, 2016

DECLARATION

I hereby declare that this submission is my own work towards the PhD and that, to the best of my knowledge, it contains no material previously published by another person, nor material which has been accepted for the award of any other degree of the University, except where due acknowledgement has been made in text.

Mariam El Boakye-Gyasi

PG 7864312

……..

Signature

……..

Date

Certified by:

Prof. Kwabena Ofori-Kwakye

……..

Signature

……..

Date

Certified by:

Prof. Kwabena Ofori-Kwakye

……..

Signature

……..

Date

ABSTRACT

Malaria is a febrile disease caused by the *plasmodium* parasite and has plagued sub-Saharan Africa for many years. Severe or complicated malaria is a medical emergency, which has very high mortality rates especially among children under five years. Many preventive and control measures have been used over the years to combat this menace. Chemotherapy through parenteral administration is the principal means of combating severe malaria. Artemether is a derivative of artemisinin antimalarial available as intramuscular injection for the treatment of severe malaria in children. The purpose of this study was to develop controlled release intramuscular PLGA microspheres of artemether to replace the multiple injection regimen of artemether drug currently available for children under five years. The improvement of current available treatment regimen for children will be a significant contribution to the management of malaria in children under five years. These children are the most affected by the disease. Two resomers (RG503H and RG502H) of a biodegradable and biocompatible polymer, PLGA were used to formulate microspheres by the single emulsion solvent evaporation method. Microspheres of the clinically relevant size range of 45-90 μm were characterized by light microscopy, scanning electron microscopy and particle size analysis. The degradation of the microspheres was studied by determining their mass loss, water uptake and molecular weight profiles by gel permeation chromatography. The *in vitro* release of artemether from the formulated microspheres in phosphate buffered saline with 0.02 % tween 80 (PBST) was studied. Experimental male Sprague-Dawley rats were injected with formulated microspheres and the *in vivo*

release of artemether was studied. A Liquid chromatography/tandem mass spectrometric method (LC-MS/MS) was used to analyze plasma samples taken from the rats and to quantify artemether present in the plasma samples. Well-formed, spherical microspheres with smooth surfaces were formulated at high drug loading (20-25 %) and loading efficiencies (59-74 %). The polydispersed microsphere sizes were normally distributed with mean size of 70 and 69 μm for RG502H and RG503H polymers, respectively. The microspheres exhibited controlled release of artemether over 21 days *in vitro* with ~ 66-73 % release in 7 days. The declining molecular weight profiles, mass loss and water uptake profiles of the drug-loaded microspheres demonstrated that artemether release from the microspheres was due to polymer erosion and diffusion through the polymer. Mathematical modeling of the release of artemether showed that the RG502H and RG503H formulations fitted the Higuchi (fickian diffusion) and Korsemeyer-Peppas (non-fickian diffusion) models, respectively. Preliminary *in vivo* tests conducted showed that the artemether is released *in vivo* and can be successfully quantified with LC-MS/MS.

ACKNOWLEDGEMENT

I wish to express my endless thanks, appreciation and gratitude to God Almighty for the marvelous things He has done. From the inception of this research project through all the challenges and victories, He is the magnificent God and His manifestations are clear for all to see.

To my indefatigable supervisor, Prof. Kwabena Ofori-Kwakye, I say a very big thank you for every second spent to effectively and actively supervise this project from beginning to the end. Your depths of knowledge, suggestions, corrections, encouragement and mentorship have all contributed to the successful completion of this project. I am very grateful to you Prof.

I wish to express thanks to Dr. Steven P. Schwendeman for providing space in his lab and for all the discussions, comments and directions for this project.

To Dr. Keiji Hirota, I say thank you (“ありがとうございました) for your patience in teaching and demonstrating, for your comments, contributions, suggestions and support.

The contributions and technical assistance of Karl Olsen and Rose Ackerman cannot be overlooked. Sincere appreciation goes to you two.

To all laboratory members of the Schwendeman Lab Group (2014-2015), I say thank you all for the support.

My husband Dr. Eric Boakye-Gyasi is the most understanding and supportive pillar and his contributions and support during and beyond the period of this project are overwhelming. Thank you so much for being the best better half in this world.

My family, my oldest group of cheerleaders, I appreciate all the prayers and encouragement. Thank you for all the love and support you continue to give me.

To all my friends, I say thank you for the never-ending encouragement. Indeed, ‘all shall pass”.

My appreciation goes to all staff of the Faculty of Pharmacy and Pharmaceutical Sciences, KNUST who in diverse ways provided assistance during this period.

Finally but not the least, my deepest gratitude goes to the University of Michigan African Presidential Scholars’ (UMAPS) Program for funding part of this research work. To all the staff of the African Studies Center of the University of Michigan I say ayekoo. I am forever grateful for the opportunity I received through your hardwork and initiative of the UMAPS program.

The words “THANK YOU” are very common words, but I am expressing them here with the deepest sense of gratitude.

DEDICATION

I dedicate this work to my parents Capt. (rtd) and Mrs. Duah. You deserve all the praise you get.

TABLE OF CONTENTS

LIST OF TABLES

LIST OF FIGURES

LIST OF PLATES

ABBREVIATIONS

ARM	Artemether
DHA	Dihydroartemisinin
IM	Intramuscular
IRS	Indoor residual spraying
IS	Internal standard
LC-MS/MS	Liquid chromatography mass spectrometry
LLIN	Long lasting insecticide-treated nets
PLGA	Poly (lactic-co-glycolic acid)
IPT	Intermittent preventive therapy
SEM	Scanning Electron Microscopy
PVA	Polyvinyl alcohol
ACT	Artemisinin-based combination therapy
RDT	Rapid diagnostic tests
IPTp	Intermittent preventive treatment in pregnancy
PLA	Poly lactic acid
PGA	Poly glycolic acid
PCR	Polymerase chain reaction
US FDA	United States Food and Drug Administration

IFA	Immunofluorescent antibody assay
ELISA	Enzyme-linked immunosorbent assay
MRM	Multiple reactions monitoring
PCL	Poly (ε- caprolactone)

Chapter 1
INTRODUCTION

1.1 GENERAL INTRODUCTION

Malaria is a protozoan infection caused by *Plasmodium* acquired through the bite of an infected female anopheles mosquito. It is a febrile infection caused by *plasmodium* parasites (WHO, 2000). It has been reported that people living in malaria-endemic regions can develop a naturally acquired immunity to malaria through repeated exposure to the parasite over five to 10 years (Doolan *et al.*, 2009). This partial immunity to malaria is protective against the most severe forms of malaria, and thus, in high transmission areas mortality from severe malaria is highest in young children and decreases with increasing age (WHO, 2010). Malaria is a major cause of morbidity and mortality especially in pregnant women and children under five years of age who are the most vulnerable groups (WHO, 2013). In 2012, malaria killed an estimated 482 000 children under five years of age. That is 1300 children every day, or one child almost every minute (WHO, 2013).

Between 2000 and 2012, a scale-up of malaria interventions saved an estimated 3.3 million lives. Approximately 90%, or 3 million, of these are in the under-five age group in sub-Saharan Africa (WHO, 2013). However, malaria is still one of the most important diseases in the developing world. *Plasmodium falciparum*, the most life-threatening form affects several hundred million people and causes 1-2 million deaths each year. The rapid emergence of drug-resistant parasite strains leaves a great need for new effective antimalarial drugs (Gilles and Warrell, 1993).

A combination of preventive and treatment methods has been used in recent times to

achieve a reduction of malaria morbidity and mortality in malaria endemic areas. The preventive measures employed involve the use of insecticide treated bed nets (ITNs) or long lasting insecticidal bed nets (LLINs) as well as indoor residual spraying (IRS). These are aimed at preventing the bite of the infected female anopheles mosquitoes. The treatment options used include the use of artemisinin-based combination therapies (ACTs) for the treatment of uncomplicated malaria, the use of quinine and artemisinin derivatives for the treatment of severe malaria and the use of sulfadoxine/pyrimethamine for intermittent preventive therapy (IPT) in pregnant women. Rapid diagnostic tests (RDTs) and microscopy are also used for quick and accurate diagnosis of malaria, which precedes chemoprophylaxis.

Delay in diagnosis and inappropriate treatment of uncomplicated malaria leads to rapid development of complicated or severe malaria. Severe malaria is diagnosed on the basis of a positive blood slide or antigen test for malaria, plus the presence of clinical or laboratory features of vital organ dysfunction. These include generalized weakness, impaired consciousness, coma, convulsions, respiratory distress, shock, systolic blood pressure < 70 mmHg in adults, < 50 mmHg in children, jaundice, haemoglobinuria, hypoglycaemia, severe metabolic acidosis, anaemia, renal impairment and pulmonary oedema (WHO, 2015).

A form of severe malaria with a very high mortality rate is cerebral malaria. According to the World Health Organization (WHO), it causes a mortality rate of up to 100 % when untreated but with prompt, effective antimalarial treatment and supportive care, the rate

falls to 10-20 %. Some of the signs and symptoms include impairment of consciousness and cognition, which can lead to slight disorientation or deep coma. The survival rate is low with persistent neurologic complications (WHO, 2015).

The WHO currently recommends parenteral artesunate or artemether as the first-line treatment for severe malaria, followed by a complete course of an effective ACT as soon as the patient can take oral medications. Intramuscular artemether is available as an oily formulation, which is administered into the anterior thigh. The initial dose of artemether is 3.2 mg/kg body weight and the maintenance dose is 1.6 mg/kg body weight intramuscularly daily (WHO, 2015).

In 2011, Murambiwa *et al* reported that the formulation and evaluation of novel drug delivery systems was not only less expensive than developing new drugs, but may also improve delivery of anti-malarials at the desired rates (Murambiwa *et al*, 2011). Many bioactive agents have been successfully microencapsulated in biodegradable synthetic polymers such as poly (lactic-co-glycolic acid) (PLGA) and related polymers in a manner suitable for injection. These injectable dosage forms make it possible to extend the duration of action of these medicines from a day to as long as six months. Unlike natural polymers, synthetic polymers exhibit high purity and reproducibility. Among the synthetic polymers, the polyester family (that is, poly (lactic acid) (PLA), poly (ε-caprolactone) (PCL), poly (glycolic acid) (PGA) are of interest in the biomedical area because of their biocompatibility and biodegradability. In particular, PLGA has been approved by the United States Food and Drug Administration (FDA) for human therapy (Anderson and Shive, 1997). Lactic acids and glycolic acids of PLGA can both be eliminated from the body, as they are biodegradable.

1.2 JUSTIFICATION

The primary aim for the treatment of severe malaria is prevention of the death of the patient. Secondary treatment aims include prevention of disabilities and reinfections.

Because mortality from severe malaria occurs within hours of admission to a healthcare facility, attainment of therapeutic levels of a highly effective antimalarial treatment cannot be overemphasized.

The WHO recommended regimen for intramuscular (IM) artemether injection used for the treatment of severe malaria requires multiple injections because of the short half-life of artemether. This poses patient compliance challenges since there is some amount of pain associated with intramuscular injections. Also in areas where the IM artemether is not readily available, a patient may receive an initial dose and there could be no more IM artemether available for the subsequent doses. Again, the health care giver to patient ratio in Ghana and other sub-Saharan African countries is woefully unbalanced and therefore in most cases, availability of skilled health care professionals to administer multiple IM injections becomes a challenge.

Moreover, children under five with severe malaria most often are administered with other parenteral medications for managing the signs and symptoms of severe malaria. The parenteral route is used because coma or lack of consciousness together with nausea and vomiting precludes the use of the oral route.

A controlled release IM dosage form, which will release the required doses of artemether at the times needed by the patient for several days with a single injection, is a promising alternative to existing dosage form and regimen. The use of a controlled release dosage

form will eliminate the need for the administration of multiple doses of IM artemether, improve the comfort of the patient and promote patient compliance. The few healthcare workers available will also be able to attend to more patients, as the number of injections required by a particular child would be reduced.

More importantly, the therapeutic effects of artemether can be maintained over a long period of time with just a single injection. Furthermore, resistance to antimalarials may develop as a result of poor patient compliance to prescribed dosage regimens, thus the improvement of patient compliance with the use of the controlled release formulation will help to combat the development of resistance due to non-compliance with medication regimens.

Moreover, the use of poly (lactic co-glycolic acid) (PLGA) in the formulation of injectable controlled release depots has been approved by the US FDA and European Medicine Agency for parenteral applications and has been successfully employed globally for controlled drug delivery. PLGA is biocompatible and biodegradable and has been proven to be well tolerated as it is used as an absorbable suture material in both adults and children daily.

Finally, this study involves the development of a delivery system from an existing potent antimalarial drug artemether, which has been successfully used in the treatment of both uncomplicated and severe *falciparum* malaria. This approach could be more cost-effective than the development of a new antimalarial drug.

1.3 AIM

To develop a controlled release formulation of artemether, for the treatment of children under five with severe malaria.

1.4 OBJECTIVES

- To determine the total dose of artemether to be administered to children under five years with the aid of pharmacokinetic data.
- To formulate artemether loaded PLGA microspheres for intramuscular administration.
- To characterize the formulated microspheres *in vitro*.
- To determine the *in vitro* drug release properties of the formulated microspheres.
- To develop a suitable method of detection of artemether in plasma after a single microsphere injection to be used in pharmacokinetic studies.
- To undertake *in vivo* pharmacokinetic studies in experimental rats.

Chapter 2
LITERATURE REVIEW

2.1 MALARIA

Malaria can be caused by many plasmodium species including but not limited to, *Plasmodium falciparum* and *Plasmodium vivax*. Other plasmodium species that infect humans are *Plasmodium malariae* and *Plasmodium ovale* but global malaria problems are caused by *P. falciparum* and *P. vivax*. The malaria parasite is transmitted from an infected person to a healthy person through the bite of an infected female anopheles mosquito (Druilhe *et al*., 1998). Malaria due to *P. falciparum* is the most deadly form and is more prevalent in Africa whereas *P. vivax* is less dangerous but more widespread, and the other species are found much less frequently (WHO, 2013). Malaria is endemic in sub-Saharan Africa and South-East Asia as shown in Figure 2.1. Although many human malaria parasites exist, *P. falciparum* is the major cause of serious disease and death

Malaria is a condition that is marked by fever. It is often mistaken for any feverish condition. The World Health Organization has clearly defined the signs and symptoms of *P. falciparum* causing malaria. Falciparum malaria can also be classified as uncomplicated or complicated (severe) malaria. Poorly managed or untreated uncomplicated malaria rapidly develops into complicated or severe malaria.

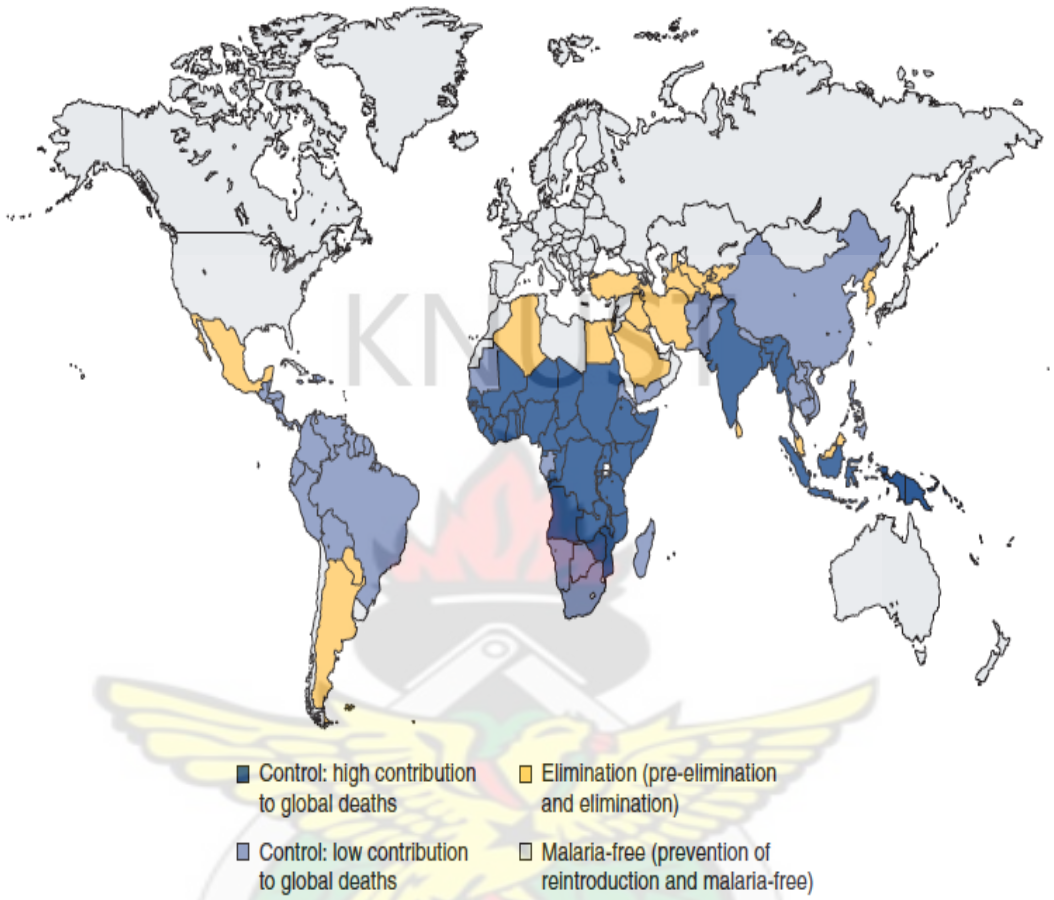

Figure 2.1 Worldwide distribution of malaria (Adapted from WHO, 2015)

2.1.1 Life cycle of plasmodium parasites

The life cycle of *plasmodium* parasites is divided between the asexual cycle, which occurs in human hosts, and the sexual cycle, which occurs in the mosquito vector as shown in Figure 2.2. The life cycle can also be classified as liver or red blood cell cycles. The sporozoites in the blood stream move into the liver and invade the liver cells. These sporozoites grow into merozoites and hypnozoites in the liver. The hypnozoites are responsible for causing malaria reinfection even after treatment. The merozoites however re-enter the blood stream and undergo asexual replication. The merozoites grow into schizonts and produce many more merozoites, which infect other red blood cells. This leads to an increase in the number of parasites in the blood stream thereby causing malaria.

The sexual life cycle involves development of some merozoites into male and female gametocytes, which upon ingestion by the anopheles mosquito grow into gametes. The male and female gametes reside in the gut of the mosquito and fuse to form diploid zygotes. These diploid zygotes also develop into ookinetes, which form oocysts. The oocyst bursts to release sporozoites into the body cavity of the mosquito and eventually move into the salivary gland of the mosquito. The sporozoites are transferred to humans through the bite of the mosquito (National Institute of Allergy and Infectious Diseases, 2016).

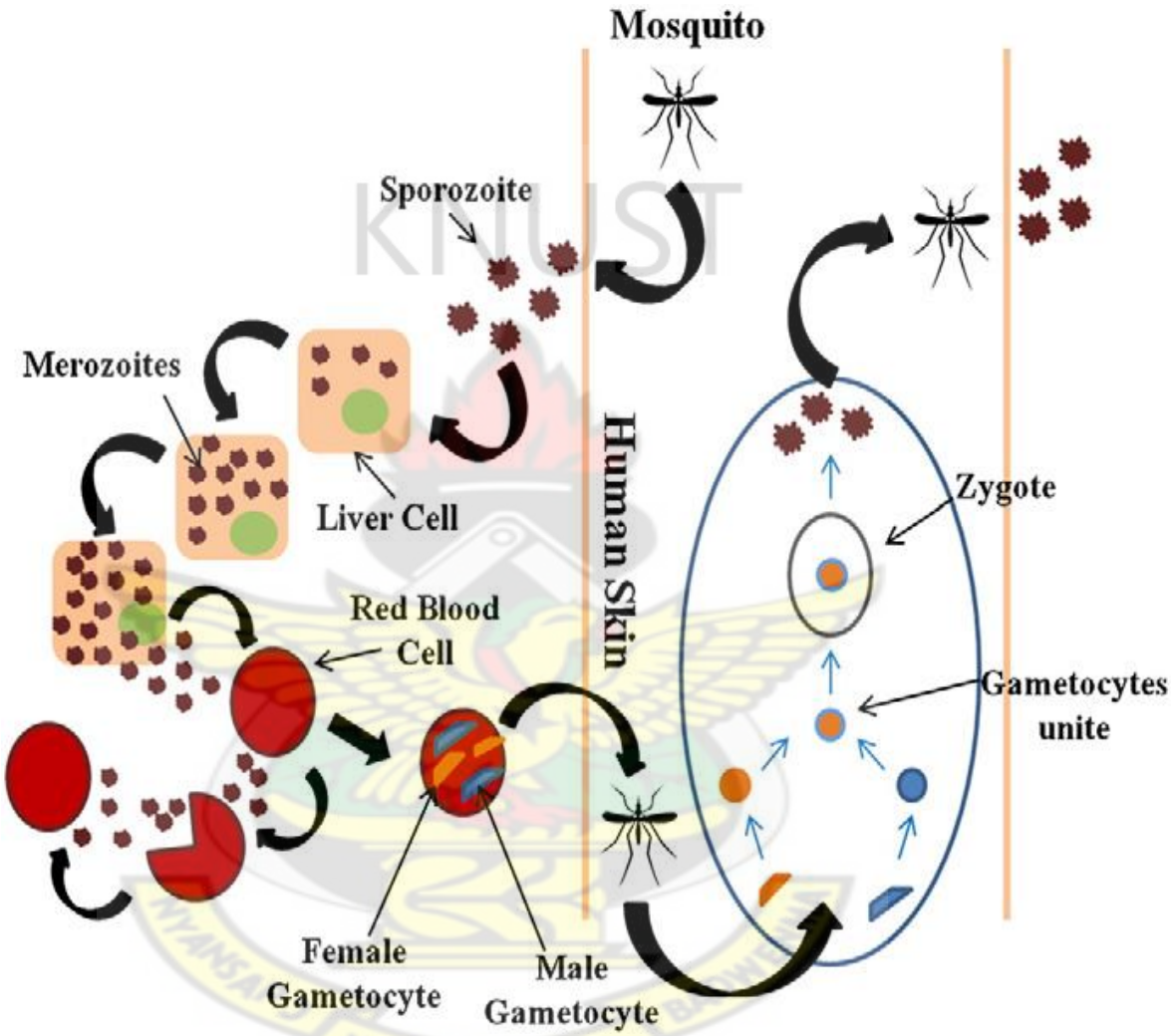

Figure 2.2 Life cycle of human malaria parasite showing sexual (in the mosquito) and asexual (in the human host) phases of life cycle (Reproduced from Aditya *et al*, 2013)

2.1.2 Malaria situation in Africa

Malaria continues to be a major cause of morbidity and mortality in sub-Saharan Africa. Although the Millennium Development Goal on malaria was to halt and begin to reverse the incidence of malaria by 2015, the United Nations (UN) Millennium Project's working group on malaria aimed to reduce malaria morbidity and mortality by 75 % by 2015 from the 2005 baseline level (UN Millennium Project, 2005). Despite significant progress in control of malaria between 2000 and 2010, it remains a major global health problem. Almost 40% of the world's population lives in malaria endemic areas, with each year about two hundred and fifty (250) million people experiencing clinical malaria and an estimated 655,000 malaria-related deaths (WHO, 2011). Globally, malaria remains a menace with an estimated 214 million cases reported worldwide in 2015 leading to 438,000 deaths, with sub-Saharan Africa accounting for 90 percent of the deaths. Malaria is an important cause of death in sub-Saharan Africa where 75 percent of 650 million people reside in malaria transmission areas (WHO, 2015).

Pregnant women and children under five are the most susceptible to malaria transmission and its subsequent effects (Bhattarai *et al.*, 2007; Barnes *et al.*, 2009). The global malaria action plan was aimed at reducing the incidence of malaria by at least 75 percent and to almost eliminate the number of malaria-related deaths by 2015(WHO, 2008). Reports showed that, almost 3.4 billion people were at risk of malaria worldwide in 2013, with populations living in sub-Saharan Africa having the

highest risk of acquiring the disease. Morbidity of 80% and mortality of 90% were estimated to occur in the sub-Saharan African Region, with children under five years of age and pregnant women most severely affected (WHO, 2015; Murray *et al*., 2012).

2.1.3 Severe malaria

Severe malaria, also known as complicated malaria, has been a major cause of mortality among children under five in sub-Saharan Africa. Vital organ dysfunction is the main distinguishing factor between severe malaria and uncomplicated malaria. The signs of vital organ dysfunction include; impaired consciousness, coma, convulsions, respiratory distress, shock, jaundice, haemoglobinuria, hypoglycaemia, severe metabolic acidosis and severe anaemia (WHO, 2010). Rapid onset of action of artemisinin and its derivatives make them most suitable for the treatment of severe malaria. Since severe malaria develops as a result of delay in diagnosis and improper management of uncomplicated malaria, early diagnosis and proper management are of prime importance. Thus, effective and timely management of uncomplicated malaria would reduce progression to severe malaria and hence the mortality rate due to severe malaria may be decreased.

2.1.4 Malaria mortality

In Africa, paediatric hospital admissions are very frequent and are as a result of conditions such as malaria and sepsis. These come with very serious and life-threatening complications such as shock and loss of consciousness. Estimated malaria mortality reportedly increased by three times through the 1980s and the 1990s with a

peak rise in 2004 (Trape, 2001; Trape *et al*., 2002; Murray *et al*., 2012). The reported mortality rate due to these conditions is 15-30 % (Nolan *et al*., 2001; English *et al*., 2004; Mulholland *et al*., 2005). In 2005, there were reports of 1-3 million deaths due to malaria and 90 % of these deaths were reported for children under five (Greenwood *et al*., 2005; Snow *et al*., 2005). Malaria mortality reportedly increased 1.3 times for children under five, 8.1 times for children five years and above and adults and 1.8 times for individuals of all ages outside the African region (WHO, 2011). Malaria was reported in 2010 as the underlying cause of death for 1.24 million people which included 714, 000 children under five years and 524, 000 children 5 years and above as well as adults (Murray *et al*., 2012). According to a study published in 2014, which was conducted across Africa and Asia, malaria mortality rates in children under 5 years are higher than in adults and children above 5 years. This study, which confirmed previous reports, was conducted using population-based registration of deaths using verbal autopsy (Streatfield *et al*., 2014).

2.1.5 Malaria diagnosis

2.1.5.1 Clinical or symptomatic diagnosis

Clinical or symptomatic diagnosis of malaria has been used widely across the globe in malaria endemic regions. However it is imprecise but remains the basis of therapeutic care for the majority of febrile patients in malaria endemic areas, where laboratory support is often out of reach. In some cases, the use of clinical diagnosis is still in existence because it is the least expensive form of diagnosis available. Unfortunately, many other diseases have symptoms similar to those of malaria and this has led to the indiscriminate use of antimalarials for the treatment of many

febrile illnesses in malaria endemic areas (Ruebush *et al*., 1995; Biritwum *et al*, 2000). The current WHO guidelines for management of malaria cases recommend parasitological confirmation before treatment with an antimalarial agent (WHO, 2010). This notwithstanding, clinical diagnosis of malaria in children under five is essential for quick commencement of potentially life-saving antimalarial treatment (WHO, 2000; Chandramohan *et al*., 2002). Moreover, various challenges with the recommended microscopic diagnosis such as false positive or negative results as well as errors in species identification have led to clinical diagnosis remaining the primary and sometimes only form of diagnostic tool (Milne *et al*., 1994; Houwen, 2002; McKenzie *et al*., 2003; Maguire *et al*., 2006).

2.1.5.2 Microscopy

In addition to symptomatic diagnosis, which involves the use of clinical signs and symptoms of the patient, laboratory confirmation of malaria diagnosis is essential. The laboratory diagnosis of malaria involves the use of light microscopy during which a blood film obtained from a drop of the patient's blood is analyzed. Microscopy is the gold standard for malaria diagnosis and all health facilities are expected to have laboratories where microscopic analyses can be carried out. Microscopic diagnosis involves the analysis of stained thick and thin blood smears of patients. A mixture of methylene blue and eosin stain, was introduced in 1904 by Gustav Giemsa known as the Giemsa-stained blood smear (Fleischer, 2004). Many alternatives have been introduced, including immunofluorescence antibody assay (IFA) and enzyme-linked immunosorbent assays (ELISA) (Sulzer *et al*., 1969). Molecular methods that involve

DNA probes and polymerase chain reaction (PCR) were introduced between 1980 and 1990 and fluorescent-staining methods also emerged (Bruce-Chwatt, 1984; Snounou *et al.*, 1993; van Vianen *et al.*, 1993; Hanscheid, 1999). However, the variability in techniques employed for the preparation of blood films accounts for the differences in parasite counts observed (Dowling and Shute, 1966; Kilian *et al.*, 2000).

2.1.5.3 Rapid Diagnostic Tests (RDTs)

The use of rapid diagnostic tests (RDTs) has been introduced since microscopic analysis requires highly skilled medical personnel who are not available at all health facilities. The introduction of RDTs also provides a diagnostic tool to be used in remote areas where access to microscopy and/or laboratories is highly limited or absent. The RDT device detects malaria antigens in a small volume of blood, approximately 5-15 µl. It involves an immunotherapy assay with monoclonal antibodies impregnated in the device that attack malaria antigens as shown in Figure 2.3.

The quick result is usually obtained between five and twenty minutes as a coloured line(s). RDTs may be in the form of a cassette or a cardboard strip (Wongsrichanalai *et al.*, 2007). The rate of diagnostic testing rose from 20 % to 47 % between 2005 and 2011 in sub-Saharan Africa. The use of RDT has increased with 40 % of all cases being tested with RDTs in 2011. Furthermore, there has been a global increase in the number of RDTs used by national malaria control programmes from less than 200, 000 in 2005 to over 74 million in 2011. This has improved diagnosis and management of malaria in peripheral health facilities especially in the rural areas (D' Acremont *et al.*, 2011; WHO, 2012). This technique is fast, reliable and a simpler method for testing for

the presence of plasmodium parasites. Due to their ease of use, individuals at home can use RDT kits, as well as pharmacists and other healthcare personnel at primary healthcare facilities (Standard Treatment Guidelines, 2010; WHO, 2013; Aditya *et al*., 2013). In Ghana, the use of RDTs increased the proportion of patients who were correctly treated from 42 % to 65 % (Ansah *et al*., 2013).

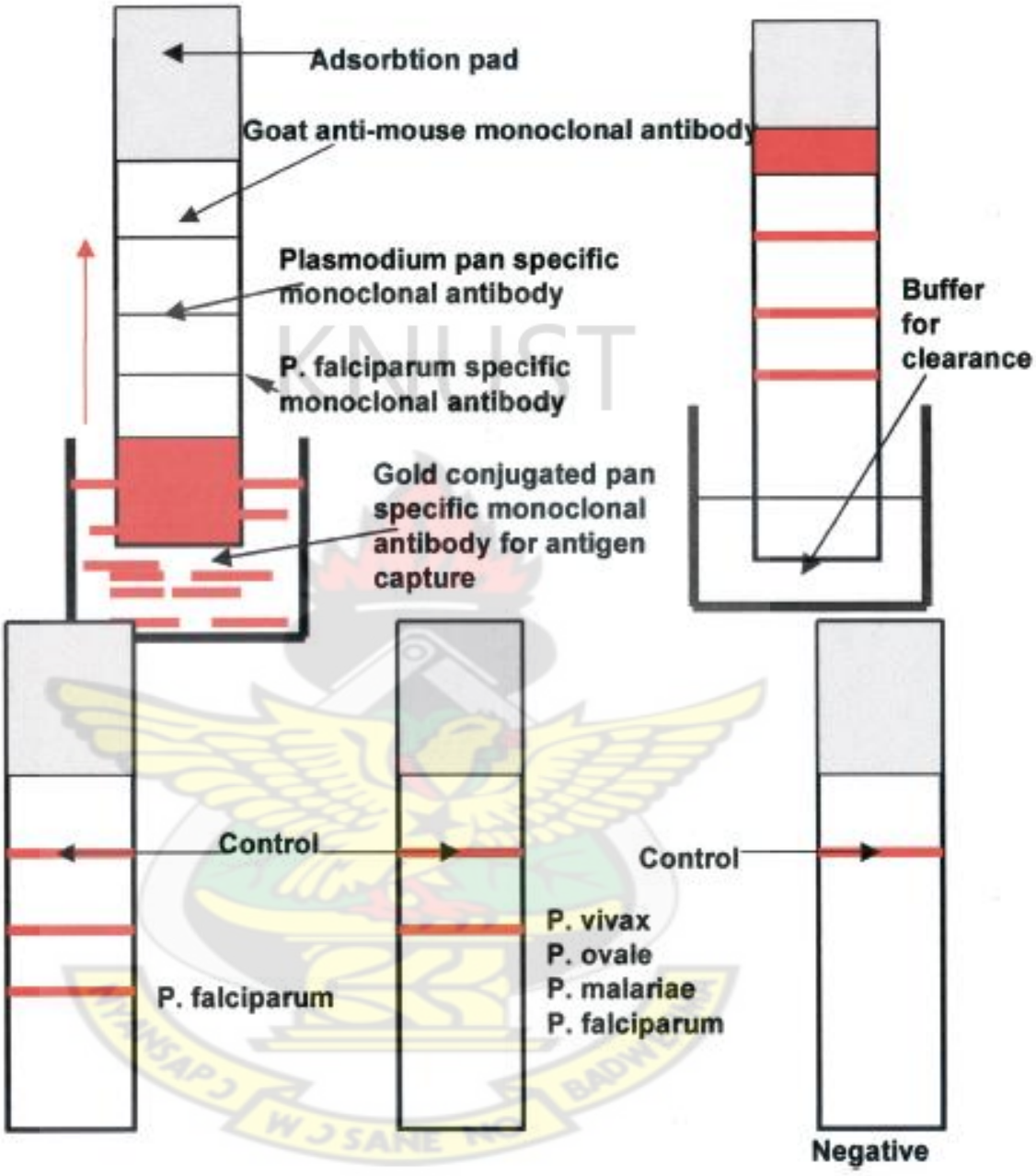

Figure 2.3 Principle of immunochromatographic RDT for Malaria (Adapted from Moody A, 2002)

2.1.6 Prevention of malaria transmission

Over the years, many approaches have been taken to prevent and control the development and spread of malaria. Prevention of transmission by vector control, indoor residual spraying and the use of insecticide sprays and lotions have been employed in the fight against malaria. The promotion of public education and awareness on malaria control also plays a vital role in the control of the disease.

2.1.6.1 Vector control

Vector control has been one of the main methods of prevention of malaria transmission in endemic areas. Vector control involves prevention of the bite of an infected female anopheles mosquito. Destruction of mosquito larva breeding sites, indoor residual spraying as well as the use of chemical mosquito repellents and topical sprays and lotions have been adopted and used. Other methods of malaria prevention include prophylactic use of selected anti-malaria medications especially for travellers to endemic regions and the development of malaria vaccines (Ockenhouse *et al.*, 1998).

2.1.6.2 Long-lasting insecticide-treated nets (LLINs)

Insecticide treated nets (ITNs) were first introduced to provide both physical and chemical means of vector control. However there were problems with the impregnation and re-impregnation of the nets during use. These problems arose because the technical skills and materials required for the above mentioned exercises were not readily available in all malaria endemic areas (Lines, 1996). LLINs were introduced to help curtail these problems. These LLINs are mosquito nets pre-treated with insecticide that lasts the life span of the net. Thus no re-impregnation is necessary

(Guillet *et al.*, 2001). The types of LLINs recommended by the WHO include Olyset®, PermaNet® and DuraNet®. Olyset® is made from polyethylene netting material (mesh 20 holes/cm^2) with 2 % permethrin incorporated into the polymer before monofilament yarn extrusion (Guillet *et al.*, 2001). Permanet® is made from polyester netting material (mesh 25 holes / cm^2) with 55 mg a / m^2 of deltamethrin incorporated in a resin coating of the fibres. DuraNet® is made from polyethylene netting material and impregnated with 261 mg/ m^2 alphacypermethrin (Table 2.1).

LLINs have been widely distributed and used in Ghana as part of the malaria control programme. Access to these insecticide treated nets has risen from 3 % in 2000 to 53 % in 2012 of households in sub-Saharan Africa. This rise in the access to these nets was as a result of recommendations made by the UN Millennium Project's working group. They recommended that the efficacy of LLINs would depend on the mass distribution of the nets to the entire population in endemic areas not just children and pregnant women (UN Millennium Project, 2005).

Table 2.1 Characteristics of some LLINs (Adapted from Atkinson *et al*., 2009)

Brand	Material	Insecticide	Mesh size	Fiber Thickness
Olyset®	Polyethylene	1, 000 mg/ m^2 permethrin	4 X 4 mm	150 denier
PermaNet®	Polyester	55 mg / m^2 deltamethrin	1.5 X 1.5 mm	100 denier
DuraNet®	Polyethylene	261 mg/ m^2 alphacypermethin	2 X 2.5 mm	145 denier

2.1.6.3 Intermittent Preventive Treatment in Pregnancy (IPTp)

In Ghana, IPTp involves the administration of a fixed dose combination of sulfadoxine and pyrimethamine (SP) to pregnant women at routine prenatal visits regardless of their malaria infection status. IPTp reduces the rate of maternal morbidity due to malaria, placental parasitaemia, low birth weight and neonatal mortality (WHO, 2002). The SP is co-administered under the supervision of a qualified health care giver on at least three occasions and can be described as 'Directly Observed Therapy" (DOT) (Anti-malaria Policy for Ghana, 2009; Standard Treatment Guidelines, 2010). The WHO recommends the use of sulfadoxine and pyrimethamine combination for the intermittent preventive therapy (IPTp) of malaria in pregnant women (WHO, 2002). The IPTp starts after quickening which is 16 gestational weeks.

The first dose is taken on the first prenatal hospital visit, which is after 16 weeks of gestation. The second dose is taken at least one month after the first dose, followed by the third dose taken at least one month after the second dose. A fourth dose may be given one month after the third dose if there is at least a month left before the

anticipated delivery date (Standard Treatment Guidelines, 2010).

2.1.7 Malaria treatment

2.1.7.1 Treatment of uncomplicated malaria

The objectives of treatment of uncomplicated malaria include the following:

- the avoidance of progression to severe malaria
- the limitation of the duration of the disease
- the minimization of the development of resistant parasites.

Therapeutic treatment of uncomplicated malaria in Ghana involves the use of WHO recommended artemisinin based combination therapies (ACTs). Oral artesunate and amodiaquine combination is recommended for first line treatment. The dose in mg / body weight is: amodiaquine 10 mg / kg and artesunate 4 mg / kg as a single dose daily for three days. However, for patients who cannot tolerate the artesunate and amodiaquine combination, alternative ACTs are recommended. These alternatives are either a combination of artemether (20 mg) and lumefantrine (120 mg) (Table 2.2) or a combination of dihydroartemisinin (40 mg) and piperaquine (320 mg base) (Table 2.3) (Standard Treatment Guidelines, 2010).

Table 2.2 Recommended Dosing Regimen for Artemether (20 mg) and Lumefantrine (120 mg)

		Number of tablets to be given					
Weight (kg)	Age	Day 1		Day 2		Day 3	
		First Dose	Second Dose (after 8 hours)	Morning	Evening (after 12 hours)	Morning	Evening (after 12 hours)
< 5	<6 m	Not recommended for children less than 5 kg					
5-15	6 m-3 yr	1	1	1	1	1	1
15-25	3-8 yr	2	2	2	2	2	2
25-35	8-12 yr	3	3	3	3	3	3
>35	>12	4	4	4	4	4	4

Table 2.3 Recommended Dosing Regimen for Dihydroartemisinin (40 mg) and Piperaquine (320 mg base)

Weight (kg)	Age (years)	Number of tablets to be given		
		Day 1	Day 2	Day 3
5-10	< 1	¼	¼	¼
11-15	1-3	½	½	½
16-24	4-6	1	1	1
24-35	7-10	1 ¼	1 ¼	1 ¼
36-50	11-13	1 ½	1 ½	1 ½
50-70	14-18	2	2	2
> 70	> 18	3	3	2

2.1.7.2 Treatment of complicated or severe malaria

The treatment objectives for severe malaria include the provision of specific parenteral anti-malarial that will ensure the presence of adequate drug levels in the blood serum that can rapidly clear the parasites. Provision of urgent treatment for life threatening conditions such as convulsions, hypoglycaemia, dehydration and renal impairment is also a must. The therapeutic agents used in the treatment of severe malaria in Ghana are intramuscular or intravenous quinine and intramuscular artemether. Rectal artesunate is also used in pre-referral treatment of severe malaria in cases where neither intramuscular quinine nor artemether is readily available. Intramuscular (IM) quinine is administered as 10 mg per kilogramme body weight and intravenous (IV) quinine is given by slow infusion over 4-8 hours. IV quinine is given as 10 mg/ kg and mixed with 5-10 ml / kg of dextrose saline or in 5 % dextrose and infused over a period of 4 to 8 hours. The infusion is repeated 8 hourly until the patient is able to swallow oral quinine. Oral quinine is given at the same dose of 10 mg / kg eight hourly to complete 7 days of treatment.

IM quinine is administered until the patient can tolerate oral therapy. The maximum single dose for all the dosage forms is 600 mg. The dosage regimen for adults and children for intramuscular artemether is the same. This is because the clearance of artemether in an adult was found to be the same in a child (Karbwang *et al*., 1998).

The current dosage regimen for intramuscular artemether in adults and children is 3.2 mg per kg body weight initially, followed 8 hours later by 1.6 mg / kg body weight.

Subsequently, 24 hours after initiation of treatment 1.6 mg / kg is given daily for up to 5 days. Intramuscular artemether injection is commercially available as an oily solution containing 80 mg of artemether in 1 ml ampoule (WHO, 1995). This IM treatment is followed by a full 3-day course of oral ACTs if the patient can tolerate oral medications (Standard Treatment Guidelines, 2010). The presence of nausea and vomiting as well as the loss of consciousness associated with severe malaria often prolongs the use of IM artemether beyond the six-day period.

2.2 ARTEMISININ AND ITS DERIVATIVES

In 1972, Chinese researchers isolated artemisinin also known as quinghaosu in Chinese, from quinhao (*Artemisia annua* L) and was reported in a published article in 1979. The structure of artemisinin was also elucidated in 1979 (Klayman, 1985). The Chinese, reportedly used this plant, which in English is called sweet wormwood, as remedy for many conditions. The use of this plant for the treatment of haemorrhoids, was first described in the "52 Prescriptions" unearthed in 168 BC from the Mawangdui Han dynasty tomb in Changsha, Hunan province. The herb was used for treatment of fevers and appeared in several Chinese literature texts as a treatment for febrile illnesses. In 1971, the Chinese discovered that a low-temperature ethyl ether extraction of the herb showed antimicrobial activity against many microorganisms including *Plasmodium berghei* (Klayman *et al*, 1984; Miller and Su, 2011; Youyou, 2011).

The maximum yield of artemisinin from cultivated Artemisia was approximately 2 % whereas the yield from the herb in the wild was between 0.01 % and 0.5 %. Also, the

highest yield was obtained just before the flowering stage of the plant (Quinghaosu Antimalarial Cordinating Research Group, 1979; Klayman, 1985; Woerdenbag *et al*., 1990). The artemisinin derived from the leaves and flowers of the plant reportedly yielded approximately 0.01% to 0.8 % of dry weight (van Agtmael *et al*., 1999).

Artemisinin derivatives include artesunate, artemether, arteether and dihydroartemisinin. Artemisinin exhibits a first order one-compartment model of metabolism and elimination. Rapid absorption of oral formulations of artemisinin and its derivatives is accompanied by incomplete absorption, which also varies from person to person. Rapidly absorbed artemisinins are widely distributed and undergo first pass metabolism to produce dihydroartemisin, an active metabolite. Metabolism of artemisinin also leads to conversion into deoxyartemisinin and dihydroxydeoxyartemisinin, which are both inactive. In addition to first pass effect, crossing the blood-brain and blood placenta barriers, is associated with primary metabolism of orally administered artemisinins. Artemisinins exhibit high levels of protein binding to α-1-acid glycoprotein and in severe cases of acute malaria; the levels of this glycoprotein are significantly raised (Li *et al*., 1982; de Vries & Dien, 1996).

These agents are increasingly used in malaria-endemic areas for the treatment of malaria because they have a fast onset of action, few side effects, and are very effective against multidrug-resistant *Plasmodium falciparum* parasites (White, 1994) The major limitation to the use of these artemisinin derivatives is a reportedly high recrudescence rate when used as monotherapy (Li *et al*., 1994). Factors that contribute

to this reduced efficacy are the short elimination half-life ($t_{1/2}$) of 1 to 3 hours and it has also been reported that the pharmacokinetics of these medicines are time dependent (Ashton *et al.*, 1998).

2.2.1 Mechanism of action of artemisinins

Artemisinins are noted for their rapid onset of action both in killing and the inhibition of the metabolic processes of plasmodium parasites. They act on various stages of the lifecycle of the plasmodium parasites. They act on both the blood stages and those found in the liver. Artemisinins also act by inhibiting cytoadherence of the plasmodium parasites.

Generally, antimalarials have nitrogen in their chemical structure but artemisinin does not share this characteristic. Artemisinin's structure consists of a sesquiterpene trioxane lactone with an endoperoxide linkage, which is reportedly essential for its activity (Antimalarials, 1972; China Cooperative Research Group, 1982; Klayman, 1985; Brossi *et al.*, 1988).

2.2.2 Artesunate

Artesunate is the water-soluble hemisuccinate derivate of artemisinin. It is available for oral, rectal and intravenous administration. Artesunate acts as a prodrug, which is converted into dihydroartemisinin and has an elimination half-life of less than thirty minutes (Na- Bangchang *et al.*, 1998).

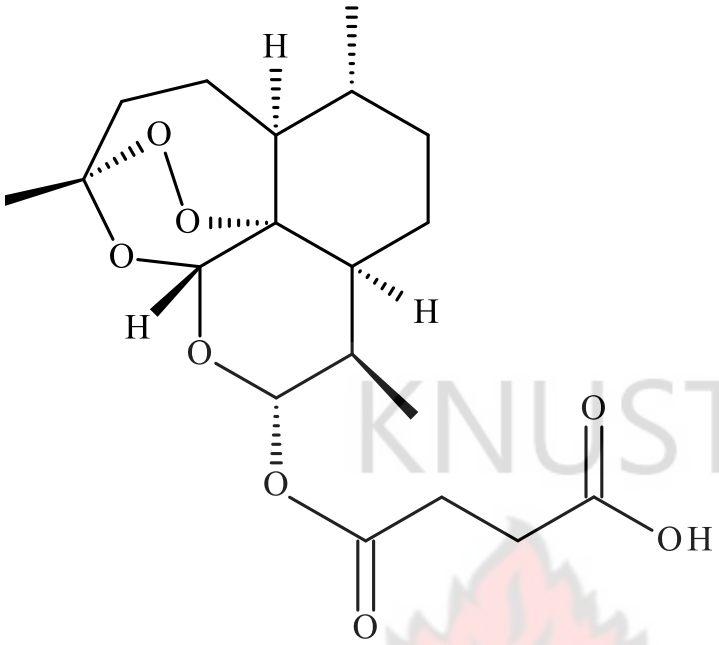

Figure 2.4 Chemical Structure of artesunate

2.2.3 Arteether

Arteether is the ethyl ether derivative of dihydroartemisinin. It has been found to be lipophilic and posses similar chemical and physical characteristics to artemether. Arteether like artemether is metabolized to dihydroartemisinin (Hien and White., 1993; Kager *et al.,* 1994). Several research studies have been undertaken to develop arteether as an antimalarial for human use (Brossi *et al*., 1988; Krishna and Flanagan, 1989; Binns and Wallace, 1989; Baker *et al*.,1993; Brewer *et al*.,1994; Kager *et al*., 1994; Davidson, 1994; Dwivedi *et al*., 2014).

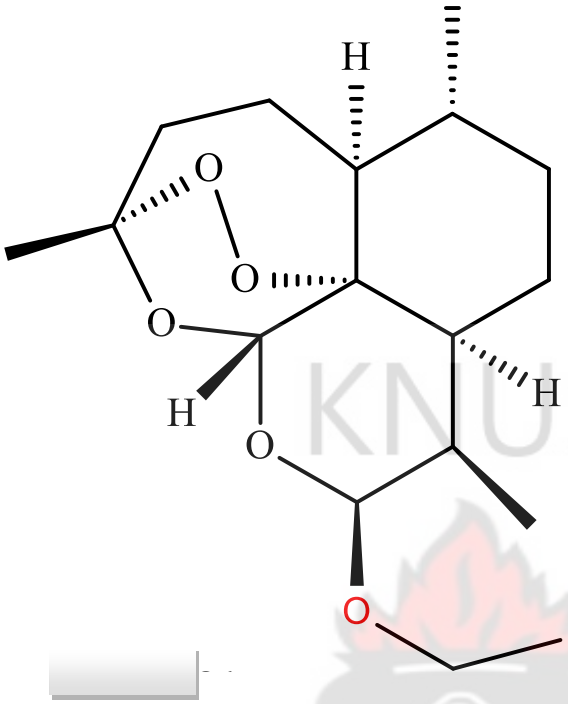

Figure 2.5 Chemical structure of arteether

2.2.4 Dihydroartemisinin

Dihydroartemisinin (DHA) is a derivative of artemisinin and the active metabolite of artemether and artesunate. DHA is obtained from the sodium borohydride reduction of artemisinin (Lin *et al*., 1987). DHA is more potent than artemisinin but has a shorter half-life (Wesche *et al*., 1994). This artemisinin derivative is reportedly three times more active than artemether (Alin *et al*., 1990). DHA is available as an oral dosage form.

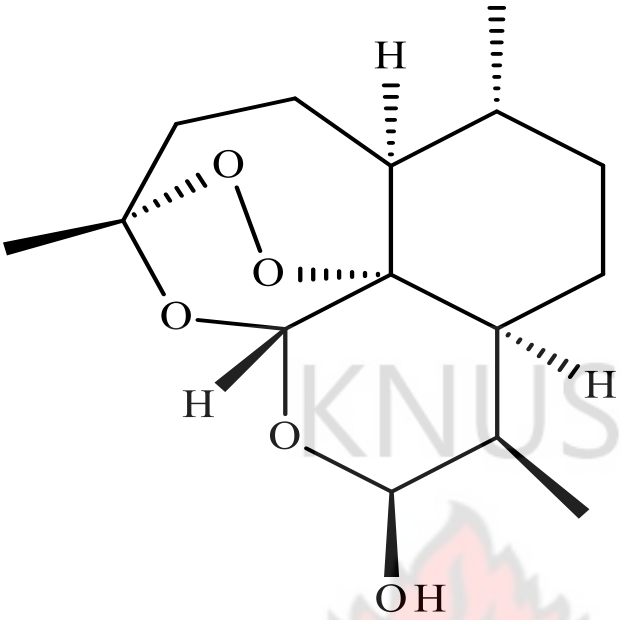

Figure 2.6 Chemical structure of dihydroartemisinin

2.2.5 Artemether

Artemether is the methyl ether derivative of DHA. It was synthesized to enhance the antimalarial activity and solubility of artemisinin. Artemether is available for oral and intramuscular administration (Kager *et al*., 1994).

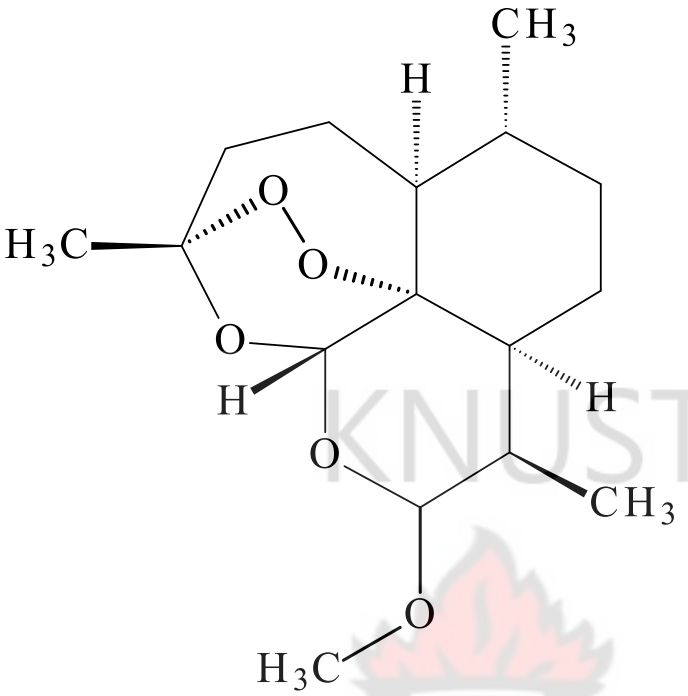

Figure 2.7 Chemical structure of artemether

2.2.5.1 Pharmacokinetics of Artemisinin and Artemether

Artemether has a short half-life of ~ 2-3 hours (Lefevre *et al*., 2001;Makanga and Krudsood, 2009). Artemisinin was found to have maximum plasma concentrations (C_{max}) and area under the plasma concentration–time curves (AUC) of 20% to 30% in patients treated for malaria after the dose at 5th day compared with the first day (Hassan Alin *et al*., 1996). A similar result was shown in healthy subjects, which suggested that this marked time-dependent decrease in bioavailability was not caused by the disease (Ashton *et al*., 1998). Van Agtmael *et al* in a study of Chinese patients with malaria, found that the mean C_{max} of artemether after the fourth dose at 48 hours was only one-third compared with the first dose, whereas the metabolite dihydroartemisinin increased over time (van Agtmael *et al*.,1999). It is thought that

artemisinin concentrations in plasma decrease over time through auto induction in multiple-dose studies. The enzymes involved in this auto induction are unknown, although it was recently found that artemisinin induced omeprazole metabolism in human beings was associated with increased hydroxylation by CYP 2C19 (Svensson *et al*., 1998).

2.2.5.2 Plasma protein binding of artemether

Artemether is 92 to 98 percent bound to plasma proteins. Artemether binds to human plasma proteins at a concentration of 3.2 mg/l and this value describe the total binding capacity of normal human plasma. However, the active metabolite of artemether, dihydroartemisinin (DHA) exhibits a lower protein binding capacity of 47 to 76 percent. The total binding capacity of normal human plasma of DHA is 0.3 mg / ml. The binding of artemether is predominantly via high affinity sites to α_1-acid glycoprotein and also via lower –affinity sites to albumin. DHA on the other hand binds predominantly to albumin (Li *et al.*, 1998). Both artemether and dihydroartemisinin bind to red blood cells with a red cell to plasma binding ratio of 0.49: 0.28 respectively (White *et al*, 1999).

2.2.5.3 Formulations of Artemether

Artemether injection is an oil soluble methyl ether of artemisinin effective against both chloroquine-resistant and chloroquine-sensitive strains of *Plasmodium falciparum*, as well as against *Plasmodium vivax*. It is also used in the management of cerebral malaria (Medana and Turner, 2006). Many formulations have been made to counteract the erratic release and erratic absorption of artemether from the

commercially available oily injection. This erratic release varies from person to person and limits the therapeutic efficacy of the artemether. It has been reported that the parenteral oily formulation leads to pain on injection as well as poor patient compliance, thus limiting its use in malaria treatment. The commercially available artemether injection has poor aqueous solubility and short half- life usually between 3 and 5 h (Mandawgade *et al*., 2008; Aditya *et al*., 2010).

The purpose of nanocarriers, is to get drugs to the targeted sites of action avoiding distribution to non target sites thereby overcoming side effects observed with conventional dosage forms. It is of utmost importance to achieve higher drug concentration in the microenvironment of parasite than in systemic circulation. Various colloidal drug carriers such as polymeric nanoparticles, liposomes, nanoemulsions, solid lipid nanoparticles (SLNs) and nanostructured lipid carriers (NLCs) have been investigated for drug delivery (Kumar *et al*., 2007; Seju *et al*., 2011; Haque *et al*., 2012; Alam *et al*., 2013).

The formulation of nanostructured lipid carriers (NLC) for intravenous delivery of artemether was reported by Joshi *et al* (2008). The NLC formulated had a particle size of 68 nm. This formulation showed a survival rate of 60 % against 0 % survival rate for the commercially available oily IM injection of artemether, for the survival rate of *Plasmodium berghei* infected mice. The encapsulation efficiency reported for this formulation was however only 30 %. The authors postulated that the remainder of the artemether may have been entrapped in the surfactant micelles and would be responsible for initial burst release. This formulation showed *in vitro* release of

artemether over 24 hours with the highest cumulative percentage release occurring at the 24th hour. Thus more than one injection is required if patients are to receive treatment for more that 24 hours which is almost always the case.

Analysis of a parenteral microemulsion formulation of artemether with a globule size of 113 nm showed ~66 % survival rate compared to 50 % for a commercially available IM injection. This result was obtained from an *in vivo* study conducted using *Plasmodium berghei* infected mice (Tayade *et al*., 2010). This formulation showed great potential, however, its administration is no different from the commercially available formulation since it is a single dose formulation. An intranasal formulation of artemether as a nanostructured lipid carrier (NLC) using central composite drug was achieved (Jain *et al*., 2015). The formulation was prepared by the microemulsion method and an average particle size of 123.4 nm was measured. The *in vitro* release study conducted showed a sustained release of artemether for up to 96 hours (4 days). The *in vivo* study showed that the NLC had a better brain targeting efficiency when compared to a solution of artemether.

The preparation of an oral nanoemulsion as a carrier for enhancing the bioavailability of oral artemether has been reported. This formulation showed 92 % release *in vivo* in 24 hours and 92 % *ex vivo* in 4 hours. A burst release of 73 % was reported in 30 minutes (Laxmi *et al*., 2015). The limitations to this formulations usefulness however outweigh the potential benefits. Artemether is a hydrophobic drug, which exhibits poor oral bioavailability, and oral monotherapy has currently been banned. The WHO recommends the use of artemisinin based-combination

therapies (ACTs) for the treatment of uncomplicated malaria. Monotherapy of artemether is only recommended for severe malaria and must be parenteral or rectal.

Gugulothu *et al* formulated a self-microemulsifying suppository formulation of β-artemether in 2010. These suppositories showed in vitro release within 30 minutes. The globule size of the suppository dispersion was ~30 μm. This formulation may be employed for pre referral management of severe malaria and may require multiple insertions of the suppositories before parenteral treatment is initiated, owing to the short half-life of artemether (Gugulothu *et al*., 2010). A sublingual spray composed of artemether in neutral oil has been shown to be more rapidly and completely absorbed than artemether tablets (Salman *et al*., 2015).

All these formulations have been made with the objective of improving malaria treatment through better delivery of artemether. The formulation of artemether dosage form with high encapsulation efficiency and controlled release properties will achieve this objective.

2.3 ARTEMISININ BASED COMBINATION THERAPIES (ACTS)

In order to prevent or slow the progression of plasmodium resistance to artemisinins, the WHO has restricted the use of artemisinin monotherapy (Warhurst, 1999). Artemisinin monotherapy is now reserved for the first line treatment of severe malaria, which involves the parenteral or rectal route. The WHO has directed that all oral artemisinins be combined with another antimalarial to produce ACTs. The artemisinin portion of this combination is responsible for the initial quick reduction in parasite load whereas the other antimalarial is for the clearing of remaining parasites since

those have a longer half-life as compared to the artemisinins. Currently, ACTs are the WHO recommended first line treatment for uncomplicated malaria and second line for complicated or severe malaria.

2.3.1 Artesunate and Amodiaquine

The WHO recommends the use of artesunate and amodiaquine combination therapy for first line treatment of uncomplicated malaria and as second line for complicated malaria (WHO, 2000). The combination of artesunate which has a quick onset of action and amodiaquine which has a long elimination half life of between nine and eighteen days (Pussard *et al*., 1987) is able to rapidly reduce parasite load and clear all residual parasites. Amodiaquine is a 4- aminoquinoline antimalarial (Ruscoe *et al*., 1998) and is active against chloroquine-sensitive and chloroquine-resistant strains of *Plasmodium falciparum.* The mechanism of action of amodiaquine is by inhibition of haem crystallization. Amodiaquine is available as oral dosage forms and undergoes first-pass metabolism (Churchill *et al*., 1985). The recommended dosing for artesunate and amodiaquine is 4 mg of artesunate per kilogramme body weight and 10 mg of amodiaquine per kilogramme body weight for oral administration (Standard Treatment Guidelines, 2010).

2.3.2 Artemether and Lumefantrine

This combination is effective against multidrug-resistant falciparum malaria. The artemether is absorbed rapidly and is metabolized to dihydroartemisinin and both are eliminated with terminal half-lives of ~ one hour. Artemether and dihydroartemisinin provide a rapid initial reduction in *plasmodium* parasite biomass, which leads to rapid

resolution of symptoms. Lumefantrine is not absorbed as rapidly as the artemether and is eliminated more slowly with a half-life of between three and six days. Absorption of lumefantrine is enhanced by ingestion of fatty food substances. Thus, the artemether-lumefantrine combination combats malaria in a two-fold action of initial clearance by artemether and clearance of residual parasites by lumefantrine. The dosage regimen for artemether-lumefantrine is shown on Table 2.2.

2.3.3 Dihydroartemisinin and Piperaquine

Dihydroartemisinin and piperaquine is available as an oral fixed dose ACT which is used as first line treatment for uncomplicated *falciparum* malaria and second line treatment for complicated *falciparum* malaria. Studies have shown that it is effective against drug-resistant *falciparum* malaria (Denis *et al*., 2002; Hien *et al*., 2004; Ashley *et al*., 2005; Smithuis *et al*., 2006). The dihydroartemisinin portion of this combination is responsible for the initial quick reduction in parasite load whereas the piperaquine is for the clearing of remaining parasites. Piperaquine is a 4-aminoquinoline like chloroquine. Research on piperaquine proved that it was effective and well tolerated (Chen *et al*., 1982). The dosing regimen for dihydroartemisinin-piperaquine is shown on Table 2.3.

2.4 CONTROLLED RELEASE DRUG DELIVERY

Controlled release systems and devices include drug delivery systems that encapsulate drugs and release them at controlled rates for relatively longer periods of time such as over several hours to a year. These systems and devices are being developed to aid in

overcoming the difficulties experienced with the use of the existing traditional or conventional methods of drug delivery. Although many materials and devices have been used for controlled delivery of drugs, biodegradable and biocompatible polymer microspheres are the most prevalent (Kim and Pack, 2006).

2.4.1 Advantages and disadvantages of controlled release drug delivery

Controlled release enables drug release to be tailored to the needs of specific applications such as the provision of a pulsatile or a constant release of drugs. Plasma levels of drugs are continuously maintained at a therapeutically desirable level. This provides less fluctuation of drug levels to achieve a more uniform effect. In addition to the improvement of patient compliance and patient comfort, the administration of fewer injections for example reduces the tasks of health care givers who may use the time saved to attend to other patients. Moreover, controlled release dosage forms serve as protection for drugs that may otherwise be rapidly destroyed by the body (Langer and Peppas, 1981; Kim and Pack, 2006).

On the other hand, dose dumping and difficulty in shutting off drug release are associated with controlled release drug delivery. Controlled drug delivery may also be associated with toxicity due to lack of biocompatibility of the polymer material used. Moreover, controlled drug release may be expensive due to the cost of the formulations used (Langer and Peppas, 1981; Kim and Pack, 2006).

2.4.2 Some controlled release PLGA dosage forms

Drug delivery of some hydrophilic and hydrophobic drugs, peptides and proteins has

been achieved through controlled release. These substances may also require parenteral formulations to avoid degradation in the digestive tract and first pass metabolism. Moreover, the short half–lives of some of these bio agents requires parenteral formulations that reduce dosing frequency. Furthermore, to avoid the inconvenience of surgical insertions of large implants, injectable biodegradable and biocompatible PLGA particles may be employed for controlled-release dosage forms. These particles include, microspheres, microcapsules, nanocapsules and nanospheres. Drug release from these particles is either by diffusion or erosion mechanisms or a combination of the two (Makadia and Siegel, 2011).

2.4.3 Natural and synthetic polymers

Both natural and synthetic polymers have been used in the formulation of controlled release dosage forms. The use of synthetic polymers however has been more prominent due to some advantages they have over natural polymers. Studies have shown that synthetic polymers are more homogenous in composition and therefore posses a higher purity compared to natural polymers (Lai *et al*., 2014). It is worth noting however that, not all synthetic polymers can be used for drug delivery. Suitable synthetic polymers should be biodegradable and have low cytotoxicity (Lai *et al*., 2014).

Synthetic polymers are mainly the polyesters and copolymers of the polyesters. The polyesters are poly (lactic acid) (PLA), poly (glycolic acid) PGA and the poly alkyl (cyano) acrylates (PCA). The copolymer of PLA and PGA known as poly (lactide-co-glycolic acid) PLGA is also used extensively. These polyester polymers have been

used extensively in medicine for many years as surgical sutures and implants (PLA) as well as wound sealing agents (PCA) (Holland *et al.,* 1986). Another advantage of synthetic polymers over natural polymers is that they are more easily engineered toward sustained release. Moreover, the degradation profiles of the synthetic polymers are well understood and have been used in the formulation of controlled release dosage forms (Lai *et al*., 2014).

Natural polymers mostly exhibit a variation in purity and also require crosslinking and further modifications, which could have an effect on the stability of the active drug formulated with them (Hans and Lowman, 2002). Natural polymers are mainly obtained from proteins from plant and animal sources. Since they are obtained from natural sources, they should be biocompatible and less cytotoxic. Natural gums (such as xanthan, cashew, albizia and khaya), gelatin and chitosan and pectin are some natural polymers used for controlled release dosage forms (Lai *et al*., 2014). Gelatine is derived from the collagen present in bones (Wang and Uludag, 2008). It possesses low antigenicity and is stable. Chitosan is obtained from the hydration of chitin in basic solutions at very high temperatures of 80-140 ^{o} C for up to ten hours (Hudson and Margaritis, 2014). The mucoadhesive, antimicrobial and antitumor properties of chitosan have been reported (Peniche and Peniche, 2011)

2.4.3.1 Biodegradable polymers

Biodegradable polymers are obtained from natural and synthetic sources and are degraded *in vivo*. The degradation may be by enzymatic or non-enzymatic pathways or a combination of the two, to produce biocompatible and toxicologically safe by-

products, which are further, eliminated by the normal metabolic pathways. Biomaterials used in drug delivery can be classified as synthetic biodegradable polymers or naturally occurring polymers. The synthetic biodegradable polymers include relatively hydrophobic materials such as hyaluronan and chitosan, which are complex sugars and inorganic hydroxyapatite (Anderson and Shive, 1997; Uhrich *et al*., 1999; Nair and Laurencin, 2007). Natural biodegradable polymers include rosin, which is obtained from the oleoresin of pine trees. Rosin and its derivatives are hydrophobic biodegradable biomaterials. The biocompatibility of rosin has also been reported. Other biodegradable natural polymers include gums, pectin, collagen and alginates (Park *et al*., 2005).

2.4.3.2 Poly (lactic-*co*-glycolic acid) PLGA

Poly (lactic-*co*-glycolic acid) is made from a copolymer consisting of PLA and PGA polymers respectively. The design and performance of PLGA makes it the best biomaterial available for controlled drug delivery. PLA is made of the D or L form of an asymmetric α-carbon and sometimes the R and S form respectively. The enantiomers of PLA are poly D-lactic acid (PDLA) and the poly L-lactic (PLLA). When the D- and L- lactic acid forms are in equal ratio, PLGA is poly D, L-lactic-*co*-glycolic acid. PGA has no methyl side groups unlike PLA and shows highly crystalline structure unlike PLA. The uses of PLGA include as surgical implants, absorbable surgical sutures and in pharmaceutical nanoparticle and microparticle formulations. The Food and Drugs Administration (FDA) in the United States of America and the European Medicine Agency have approved PLGA for use in human therapy

(Anderson and Shive, 1997, Danhier *et al.*, 2012).

PLGA formulations are more reproducible because of the high purity of PLGA. Furthermore, it offers an advantage over PLA and PGA of being more stable against hydrolytic cleavage. Modification of the surface properties of PLGA is easily achieved for drug targeting purposes (Danhier *et al.*, 2012). PLGA can be formulated into almost any shape and size and various sizes of molecules can be successfully encapsulated by it. Its solubility in many common solvents such as chlorinated solvents, tetrahydrofuran, acetone and ethyl acetate is an added advantage for various formulations (Uhrich *et al.*, 1999; Wu and Wang, 2001).

2.4.3.3 Physicochemical Properties of PLGA

The crystallinity of the PLGA is dependent on the type and molar ratio of the individual monomers in the copolymer chain. The crystallinity of PLGA influences the mechanical strength, swelling behavior, capacity to undergo hydrolysis and the biodegradation rate. Generally, the higher the content of PGA, the quicker the rate of degradation, although a 50:50 ratio of PLA/ PGA exhibits the fastest rate of degradation with a higher PGA content leading to increased degradation interval below 50 %. The degree of cystallinity and melting point range of the polymers are directly related to the molecular weight of the polymer. The glass transition temperature (Tg) of PLGA polymers is above the physiological temperature of 37 ^{o}C. This makes PLGA copolymers glassy and they exhibit a fairly rigid chain structure. It has been reported that Tg of PLGA decrease with a decrease of lactide content in the copolymer composition and with a decrease in molecular weight (Passerini and Craig, 2001).

The intrinsic viscosity, which is directly related to molecular weights, is used to characterize commercially available PLGA. Another important property of PLGA is its highly biodegradable nature. It biodegrades by hydrolysis of its ester linkages in water. Lactide rich PLGA copolymers degrade more slowly because they are less hydrophilic and absorb less water since the methyl side groups of PLA make it more hydrophobic. Biodegradation of PLGA yields lactic and glycolic acids, which are the same as the natural metabolites, found in humans and thus are eliminated easily from the body (Kumari *et al*., 2010; Makadia and Siegel, 2011). The physical properties of PLGA are dependent on many different factors which include, the initial molecular weight, the lactide to glycolide ratio, device size, water exposure or surface shape and storage temperature (Houchin and Topp, 2009). The molecular weight and polydispersity index predict the mechanical strength of PLGA. The type of drug encapsulated affects the release rate of drugs from PLGA (Siegel *et al*., 2006)

2.4.3.4 Pharmacokinetics of PLGA

Many active pharmaceutical ingredients (API) have been successfully encapsulated into PLGA for drug delivery. The success of such formulations depends on the ability of the PLGA to deliver the drug at the appropriate times to achieve the intended therapeutic effect. Thus the material, geometry and location design must incorporate mechanisms of degradation and clearance of the vehicle as well as the API. Bioavailability and pharmacokinetics of PLGA follows a non-linear and dose dependent profile (Yang *et al*., 2001). It has been reported that blood clearance and uptake by mononuclear phagocyte system (MPS) may depend on dose and composition of PLGA carrier systems (Panagi *et al*., 2001). The degradation of PLGA

formulations is almost 30 % initially followed by a slow phase, which leads to the clearance of the metabolites via respiration by entering the tricarboxylic acid cycle (Bazile *et al*., 1992). Surface modifications have been proposed to increase blood circulation half -life of PLGA formulations (Esmaeli *et al*., 2008).

2.4.3.5 Drug release from PLGA formulations

The release of drugs from PLGA formulations has been described as diphasic (Crotts and Park, 1998; Ramchandani and Robinson, 1998) and triphasic (O'Donnell and McGinity, 1997; Makino *et al.,* 2000). The diphasic release was described as an initial burst of drug release from the surface in contact with the medium followed by a second phase, which occurs as a result of water inside the polymer matrix, which hydrolyzes the polymer. The initial phase is related to drug type, drug concentration and polymer hydrophobicity and also is a function of solubility as well as penetration of water into the polymer matrix. In the initial phase, random scission of PLGA decreases the molecular weight of polymer significantly with no significant corresponding mass loss and no soluble monomer products formed. The second phase involves the continuous release of the drug through the thicker drug depleted layer.

Soluble oligomeric and monomeric products are formed when water inside the polymer hydrolyzes the polymer. A passage is thus created for the drug to be released by both diffusion and erosion until the polymer is completely solubilized. The nature of the drug encapsulated is a major factor that affects the entry of the aqueous phase into the polymer matrix (Crotts and Park, 1998; Ramchandani and Robinson, 1998).

The triphasic release was described as an initial burst release that was followed by a slow diffusion controlled release and the third phase was as a result of rapid degradation of the polymer matrix (O'Donnell and McGinity 1997; Makino *et al.,* 2000).

2.4.4 Microcapsules and/or microspheres

These are particles that fall in the micrometer size range but are however considered under the broad definition of nanoparticle. This is due to their clinical applications in drug delivery. These particles are basically spherical and may be solid or porous. They are often described as microspheres or microspheres having the same basic composition as nanoparticles. Microspheres like nanoparticles can be formulated from many natural and synthetic materials including polymers, proteins and lipids. Poly lactic acid (PLA) and Poly lactic co- glycolic acid (PLGA) are the polymers that are usually used in microsphere formulations. Drugs have been successfully incorporated into matrix systems, which control the rate of drug release from the matrix. Thus, the degradation rate of the matrix is directly linked to the rate of drug release (Aulton and Taylor, 2013).

2.4.5 Microspheres as a dosage form

Microspheres formulated from biodegradable polymers are easily administered with a syringe and needle. They have the ability to encapsulate many drugs, large and small molecules as well as bioactive compounds such as proteins and nucleic acids. Microspheres provide high bioavailability and are easily eliminated due to their biodegradable nature. Microspheres made from synthetic polymers are generally well

tolerated due to their biocompatibility (Kim and Pack, 2006). Formulation and use of microspheres for controlled drug delivery are not without challenges.

There has been reports of difficulty with large-scale manufacturing, poor control of drug release and inactivation of drugs during formulation. However, many of these challenges are mainly with the encapsulation of bioactive compounds such as hormones and alteration of formulation parameters have been used to avoid many of these challenges (Kim and Pack, 2006). Not withstanding the challenges, many controlled release dosage forms have been successfully formulated as microspheres and are commercially available. Examples include suspensions of microspheres for subcutaneous injection (Trenantone®) and microsphere intramuscular injection (Sandostatin LAR®) among others (Aulton and Taylor, 2013).

Formulation parameters for microspheres to be considered include, the:

- nature and solubility of the drug being encapsulated
- polymer concentration, composition and molecular weight
- drug / polymer ratio
- organic solvent used
- concentration and nature of emulsifier used
- temperature and agitation speed of the emulsification process
- viscosities and volume ratio of the dispersed and continuous phase

Moreover, microspheres are easily administered by injection and no surgical removal is necessary and the drug release rates can be controlled by manipulation of the microparticle size (Cohen *et al.*, 1991; Narayani and Rao, 1994).

2.4.6 Methods of encapsulation/ Microparticle formulation

Drug encapsulation using PLGA can be achieved by various methods and techniques. The methodology employed depends on the nature of the drug to be encapsulated. Thus hydrophilic drugs are successfully encapsulated using different techniques from those for hydrophobic drugs. The commonest methods that have been employed over the years involve emulsification and solvent evaporation or extraction (Wischke and Schwendeman, 2008). Single emulsion processes are used for lipid soluble drugs whereas double or multiple emulsion processes are employed for hydrophilic drugs.

One reason assigned to this is that poor encapsulation efficiencies are obtained when water-soluble drugs are encapsulated with the single-emulsion methods. Another reason assigned is that an initial burst release is associated with hydrophilic drug microspheres formulated with the single emulsion technique. This initial burst release of the drug is undesirable since the purpose of encapsulation is to produce a controlled release dosage form that releases the drug gradually over a specified period of time (Wischke and Schwendeman, 2008).

Artemether is a hydrophobic drug and thus the single emulsion method is best suited for its microencapsulation. Hydrophobic drugs are a heterogeneous group of molecules that exhibit poor solubility in water but are not always soluble in various organic solvents. Determination of the solubility of the drug to be encapsulated in various organic solvents for the microencapsulation process is essential. Generally, microencapsulation of hydrophobic drugs involves the use of volatile organic solvents. These solvents dissolve the polymer matrix and sometimes, the drug as well. These

solvents include, methylene chloride, ethyl acetate and butyl acetate. Co-solvents such as methanol, ethanol, acetone and tetrahydrofuran are also used in hydrophobic drug encapsulation (Wischke and Schwendeman, 2008).

Hydrophilic drugs are those that have an affinity for water and readily absorb and /or dissolve in water and aqueous media. The selection of a method for encapsulation of drugs depends on its hydrophobic or hydrophilic nature (Li *et al*., 2008). Multiple emulsions are mainly used for encapsulation of hydrophilic drugs and the w/o/w method has been successfully employed for this purpose (Crotts and Park, 1998; Okochi and Nakano, 2000; Sinha and Trehan, 2003). Many anticancer, anti-inflammatory and antibiotic drugs have been encapsulated using the multiple emulsion techniques. The microencapsulation of hydrophilic drugs also involves the use of volatile organic solvents such as dichloromethane and chloroform (Li *et al*., 2008).

2.4.6.1 Single Emulsion Encapsulation Techniques

2.4.6.1.1

Oil-in-water (o/w) emulsion

This is the formulation of an oil-in-water (o/w) emulsion. The polymer and drug are dissolved in an appropriate organic solvent. Volatile solvents for easy removal either by evaporation or extraction are used. The dispersion produced by a mixture of the drug, polymer and organic solvent is emulsified in a large volume of water in the presence of an emulsifying agent at an appropriate temperature while stirring. Polyvinyl alcohol (PVA) is the agent most often used. The organic solvent is then removed from the resultant oil-in-water emulsion either by extraction or evaporation to

harden the oil droplets. During evaporation, the emulsion is maintained at reduced or atmospheric pressure while controlling the stirring rate as the solvent evaporates. Extraction of the solvent involves transfer of the emulsion into a large volume of water that may contain a surfactant or into another medium to diffuse out the solvent associated with the oil droplets. The resultant solid microspheres are washed and dried by freeze-drying or other methods to give a final injectable microsphere formulation (Arshady, 1991; Sah, 1997; King and Patrick, 2000; Rosca *et al*., 2004).

2.4.6.1.2

Oil-in-oil (o/o) emulsion

This method is used for encapsulation of drugs such as hydrocortisone, which exhibit an appreciable solubility (~ 280 µg/ ml of water) in aqueous media although they are classified as hydrophobic drugs. The use of o/w emulsification process for encapsulation of such drugs leads to low encapsulation efficiency due to flux of the active ingredients from the dispersed phase to the larger volume of the aqueous continuous phase. Oil-in-oil emulsification involves the extraction of the oil phase solvent by a solution of the emulsifier in oil such as cottonseed or mineral oil which should be a non solvent for both the drug and the polymer (Jalil and Nixon, 1990 a,b,c; Wada *et al* 1990; Herrmann and Bodmeier, 1998)

2.4.6.2 Multiple Emulsion Encapsulation techniques

The encapsulation of water-soluble drugs by the conventional o/w solvent evaporation method will generally result in rapid partitioning of the drug from the organic phase and into the aqueous phase resulting in microspheres with little or no

drug loading. Multiple emulsion encapsulation methods have been used to produce formulations of hydrophilic drugs with good drug loading and encapsulation efficiencies. Water-oil-water (w/o/w), water-oil-oil (w/o/o) and water-oil-oil-oil (w/o/o/o) emulsions have been used to encapsulate a number of hydrophilic drugs (O'Donnell and McGinity, 1997). The multi-phase microspheres of the w/o/o/o type belong to the class of reservoir type drug delivery devices. Utilization of this type of multiple emulsion system allows the encapsulation of a primary water-in-oil emulsion within a polymeric microsphere. The oil in the primary emulsion prevents contact between the internalized protein and the polymer / solvent systems (O'donnell *et al.*, 1995).

2.4.6.3 Double Emulsion Encapsulation techniques

2.4.6.3.1

Water-in-oil –in water (w/o/w) emulsion

This method is suitable for encapsulation of water soluble or hydrophilic drugs such as peptides, proteins and vaccines. An appropriate amount of drug is dissolved in aqueous phase usually deionized water. This solution is added to an organic phase consisting of PLGA and / or PLA solution in dichloromethane (DCM) or chloroform with vigorous stirring to produce a water-in-oil emulsion. The water-in-oil (w/o) primary emulsion formed is poured into a PVA aqueous solution for further emulsification (w/o/w) for an appropriate time under appropriate conditions of agitation mixing. The organic solvent is then removed by evaporation or extraction as for oil-in-water emulsions. The encapsulation efficiency and particle size are affected by the choice of solvents and

rate of stirring (Arshady, 1991; Mao *et al*., 2007; Chaisri *et al*., 2009). The w/o/w method produces efficient loading of hydrophilic drugs and is the most commonly used method for encapsulating peptides and proteins (Kent *et al*, 1987; Yamamoto *et al*., 1994). This method has an advantage over the w/o technique in that, the cumbersome oil removal by repeated washing is avoided and no aggregates are formed during preparation (Yamamoto *et al*, 1994).

2.4.6.3.2

Solid-in-oil-in-water (s/o/w) emulsion

This technique is employed for active ingredients that cannot dissolve in the carrier solvent or solvent mixture. The s/o/w method is also used for formulations in which a greater portion of the drug is lost in the continuous phase when co-solvent systems are used. This technique has been used for encapsulation of many hydrophobic drugs including levonorgestrel, β–estradiol and camptheric in and its derivatives (Shenderova *et al*., 1997, 1999; Ertl *et al*., 1999; Birnbaum *et al* 2000; Mogi *et al* 2000; Wang *et al*., 2005).

2.5 PARENTERAL DRUG ADMINISTRATION

Many drug formulations are administered to patients by injection into the vascular system, muscle or soft tissue for systemic action or into specific organs for local action. Some drug formulations are also injected into joint spaces. Drug administration by injection is generally referred to as parenteral administration.

Medicines that are poorly absorbed orally and/ or are inactivated by the secretions of the gastrointestinal tract are administered parenterally. In emergency situations where

rapid effects of medications are required or where the oral route is precluded such as in unconscious patients, the parenteral route is utilized. In practice, medicines are injected by many different routes on the basis of the purpose of treatment as well as the volume of medication to be administered. There are many different types of parenteral injections that have been described below (Aulton and Taylor, 2013; Allen and Ansel, 2013).

2.5.1 Intravenous injections and infusions

Intraveneous (IV) injections and infusions are very widely administered to in-patients at healthcare facilities. They are administered into a vein that is easily accessible, prominent and near the skin's surface usually on the back of the hand or in the internal flexure of the elbow. The difference between IV injection and IV infusion is the volume administered. Smaller volumes (usually 1 ml) are administered as IV injections whereas lager volumes of up to several litres are given as IV infusions. IV injections produce a more rapid effect than IV infusions that are delivered at a slow and controlled rate with the aid of a pump (500 ml to 1 litre per infusion bag). The rapid onset of intraveneous injections is especially useful in emergency situations. Parenteral formulations made of water-in-oil emulsions or suspensions contain drug particles that can physically block blood capillaries and the oil phase of the emulsion could cause a fat embolism, which can block the blood vessels. This can lead to clinical fatalities. Thrombophlebitis, which is associated with pain and inflammation, may also occur with the IV route when hypertonic solutions are administered (Aulton and Taylor, 2013; Allen and Ansel, 2013).

2.5.2 Intra-arterial and intracardiac injections

Intra-arterial injections are given by administration of drugs into an artery. These types of injections are not often given due to the risk associated with their administration. The arteries are not as accessible as veins and this administration is considered more invasive but useful when intravenous access is not possible such as in premature infants. Premature infants have vein sizes that are relatively smaller compared to catheter tubes that need to be inserted to provide vascular access for drug administration. Intra-arterial injections are also utilized in the treatment of liver cancer and other cancers to ensure the medications reach the tumor before distribution around the body. The benefits of this type of injection however do not significantly outweigh the risks. On the other hand, intracardiac injections are used in life threatening emergency situations to administer drugs directly to the cardiac muscle or into a ventricle of the heart. A common application is the injection of an aqueous solution of adrenaline to produce a local effect in the heart during a heart attack or circulatory collapse (Aulton and Taylor, 2013; Allen and Ansel, 2013).

2.5.3 Intradermal injections

Intradermal injections involve the injection of small volumes of up to 0.2 ml into the skin between the epidermis and the dermis. Absorption of drug from the site of injection is slow and these types of injections are employed for administration of vaccines (BCG tuberculosis) and allergy tests (Aulton and Taylor, 2013; Allen and Ansel, 2013)

2.5.4 Subcutaneous or hypodermic injections

These injections are given into the loose connective and adipose tissues immediately beneath the dermal skin layer usually of the abdomen, upper and lower legs. Aqueous solutions or suspensions of drugs with volumes of up to 1 ml are administered via this route and are absorbed fairly rapidly and predictably. Insulin is administered by subcutaneous injection. Subcutaneous injections are widely utilized as a delivery route for compounds with limited oral bioavailability or as a means to modify or extend the release profile (Aulton and Taylor, 2013; McLennan *et al*., 2005).

2.5.5 Intraspinal injections and intrathecal injections

The site of injection differentiates intraspinal and intrathecal injections. Injections given between the vertebrae of the spine into the area of the spinal column are intraspinal injections. Intrathecal injections on the other hand are administered into the cerebrospinal fluid (CSF) in the subarachnoid space between the arachnoid mater and the pia mater, which are the two innermost protective membranes surrounding the spinal cord. It is worth noting that the intraspinal route administers only drugs in aqueous solution. The intrathecal injections are used for spinal anaesthesia and administration of drugs that cannot diffuse across the blood brain barrier when other routes are used.

Epidural injections are a form of spinal anaesthesia that is given into the peridural space between the dura mater and the vertebrae (Aulton and Taylor, 2013; Allen and Ansel, 2013).

2.5.6 Intra-articular injections

The administration of aqueous solutions or suspensions into the synovial fluid of joint cavities such as the knee is referred to as intra-articular injection. This type of injection produces a local effect and is commonly used in treatment of arthritis using anti-inflammatory drugs (Aulton and Taylor, 2013: Lavelle *et al.*, 2007)

2.5.7 Ophthalmic injections

As the name suggests, ophthalmic injections are administered into the eye or around the eye. However, injections into the eye are specifically called intraocular injections, which are further classified as intracameral or intravitreal. Intracameral injections are administered in front of the lens of the eye whereas intravitreal injections are administered behind the lens of the eye. A maximum volume of 0.1 ml of preparation can be administered via the intravitreal route because there is the risk of damage to the retina as a result of increased intraocular pressure from large volumes of medication. Intracameral injections however can be from 0.1 to 1 ml volume of injection (Aulton and Taylor, 2013; Kahook *et al*., 2009).

2.5.8 Intramuscular injections

Intramuscular injections are given into tissues of relaxed muscles of the thigh, buttock or shoulders. Volumes of up to 4 ml of aqueous or oily solutions or suspensions are administered by IM injections. The gluteal or buttock muscle of adults or the thigh muscle of children is the site used for larger volumes of IM injections. Compared to the subcutaneous route, drugs administered via the IM route are more slowly absorbed from the site of injection into systemic circulation. Thus, by manipulation of IM

injections a prolonged and delayed release of medications from the injection site is possible and allows doses to be required at monthly intervals. Intramuscular injections have also been used to deliver depot preparations. A limitation to the use of IM injections however is the risk of sciatic nerve injury if the injection is not administered skillfully. (Chan *et al*., 2006; Aulton and Taylor, 2013; Allen and Ansel, 2013).

The choice of the intramuscular route of administration of a controlled release drug formulation is an added advantage in terms of the control of the release of the drug from the formulation.

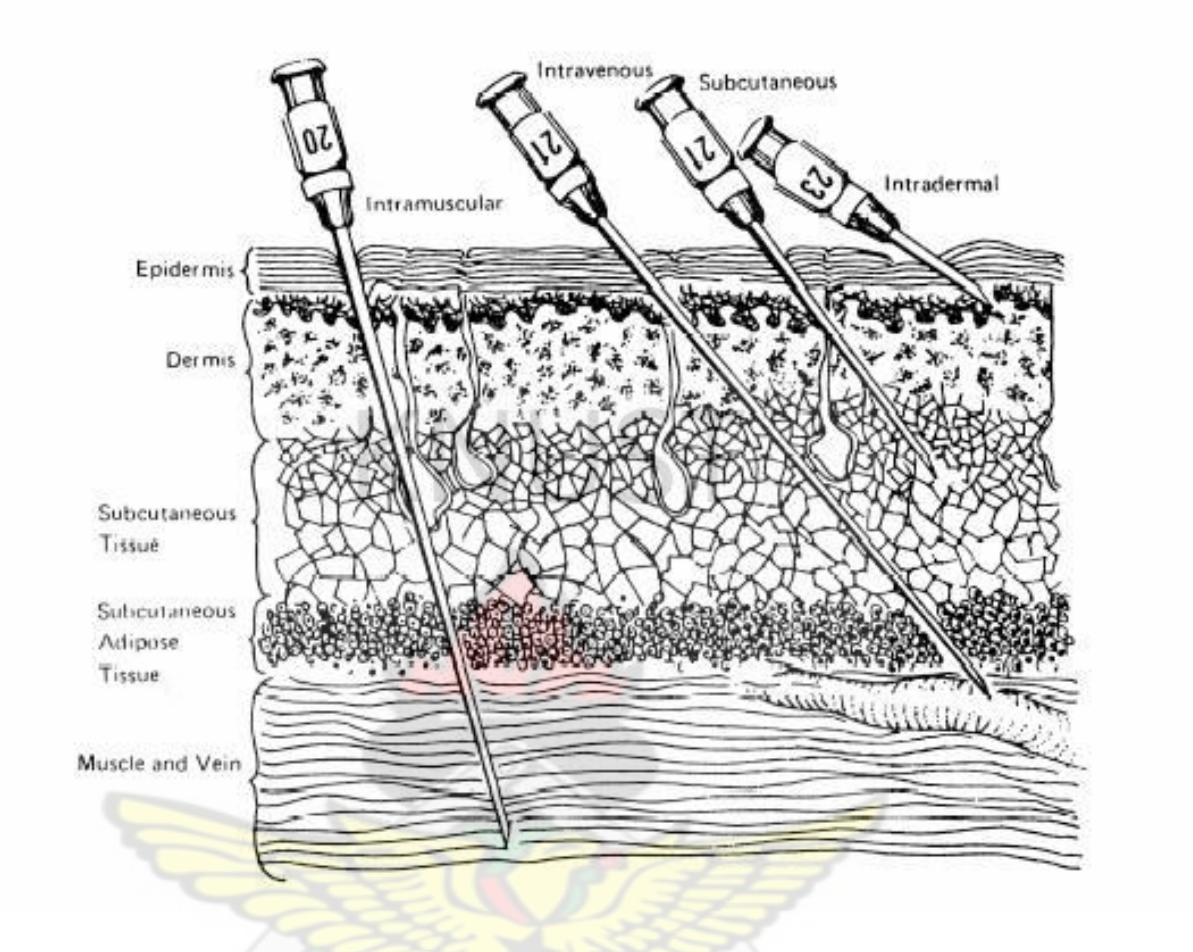

Figure 2.8 Intramuscular, intravenous, subcutaneous and intradermal routes of administration (Adapted from Google images ©, 2016)

Chapter 3

MATERIALS AND METHODS

3.1 MATERIALS

Distilled water, double distilled water and deionized water were freshly prepared and used. All other reagents used were of analytical grade.

Table 3.1 (a) Materials used for formulation, characterisation, *in vitro* and *in vivo* studies of microspheres

Materials	**Source**
Poly (lactic-co-glycolic acid) PLGA resomers RG502H (inherent viscosity = 0.21 dl/g) and RG503H (inherent viscosity = 0.37 dl/g)	Evonik Industries AG, Essen, Germany
Artemether	Tokyo Chemical Industry Co., Ltd., Tokyo, Japan
Dihydroartemisinin	Selleck chemicals, Houston TX, USA
Artemisinin	Alfa Aesar, Ward Hill, MA, USA
Polyvinyl alcohol (PVA) (88 mol.% hydrolysed, Mw~25 kDa	Polysciences, Inc., Warrington, PA, USA
Methylene chloride	Fisher Scientific, Fair Lawn, NJ, USA
Tetrahydrofuran (THF)	Fisher Scientific, Fair Lawn, NJ, USA
Nylon membrane filters	Merck Millipore limited, Tullagreen, Co. Cork, Ireland

Table 3.1(b) Materials used for formulation, characterisation, *in vitro* and *in vivo* studies of microspheres

Materials	**Source**
Mannitol	Sigma-Aldrich, St. Louis, MO, USA
Trifluoroacetic acid	Fisher Scientific, Fair Lawn, NJ, USA
Acetonitrile	Sigma-Aldrich, St. Louis, MO, USA
Sterile phosphate buffered saline	Fisher Scientific, Fair Lawn, NJ, USA
Isoflurane (Matrx VIP 3000®)	Paragon medical, Coral Springs, FL, USA
Oxygen	Paragon medical, Coral Springs, FL, USA
Carboxymethylcellulose-sodium salt (low viscosity)	Sigma-Aldrich, St. Louis, MO, USA
Tween 80	Sigma-Aldrich, St. Louis, MO, USA
Ethanol	Sigma-Aldrich, St. Louis, MO, USA

Table 3.2 (a) Equipment used for formulation, characterisation, *in vitro* and *in vivo* studies of microspheres

Equipment	**Source**
Tempest I.Q.^{2} homogenizer	The VirTis Co., Gardiner, NY, USA
Freeze-dryer	VirTis, SP Scientific, Warminster, PA, USA
Light microscope	Axiolab, Carl Zeiss Microscopy GmbH, Jena, Germany
Mechanical shaker	KS125 basic IKA Works, Inc.,Wilmington,NC,USA
Electronic balance (AG 285)	Mettler-Toledo, Columbus, OH,
pH meter and electrode	Corning, NY, USA, Thermo Fisher Scientific, Inc., Waltham, MA, USA
Scanning electron microscope	Philips XL30 FEG SEM (FEI, Hillsboro, OR, USA
Ultra performance liquid chromatography (UPLC) system and (Acquity UPLC BEH C18 1.7 µm, 2.1 x 100 mm column	Acquity UPLC ,Waters, Ireland
Mastersizer 2000® particle size analyzer	Malvern Instruments, Worcestershire, UK
Xbridge C-18 column, 50 mm × 2.1 mm ID, 3.5 µm	Waters, Milford, MA, USA

Table 3.2 (b) Equipment used for formulation, characterisation, *in vitro* and *in vivo* studies of microspheres

Equipment	**Source**
An ABI-4500 QTrap mass spectrometer with electrospray ionization probe	Applied Bio-systems (MDS SCIEX), Foster City, CA, USA
Shimadzu high performance liquid chromatography (HPLC) system	Shimadzu Corporation, Kyoto, Japan
Waters 1525 HPLC system with HR 1 and HR 5E columns	Waters, Milford, MA, USA
Eppendorf centrifuge 5810 R 15 amp version	Eppendorf , Hamburg, Germany
Sterile 21-gauge needle	Becton Dickinson (BD), Franklin Lakes, NJ, USA
Sterile 1 ml syringes	Becton Dickinson (BD), Franklin Lakes, NJ, USA
VWR analog vortex mixer	VWR, Radnor, PA, USA

3.2 CALCULATION OF DOSE OF INTRAMUSCULAR ARTEMETHER FOR A SIX MONTHS OLD INFANT WITH A BODY WEIGHT OF 5 KILOGRAMMES

The clearance (CL) of artemether for an adult = 19.1 ml/min/kg (Karbwang *et al*., 1998).

The weight of adult = 70 kg

Therefore clearance in a 70 kg adult = 19.1 X 70= 1337 ml/min

Calculation of clearance in the child,

$CL_{in\ child}$ = adult CL **x** (weight of child/ 70) $^{1.0}$ (Mahmood, 2010)

$CL_{in\ child}$ = 1337 X (5/70) $^{1.0}$

$CL_{in\ child}$ = 95.5 ml/min

$CL_{in\ child}$ = 95.5 /5 = 19.1 ml/min/kg same as adult CL

Dose $_{in\ child}$ = CL $_{in\ child}$ (dose $_{in\ adult}$/CL $_{in\ adult}$)

Loading dose in adults = 3.2 mg/kg

Dose $_{in\ child}$ = 3.2 X 5= 16 mg

Dose after 8 hours in adult = 1.6 mg/kg

Dose $_{in\ child}$ = 1.6X5= 8 mg

Subsequent doses in adult = 1.6 mg/kg daily for up to 5 days

Subsequent Dose $_{in\ child}$ = 5 x (1.6X5)=40 mg

Total amount of artemether required for the formulation =

(16+8+(8+8+8+8+8)= 64 mg

7 doses over a period of six days = 64 mg

3.2.1 Preparation of 100 ml of 5 % w/v Polyvinyl alcohol (PVA) solution

Five grammes of PVA was weighed in a beaker and the beaker was placed on a magnetic stirrer. The speed of stirring was set between 125 -350 rpm. One hundred millilitres of distilled water was slowly added and the temperature was set to 180 ^{o}C. A thermometer was mounted in the solution and the beaker was covered with aluminum foil. The heat was turned off when the temperature of the solution reached 75 ^{o}C. Stirring was continued for 15 to 30 minutes for all the PVA to dissolve. The PVA solution was transferred into a glass bottle when the temperature dropped below 30 ^{o}C. The solution was stored in a refrigerator and used within 3 weeks.

3.2.2 Preparation of 100ml of 0.5 % w/v Polyvinyl alcohol (PVA) Solution from 5 % w/v PVA solution

Ten millilitres of 5 % PVA was measured and poured into a volumetric flask and made up to 100 ml with distilled water. The solution was transferred into a glass bottle and stored in a refrigerator.

a b c

Plate 3.1 (a) A set up for preparation of 5 % PVA solution (b), (c) 5 % and 0.5 % Polyvinyl alcohol solutions

3.2.3 Preparation of 100 ml of 1% w/v Polyvinyl alcohol (PVA) solution

One gramme of PVA was weighed in a beaker and used to prepare 100 ml of 1 % PVA solution using the procedure described previously in Section 3.2.1.

3.2.4 Preparation of 200 ml of 0.3 % w/v Polyvinyl alcohol (PVA) solution from 1 % w/v PVA solution

Sixty millilitres of 1 % w/v PVA was measured and poured into a volumetric flask and made up to 200 ml with distilled water. The solution was transferred into a glass bottle and stored in a refrigerator.

3.3 PREPARATION OF 100 ML OF MANNITOL SOLUTION (100 MG/ML)

Ten grammes of powdered mannitol was weighed and transferred into a beaker. Twenty millilitres of distilled water was added and placed on a magnetic stirrer. More distilled water was added slowly to the 100 ml mark. Stirring was continued until all the mannitol dissolved in the water. It was transferred into a plastic bottle and labeled appropriately for use.

3.4 PREPARATION OF BLANK RG503H PLGA MICROSPHERES BY SINGLE EMULSION SOLVENT EVAPORATION METHOD

A mass of 600 mg of RG503H PLGA polymer was weighed in a glass tube and 1 ml of methylene chloride added. This mixture was dissolved using a mechanical shaker (KS125 basic IKA Works, Inc., Wilmington, NC, USA) at 600 rpm for 30 to 40 minutes. A volume of 4 ml of 5 % w/v PVA solution was added to the glass tube and the resulting solution was homogenized at 10,000 revolutions per minute (rpm) for 1 minute using a Tempest I.Q.^{2} homogenizer (The VirTis Co., Gardiner, NY, USA). The glass tube was held such that the tip of the homogenizer was completely submerged in the solution. The emulsion formed was poured into a beaker containing 100 ml of 0.5 % w/v PVA solution. The 0.5 % PVA solution was stirred at a speed, which made the vortex reach half the height of the solution in the 100 ml beaker. The rest of the emulsion was suspended by adding 0.5 % w/v PVA solution from the beaker and then poured back into the beaker. Stirring with the magnetic stirrer was continued for 3 hours at room temperature in the chemical hood to allow evaporation of the methylene chloride.

The microspheres were collected with sieves with aperture sizes of 90, 45 and 20 microns. These sieves were placed on top of each other in the order of decreasing aperture from top to bottom. The sieves were placed over a 400 ml beaker and the microspheres were washed with 1000 ml of double distilled water until the wastewater appeared clear. Microspheres collected on each sieve were transferred into pre-weighed 15 ml centrifuge tubes with double distilled water. The microspheres were centrifuged (Eppendorf centrifuge 5810 R 15 amp version) at 3000 relative centrifugal force (rcf) for 5 minutes at 25 ^{o}C. The supernatant was decanted and discarded and mannitol was added as a cryoprotectant (42 mg of mannitol per 1 ml of micro particles). The centrifuge tubes were soaked in liquid nitrogen for 30-60 seconds. The covers of the tubes were loosened to allow for solvent evaporation. The microspheres were freeze dried (VirTis, SP Scientific, Warminster, PA, USA) under vacuum for 24 hours and stored at -20 ^{o}C. The microspheres were collected and weighed.

3.4.1 Reformulation of Blank RG503H PLGA microspheres by single emulsion solvent evaporation method

The method described previously was employed with modifications. The modifications were; the reduction of concentration and volume of PVA, 4 ml of 5 % PVA to 2 ml of 1 % PVA, and 100 ml of 0.5 % PVA to 100 ml of 0.3 % PVA. The mixture was vortex mixed for 15 seconds instead of homogenization.

3.4.2 Characterisation of formulated microspheres by light microscopy

The microspheres were observed under a light microscope (Axiolab, Carl Zeiss Microscopy GmbH, Jena, Germany) and images of particles captured with the live view camera. Ten milligrammes of microspheres was suspended in 200 µl of distilled water in a 1.5 ml centrifuge tube. The tube was vortex mixed for 10 seconds to suspend the microspheres in the water. A drop of the suspension was placed on a microscope slide, covered with a cover slip and observed (objective lens x 5).

3.4.3 Formulation of artemether-loaded RG503H PLGA microspheres by single emulsion solvent evaporation method

Six hundred milligrammes of RG503H PLGA polymer and 300 mg of artemether were weighed in a glass tube and 1 ml of methylene chloride was added. A mechanical shaker (KS125 basic, IKA Works, Inc., Wilmington, NC, USA) at a speed of 600 rpm was used to dissolve this mixture for 30 to 40 minutes. A volume of 2 ml of 1 % w/v PVA solution was added to the glass tube and the resulting solution was vortex mixed at the highest speed for 15 seconds. The emulsion formed was poured immediately into a beaker containing 100 ml of 0.3 % w/v PVA solution. The 0.3 % PVA solution was stirred at a speed, which made the vortex reach half the height of the solution in the 100 ml beaker. The rest of the emulsion was suspended by adding 0.3 % w/v PVA solution from the beaker and then poured back into the beaker. Stirring on the magnetic stirrer was continued for 3 hours at room temperature in the chemical hood to allow for evaporation of methylene chloride. The microspheres were collected with sieves with aperture sizes of 90, 45 and 20 microns.

These sieves were placed on top of each other in order of decreasing aperture from top to bottom. The sieves were placed over a 400 ml beaker and the microspheres were washed with 1000 ml of double distilled water until the wastewater appeared clear. Microspheres collected on each sieve were transferred into 15 ml centrifuge tubes (previously weighed) with double distilled water. The microspheres were centrifuged (Eppendorf centrifuge 5810 R 15 amp version) at 3000 relative centrifugal force for 5 minutes at 25 ^{o}C. The supernatant was decanted and discarded and 100 mg/ml of mannitol was added as a cryoprotectant (42 mg of mannitol per ml of particles). The tubes were soaked in liquid nitrogen for 30-60 seconds. The covers of the tube were loosened to allow for solvent evaporation. The microspheres were freeze dried (VirTis, SP Scientific, Warminster, PA, USA) under vacuum for 24 hours and stored at -20 ^{o}C. The microspheres were collected and weighed.

a **b**

Plate 3.2 (a) Freeze drying of PLGA microspheres and (b) Microspheres after freeze-drying

3.4.4 Reformulation of artemether-loaded RG503H PLGA microspheres by single emulsion solvent evaporation method

The method previously described was used with some modifications. The modifications involved the use of homogenization instead of 15-second vortex. The homogenization speeds and times used respectively were; 5,000 rpm for 30 seconds, 5,000 rpm for 45 seconds, 5,000 rpm for 60 seconds, 10,000 rpm for 15 seconds and 10,000 rpm for 30 seconds. Five batches of microspheres were prepared.

3.4.5 Characterisation of formulated artemether-loaded RG5O3H PLGA microspheres by light microscopy

The method previously described in 3.4.2 was used to observe the characteristics of the formulated microspheres.

3.5 PREPARATION OF 1 LITER OF 10MM OF PHOSPHATE BUFFERED SALINE WITH TWEEN 80

Table 3.3 Composition of Phosphate Buffered Saline prepared

Components	Quantity in grammes
$Na_2HPO_4.7H_2O$	1.7961
$NaH_2PO_4.H_2O$	0.4554
NaCl	8.0
KCl	0.2236
NaN_3	0.2
Tween 80	0.2

All the components with the exception of Tween 80 were dissolved in 800 ml of distilled water. The pH of the solution was determined with a pH meter (Corning, NY, USA) and electrode (Thermo Fisher Scientific, Inc., Waltham, MA, USA) and the pH was adjusted to 7.4. using 0.1 M HCl and 0.1 M NaOH respectively. Distilled water was added to make up a one litre buffer solution in a volumetric flask. Tween 80 was added to the buffer in a beaker and dissolved by heating at 65 ^{o}C on a magnetic stirrer for 20 minutes. The solution was poured in a one litre volumetric flask after it cooled.

3.6 CALIBRATION CURVE FOR ARTEMETHER

A stock solution of 10 mg/ml of artemether was prepared and six concentrations namely: 1, 0.75, 0.5, 0.25, 0.1 and 0.05 mg/ml of artemether in acetonitrile and distilled water mixture (60:40) were respectively prepared. Trifluoroacetic acid (TFA) was used as ion- pairing agent at 0.1 % v/v. The calibration curve was obtained by running the 6 concentrations by Ultra performance liquid chromatography (UPLC) analysis (Acquity UPLC BEH C18 1.7 μm, 2.1 x 100 mm column from Waters, Ireland). The mobile phase used was acetonitrile with 0.1 % trifluoroacetic acid (TFA) as an ion-pairing agent, and distilled water in a ratio of 60:40.

The choice of 60 % acetonitrile solution as the solvent was based on the test of the solubility of artemether in phosphate buffered saline with 0.02 % tween 80 (PBST) and 60 % acetonitrile respectively. Standard solutions of artemether were prepared at concentrations of 1, 0.75, 0.5, 0.25, 0.1 and 0.05 mg/ml respectively in PBST and 60 % acetonitrile in water. UPLC analysis was used to obtain the calibration curves for comparison.

3.7 PREPARATION OF BLANK RG502H PLGA MICROSPHERES BY SINGLE EMULSION SOLVENT EVAPORATION METHOD

One gramme of RG502H PLGA polymer was weighed in a glass tube and 1 ml of methylene chloride added. A mechanical shaker (KS125 basic, IKA Works, Inc., Wilmington, NC, USA) at 600 rpm was used to dissolve this mixture for 30 to 40 minutes. Two millilitres of 1 % w/v PVA solution was added to the glass tube and the resulting solution homogenized at 5,000 rpm for 30 seconds using a Tempest I.Q.[2]

homogenizer (The VirTis Co., Gardiner, NY, USA). The glass tube was held such that the tip of the homogenizer was completely submerged in the solution. The emulsion formed was poured into a beaker containing 100 ml of 0.3 % w/v PVA solution. The 0.3 % PVA solution was stirred at a speed, which made the vortex reach half the height of the solution in the 100 ml beaker. The rest of the emulsion was suspended by adding 0.3 % w/v PVA solution from the beaker and then poured back into the beaker. Stirring on the magnetic stirrer was continued for 3 hours at room temperature in the chemical hood.

The microspheres were collected with sieves with aperture sizes of 90, 45 and 20 microns. These sieves were placed on top of each other in the order of decreasing aperture from top to bottom. The sieves were placed over a 400 ml beaker. The microspheres were washed with 1000 ml of double distilled water until the wastewater appeared clear. Microspheres collected on each sieve were transferred into 15 ml centrifuge tubes respectively with double distilled water. The microspheres were centrifuged (Eppendorf centrifuge 5810 R 15 amp version) at 3000 rcf for 5 minutes at 25 ^{o}C. The supernatant was decanted and discarded and mannitol was added as a cryoprotectant (42 mg of mannitol per ml of particles). The tubes were soaked in liquid nitrogen for 30-60 seconds. The covers of the tube were loosened to allow for solvent evaporation. The microspheres were freeze dried (VirTis, SP Scientific, Warminster, PA, USA) under vacuum for 24 hours and stored at -20 ^{o}C. The microspheres were collected and weighed.

3.7.1 Characterisation of blank RG502H PLGA microspheres by light microscopy

The method previously described in Section 3.4.2 was used to observe the characteristics of the formulated microspheres.

3.8 REFORMULATION OF ARTEMETHER - LOADED RG502H PLGA MICROSPHERES WITH SINGLE EMULSION SOLVENT EVAPORATION METHOD

The method previously described for RG503H in Section 3.4.3 was used with modifications. The modifications were the use of 1 g of RG502H PLGA polymer instead of 600 mg of RG503H polymer. The homogenization speeds and times used were; 5000 rpm for 30 seconds, 10,000 rpm for 45 seconds and 5000 rpm for 45 seconds.

3.9 CHARACTERISATION OF FORMULATED ARTEMETHER-LOADED RG503H AND RG502H POLYMER MICROSPHERES

3.9.1 Particle size analysis using the Mastersizer 2000®

A Mastersizer 2000® (Malvern Instruments, Worcestershire, UK) was switched on and warmed up for 15 minutes. The computer with the software was also switched on. The measurement zone was cleaned with distilled and deionized (DI) water. This was done three times and the distilled and deionized water was drained and refilled by clicking empty and fill on the computer. Detector 1 with background value of less than 100 was used. The stirring speed was set at 2975 rpm. The background, which was the DI water, was measured first. The particles were dispersed in DI water and added into the measurement zone with the aid of a pipette until an optimal obscuration was attained

(2.52 % for RG503H formulation, 1.76 % for RG502H formulation). Multiple measurements were made and recorded, (12 for RG503H microspheres and 21 for RG502H microspheres). The measurement zone was emptied and cleaned three times with DI water. The software generated histograms of the particle size distribution of the microspheres measured.

3.9.2 Morphological analysis using Scanning Electron Microscopy

3.9.2.1 Preparation of samples for SEM

A scanning electron microscope (Philips XL30 FEG SEM (FEI, Hillsboro, OR, USA) was used to study the surface morphology, size and shape of the microspheres. An SEM stub was used. Double-sided carbon tape was cut into various shapes depending on the number of different samples to be analyzed. The different shapes were pasted on the SEM stub by removing the covering on one side of the tape with the aid of tweezers. The covering on the other side of the tape was removed and the microspheres were spread thinly and evenly on the tape. Each sample was spread on a different shape of tape and subsequently sputter coated with gold prior to SEM analysis.

3.9.2.2 Sputter coating-SPI sputter coater with Etch mode

Gold was used to sputter coat the microspheres. 19.4 g/cc was dialled in and the zero adjustment was used to set the display to 0.00. The timer was set to 60 seconds. It was ensured that the leak valve was fully closed. The SPI-Module control and the SPI-Module sputter coater switches were both turned on. The rotary pump started

immediately and the vacuum was indicated on the meter. The gas leak valve was partially opened to flush the work chamber with argon for about 10-15 seconds. The leak valve was closed and the work chamber was allowed to pump down to approximately 10^1 millibar. The gas leak valve was opened until the pressure just began to rise and the test button was depressed whiles adjusting the gas leak valve, the plasma current was set to 18 mA. A visible discharge was observed in the chamber as a purple colour. The start button was depressed and gold was sputtered onto the microspheres for 60 seconds. The plasma automatically extinguished at the end of 60 seconds. The mode switch was turned off to extinguish the sputtering. Both power switches were turned off and the leak valve was opened to allow air into the glasswork chamber. The glass chamber and the quartz crystal thickness monitor were both cleaned with isopropanol.

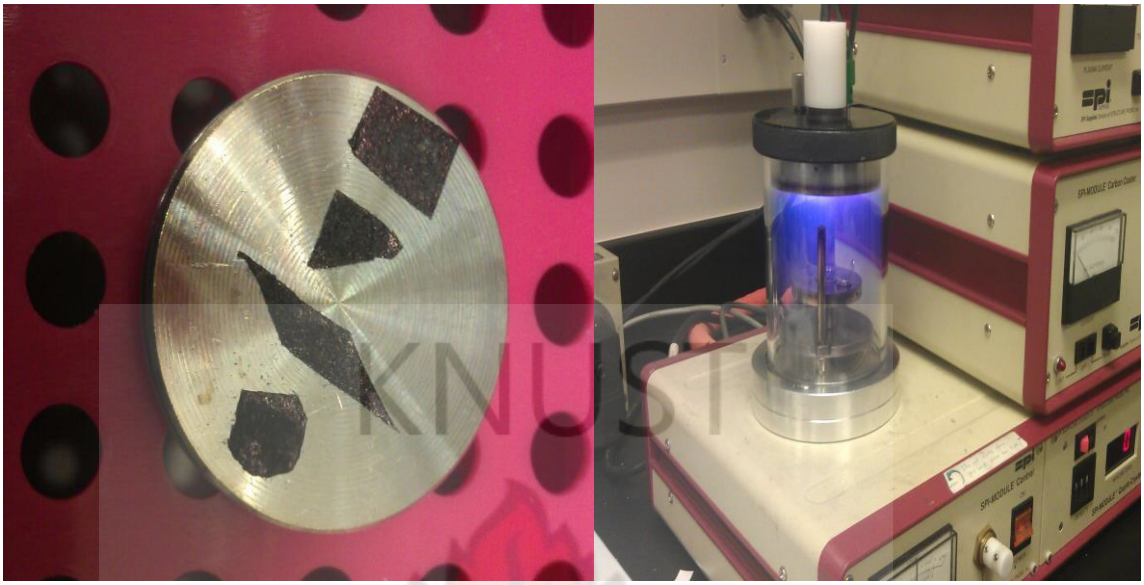

a **b**

Plate 3.3 (a) Microspheres on carbon tape that have been sputter coated (b) A visible discharge observed in the chamber as a purple colour during sputter coating

3.9.2.3 Scanning electron microscopy (SEM)

The sample on the SEM stub was placed in the chamber. The stub was tightened and the height adjusted. The door to the chamber was closed and the pump was switched on. This was switched off when the vacuum button turned yellow. The detector selected was the secondary electron detector (SE), the beam was turned on and a voltage of 3kV was selected. The image was focused before selecting 'OK.' The brightness and contrast were also adjusted. Images of the samples were captured and saved after which the sample was removed from the chamber. The chamber was closed and the pump turned on, the beam was turned off and the chamber was vented for 30 seconds before switching off the microscope.

a

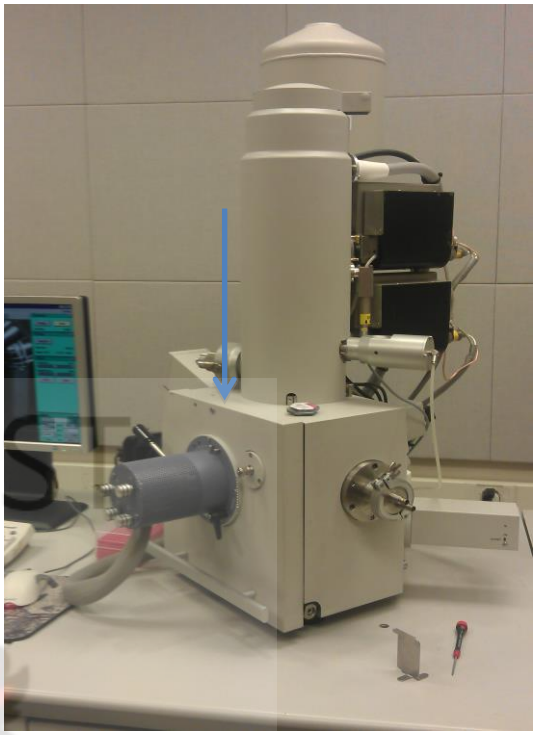

b

Plate 3.4 (a) Chamber where the stub with samples was placed for SEM analysis (open)
Plate 3.4 (b) SEM with arrow pointing to the analysis chamber (closed)

3.9.3 Drug loading and loading efficiency

The loading of artemether in both the artemether-loaded RG503H and RG502H PLGA microspheres was determined. A mass of microspheres equivalent to 10 mg of microspheres was dissolved with a combination of tetrahydrofuran (0.5 ml) (THF) and ethanol (9.5 ml). The mixture was vortex mixed and centrifuged (Eppendorf centrifuge 5810 R 15 amp version). The supernatant was analyzed using Ultra Performance Liquid Chromatography with an ultraviolet detector (UPLC-UV) (Acquity UPLC Waters, Ireland). The absorbance of the artemether was measured at a wavelength of 220 nm. The percentage of the amount of artemether loaded was calculated from the

peak area of artemether which appeared at ~ 3 minutes of retention time using a Waters® Empower™ chromatography software (Acquity UPLC Waters, Ireland). The percentage loading efficiency was obtained by finding the ratio of the actual mass of artemether loaded to the initial mass of artemether used.

3.9.4 *In vitro* release of artemether from microspheres

The equivalent of 10 mg of microspheres or free drug was suspended in 50 ml of phosphate buffered saline with 0.02 % Tween 80 (PBST) at a pH of 7.4 and kept in an incubator at 37 ^{o}C with agitation at 240 rpm. The microspheres were washed three times with double distilled water (ddH_2O) to remove the buffer salts. Ultra performance liquid chromatography with an ultraviolet detector (UPLC-UV) was used to determine the concentration of artemether released at each time point (Days 0, 1, 3, 7, 14 and 21) at a wavelength of 220 nm. The percentage of artemether released was calculated relative to initial artemether loaded. The residual method of quantification was used. The amount of artemether remaining in the microspheres was quantified and the release was calculated relative to these values. All the analyses were carried out in triplicate.

3.9.5 Kinetics and mechanism of drug release from formulated microspheres

In order to develop mathematical modelling of the release kinetics of artemether from PLGA microspheres, zero order, first order, Higuchi, Hixson-Crowell and Korsemeyer-Peppas models were employed as follows; cumulative amount of drug

released versus time was plotted for the zero order model; the cumulative percentage drug released versus the square root of time for the Higuchi model; a plot of the cube root of drug percentage remaining in microspheres versus time for the Hixson-Crowell model; the log of percentage drug released versus log of time for the Korsemeyer-Peppas model; and the log of cumulative of percentage drug remaining versus time for the first order model (Hixson and Crowell, 1931; Higuchi, 1963; Gibaldi and Feldman, 1967; Wagner, 1969; Korsemeyer *et al.*, 1983; Varelas *et al.*, 1995). The equations employed were the following

For zero order kinetics;

$Q = Q_o + K_o t$ Eqn (1)

where, Q is the amount of drug released

Q_o is the initial amount of the drug in solution (usually zero)

Thus,

$Qt = Kot$ Eqn (2)

where, Qt = amount of drug released in time t

Ko = zero order release constant

t = release time (Hadjiioannou *et al.*, 1993)

First order kinetics;

$\text{Log } C = \log Co - kt / 2.303$ Eqn (3)

Where, C = the amount of drug released

Co = the initial concentration of the drug

k = first order release constant (Dash *et al.*, 2010)

Higuchi model;

$Q = K_H t^{1/2}$ Eqn (4)

Where Q = the amount of drug released at time t

K_H = release rate constant for Higuchi model (Higuchi, 1963)

Hixson – Crowell model;

$Qo^{1/3} - Qt^{1/3} = K_{HC}\, t$ Eqn (5)

Where, Qo = the initial amount of the drug in microspheres

Qt = the amount of drug released at time t

K_{HC} = release rate constant for Hixson – Crowell model (Singhvi and Singh, 2011)

Korsemeyer – Peppas model;

$mt / mT = kt^n$ Eqn (6)

where, mt / mT = fraction of drug release

k = kinetic constant which incorporates the structural and the geometric characteristics of the polymer system

t = release time of drug

n = the diffusional exponent which characterizes the release mechanism of the drug (Korsemeyer *et al.*, 1983)

3.10 POLYMER DEGRADATION ANALYSIS

3.10.1 Mass loss and water uptake study

The mass loss and water uptake amounts of particles were determined at time points of Days 0, 1, 7 and 14. Phosphate buffered saline with 0.02 % Tween 80 (PBST) was used. Ten milligrammes of artemether-loaded PLGA microspheres was weighed and transferred into a 50 ml centrifuge tube. A volume of 50 ml of PBST was added to the microspheres in the 50 ml tube. Dry and wet masses of 0.20 µm filter papers were

weighed and recorded. The filter paper was made wet with the aid of a filtration assembly. The filter paper was placed on the filter. The vacuum was turned on and clean double distilled and deionized water was used to wet the filter paper. A spatula was used to raise the edge of the filter paper to half of its diameter in order for water trapped underneath to be removed. The filter paper was replaced and the stop clock was set for 60 seconds, after which the vacuum was switched off and the filter paper was removed and weighed immediately, and the mass was recorded. Empty 2 ml centrifuge tubes were weighed and the masses recorded. The pre-weighed filter paper was placed on the filter of the filtration assembly. The vacuum was switched on.

The suspended particles were poured on the filter paper through the glass tube; the particles were washed with 50 ml of distilled and deionized water. The glass tube was removed after all the liquid had drained leaving the microspheres on the filter paper. Any particles stuck on the glass tube were rinsed onto the filter paper. The filter paper with the particles on it was carefully lifted halfway to remove trapped water and carefully placed back on the filter. The filter paper with the microspheres was carefully transferred after 60 seconds into a pre-weighed 2 ml centrifuge tube and weighed. The mass of the tube with the filter paper and microspheres was recorded. This process was repeated in order to have the results in duplicate.

The tubes were placed on a rack and the lids were opened. The rack was placed in a drying oven and the chamber was vacuumed to a pressure of 23 mmHg and the samples were left in the drying oven at room temperature for 24 hours. The tubes, which contained the filter paper and samples, were weighed after 24 hours to obtain

the dry weight. They were kept in the drying oven until a constant dry weight was obtained. A change in mass required further drying until no change in mass was recorded. The Day zero PBST was cooled to 4 ^{o}C. For the subsequent days, PBST at room temperature, 25 ^{o}C was used. Amber coloured 50 ml tubes were labeled for days 1, 7 and 14 mass loss studies respectively. Each day was assigned two tubes. Individual masses of 10 mg were weighed in each tube and 50 ml of PBST added and stored in an incubator on the shaker (160 rpm). At each time point, the samples were taken through the method described above.

The mass loss (%) was obtained by calculation as follows:

Mass loss (%) = $(M_1 - M_2 / M_1) \times 100$

where M_1 is the initial weight of microspheres and M_2 is the final weight of microspheres.

The water uptake amount was obtained by calculation as follows;

Water uptake (%) = $(W_1 - W_2 / W_1) \times 100$

where W_1 is the weight of wet microspheres and W_2 is the weight of dry microspheres.

The individual parameters that yielded the above are as follows

Dry particle amount G =H - (E + B)

Water uptake amount = F- (E +C + G)

Weight of water absorbed by filter paper D= C – B

A = initial weight of particles

B = weight of dry filter paper

C = weight of wet filter paper

D = weight of water absorbed by filter paper

E = weight of empty 2 ml centrifuge tube

F = weight of tube and particles and filter paper (WET)

G = dry particle weight

H = final total dry weight (weight of particles, filter paper and tube)

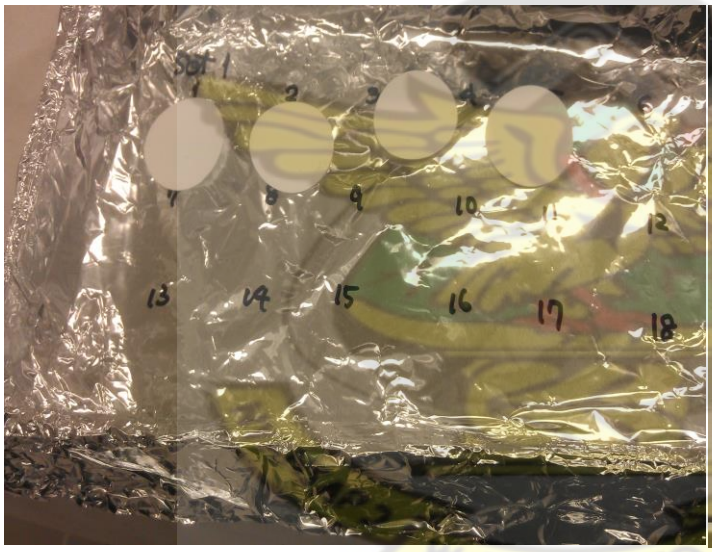

a

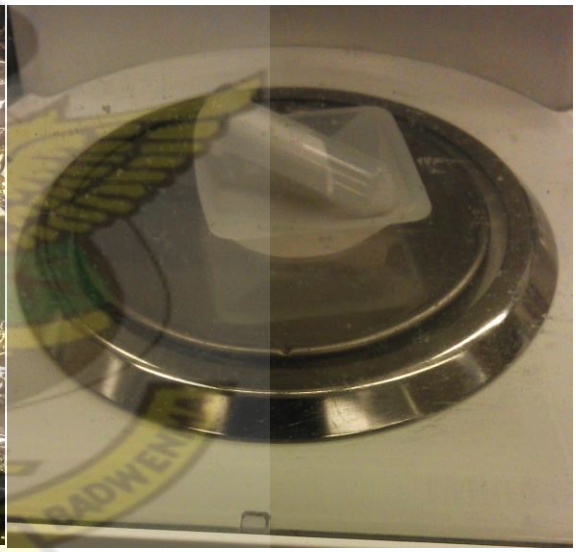

b

Plate 3.5 (a) 0.20 µm filter papers and Plate 3.5 (b) Filter paper with microspheres weighed together with 2 ml centrifuge tube.

a

b

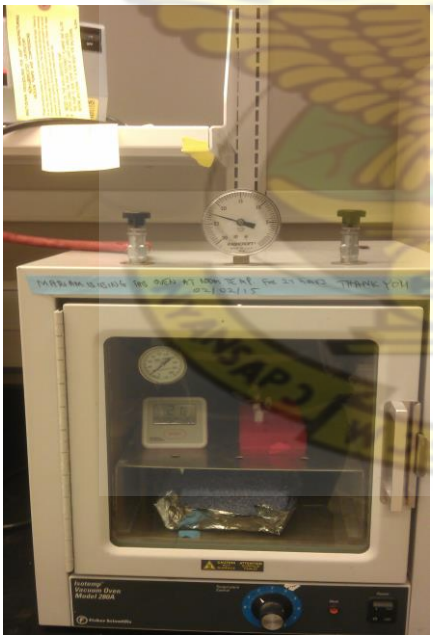

c

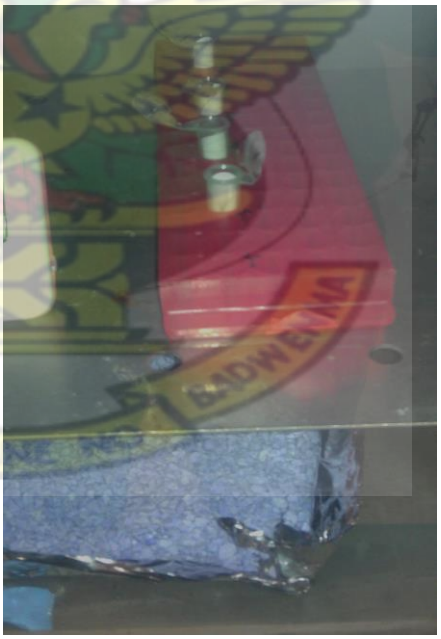

d

Plates 3.6 (a) and (b) Set up of filtration assembly with vacuum pump, Plates 3.6 (c) and (d) Microspheres dried in drying oven

3.10.2 Determination of molecular weight profiles of microspheres

The molecular weights of the microspheres were determined by gel permeation chromatography (GPC) using two styragel columns (HR 1 and HR 5E columns) (Waters, Milford, MA, USA), with Waters 1525 HPLC system with a refractive index detector. The GPC analysis was performed by dissolving the microspheres in tetrahydrofuran and injecting the supernatant onto the columns. The weight – averaged molecular weight (Mw) was obtained with the use of Breeze GPC software (Waters, Milford, MA, USA). The Mw was calculated using monodisperse polystyrene as a standard *(*regression data: $y = -1.2404x + 7.629$, $R^2 = 0.97736$*).*

3.11 *IN VIVO* STUDY / PHARMACOKINETIC STUDY

A preliminary *in vivo* study was conducted using RG503H microsphere formulations only. This study was conducted to obtain a suitable means of quantifying artemether in the plasma samples.

3.11.1 Pilot *in vivo* study

A preliminary pilot study was conducted with three male Sprague-Dawley rats 7-9 weeks old and weighed 250-300 grammes. The three rats were given a subcutaneous injection of pure artemether at 25 mg/ kg (6.25 mg of artemether in 1 ml of injection vehicle), 12.5 mg/kg of artemether-loaded microspheres (low dose) and 25 mg/kg of artemether-loaded microspheres (high dose), respectively. This study was carried out to determine the viability of the method used (HPLC-MS/MS).

3.11.2 Main *in vivo* Study

Twenty male Sprague-Dawley rats, 7-9 weeks old and weighing 250-300 grammes were used for the main animal study. The rats were in five groups (n=4).

Table 3.4 Protocol used for animal study

Animals	**5 groups (n=4)**	**Time points**
Male Sprague-Dawley Rats	a) Negative control Group b) Low dose artemether-microsphere single injection c) High dose artemether-microsphere single injection d) Artemether multiple injections (conventional dosing) e) High dose artemether single injection	1 hour Day 1 Day 3 Day 5 Day 7 Day 14 Day 21

The male Sprague-Dawley rats used in the study were purchased from Charles River Breeding Laboratories (USA) and housed at the animal housing facilities at the North Campus Research Complex at the University of Michigan. Each vivarium room and caging system met all the Association for Assessment and Accreditation of Laboratory Animal Care (AAALAC) and National Institute of Health (NIH) Guidelines and requirements. The vivarium used met all the requirements for ventilation, temperature control, air exchanges, food, water and animal husbandry practices. Specific Pathogen Free environment was maintained and monitored by the Unit for Laboratory Animal Medicine (ULAM). ULAM also provided daily health checks of all animals by trained Animal Care Technicians. Veterinary care was available to all animals at any time. A

laminar flow hood, water bottles, disinfectant sprays and solutions, as well as personal protection equipment (hair bonnets, shoe cover, gowns, latex gloves and masks) were all available for use in the vivarium. The animals were housed in groups of three in the stainless steel cages. All animal testing protocols were approved by, the University Committee for the Use and Care of Animals (UCUCA).

3.11.2.1 Preparation of injection vehicle

Sterile phosphate buffered saline was purchased from the Biomedical Research Stores at the North Campus Research Complex, University of Michigan, Ann Arbor, USA. A concentration of 5 % w/v low viscosity carboxymethylcellulose and 0.1 % tween 80 was the injection vehicle used.

3.11.2.2 Preparation of rats for study

The tails of the rats were labeled respectively for ease of identification. The rats were anaesthetized with a combination of 3 % isoflurane and oxygen in an anesthesia induction chamber at a flow rate of 1 litre per minute. Anaesthesia was maintained during rat dosing and blood sample collection through a nose cone. The rats were kept on a heating pad for the duration of the procedure to prevent a drop in their body temperatures.

3.11.2.3 Collection of baseline blood samples and injection of microspheres

Baseline blood samples were drawn from the jugular vein of each rat with a sterile 23-gauge needle and 1 ml syringe. The blood was kept in BD vacutainer K2 (K2E) with 3.6 mg of EDTA blood collection tubes. The tubes were kept in an icebox on ice. The

rats in the various groups received one milliliter each of subcutaneous injections of different preparations shown in Tables 3.4. and 3.5 respectively.

Table 3.5 Protocol for the *in vivo* study

Rat Group	Treatment	Dosing per rat
1	Negative control (single injection)	1 ml injection vehicle only
2	Low dose artemether-microsphere single injection (1 ml)	12.5 mg artemether-loaded microspheres
3	High dose artemether-microsphere single injection (1 ml)	25 mg artemether-loaded microspheres
4	Conventional artemether multiple injections	0.8 mg artemether as first dose, 0.4 mg after 8 hours and 0.4 mg daily for 5 days
5	Artemether single injection	3.2 mg artemether

3.11.2.4 Blood sample collection

Blood samples (1 ml) from the jugular vein were collected from each rat after administration of the injections. These samples were collected at one hour, 24 hours, 3 days, 7 days, 14 days and 21 days after administration of the injections.

Plate 3.7 (a) Isoflurane tank used for anaesthesia in rats, (b) Anaesthesia chamber (c) Heating pad used for maintenance of rat body temperature and (d) Labeled rat tail for identification of rats (e) Administration of microspheres and drug samples (f) Blood sample collection from the jugular vein of a rat.

3.11.2.5 Separation of plasma

The blood samples were centrifuged (Eppendorf centrifuge 5810 R 15 amp version) at 1500 rpm at 4 ºC for 10 minutes. The plasma layer was drawn off by pipetting and kept at -80 ºC for analysis.

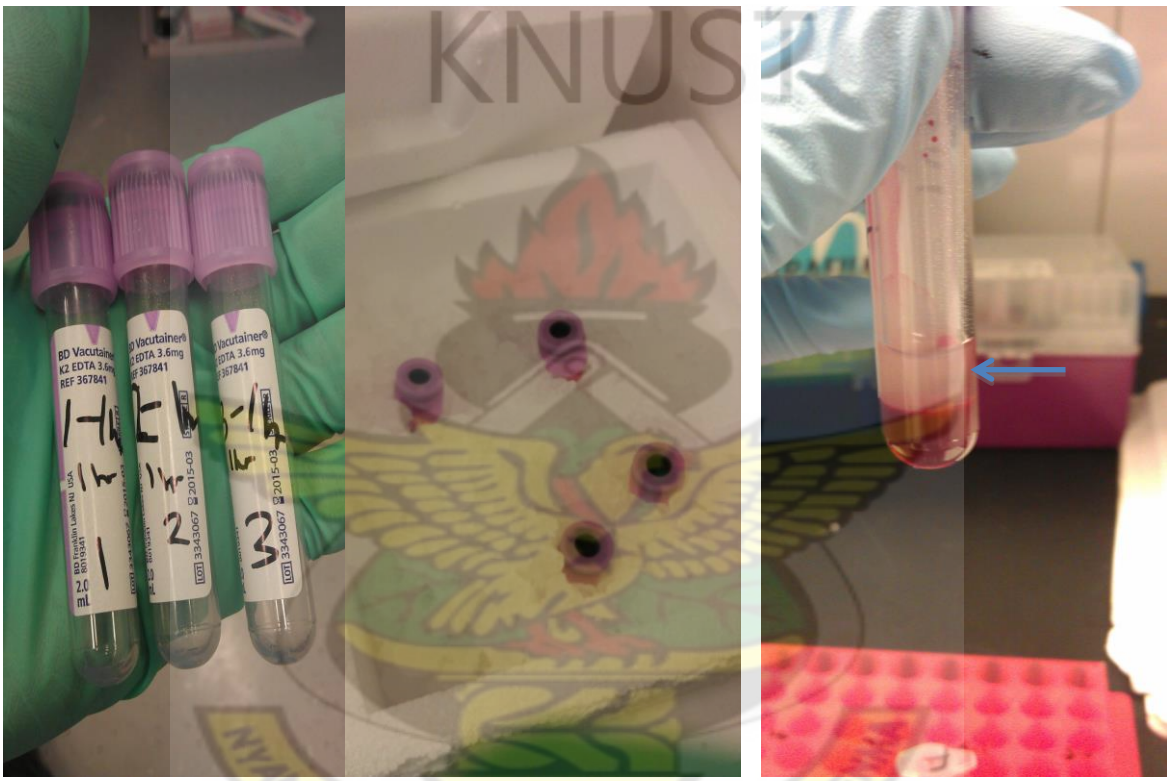

a **b** **c**

Plate 3.8 (a) BD vacutainer K2 (K2E) with 3.6 mg of EDTA blood collection tubes used for storage of blood samples drawn (b) Blood samples stored in ice (c) Separated plasma after centrifugation shown with arrow

3.12 ANALYSIS OF PLASMA CONTENT OF ARTEMETHER

3.12.1 Preparation of plasma samples for liquid chromatography - mass spectrometry analysis

3.12.1.1 Calibration curve

A volume of 200 µl of rat plasma was used. The plasma was spiked with 10 µl of the internal standard, artemisinin, and 30 µl of artemether and 30 µl of the metabolite dihydroartemisinin, respectively. This mixture was mixed with the aid of a vortex mixer. A volume of 200 µl of methanol was added to the mixture and centrifuged at 2250 rpm for 10 minutes at 4 ºC. The supernatant of the resulting mixture was collected and dried with nitrogen gas. The dried sample was reconstituted with 100 µl of 60 % acetonitrile solution in distilled water and the solution filtered with a 4 mm syringe driven filter unit. The concentrations of artemether used for the calibration curve were 10, 150, 250, 500, 750,850 and 1000 ng/ml respectively.

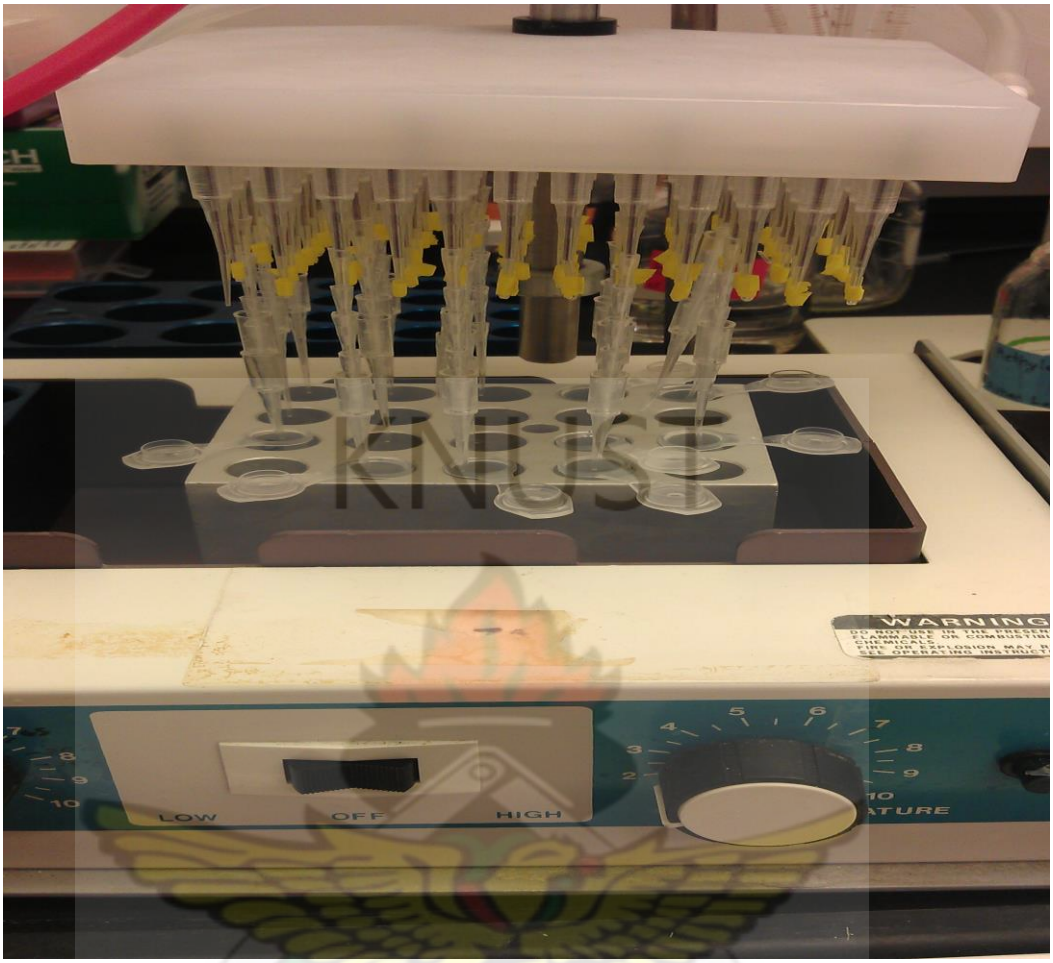

Plate 3.9 Drying of plasma samples with nitrogen gas in the chemical hood

3.12.2 Quantification of artemether with liquid chromatography - mass spectrometry analysis (LC-MS/MS) method

LC-MS/MS involves the combination of liquid chromatography and mass spectrometry whereby two mass analyzers are combined in one mass spectrometer. Plasma samples were analyzed at University of Michigan Pharmacokinetics-Core (UM PK-core) Facility. An ABI-4500 QTrap mass spectrometer with electrospray ionization probe (Applied Bio-systems (MDS SCIEX), Foster City, CA, USA) was interfaced with a Shimadzu high performance liquid chromatography (HPLC) system

(Shimadzu Corporation, Kyoto, Japan). The Analyst Software Version 1.6.2 package supplied by Applied Bio-systems (MDS SCIEX) was used to control the LC–MS/MS system, as well as for data acquisition and processing. Artemether and artemisinin (internal standard) were separated on an Xbridge C-18 column, 50 mm × 2.1 mm ID, 3.5 μm (Waters, Milford, MA, USA) at a flow rate of 0.4 ml/min. The mobile phase A was 100 % water and B was 100 % acetonitrile. Both mobile phases consisted of 5 mM ammonium formate.

The gradient separation was started with 10 % B for 0.5 minutes, then raised to 80 % B at 1.5 minutes; at 1.6 minutes, the percentage of B was switched to 95 % and kept for 2.5 minutes, then back to 10 % for another 2.5 minutes. The mass spectrometer was operated in the positive mode with multiple reaction monitoring (MRM) for the analysis. The gas temperature was 100 ℃ with an ion spray voltage of 5500 V, declustering potential (DP) of 8, curtain gas of 30 and collision energy of 11. The mass transitions were monitored at *m*/*z* 316.2→267.2 for artemether and *m*/*z* 300.1→209.1 for the internal standard. The plasma concentrations of the artemether were calculated by comparing the peak-area ratio of the peaks of interest with those of a calibration curve run with different concentrations of artemether and artemisinin (IS).

3.13 STATISTICAL ANALYSIS

Data was analyzed with Excel from Microsoft Office for Mac (2011) and Graph pad prism version 6.0 for windows. Two-way ANOVA followed by Sidak's multiple comparison test was used to analyze the mass loss, water uptake and molecular weight profiles and the cumulative percentage drug release from the two formulations. PK

Solutions 2.0 ™ Noncompartmental Pharmacokinetics Data Analysis for windows version 2.0.6 (Excel 2002 Edition) software was used to analyze the pharmacokinetics data.

Chapter 4

RESULTS

4.1 DOSE OF ARTEMETHER TO BE INCORPORATED

From the calculations previously shown in Section 3.2, the total mass of artemether to be incorporated into the microsphere formulations for controlled release was 64 mg.

Total amount of artemether required for the formulation =

(16+8+(8+8+8+8+8)= 64 mg

7 doses over a period of six days = 64 mg

4.2 FORMULATION OF MICROSPHERES

The use of 5 % and 0.5 % PVA as homogenizers yielded microspheres that were not spherical in shape when observed with the light microscope. There were particles engulfed by other particles and the particles were aggregated together. This observation is shown in Figure 4.1. Artemether was however successfully encapsulated in RG503H and RG502H polymers using 0.3 % PVA to form microspheres that were not clumped together and were spherical in shape as shown in Figures 4.2 and 4.3. From Table 4.1(a) and (b), Table 4.2 (a) and (b) and Figures 4.6, 4.7, 4.8 and 4.9 the highest total yields of microspheres did not correspond to the highest yield of the required size range of 45-90 μm.

For RG503H polymer formulations, Table 4.1(a) and (b) and Figure 4.6 show that for homogenization speed of 5000 rpm, there was an increase in total yield with increase in time of homogenization. This observation did not occur at a homogenization speed

of 10,000 rpm for RG503H polymer formulations. It was observed that for RG503H polymer formulations, similar duration of homogenization (30 s) with differing speeds produced a higher yield at the lower homogenization speed of 5000 rpm. The reverse was true for RG502H polymer microspheres as seen in Table 4.2 (a), (b) and Figure 4.7.

The yields and particle size fractions obtained using different formulation processes are shown in Figures 4.6 to 4.7. For the two PLGA resomers, formulation B (5 000 rpm for 45 s) and formulation D (10 000 rpm for 45 s) produced the highest yield of 45-90 µm particles for RG503H and RG502H microspheres, respectively.

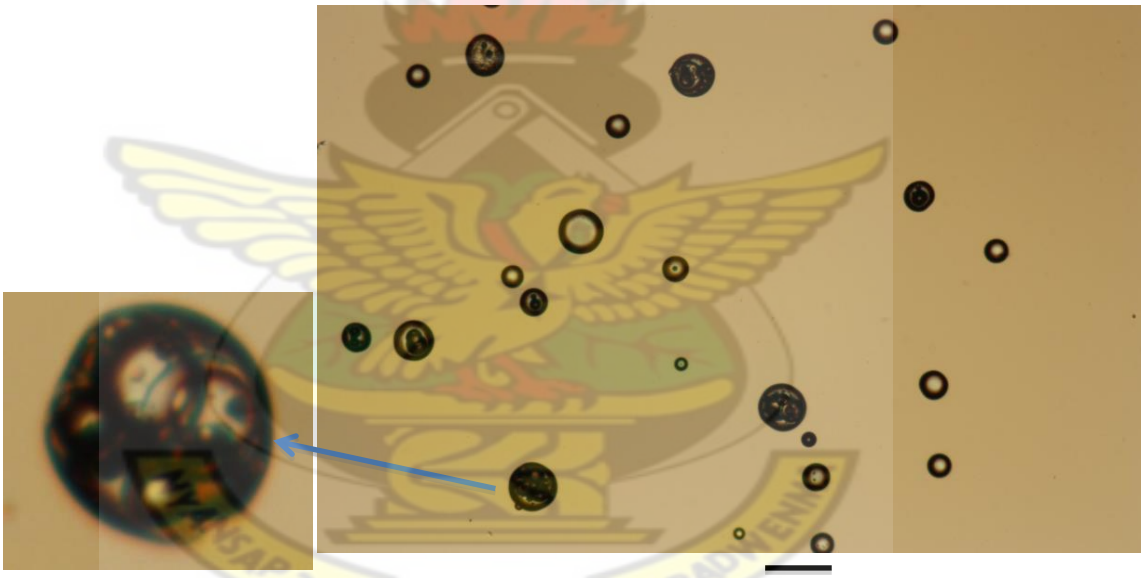

scale bar = 100 µm

Figure 4.1 Light microscope image of formulated microspheres showing clumps and aggregates

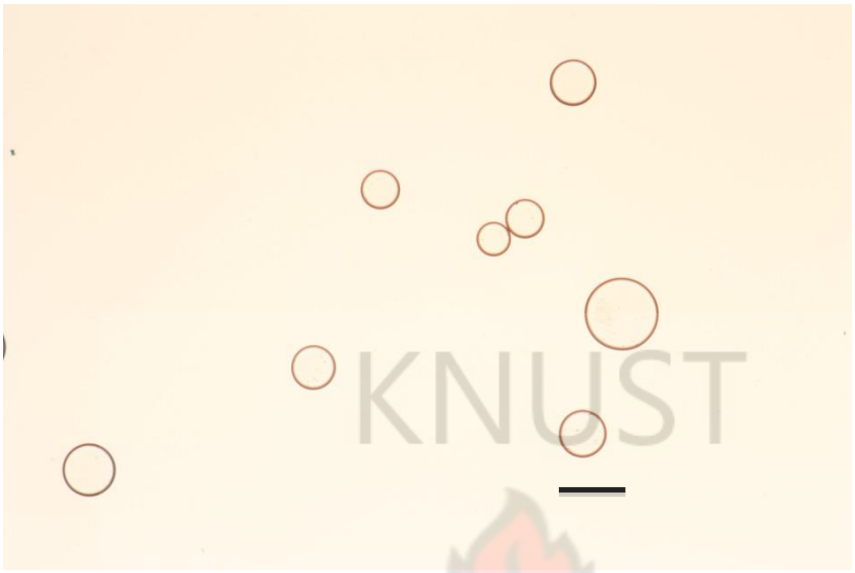

scale bar = 100 µm

Figure 4.2 (a) Light microscope image of well-formed blank RG503H PLGA microspheres

scale bar = 100 µm

Figure 4.2(b) Light microscope image of well-formed artemether-loaded RG503H PLGA microspheres

scale bar = 100 µm

Figure 4.3 (a) Light microscope image of well-formed blank RG502H PLGA microspheres

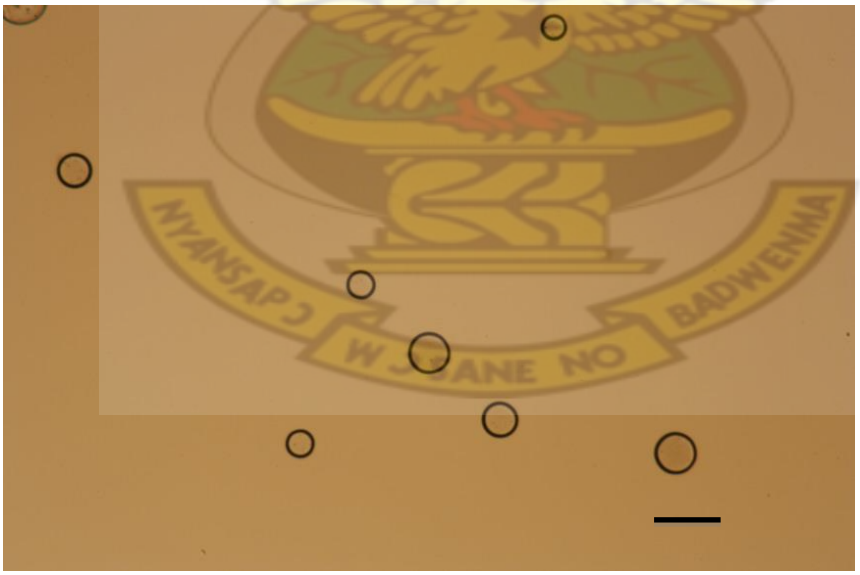

scale bar = 100 µm

Figure 4.3 (b) Light microscope image of well-formed artemether-loaded RG502H PLGA microspheres.

Table 4.1 (a) Yields of RG503H polymer microspheres under varied conditions

Particle size (μm)	Mass of empty centrifuge tube (g)	Volume of particles before freeze drying (ml)	Volume of mannitol added (ml)	Mass of microspheres, centrifuge tube and mannitol after freeze drying (g)
5, 000 rpm for 30 seconds **(A)**				
20-45	7.06927	0.26	1.1	7.23294
45-90	7.15278	0.26	1.1	7.39996
> 90	7.21115	0.5	2.1	7.7267
5, 000 rpm for 45 seconds **(B)**				
20-45	7.05142	0.35	1.26	7.36850
45-90	7.05564	0.6	2.52	7.67990
> 90	7.03584	0.3	1.26	7.37350
5, 000 rpm for 60 seconds **(C)**				
20-45	6.98905	0.1	0.42	7.14800
45-90	7.05540	0.3	1.26	7.43580
> 90	6.99030	0.6	2.52	7.58050
10, 000 rpm for 15 seconds **(D)**				
20-45	7.09640	0.2	0.84	7.33960
45-90	7.01523	0.4	1.68	7.49300
> 90	7.01442	0.6	2.52	7.57000
10, 000 rpm for 30 seconds **(E)**				
20-45	7.06927	0.26	1.1	7.22599
45-90	7.21944	0.26	1.1	7.42944
> 90	7.12926	0.5	2.1	7.33926

Table 4.1 (b) Yields of RG503H polymer microspheres under varied conditions

Particle size (µm)	Mass of microspheres with mannitol (mg)	Mass of mannitol (mg)	Mass of microspheres (mg)
5, 000 rpm for 30 seconds **(A)**			
20-45	163.67	110.00	53.67
45-90	247.18	110.00	137.18
> 90	515.55	210.00	305.55
Total yield			**496.40**
5, 000 rpm for 45 seconds **(B)**			
20-45	317.08	140.00	177.08
45-90	624.26	252.00	372.26
> 90	337.66	140	197.66
Total yield			**747.00**
5, 000 rpm for 60 seconds **(C)**			
20-45	158.95	42.00	116.00
45-90	380.40	126.00	254.40
> 90	590.20	252.00	338.20
Total yield			**708.60**
10, 000 rpm for 15 seconds **(D)**			
20-45	243.20	84.00	159.20
45-90	477.77	168.00	309.77
> 90	555.58	252.00	303.58
Total yield			**772.55**
10, 000 rpm for 30 seconds **(E)**			
20-45	156.72	110.00	46.72
45-90	313.84	110.00	203.84
> 90	223.66	110.00	113.66
Total yield			**364.22**

Table 4.2 (a) Yields of RG502H polymer microspheres under varied conditions

Particle size (μm)	Mass of empty centrifuge tube (g)	Volume of particles before freeze drying (ml)	Volume of mannitol added (ml)	Mass of microspheres, centrifuge tube and mannitol after freeze drying (g)
5, 000 rpm for 30 seconds **(A)** blank				
20-45	7.0258	0.1	0.042	7.1175
45-90	7.0012	0.2	0.084	7.2272
> 90	6.9886	0.6	0.252	7.6663
5, 000 rpm for 30 seconds **(B)**				
20-45	6.9681	0.1	0.042	7.0845
45-90	7.0955	0.4	0.168	7.4184
> 90	7.0670	1.0	0.420	8.1295
5, 000 rpm for 45 seconds **(C)**				
20-45	6.9874	0.1	0.042	7.1157
45-90	7.0335	0.4	0.168	7.3727
> 90	6.9511	1.0	0.420	7.9682
10, 000 rpm for 45 seconds **(D)**				
20-45	7.1049	0.3	0.126	7.4572
45-90	6.8960	0.8	0.336	7.6598
> 90	7.0894	0.2	0.084	7.2357

Table 4.2 (b) Yields of RG502H polymer microspheres under varied conditions

Particle size/ µm	Mass of microspheres and mannitol/ mg	Mass of mannitol/mg	Mass of microspheres/ mg
5, 000 rpm for 30 seconds **(A) blank**			
20-45	91.7	4.2	87.5
45-90	226.0	8.4	217.6
> 90	677.7	25.2	652.5
Total yield			**957.6**
5, 000 rpm for 30 seconds **(B)**			
20-45	116.4	4.2	112.2
45-90	322.9	16.8	306.1
> 90	1062.5	42	1020.5
Total yield			**1438.8**
5, 000 rpm for 45 seconds **(C)**			
20-45	128.3	4.2	124.1
45-90	339.2	16.8	322.4
> 90	1017.1	42	975.1
Total yield			**1421.6**
10, 000 rpm for 45 seconds **(D)**			
20-45	352.3	12.6	339.7
45-90	763.8	33.6	730.2
> 90	146.3	8.4	37.9
Total yield			**1207.8**

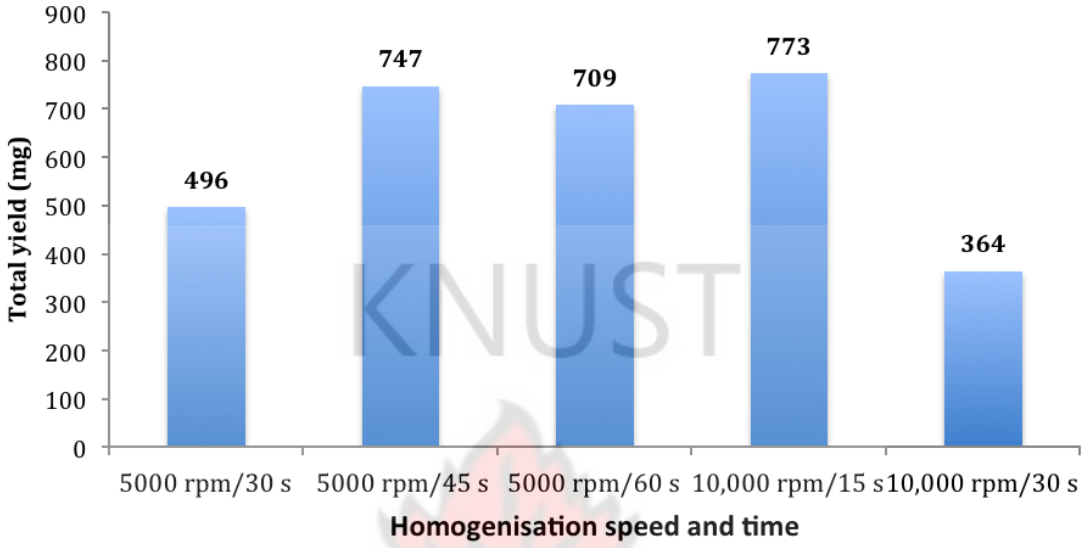

Figure 4.4 Total yields of various artemether -loaded RG503H formulations

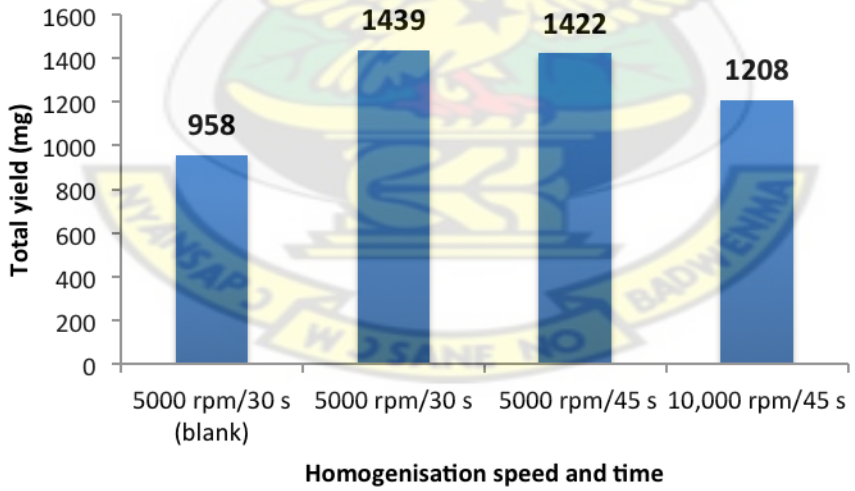

Figure 4.5 Total yields of various artemether -loaded RG502H formulations

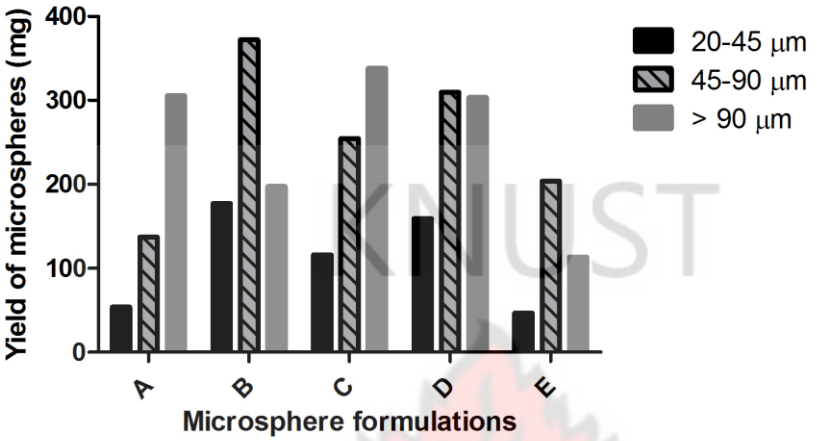

Key:
A: 5, 000 rpm for 30 seconds
B: 5, 000 rpm for 45 seconds
C: 5, 000 rpm for 60 seconds
D: 10, 000 rpm for 15 seconds
E: 10, 000 rpm for 30 seconds

Figure 4.6 Total yields of different RG503H PLGA microsphere formulations produced under various processing conditions

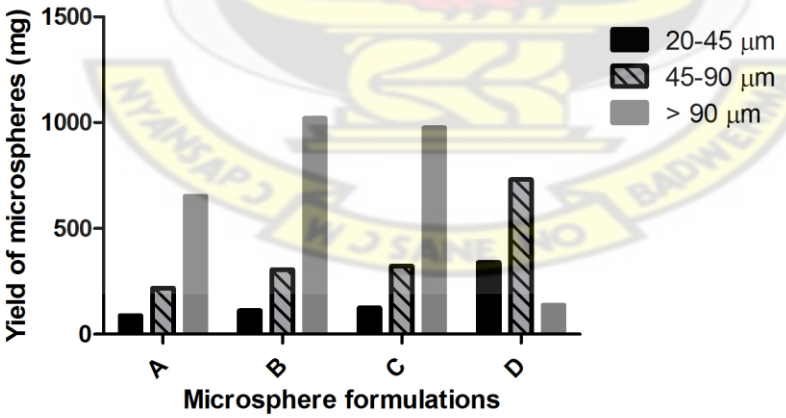

KEY:
A: 5, 000 rpm for 30 seconds (BLANK)
B: 5, 000 rpm for 30 seconds
C: 5, 000 rpm for 45 seconds
D: 10, 000 rpm for 45 seconds

Figure 4.7 Total yields of different RG502H PLGA microsphere formulations produced under various processing conditions

4.3 SOLUBILITY OF ARTEMETHER IN RELEASE BUFFER (PBST) AND 60 % ACETONITRILE IN WATER

A higher correlation coefficient of (0.9979) was obtained for artemether in 60 % acetonitrile in water than in PBST buffer (0.79469) as shown in Figures 4.8 and 4.9 respectively. There was no linear relationship between the concentration of artemether dissolved in PBST and the peak areas obtained from the UPLC analysis. A clear linear relationship is seen in Figure 4.8 between concentration of artemether dissolved in 60 % acetonitrile in water and the peak areas obtained. The chromatograms obtained for artemether showed that the retention time was ~ 3 minutes as shown in Figures 4.10 and 4. 11. Sharp peaks were observed on the chromatograms for artemether.

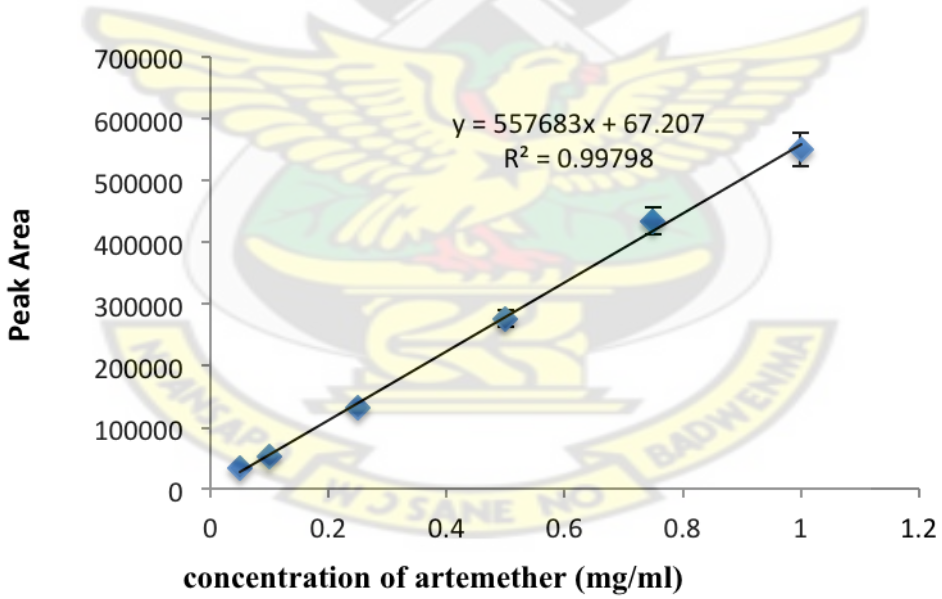

Figure 4.8 Calibration curve for artemether in 60 % acetonitrile in water

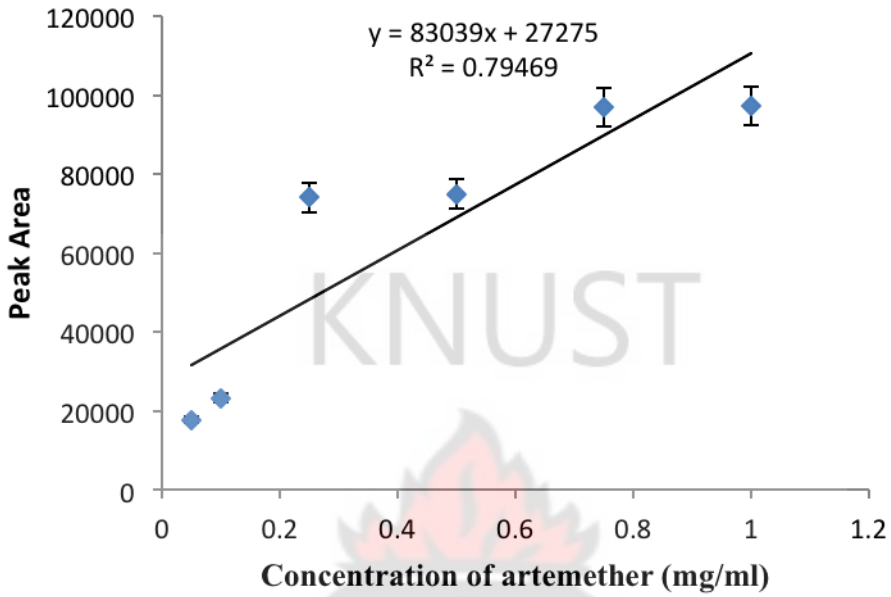

Figure 4.9 Calibration curve for artemether in PBST

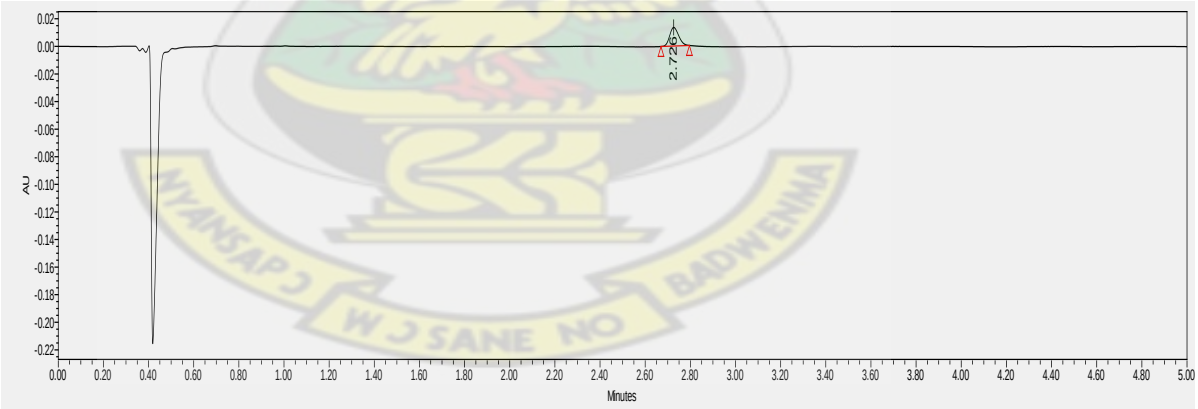

Figure 4.10 Chromatogram of 0.05 mg /ml artemether

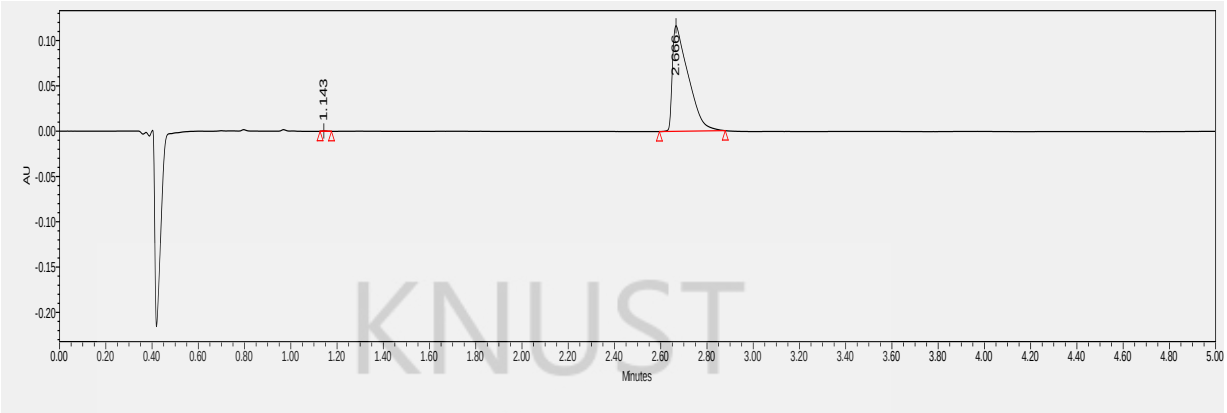

Figure 4.11 Chromatogram of 1 mg /ml artemether

4.4 PARTICLE SIZE ANALYSIS OF FORMULATED MICROSPHERES

The particle size analysis histograms shown in Figures 4.12 and 4.13 demonstrated normally distributed microspheres for both RG503H and RG502H polymer microspheres. The characteristics of the microspheres are shown in Table 4.3. The average particle size (D_{50}) of RG502H microspheres was larger (70.41 μm) than that of RG503H (69.06 μm).

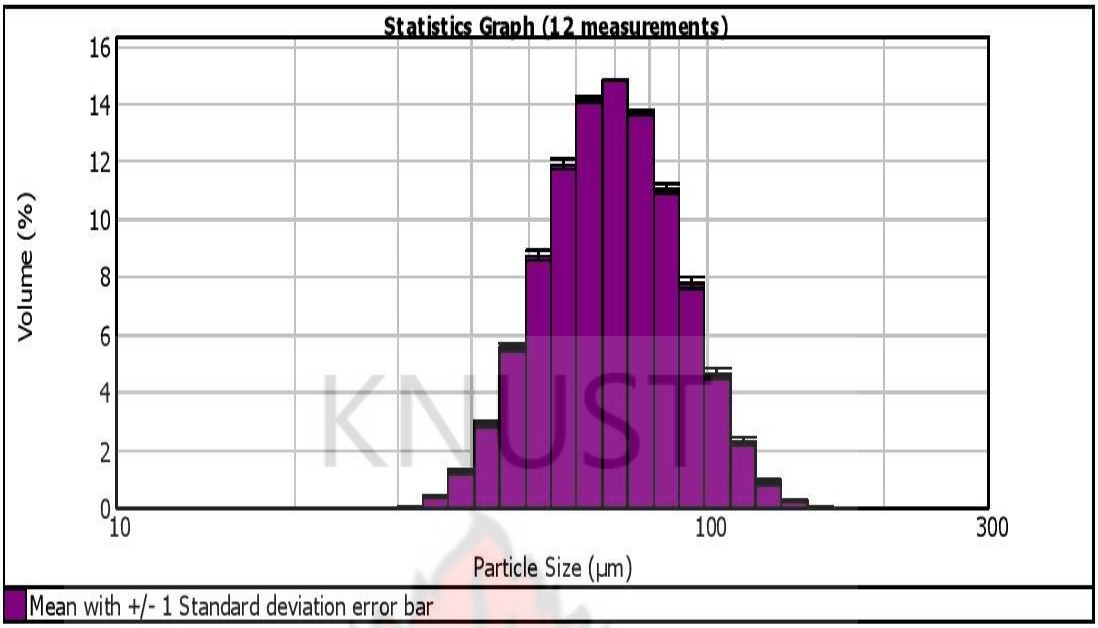

Figure 4.12 Particle size distribution of artemether-loaded RG503H PLGA microspheres

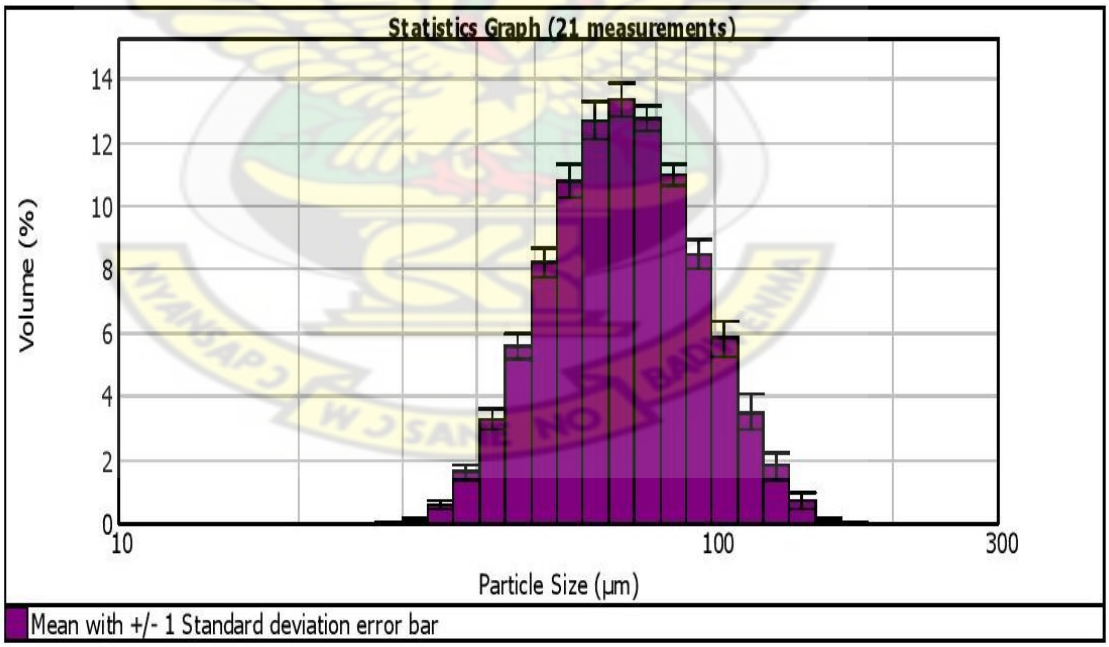

Figure 4.13 Particle size distribution of artemether-loaded RG502H PLGA microspheres

4.5 CHARACTERISTICS OF ARTEMETHER-LOADED PLGA MICROSPHERES

The characteristics of PLGA microsphere formulations selected for further processing are shown in Table 4.3. Although the total yield for RG503H microspheres was greater (83.00 %) than 80.53 % for RG502H, the yield of the desired particle size range did not follow this trend. The yield of RG502H microspheres of the 45-90 μm size range was 60.43 %, which was higher than that of RG503H microspheres (50.13 %). The drug loading content as well as drug loading efficiencies were higher for RG503H (25 %, 74 %) microspheres as compared to RG502H microspheres (20 %, 59 %). The percentage drug loading and corresponding encapsulation efficiency of artemether was high for both the low and high molecular weight PLGA microsphere formulations, but were higher with the higher molecular weight RG503H PLGA formulations.

Table 4.3 Characteristics of 45-90 μm size range artemether-loaded PLGA microspheres

Formulation type	D_{10} (μm)	D_{50} (μm)	D_{90} (μm)	Total Yield (%)	Yield of 45-90 μm size range (%)	Drug Loading Content (%)	Drug Loading Efficiency (%)
RG502H polymer	48.61	70.41	102.13	80.53	60.43	20 ± 0.87	59 ± 2.62
RG503H polymer	49.41	69.06	96.38	83.00	50.13	25 ± 0.21	74 ± 0.64

4.6 MORPHOLOGICAL CHARACTERISTICS OF MICROSPHERES

Figures 4.16 and 4.17, present the SEM images of blank and artemether- loaded microspheres of RG502H and RG503H resomers observed. The microspheres formulated with both RG502H and RG503H PLGA respectively were spherical with smooth surfaces. The sizes of the microspheres observed were within the 45-90 μm size range. In general, the microspheres were spherical in shape. The microspheres had smooth surfaces and were without any free drug on the surfaces. The particle size range obtained from the SEM analysis corresponded with the size range obtained from the particle size analysis. The spherical shape of the particles observed under light microscopy (Figures 4.1- 4.3) also corresponded with the shape observed in the SEM analysis. Figures 4.14 and 4.15 show that there was no difference in particle size and particle morphology between the blank microspheres and the artemether-loaded microspheres.

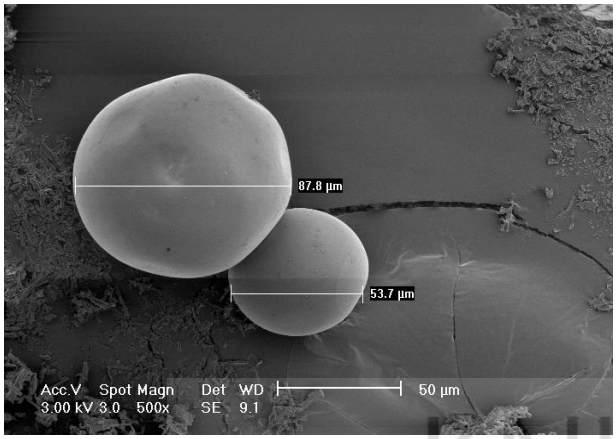

a

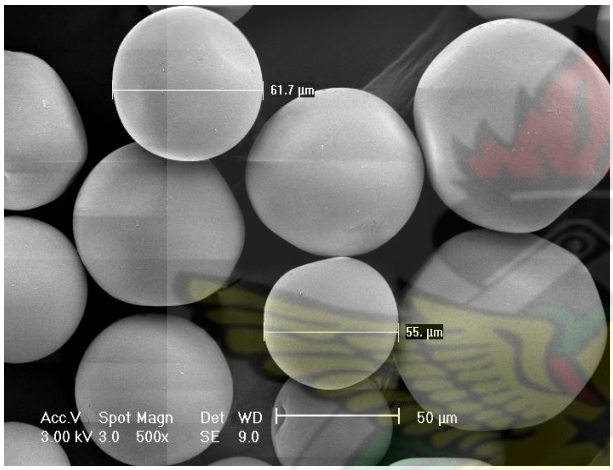

b

Figure 4.14(a) SEM image of blank RG503H PLGA microspheres and (b) SEM image of artemether-loaded RG503H PLGA microspheres

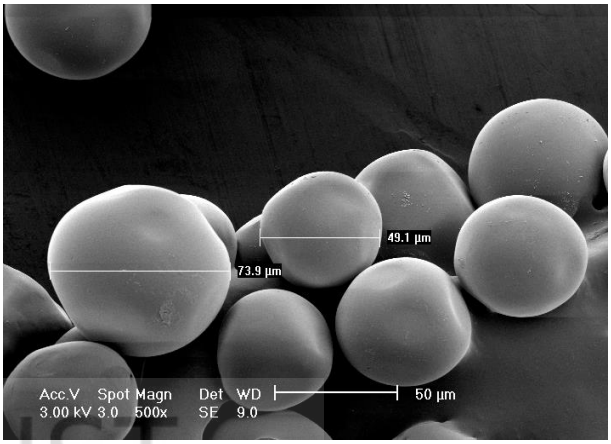

a

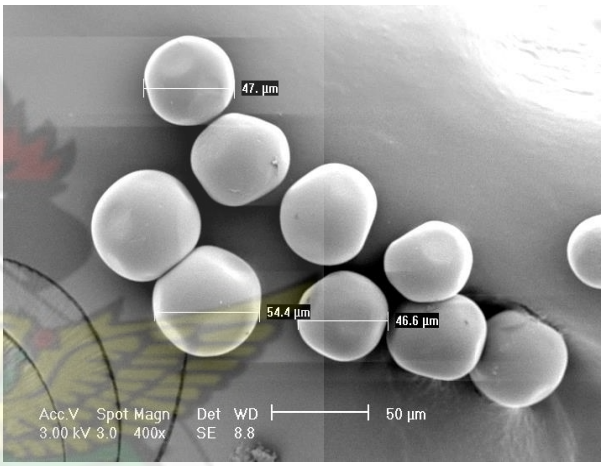

b

Figure 4.15(a) Figure 4.15 SEM image of blank RG502H PLGA microspheres and (b) SEM image of artemether-loaded RG502H PLGA microspheres

4.7 ARTEMETHER RELEASE FROM PLGA MICROSPHERE FORMULATIONS

The release profiles of RG503H and RG502H microsphere formulations are shown in Figures 4.17 and 4.19 respectively. From Figure 4.20, RG503H and RG502H microsphere formulations showed a triphasic and biphasic release of artemether, respectively. For the RG502H formulation, there was a burst release within the first three days followed by a slower release up to the fourteenth day. The release curve of artemether from the RG502H also corresponds to a normal cumulative release curve. Also, RG503H formulations showed a burst release on day one and slowed on day 3. There was however a rapid release from day 3 to day 7 which became slow and almost constant from day 7 to 21. The amount of drug released from day 0 to day 7 was higher with the RG502H formulation (72.9 %) than the RG503H formulation (66.3 %). In general, the RG503H microsphere formulation exhibited a greater control of the release of artemether than the RG502H formulation. Using Two-way ANOVA followed by the Sidak's multiple comparison test, the release of artemether from the two microspheres formulations was analyzed. There was no significant difference between the release of artemether from the two formulations RG502H and RG503H on Day 1, Day 7 and Day 21. However, for Day 3 the difference between the releases from the two formulations was very significant (*** $p < 0.0001$). The release of artemether on Day 14 was also significantly different (* $p < 0.01$) for the two formulations.

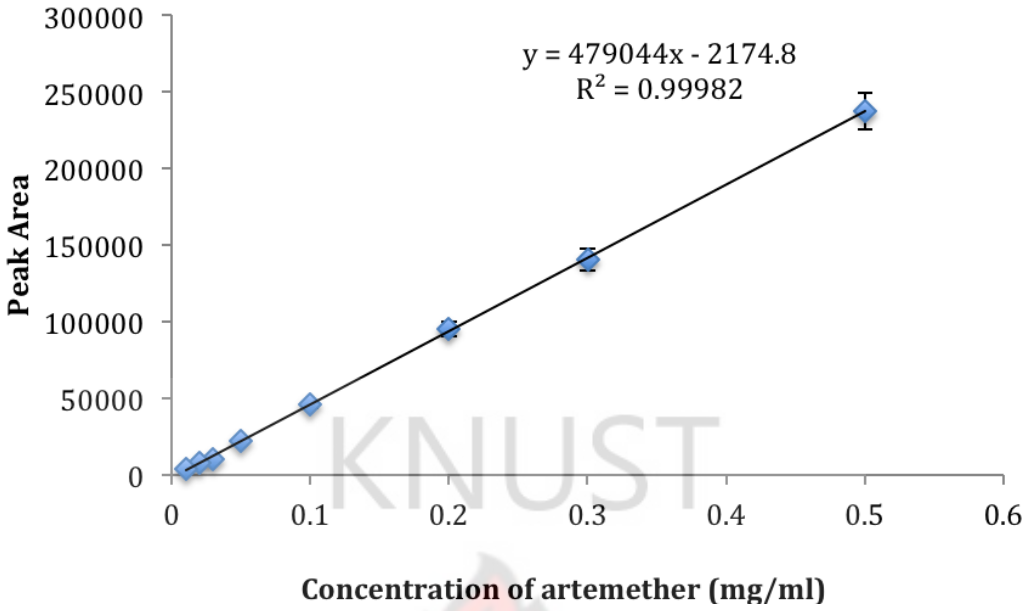

Figure 4.16 Calibration curve of artemether for drug loading in RG503H formulation

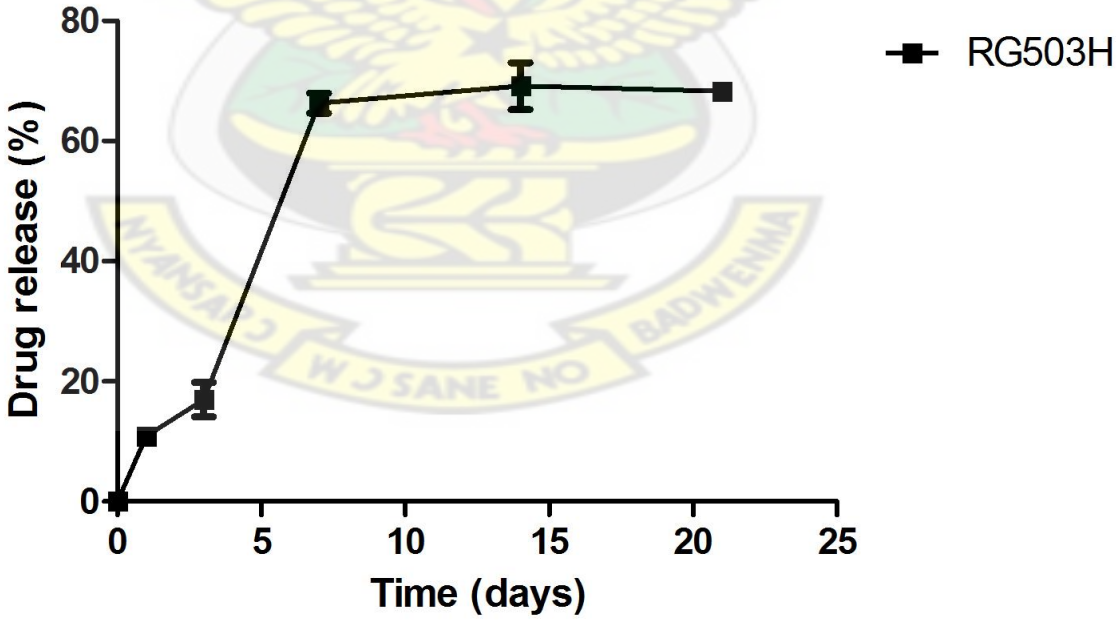

Figure 4.17 Cumulative percentage drug release profile of artemether-loaded RG503H PLGA microspheres

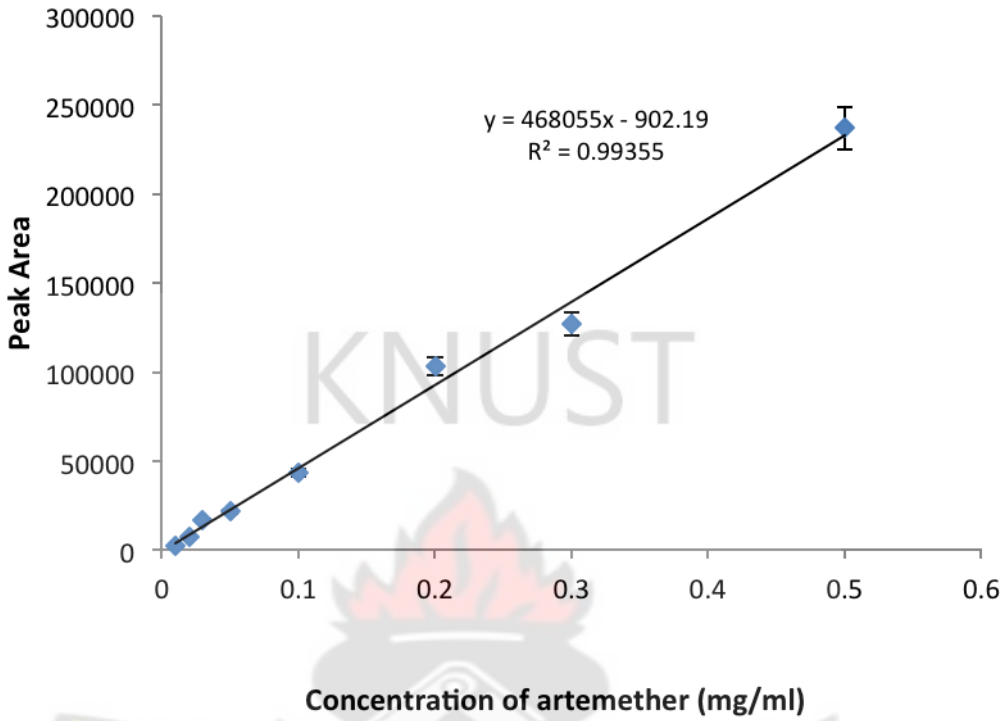

Figure 4.18 Calibration curve of artemether for drug loading in RG502H formulation

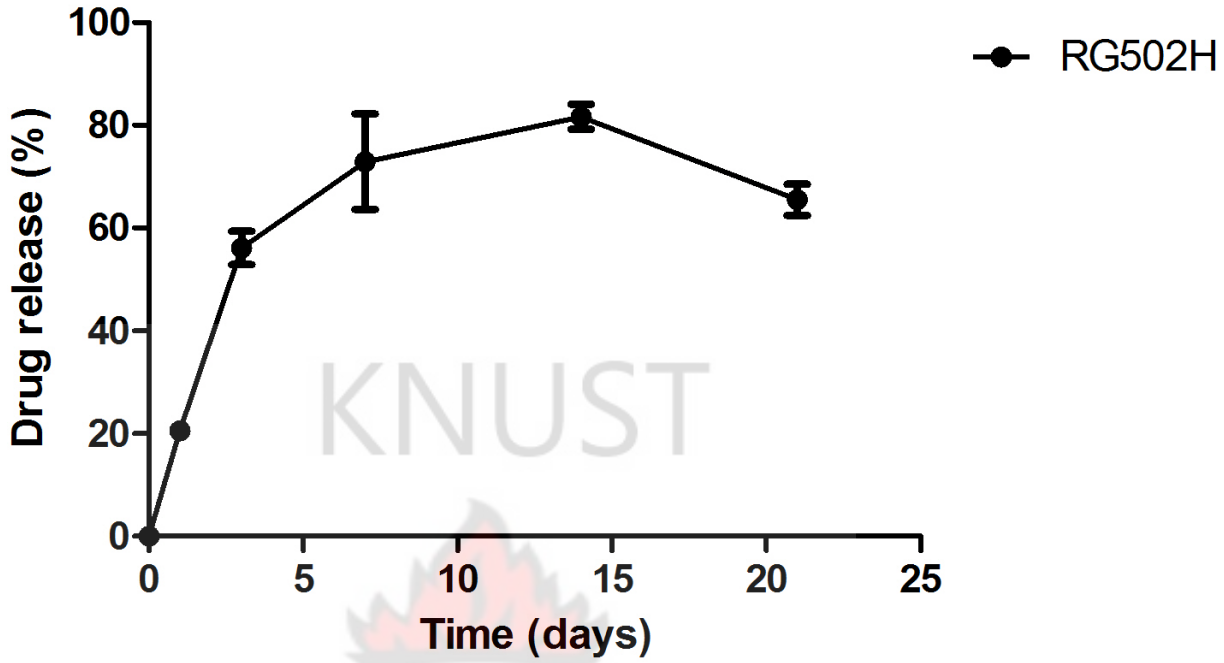

Figure 4.19 Cumulative percentage drug release profile of artemether-loaded RG502H PLGA microspheres

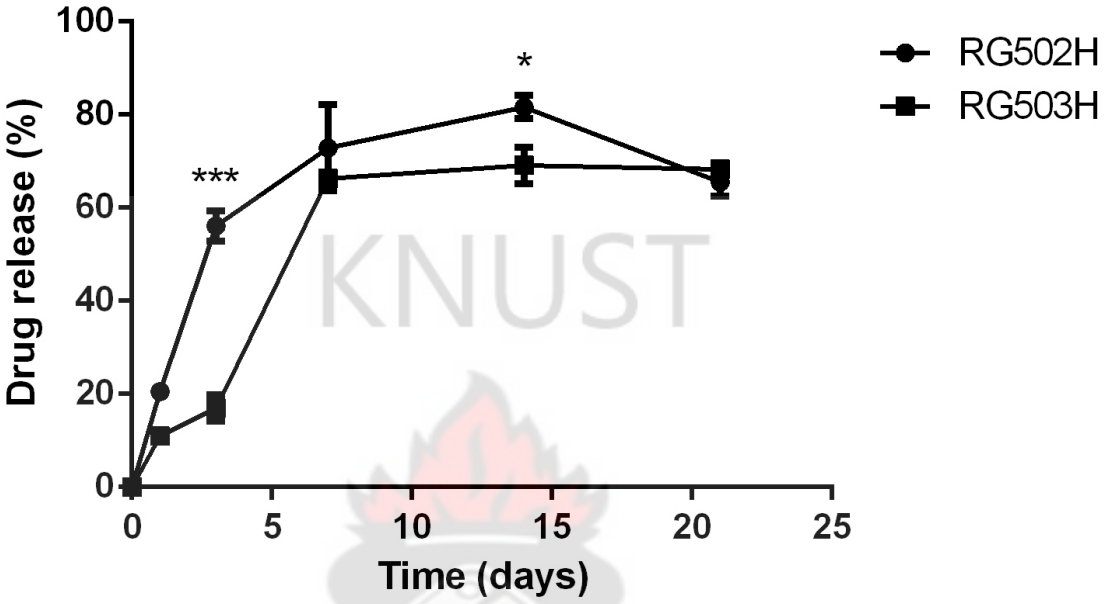

Figure 4.20 Cumulative percentage drug release profiles for artemether-loaded RG502H and RG503H polymer microspheres over 21 days. Values are mean ± SEM, n = 3 *p < 0.01, *** p< 0.0001 comparing RG502H and RG503H polymer microspheres (Two-way ANOVA followed by Sidak's multiple comparison test)

4.8 POLYMER DEGRADATION

The degradation behaviour of the microspheres was studied by assessing the mass loss, water uptake and the molecular weight profile of the microspheres over time. The molecular weight (Mw) profiles of the two resomer formulations over a period of 14 days are shown in Figure 4.23. The Mw of the RG503H formulation remained steady from Day 0 to Day 1 after which it declined markedly to Day 14. The RG502H formulation exhibited continuous decline in molecular weight over 14 days.

The masses of microspheres recorded over the fourteen-day period are shown in Tables 4.4 – 4.7 for the various formulations respectively. The water uptake amount for RG502H polymer microspheres was significantly higher (57.30 %) than that of RG503H polymer microspheres (30.28 %) on the fourteenth day as shown in Table 4.8. The change in weight of the microspheres over 21 days was measured in the mass loss experiment. The mass loss of RG503H polymer microspheres was lower (35.36 %) than that for RG502H (46.47 %) on Day 14.

Using Two-way ANOVA followed by the Sidak's multiple comparison test, the water uptake, mass loss and molecular weight profiles of the two formulated microspheres formulations RG502H and RG503H were analyzed (Figures 4.21, 4.23 and 4.24). There was no significant difference in the water uptake amounts of the two formulations from Day 0 to Day 7. However, there was a significant difference (*** $p < 0.0001$) observed on Day 14. The mass loss study showed significant difference in mass loss of the two microspheres formulations on Day 7 (** $p < 0.001$) and Day 14 (* $p < 0.01$). There were significant differences (*** $p < 0.0001$) in the molecular weights of both formulations from Day 0 to Day 7. The molecular weights recorded on Day 14 did not differ significantly.

Dry particle amount G =H - (E + B)

Water uptake amount = F- (E +C + G)

Weight of water absorbed by filter paper D= C - B

A = initial weight of particles

B = weight of dry filter paper

C = weight of dry filter paper

D = weight of water absorbed by filter paper

E = weight of empty 2 ml centrifuge tube

F = weight of tube and particles and filter paper (WET)

G = dry particle weight

H = final total dry weight (weight of particles, filter paper and tube)

Table 4.4 Mass of microspheres measured on Day 0

	A (mg)	B (mg)	C (mg)	D (mg)	E (mg)	F (mg)	G (mg)	H (mg)
RG502H T_1	10.2	32.4	86.2	53.8	1185.04	1286.39	8.53	1226.47
RG502H T_2	10.3	32.3	87.0	54.7	1185.52	1282.43	8.16	1225.98
RG503H T_1	10.3	32.4	86.3	53.9	1185.20	1285.84	8.87	1226.47
RG503H T_1	10.3	32.5	86.2	53.7	1188.04	1283.95	8.54	1229.08

Table 4.5 Mass of microspheres measured on Day 1

	A (mg)	B (mg)	C (mg)	D (mg)	E (mg)	F (mg)	G (mg)	H (mg)
RG502H T_1	10.01	32.83	86.5	53.67	1189.09	1285.15	8.82	1230.74
RG502H T_2	10.03	33.02	87.03	54.01	1189.67	1287.68	8.27	1230.96
RG503H T_1	10.12	32.92	86.57	53.65	1187.90	1285.22	7.99	1228.81
RG503H T_1	10.14	33.01	87.02	54.01	1187.64	1286.44	7.75	1228.40

Table 4.6 Mass of microspheres measured on Day 7

	A (mg)	B (mg)	C (mg)	D (mg)	E (mg)	F (mg)	G (mg)	H (mg)
RG502H T_1	10.20	33.84	89.96	53.67	1195.08	1292.91	7.52	1236.44
RG502H T_2	10.28	33.85	90.53	54.01	1190.37	1291.77	7.88	1232.10
RG503H T_1	10.11	33.84	90.12	53.65	1183.32	1296.94	8.63	1225.79
RG503H T_1	10.30	33.74	90.42	54.01	1189.86	1295.30	9.5	1233.10

Table 4.7 Mass of microspheres measured on Day 14

	A (mg)	B (mg)	C (mg)	D (mg)	E (mg)	F (mg)	G (mg)	H (mg)
RG502H T_1	10.09	33.84	89.96	53.67	1195.08	1292.91	5.39	1222.02
RG502H T_2	10.03	33.85	90.53	54.01	1190.37	1291.77	5.38	1226.59
RG503H T_1	10.09	33.84	90.12	53.65	1183.32	1296.94	6.88	1233.76
RG503H T_1	10.23	33.74	90.42	54.01	1189.86	1295.30	6.25	1229.92

Table 4.8 Water uptake amounts (%)

Time (days)	RG502H	RG503H
0	1.85 ± 0.2569	3.09 ± 2.8491
1	0.44 ± 0.3717	3.17 ± 0.8388
7	1.60 ± 1.7845	4.85± 0.4292
14	57.30 ± 0.4052	30.28 ± 2.3050

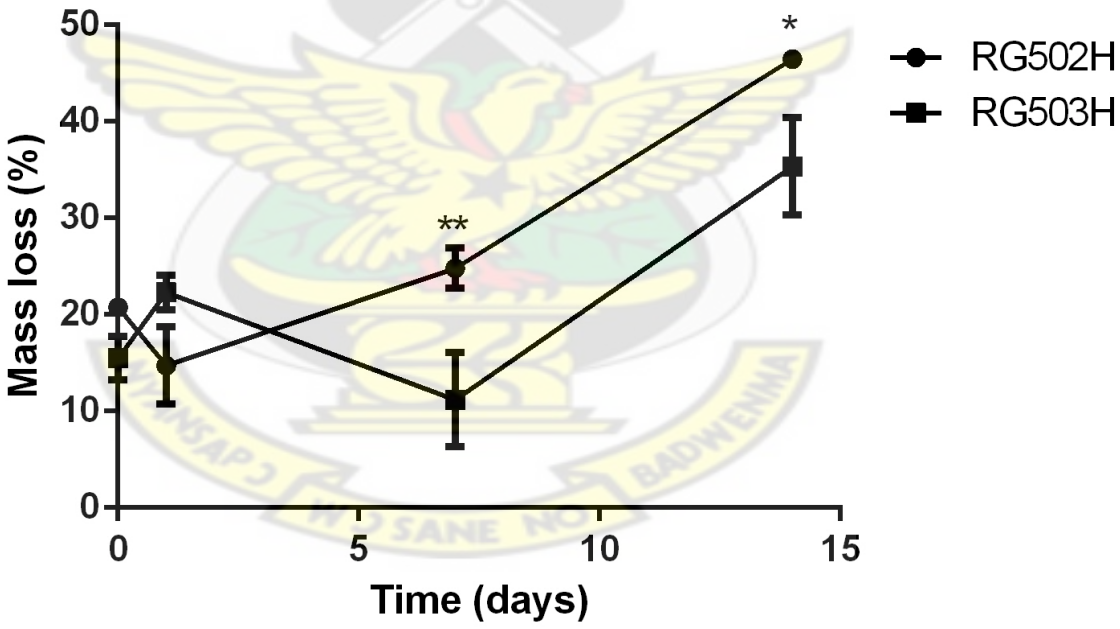

Figure 4.21 Mass loss of artemether-loaded PLGA microspheres. Values are mean ± SEM, n = 2 * $p < 0.01$, ** $p < 0.001$ comparing RG502H and RG503H polymer microspheres (Two-way ANOVA followed by Sidak's multiple comparison test)

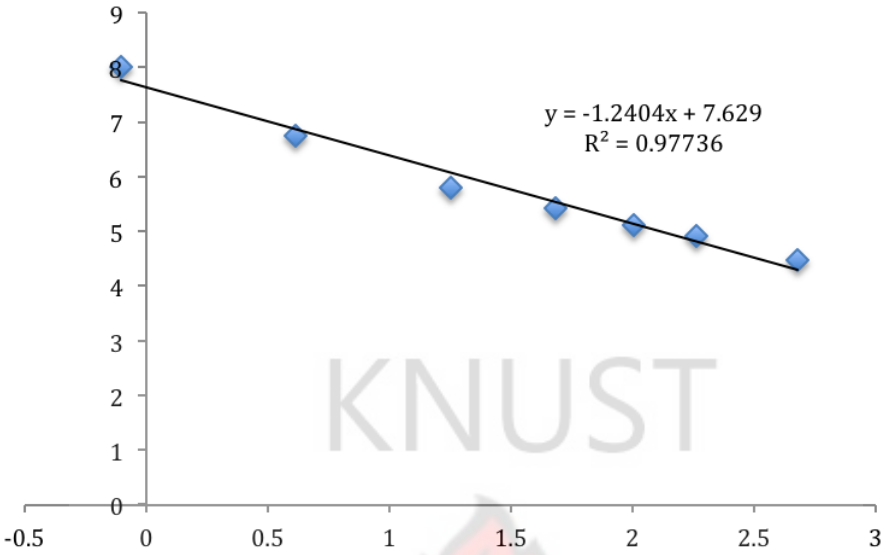

Figure 4.22 Calibration curve for GPC profiles of artemether- loaded PLGA microspheres with monodisperse polystyrene as a standard

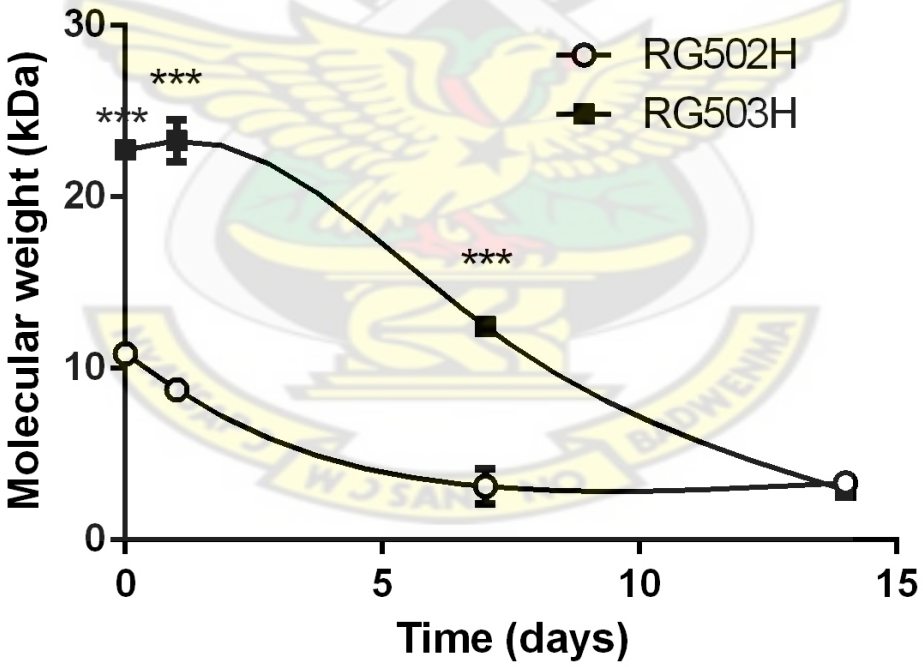

Figure 4.23 Molecular weight profiles of artemether-loaded PLGA microspheres incubated at pH 7.4 and 37 ^{o}C. Values are mean ± SEM, n = 2, *** $p < 0.0001$ comparing RG502H and RG503H polymer microspheres (Two-way ANOVA followed by Sidak's multiple comparison test)

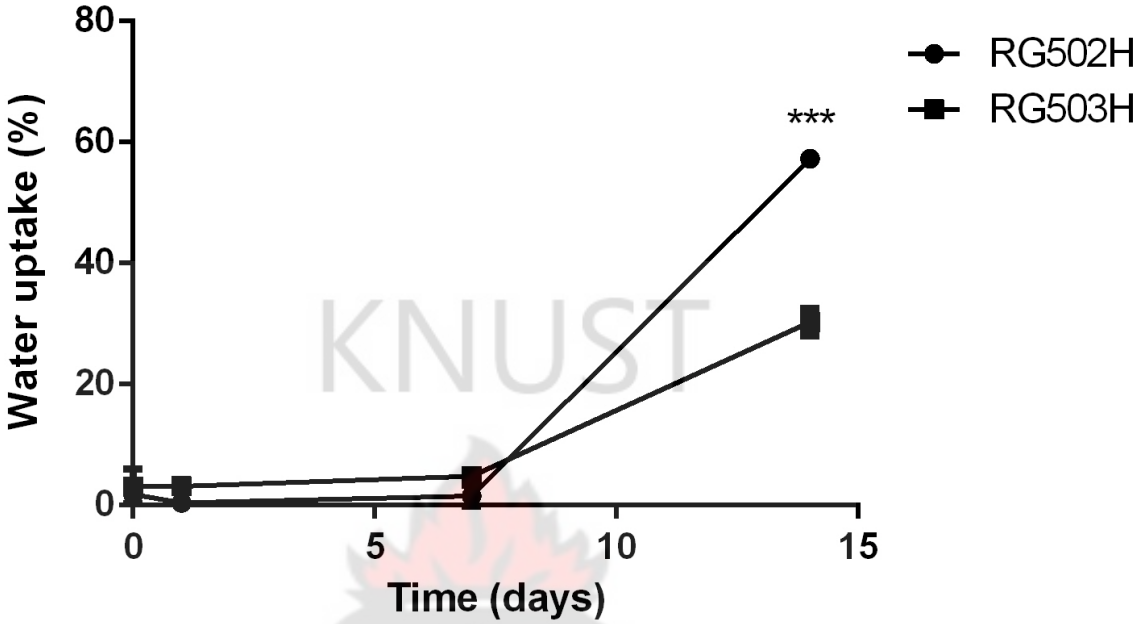

Figure 4.24 Water uptake of artemether loaded -PLGA microspheres. Values are mean ± SEM, n = 2 *** $p < 0.0001$ comparing RG502H and RG503H polymer microspheres (Two-way ANOVA followed by Sidak's multiple comparisons test)

4.9 KINETIC MODELLING OF ARTEMETHER RELEASE FROM MICROSPHERES

The parameters of the kinetic models used to assess the release of artemether from the microsphere formulations are shown in Table 4.9. Both the Higuchi and Korsemeyer-Peppas models produced relatively high correlation coefficients (R^2). For both models the R^2 value for RG503H formulation was higher than RG502H formulation. The R^2 values for RG503H formulation from the Higuchi and Korsemeyer-Peppas models are 0.8555 and 0.8801 respectively. The R^2 values for RG502H formulation from the

Higuchi and Korsemeyer-Peppas models are 0.7493 and 0.7425 respectively. The release exponent *n* obtained from Korsemeyer-Peppas model was 0.6854 and 0.3920 for the RG503H and RG502H formulations respectively. The correlation coefficients (R^2) obtained by fitting the parameters in all the equations are shown in Figures 4.25 – 4.34.

Table 4.9 Parameters of various models of kinetics of artemether release from microspheres

Formulation Type	Zero Order		First Order		Hixson-Crowell		Higuchi		Korsmeyer-Peppas	
	K_0	R^2	K_1	R^2	K_{HC}	R^2	K_H	R^2	n	R^2
RG502H	0.1147	0.5013	0.0008	0.3788	0.0055	0.415	3.3184	0.7493	0.3920	0.7425
RG503H	0.1398	0.7285	0.0016	0.6488	0.0062	0.5768	3.586	0.8555	0.6854	0.8801

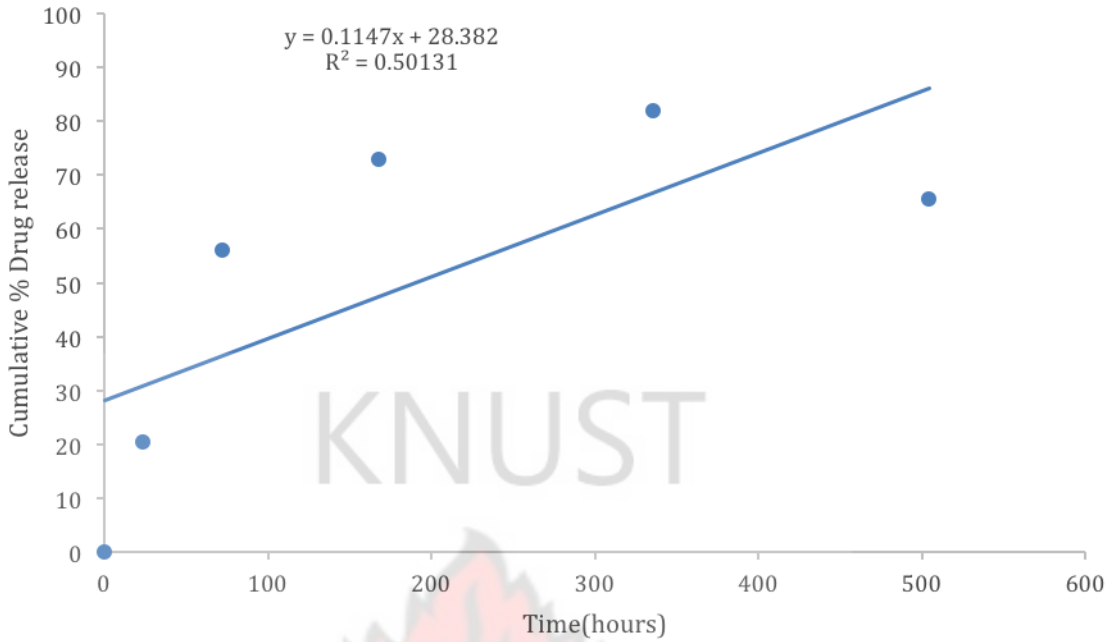

Figure 4.25 Zero order release kinetics modelling for RG502H polymer microspheres

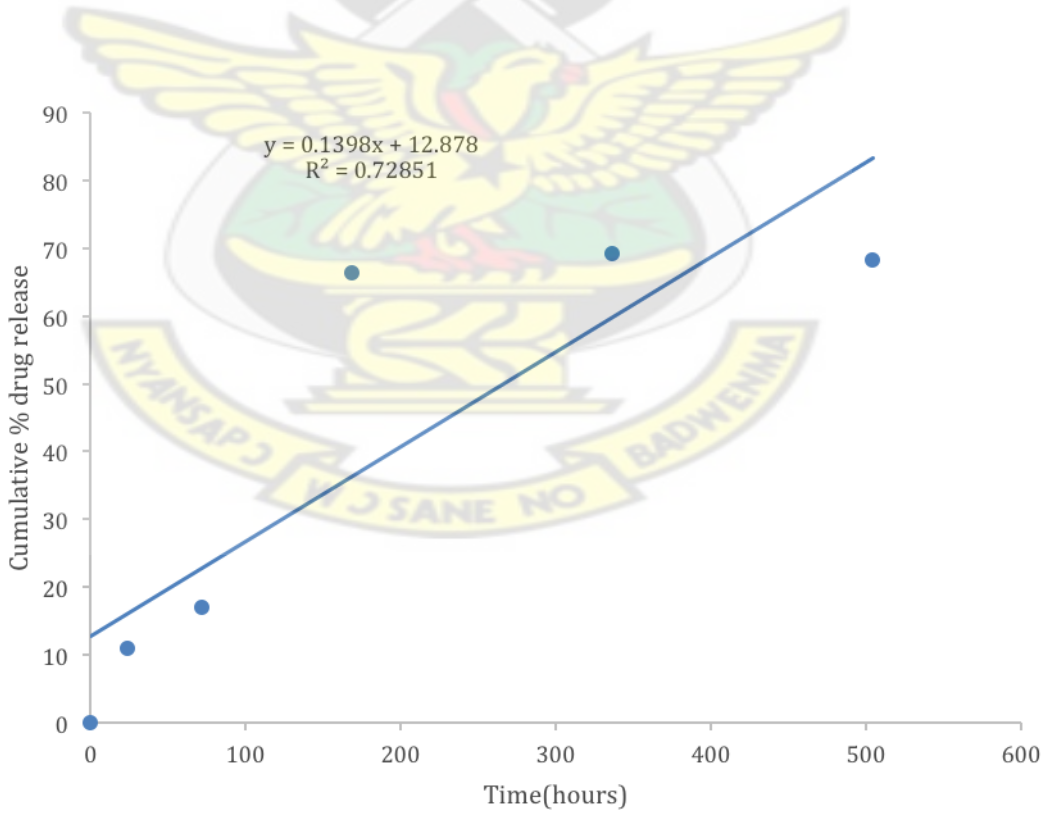

Figure 4.26 Zero order release kinetics modelling for RG503H polymer microspheres

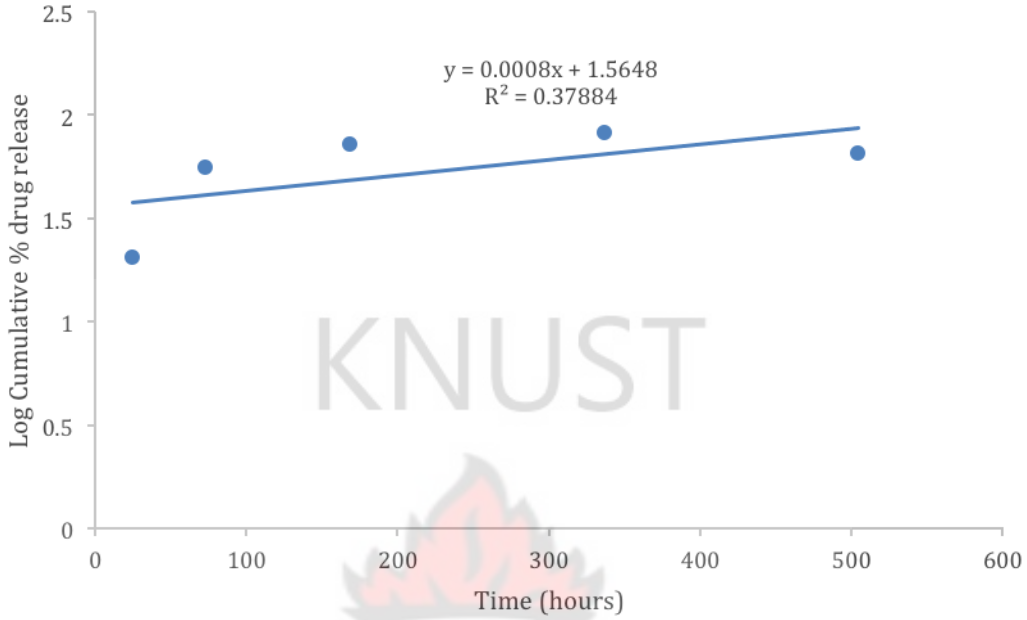

Figure 4.27 First order release kinetics modelling for RG502H polymer microspheres

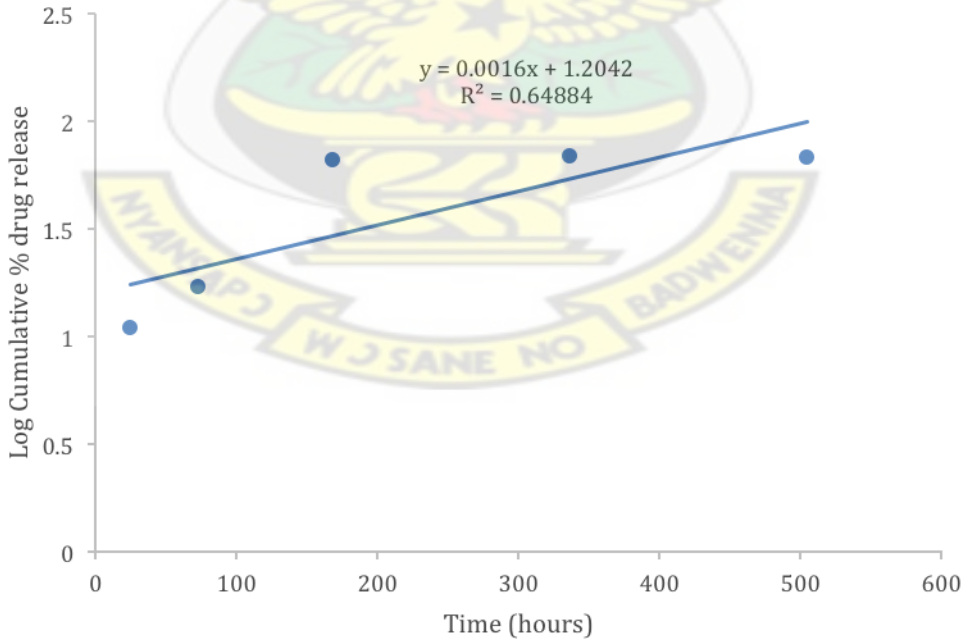

Figure 4.28 First order release kinetics modelling for RG503H polymer microspheres

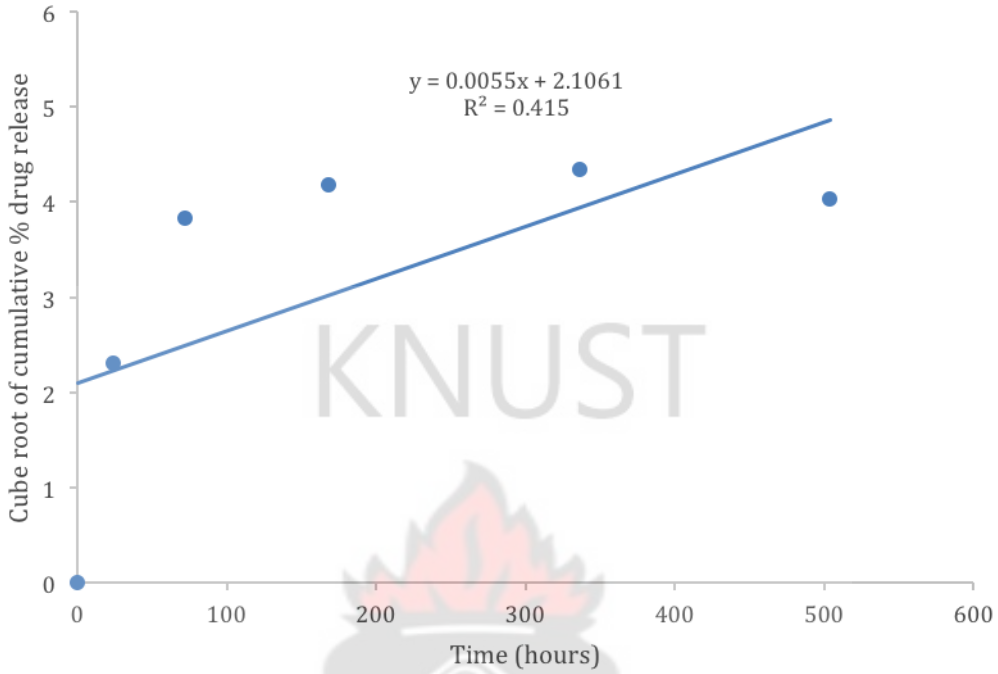

Figure 4.29 Hixson Crowell release kinetics modelling for RG502H polymer microspheres

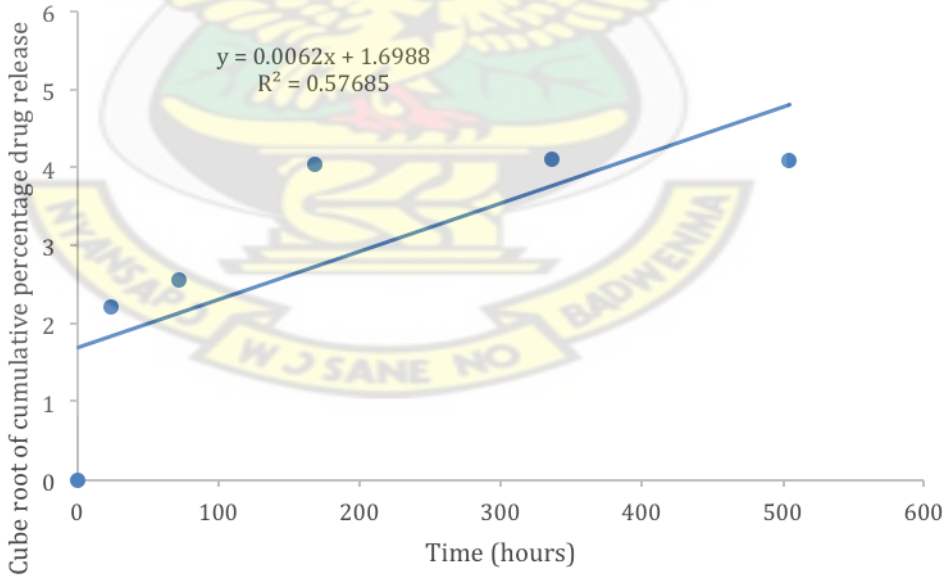

Figure 4.30 Hixson Crowell release kinetics modelling for RG503H polymer microspheres

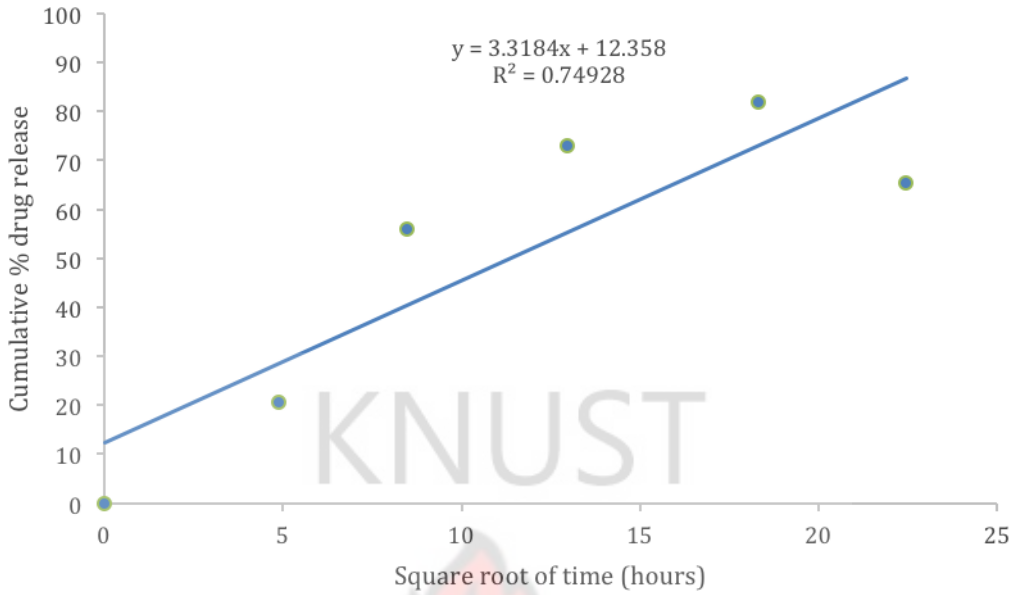

Figure 4.31 Higuchi release kinetics modelling for RG502H polymer microspheres

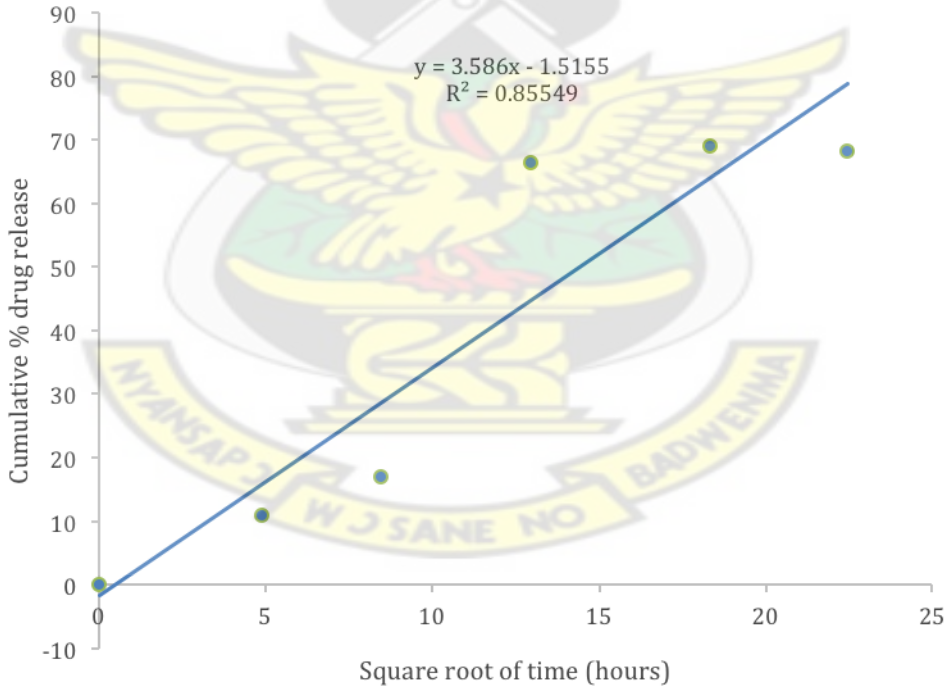

Figure 4.32 Higuchi release kinetics modelling for RG503H polymer microspheres

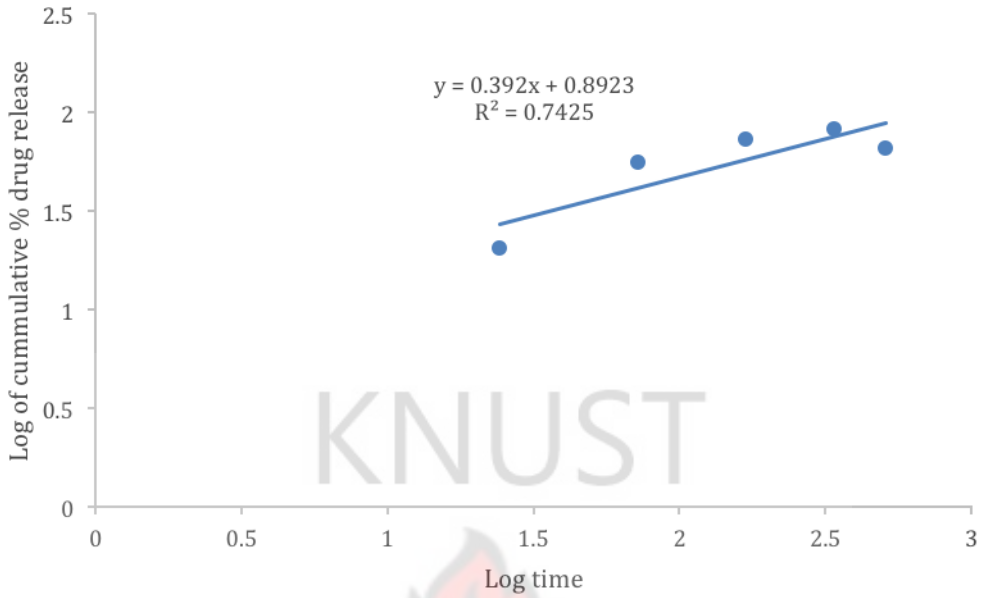

Figure 4.33 Korsemeyer-Peppas release kinetics modelling for RG502H polymer microspheres

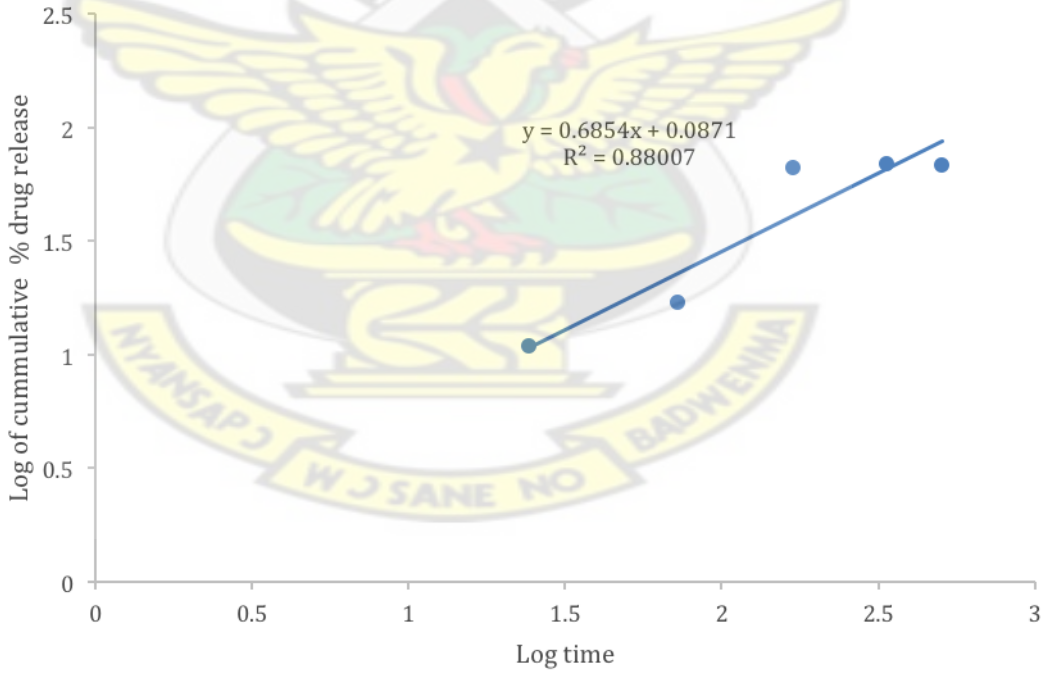

Figure 4.34 Korsemeyer-Peppas release kinetics modelling for RG503H polymer microspheres

4.10 QUANTIFICATION OF ARTEMETHER EXTRACTED FROM RAT PLASMA

The concentration of artemether measured in plasma samples of the rats used in the preliminary study is shown in Table 4.10. The concentration of artemether extracted from the plasma samples increased from the 1-hour sample to the 7th day sample for Rats 2 and 3. The concentration of artemether measured in the plasma samples for 1-hour and day 7of Rat 2 and Rat 3 were (191 and 643 ng/ml) and (328 and 3310 ng/ml) respectively. The highest concentration of artemether for Rat 1 was recorded on Day 3 (3050 ng/ml) and decreased to 360 ng/ml on Day 7.

Figures 4.40 – 4.69 represent chromatograms obtained from plasma samples of rats used in the pilot study. The chromatogram of isolated metabolite dihydroartemisinin (DHA), the internal standard artemisinin (IS) and artemether (ARM) is represented in Figure 4.35. The retention times recorded for the DHA, IS and ARM are 2.98, 3.11 and 3.50 minutes respectively. Figures 4.36 to 4.41 show chromatograms for 10, 750 and 1000 ng/ml of ARM and IS respectively, used to obtain the standard curve.

The extracted ARM and metabolite DHA as well as IS obtained from plasma samples of the rats in the pilot study are shown in Figures 4.42-4.65. The chromatograms show the presence of DHA, ARM and IS in all samples from the first hour to Day 7.

The plasma concentration-time profile of artemether is shown in Figure 4.66. Each data point represents mean concentrations of artemether from rat plasma. LC-MS/MS was used in analyzing artemether in the plasma of rats for the various groups and a chromatogram for one rat plasma sample from each group have been represented in Figures 4.67 to 4.70. Identification of primary ion species for artemether and

artemisinin (IS) seen on the chromatograms indicate that the precursor-product ion pairs for artemether and artemisinin (IS) were m/z 316.200 /267.200 and m/z 300.100 / 209.100 respectively.

The concentration of artemether extracted from all the rat groups is represented in the plasma concentration-time graph shown in Figure 4.66. The concentration of artemether in the plasma measured over 21 days showed that the drug detected in the plasma was relatively constant from the first hour to day 5. However, Day 14 and Day 21 plasma samples showed the presence of artemether in the rats dosed with artemether-loaded microsphere formulations only.

The pharmacokinetic parameters of artemether extracted from rat plasma are depicted in Table 4.12. The highest value (12011.25 ng/ml), for maximum concentration (C_{max}) was exhibited by rats' plasma samples from rats in Group 2, which were injected with a single injection of 12 mg/kg of artemether-loaded microspheres respectively. This concentration was observed on Day 21 (504 hours). The highest numerical value (6.8215 μg.h/ml) for area under the concentration-time curve (AUC_{0-504}) was observed for Group 2 rats' plasma samples. The lowest value (13.75 ng/ml) for C_{max} was observed for Group 3 rats' plasma samples. Rats in Group 3 received a single injection of 25 mg/kg of artemether-loaded microspheres respectively. The lowest (8.5225 μg.h/ml) $AUC_{(0-504)}$ was obtained from rats' plasma samples of rats in Group 5, which received a single injection of artemether only. The key to the rat groups is shown on Table 4.13.

Table 4.10 Concentrations of artemether extracted from plasma of rats used in the pilot study

Rat	**Drug treatment**	**Concentration of artemether (ng/ml)**			
		1 hour	**Day 1**	**Day 3**	**Day 7**
1	25 mg/ kg artemether	742	443	3050	360
2	12.5 mg/ kg artemether-loaded microspheres	191	172	480	643
3	25 mg/ kg artemether-loaded microspheres	328	133	183	3310

Table 4.11 Key to samples on chromatograms

Code	Sample description
AA	1 hour plasma sample from Rat 1
BB	1 hour plasma sample from Rat 2
CC	1 hour plasma sample from Rat 3
D	24 hour plasma sample from Rat 1(Day 1)
E	24 hour plasma sample from Rat 2 (Day 1)
F	24 hour plasma sample from Rat 3 (Day 1)
G	72 hour plasma sample from Rat 1(Day 3)
H	72 hour plasma sample from Rat 2 (Day 3)
I	72 hour plasma sample from Rat 3 (Day 3)
Q	168 hour plasma sample from Rat 1(Day 7)
R	168 hour plasma sample from Rat 2 (Day 7)
S	168 hour plasma sample from Rat 3 (Day 7)
ARM	Artemether
DHA	Dihydroartemisinin
IS	Artemisinin

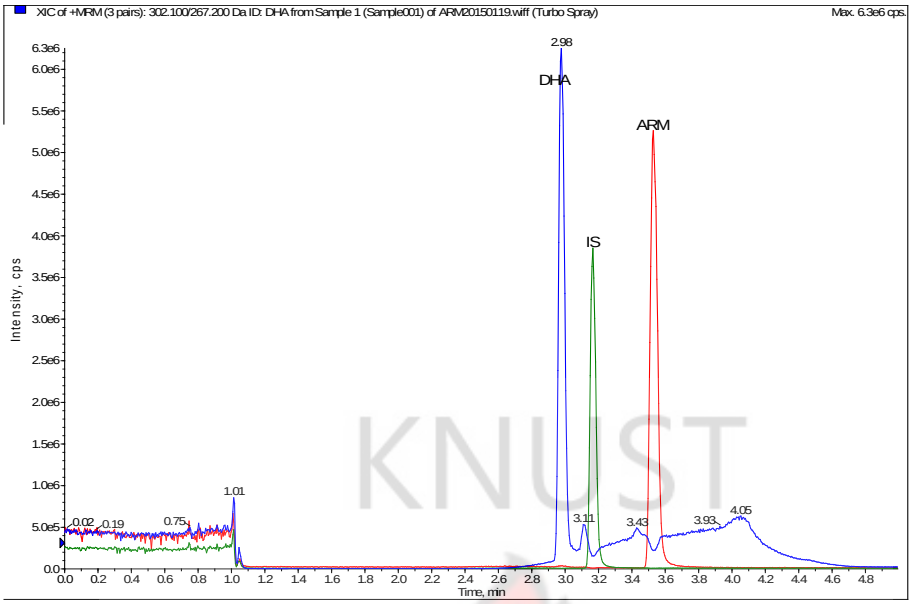

Figure 4.35 Chromatogram showing peaks for extracted metabolite DHA, IS and ARM (10 ng/ml standard) with retention times of 2.98, 3.11 and 3.50 minutes respectively.

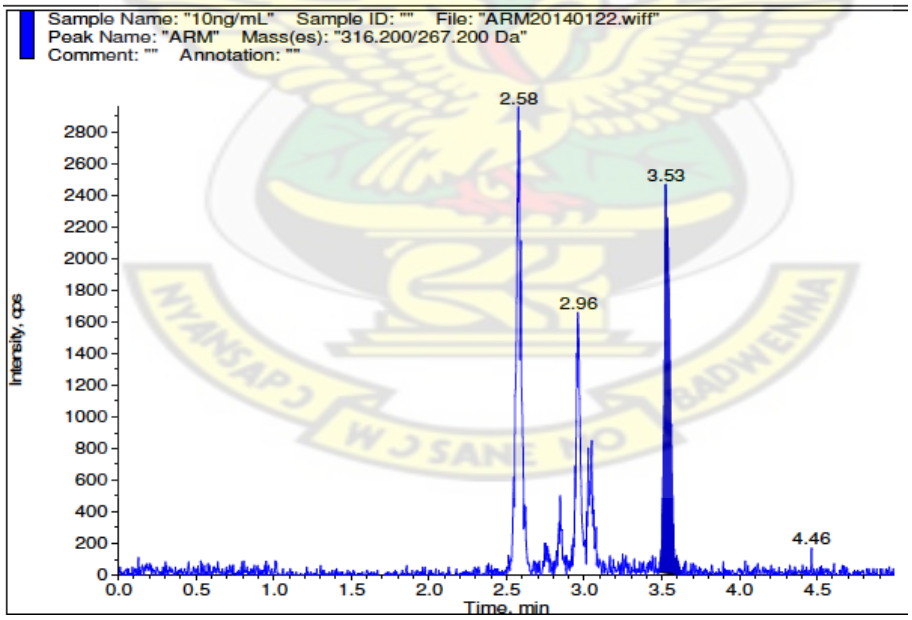

Figure 4.36 Chromatogram of extracted metabolite DHA 10 ng/ml and ARM 10 ng/ml with retention times of 2.96 and 3.53 minutes (standard) respectively

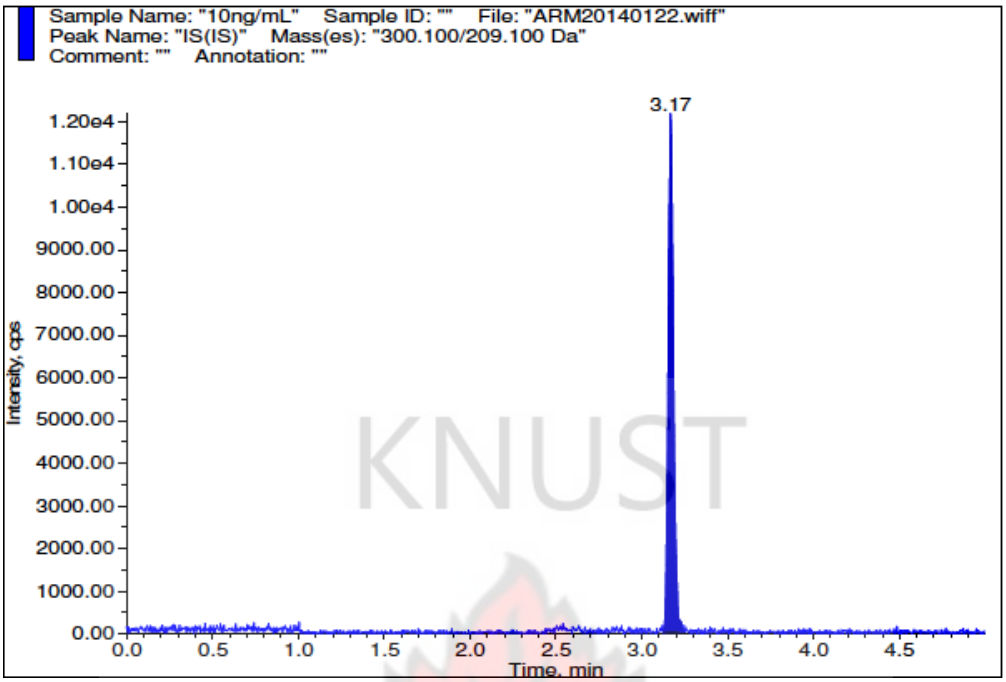

Figure 4.37 Chromatogram of 10 ng/ml IS (standard) with retention time of 3.17 minutes

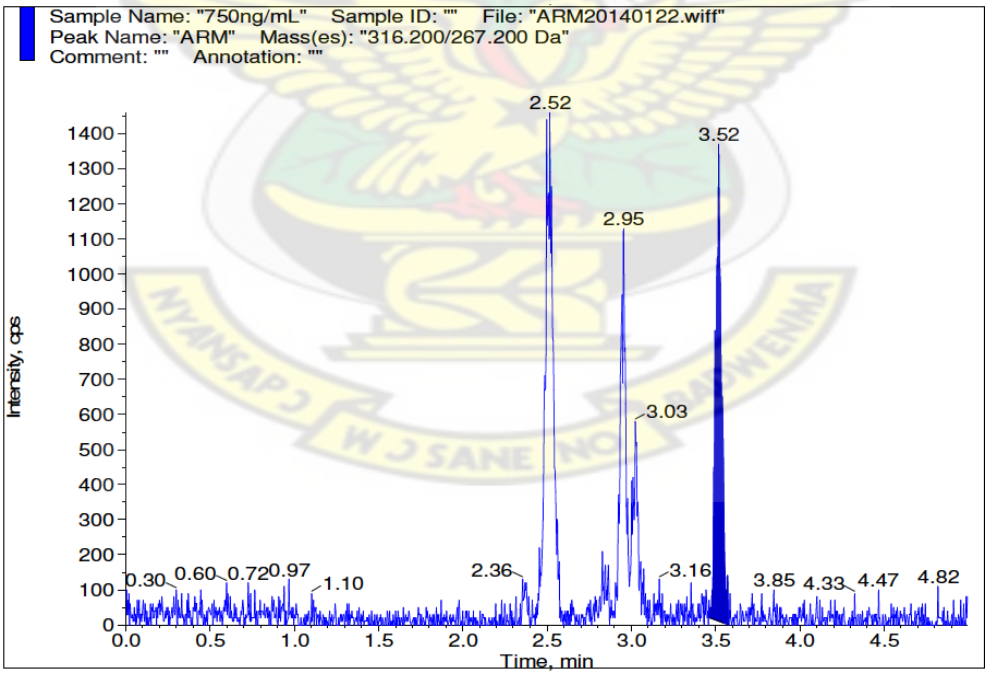

Figure 4.38 Chromatogram of extracted metabolite DHA 750 ng/ml and ARM 750 ng/ml with retention times of 2.95 and 3.52 minutes (standard) respectively

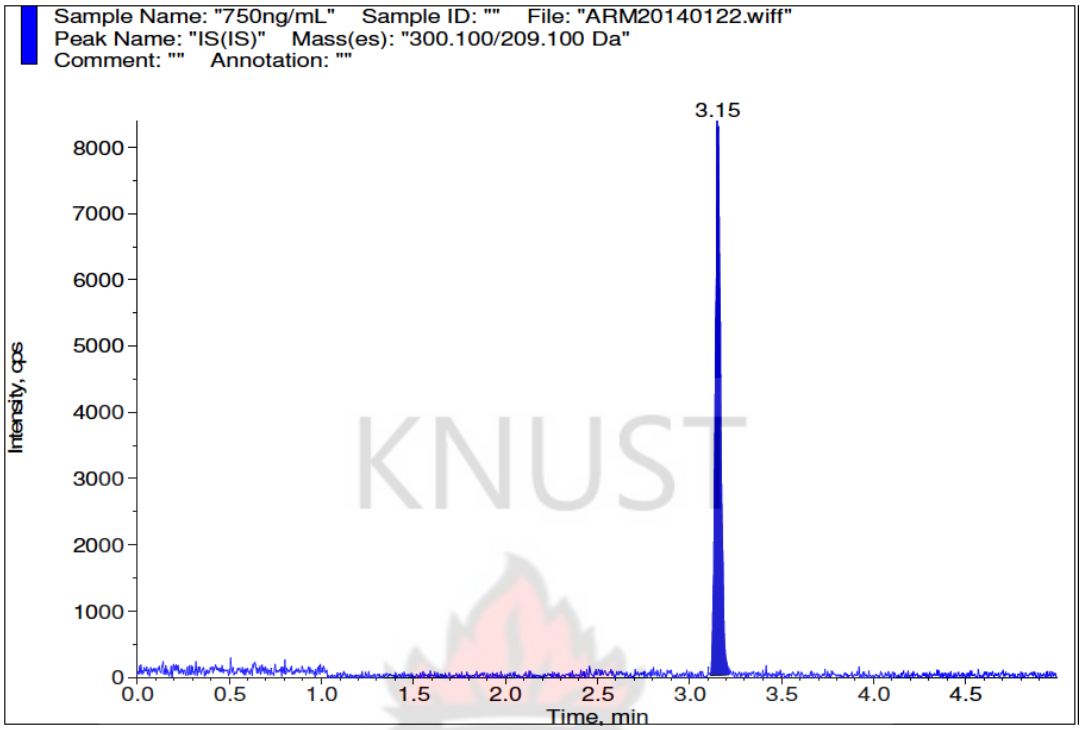

Figure 4.39 Chromatogram of 750 ng/ml IS (standard) with retention time of 3.15 minutes

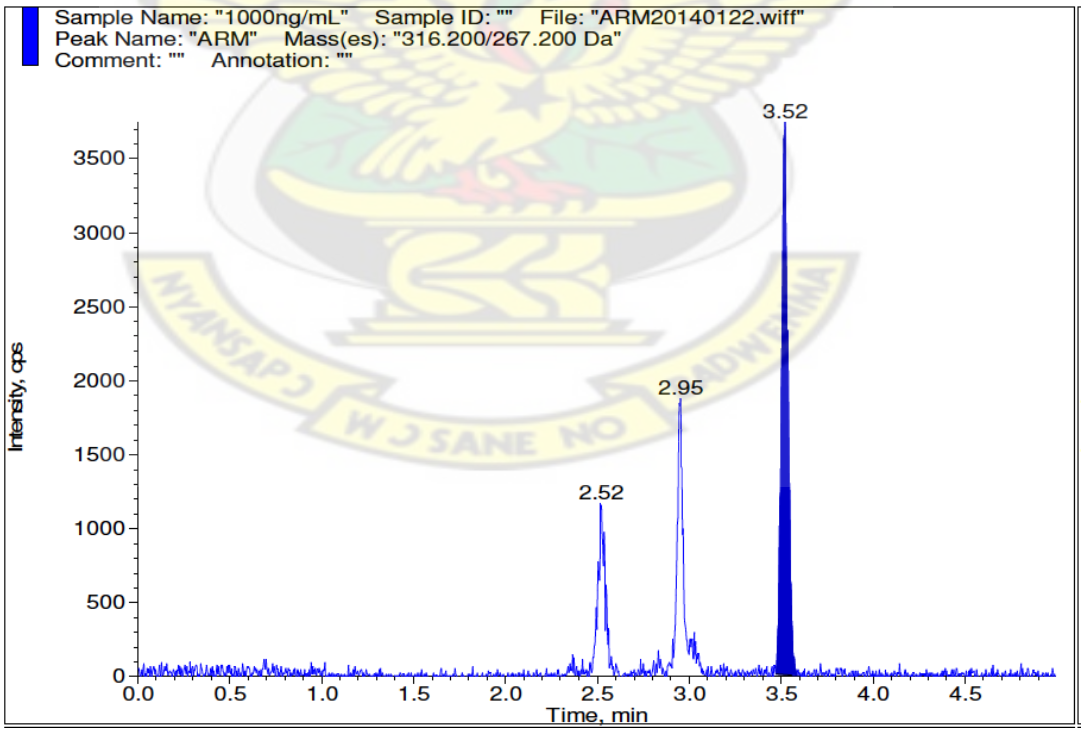

Figure 4.40 Chromatogram of extracted metabolite DHA 1000 ng/ml and ARM 1000 ng/ml with retention times of 2.95 and 3.52 minutes (standard) respectively

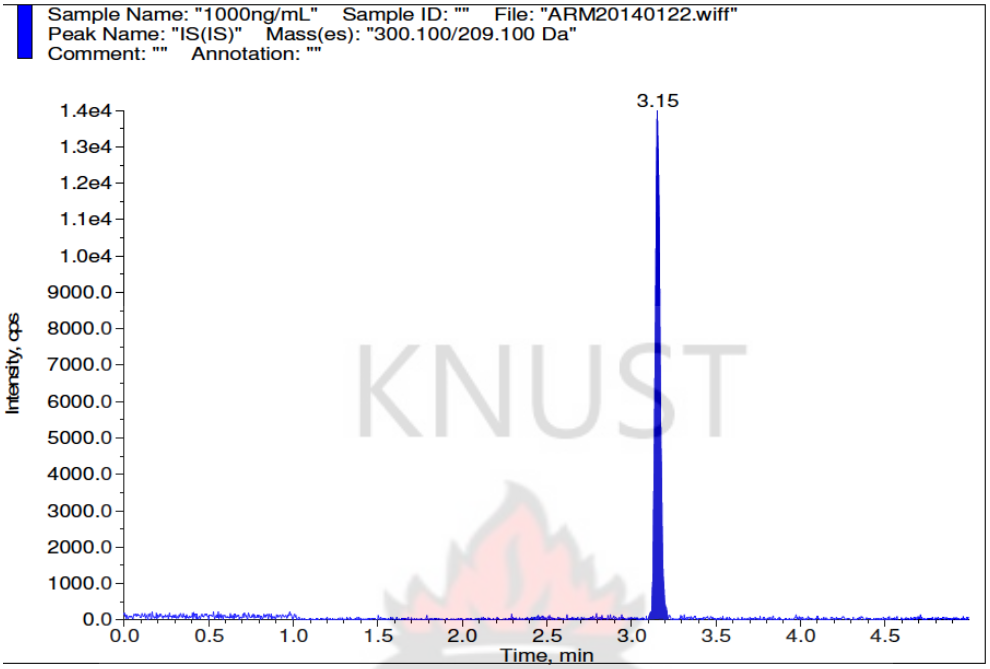

Figure 4.41 Chromatogram of 1000 ng/ml IS (standard) with retention time of 3.15 minutes

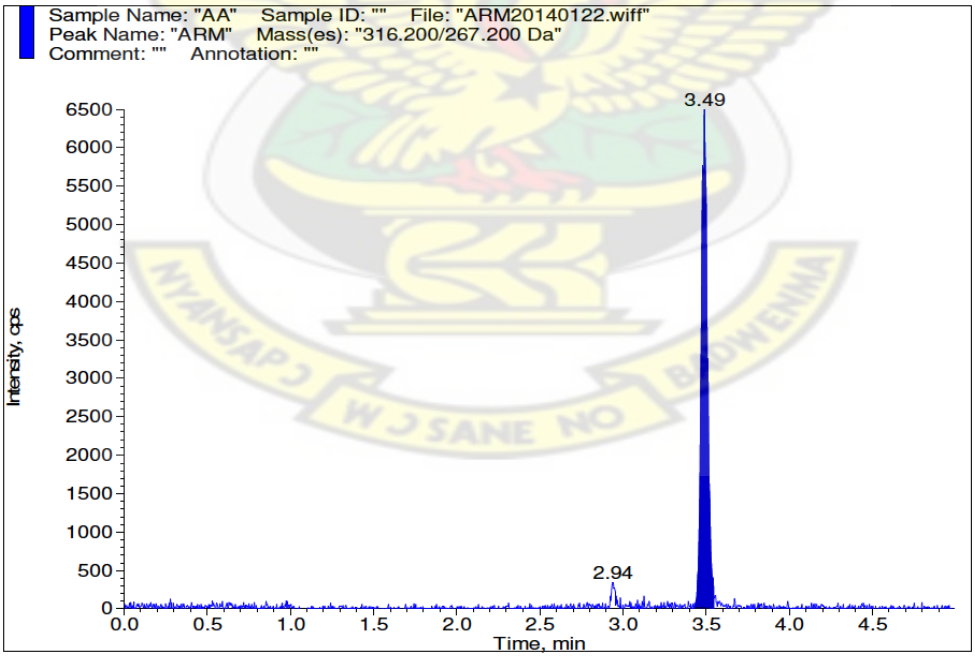

Figure 4.42 Chromatogram of extracted metabolite DHA and ARM with retention times of 2.94 and 3.49 minutes from 1-hour plasma sample of rat 1

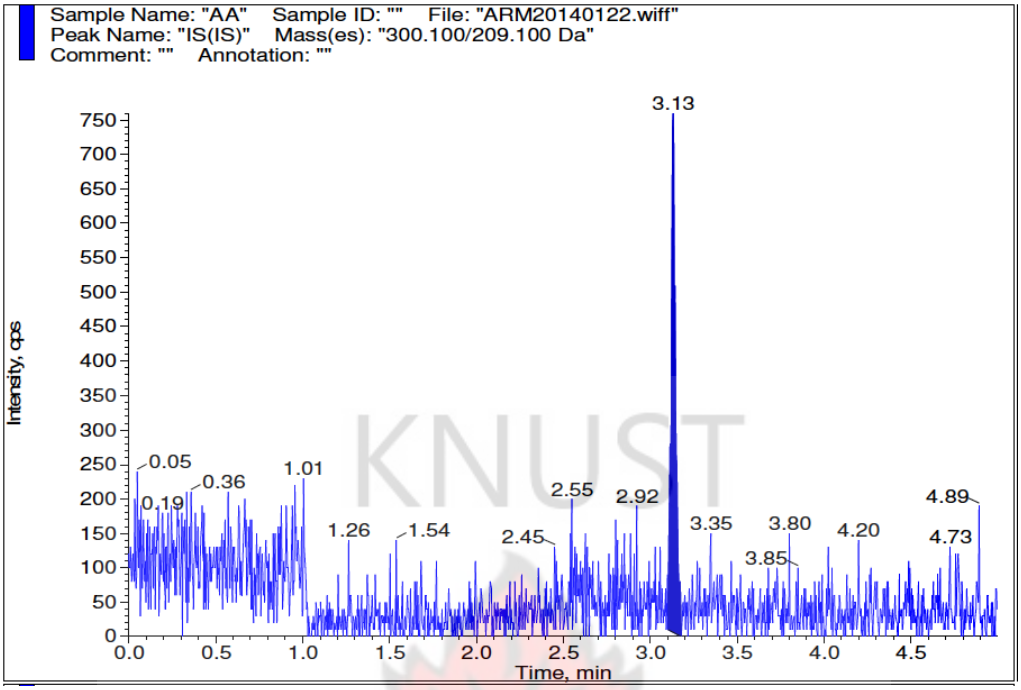

Figure 4.43 Chromatogram of extracted IS with retention times of 3.13 minutes, from 1-hour plasma sample of rat 1

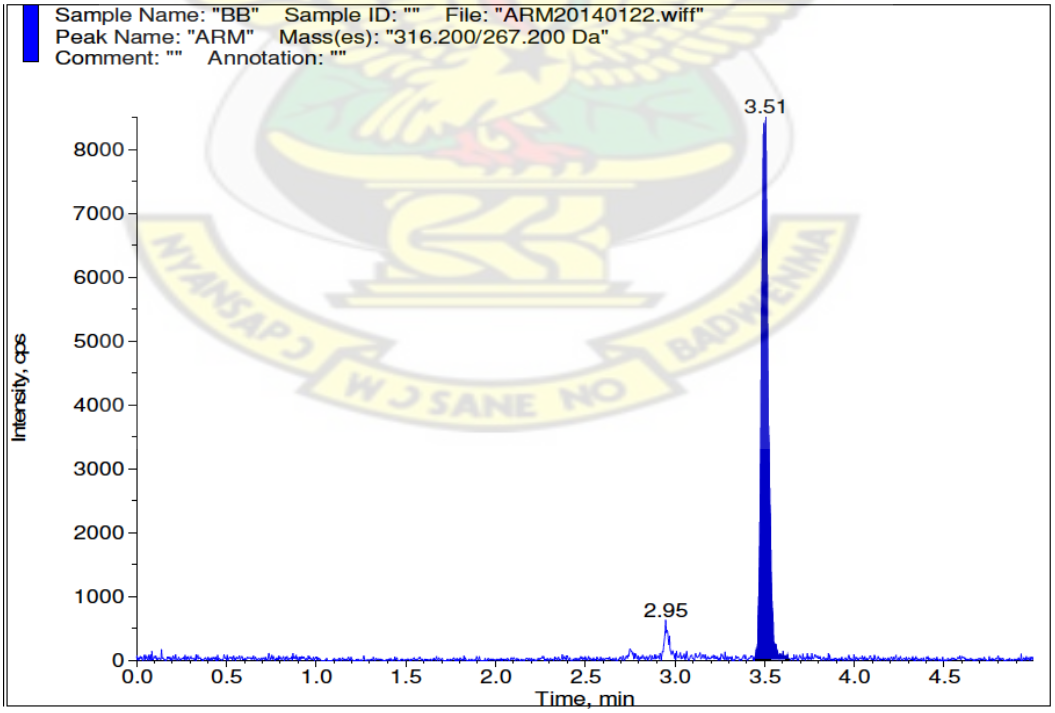

Figure 4.44 Chromatogram of extracted metabolite DHA and ARM with retention times of 2.95 and 3.51 minutes respectively from 1-hour plasma sample of rat 2

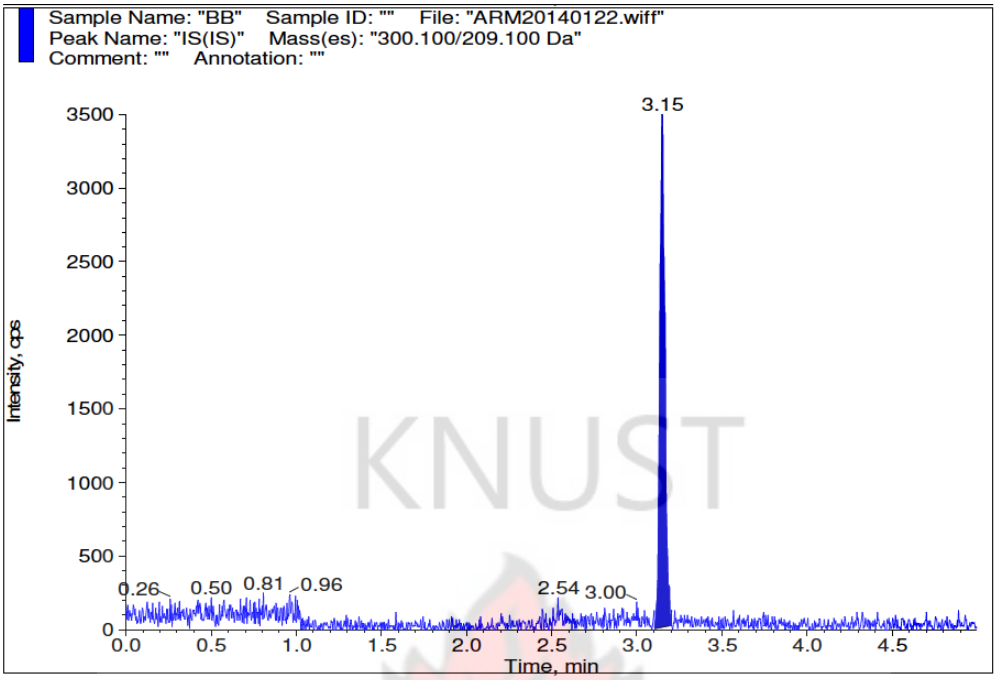

Figure 4.45 Chromatogram of extracted IS with retention time of 3.15 minutes, from 1-hour plasma sample of rat 2

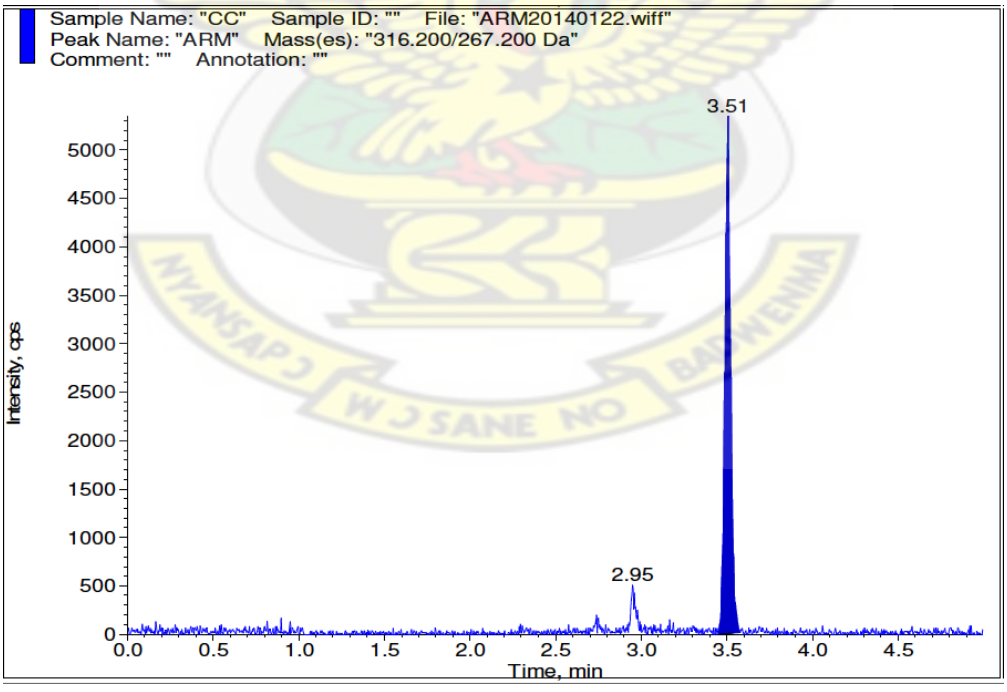

Figure 4.46 Chromatogram of extracted metabolite DHA and ARM with retention times of 2.95 and 3.51 minutes from 1-hour plasma sample of rat 3

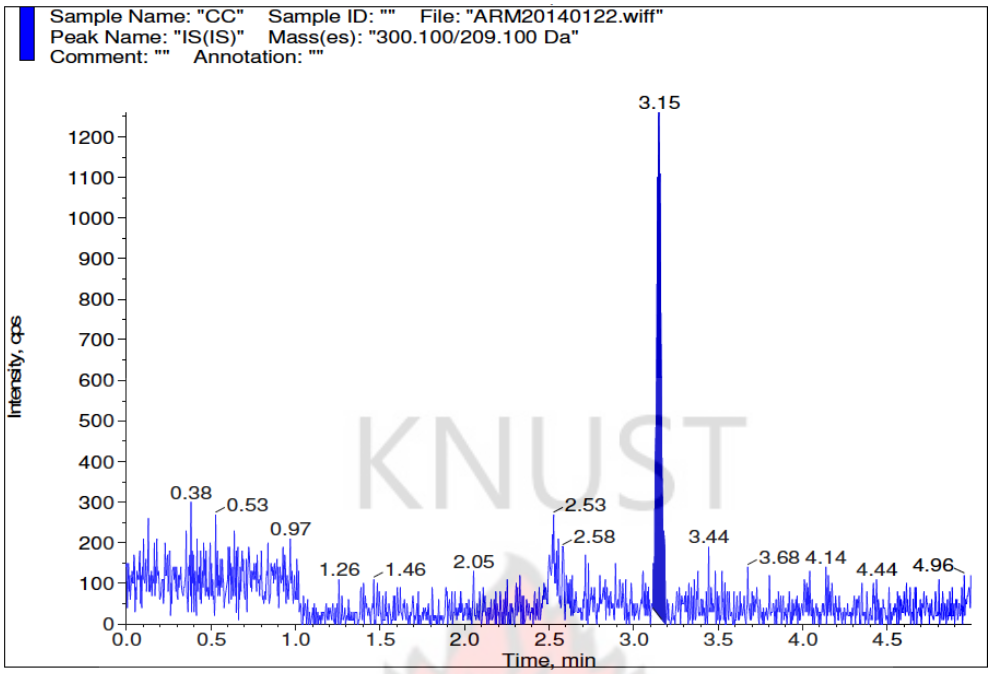

Figure 4.47 Chromatogram of extracted IS with retention time of 3.15 minutes, from 1-hour plasma sample of rat 2

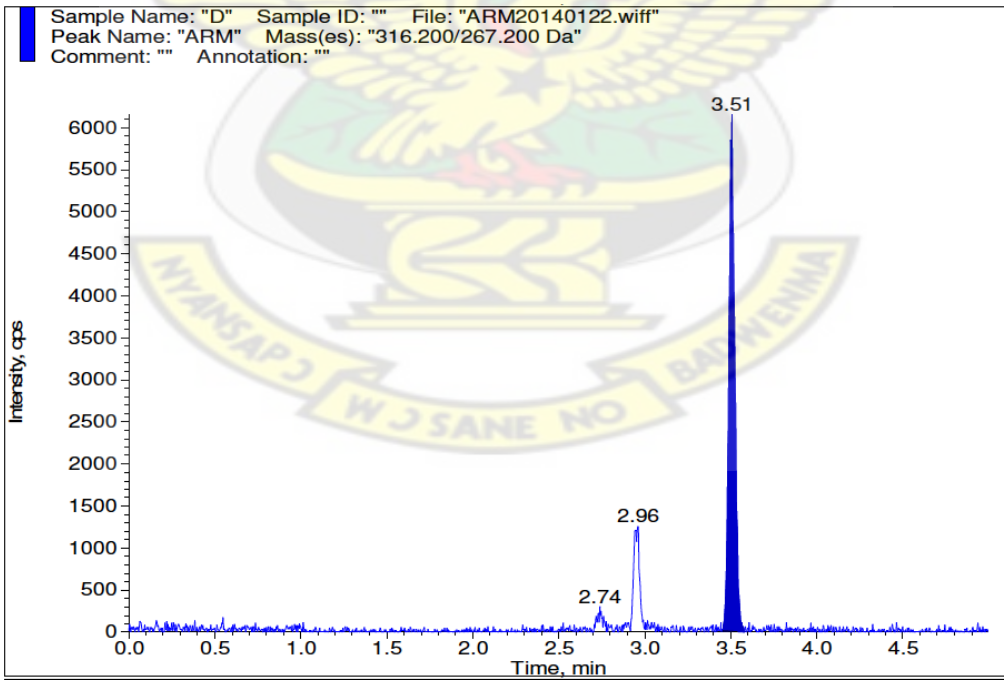

Figure 4.48 Chromatogram of extracted metabolite DHA and ARM with retention times of 2.96 and 3.51 minutes respectively from 24-hour plasma sample of rat 1

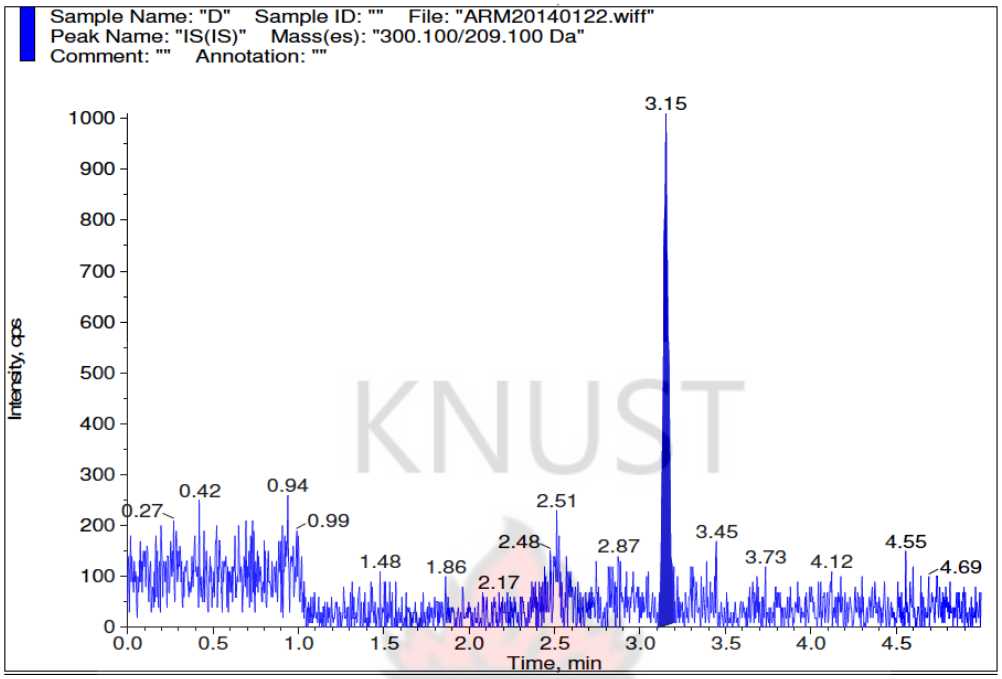

Figure 4.49 Chromatogram of extracted IS with retention time of 3.15 minutes, from 24-hour plasma sample of rat 1

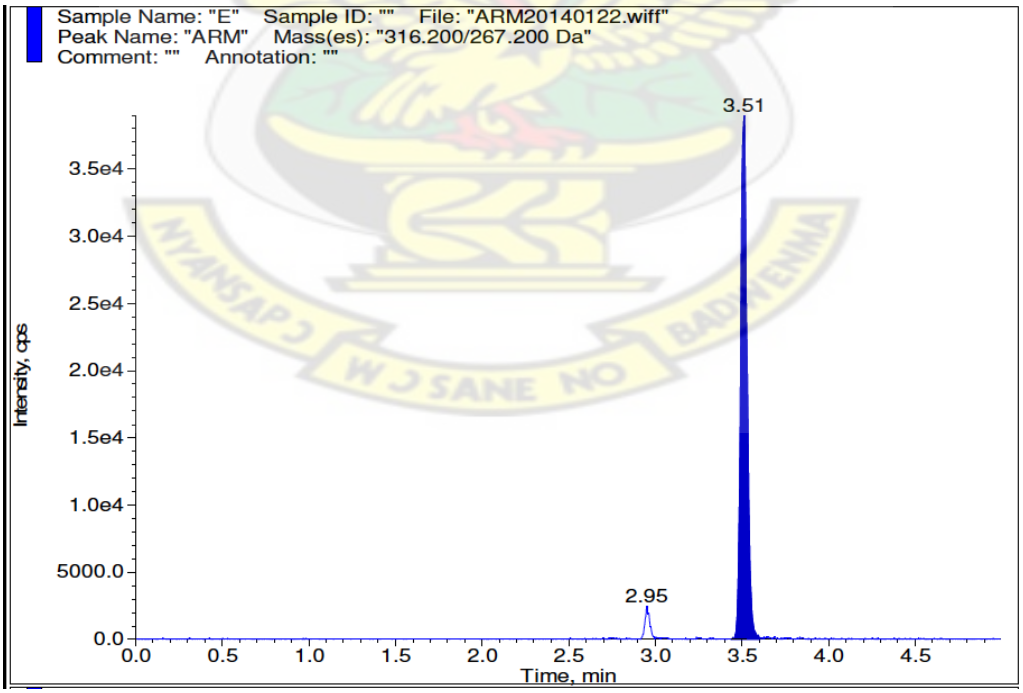

Figure 4.50 Chromatogram of extracted metabolite DHA and ARM with retention times of 2.95 and 3.51 minutes from 24-hour plasma sample of rat 1

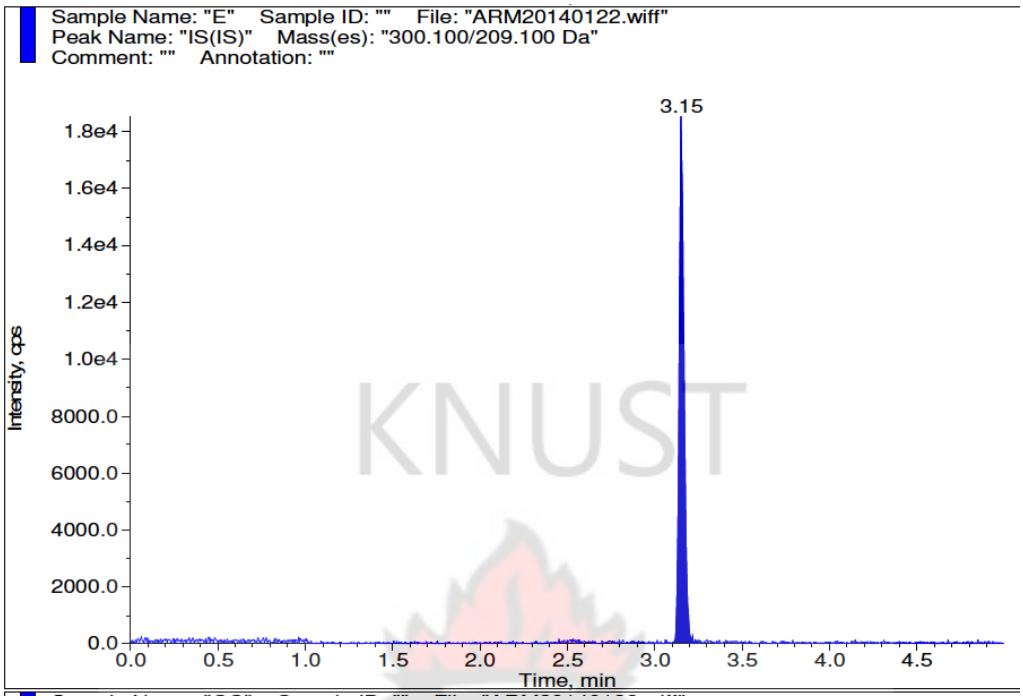

Figure 4.51 Chromatogram of extracted IS with retention of time 3.15 minutes, from 24-hour plasma sample of rat 2

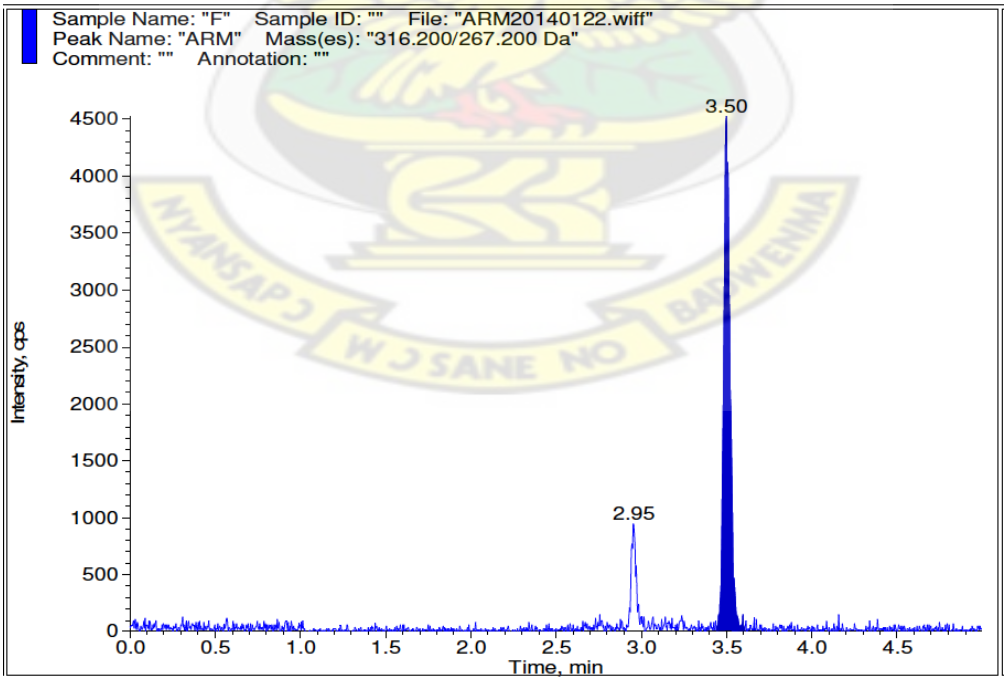

Figure 4.52 Chromatogram of extracted metabolite DHA and ARM with retention times of 2.95 and 3.50 minutes respectively from 24-hour plasma sample of rat

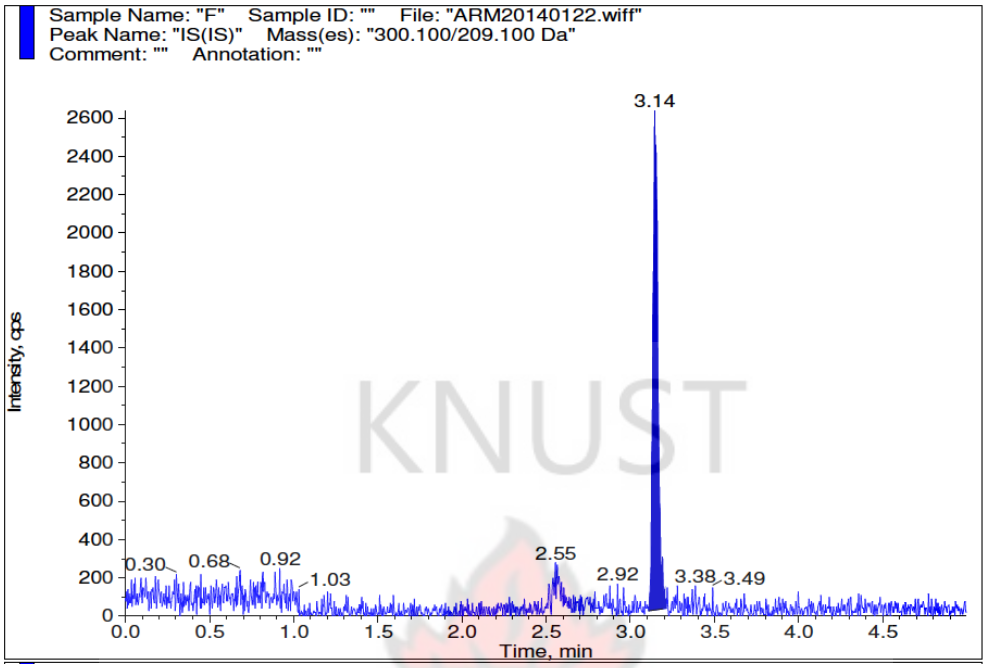

Figure 4.53 Chromatogram of extracted IS with retention time of 3.14 minutes, from 24-hour plasma sample of rat 2

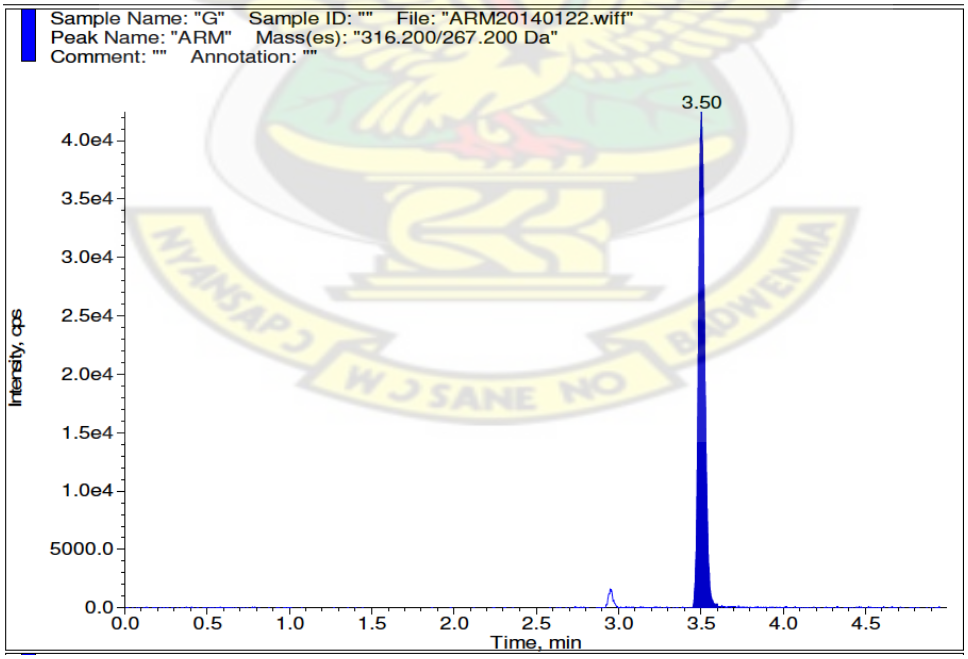

Figure 4.54 Chromatogram of extracted metabolite DHA and ARM with retention times of 2.90 and 3.50 minutes respectively from 24-hour plasma sample of rat 1

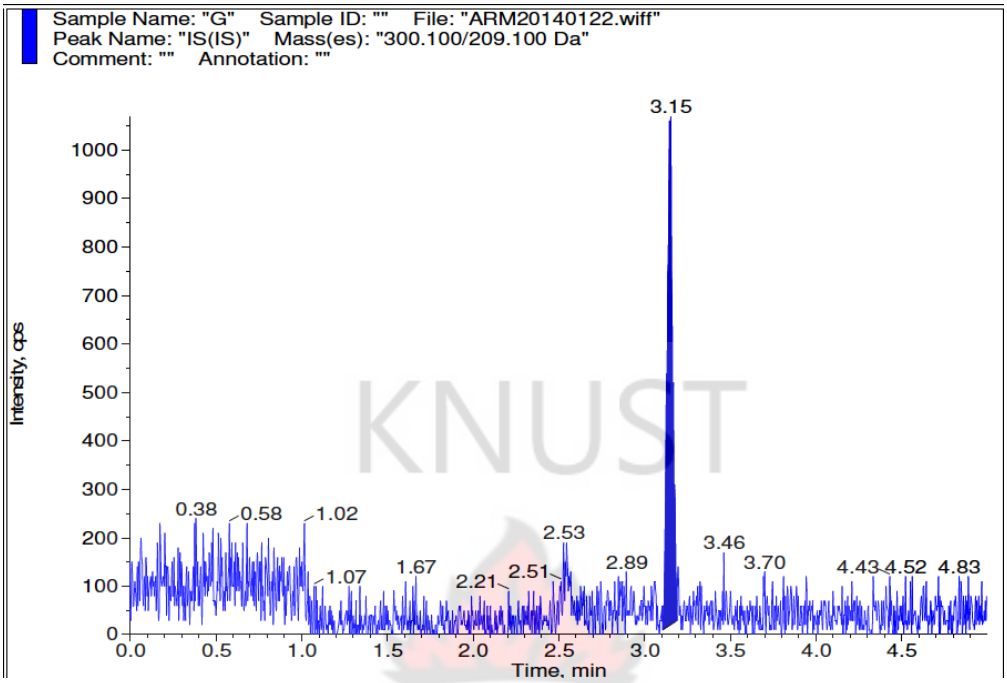

Figure 4.55 Chromatogram of extracted IS with retention time of 3.15 minutes, from 72-hour plasma sample of rat 1

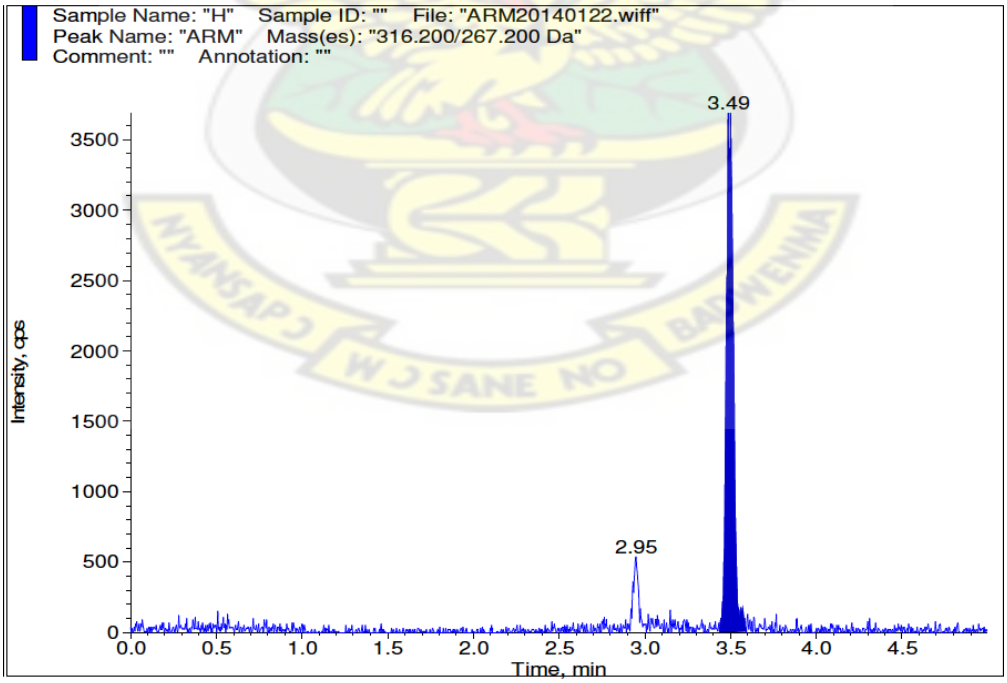

Figure 4.56 Chromatogram of extracted metabolite DHA and ARM with retention times 2.95 and 3.49 minutes respectively from 24-hour plasma sample of rat 2

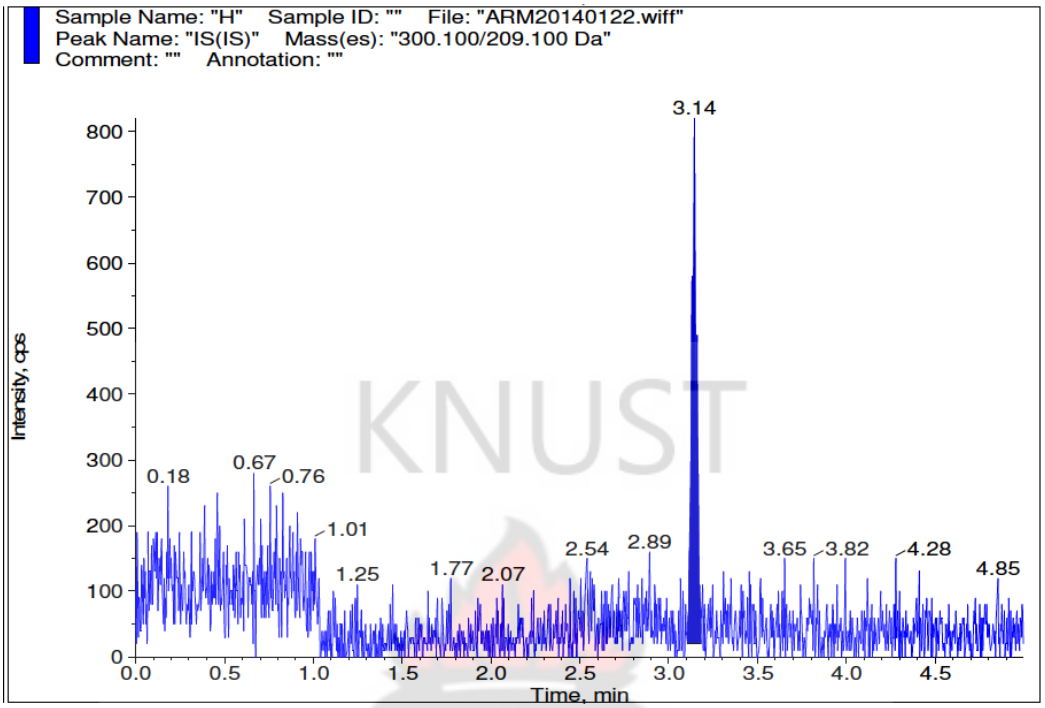

Figure 4.57 Chromatogram of extracted IS, retention time 3.14 minutes, from 72-hour plasma sample of rat 2

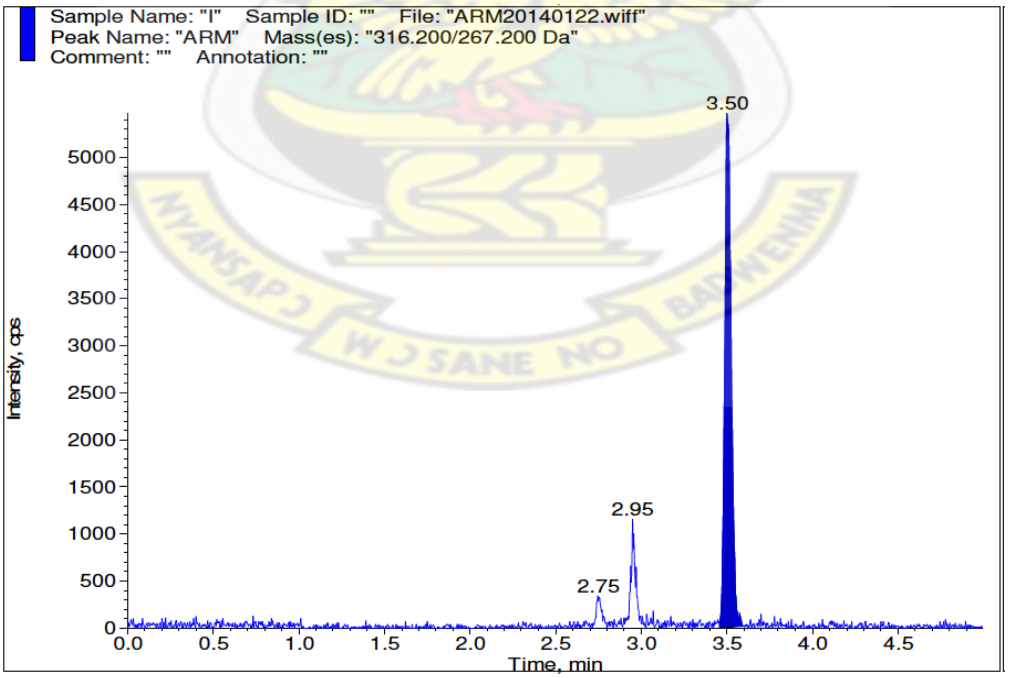

Figure 4.58 Chromatogram of extracted metabolite DHA and ARM retention times 2.95 and 3.50 minutes from 24-hour plasma sample of rat 3

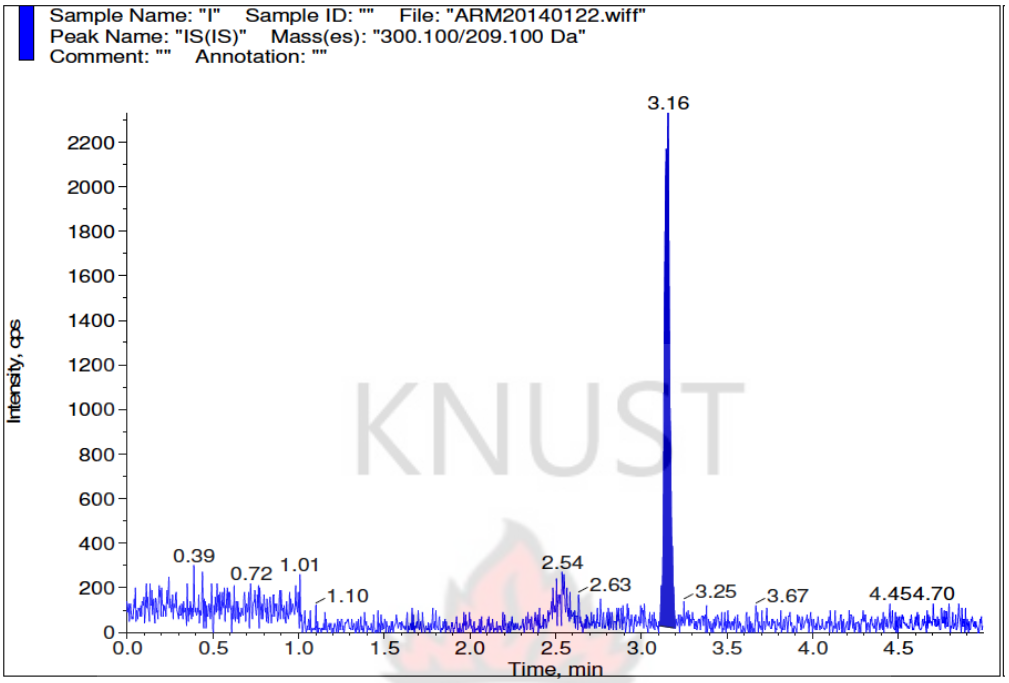

Figure 4.59 Chromatogram of extracted IS with retention time of 3.16 minutes, from 72-hour plasma sample of rat 2

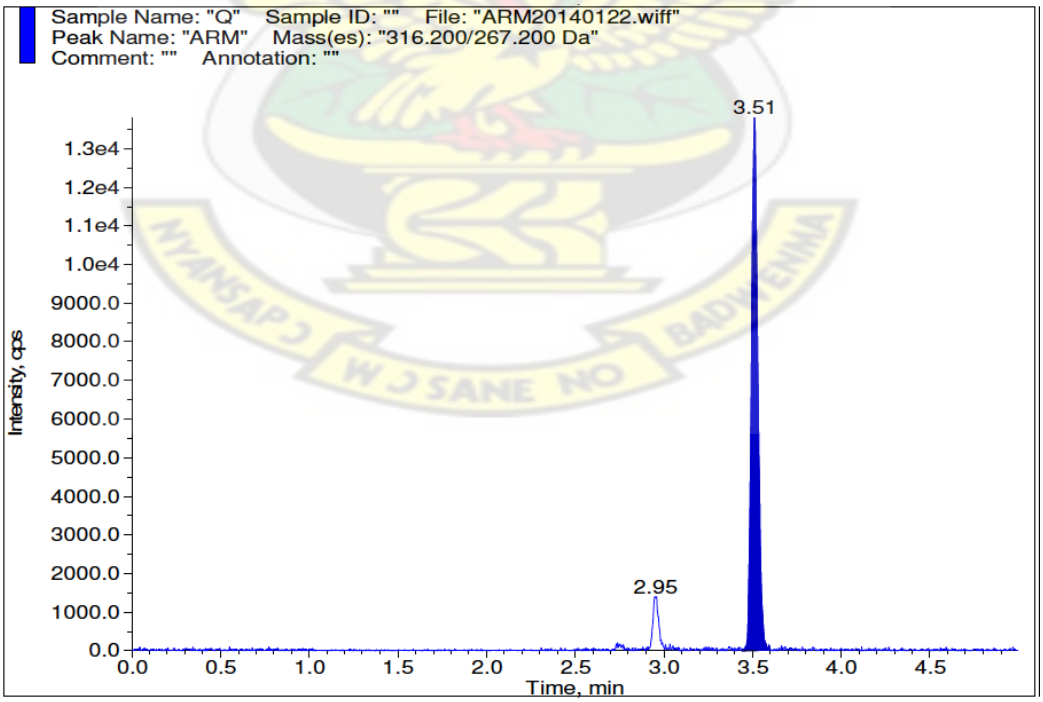

Figure 4.60 Chromatogram of extracted metabolite DHA and ARM with retention times of 2.95 and 3.51 minutes respectively from 168-hour plasma sample of rat 1

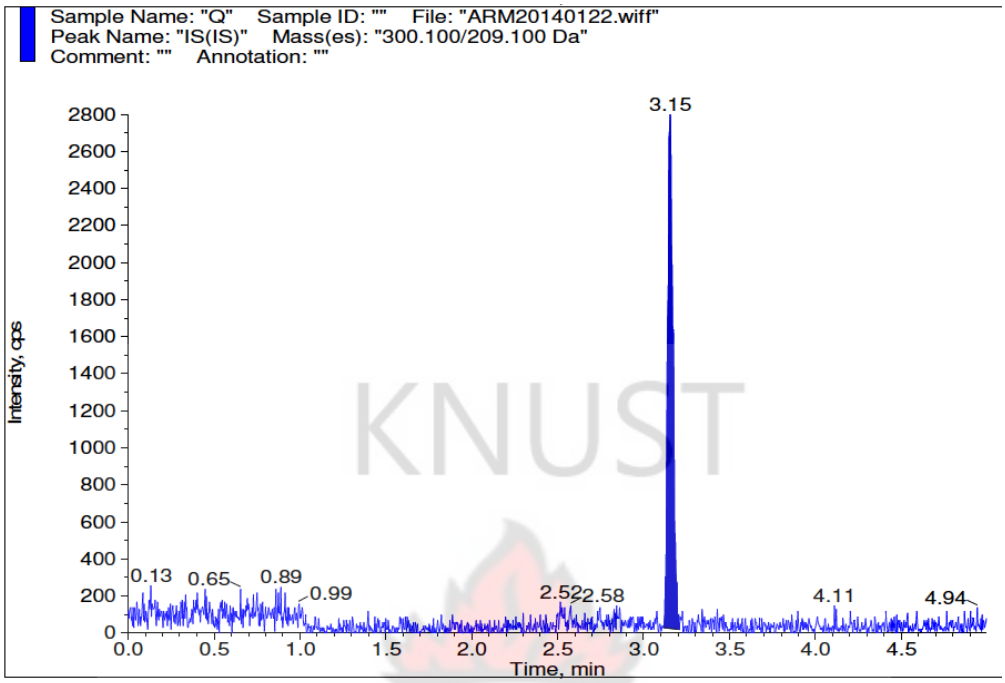

Figure 4.61 Chromatogram of extracted IS with retention time of 3.15 minutes, from 168-hour plasma sample of rat 1

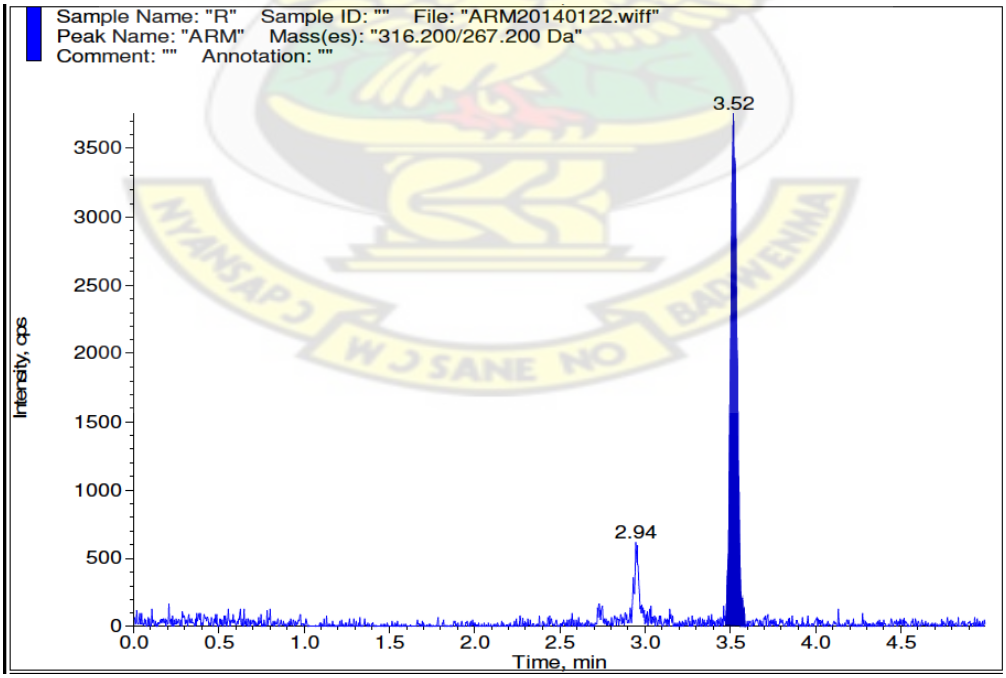

Figure 4.62 Chromatogram of extracted metabolite DHA and ARM with retention times of 2.94 and 3.52 minutes from 168-hour plasma sample of rat 2

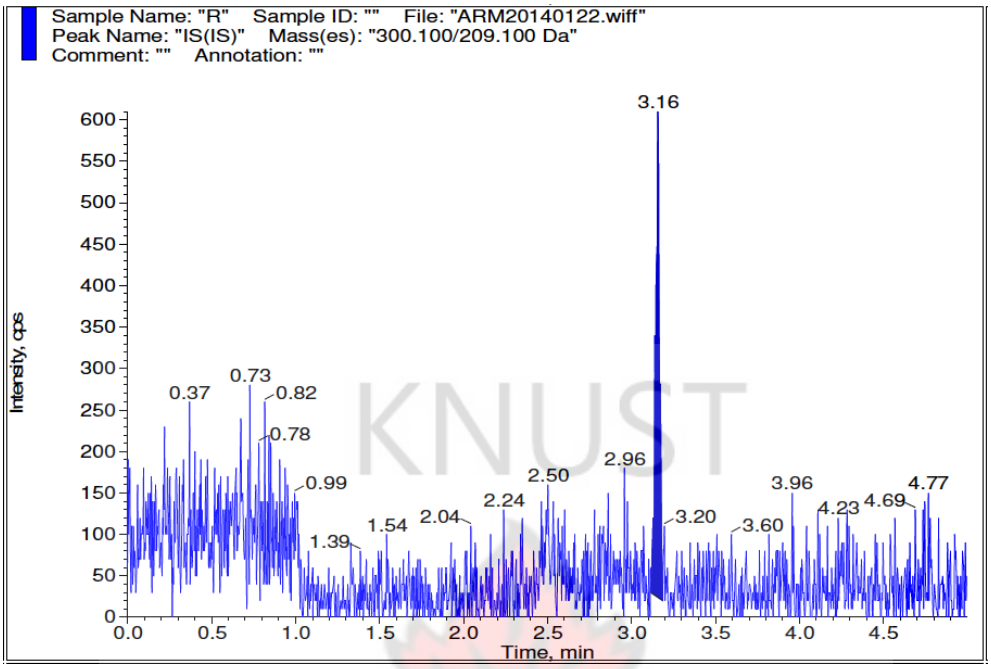

Figure 4.63 Chromatogram of extracted IS with retention time of 3.16 minutes, from 168-hour plasma sample of rat 2

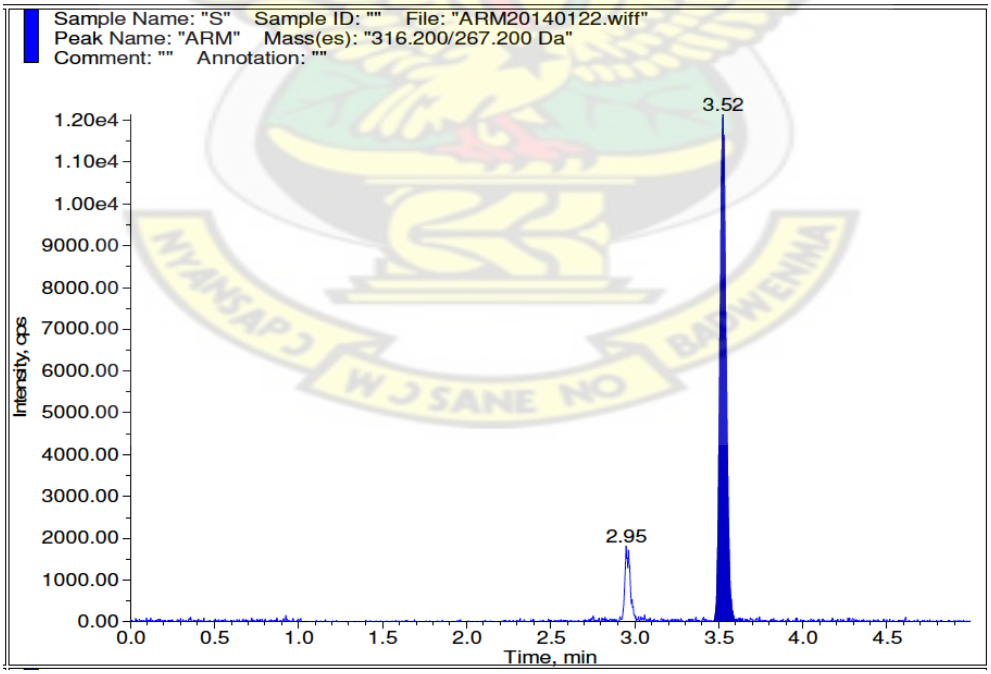

Figure 4.64 Chromatogram of extracted metabolite DHA and ARM with retention times of 2.95 and 3.52 minutes from 168-hour plasma sample of rat 3

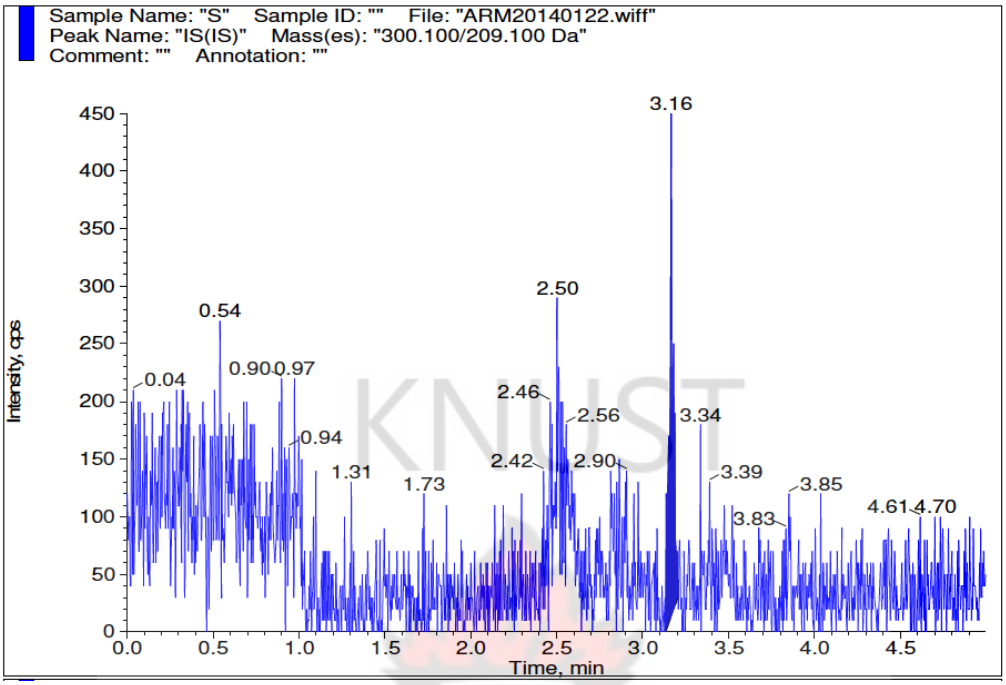

Figure 4.65 Chromatogram of extracted IS with retention time of 3.16 minutes, from 168-hour plasma sample of rat 3

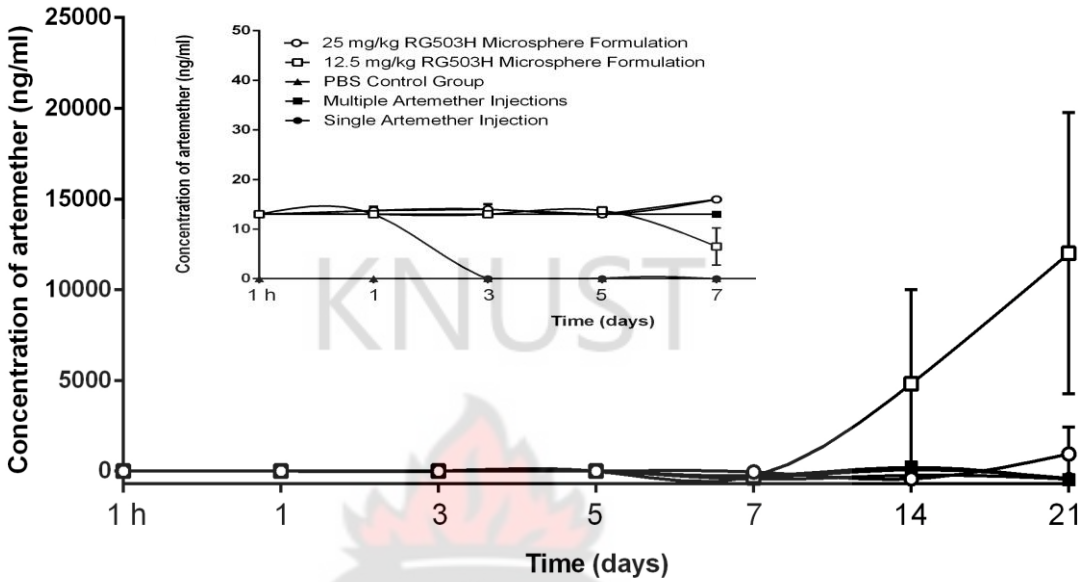

Figure 4.66 Plasma concentration-time profile of artemether extracted from rat plasma in 21 day *in vivo* release study.

Table 4.12 Pharmacokinetic parameters of artemether by non-compartmental model using trapezoidal rule following SC injections of male Sprague-Dawley rats (n = 4 per group)

	Group 2	**Group 3**	**Group 4**	**Group 5**
C_{max} (μg/ml)	12.01125	0.01375	0.21975	0.08225
T_{max} (h)	504	24	336	336
AUC (μg.h/ml) **SD**	1815.8995 ±1468.25	6.8215 ± 6.14	59.8675 ± 44.57	8.5225 ± 13.94

Table 4.13 Key to rat groupings for plasma concentration-time profile and pharmacokinetic parameters of artemether

Rat groups	**Treatment**
Group 1	Negative control group (injection vehicle only)
Group 2	Low dose artemether-loaded microsphere single injection
Group 3	High dose artemether-loaded microsphere single injection
Group 4	Artemether multiple injections (conventional dosing)
Group 5	High dose artemether (single injection)

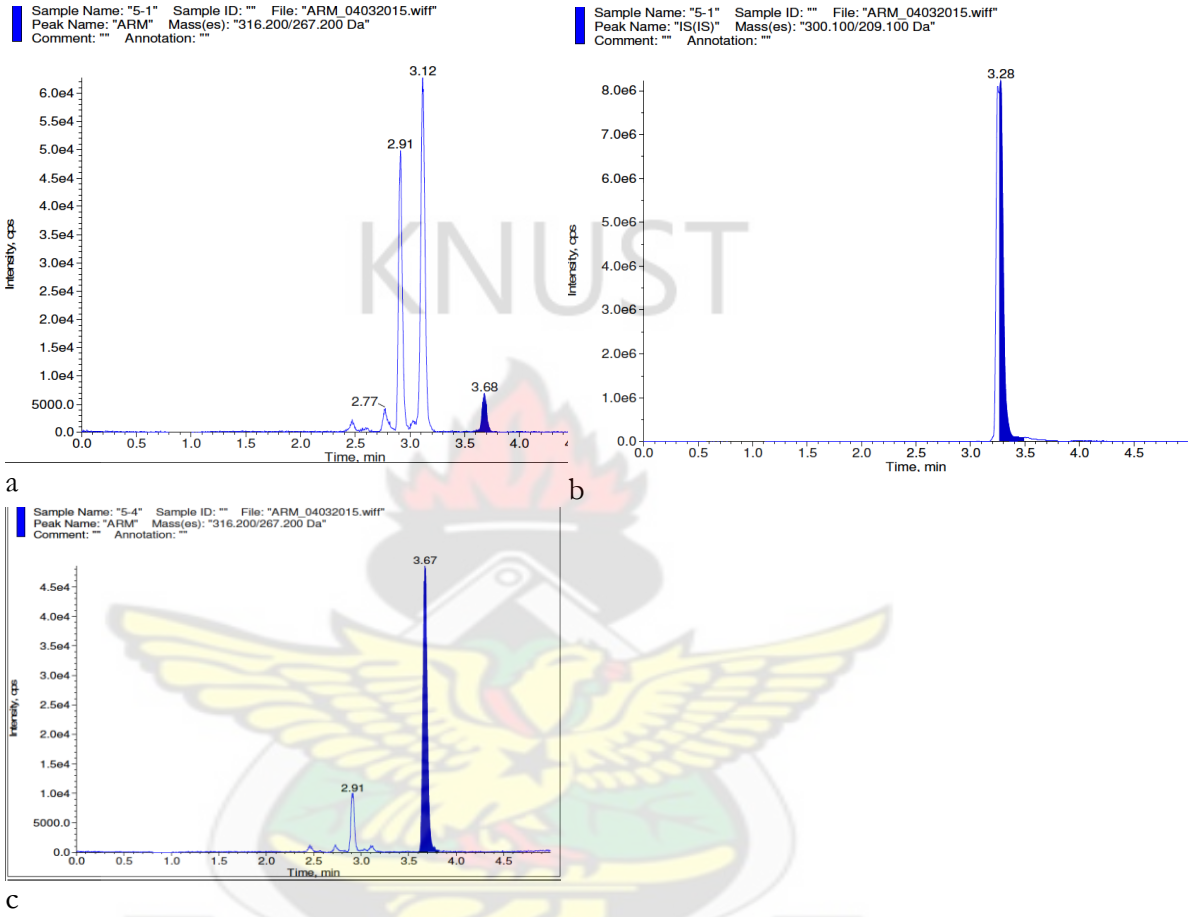

Figure 4.67 Chromatograms for low dose microsphere group (a) Artemether and dihydroartemisinin (b) Artemisinin (IS) one hour plasma sample and (c) presence of artemether and dihydroartemisinin in day 7 plasma sample

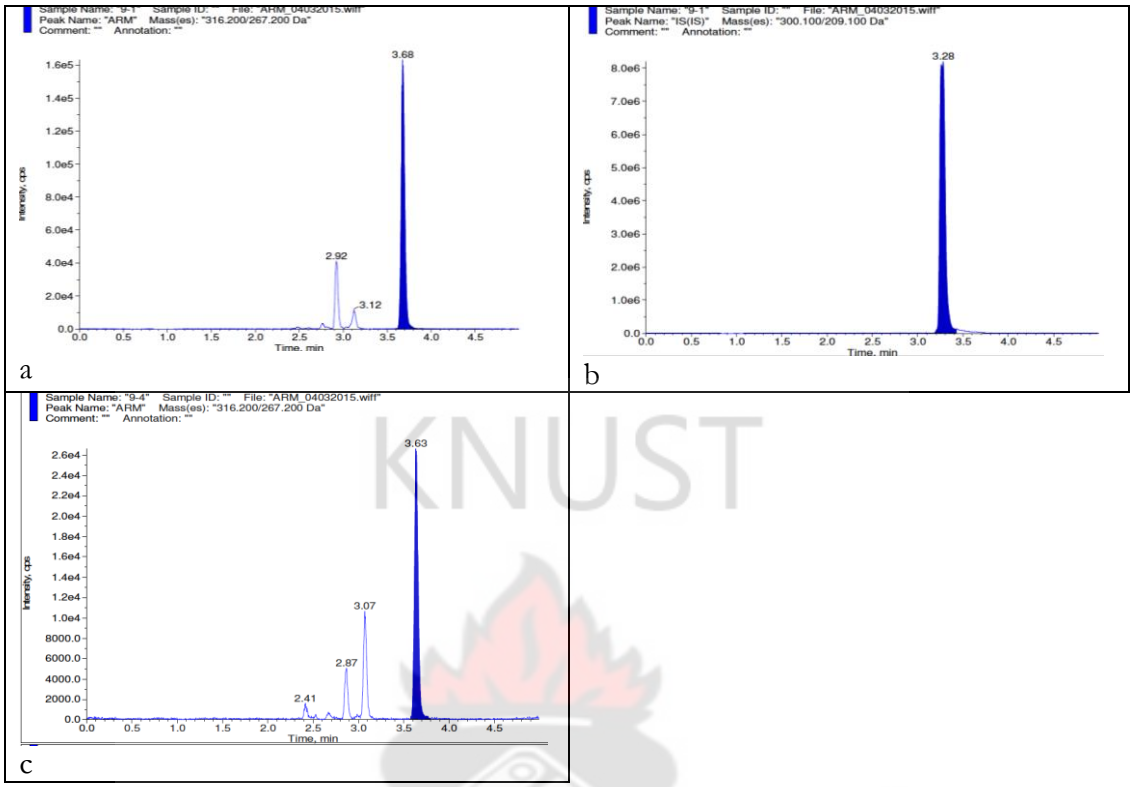

Figure 4.68 Chromatograms for High dose microsphere group (a) Artemether and dihydroartemisinin (b) Artemisinin (IS) one hour plasma sample and (c) presence of artemether and dihydroartemisinin in day 7 plasma sample

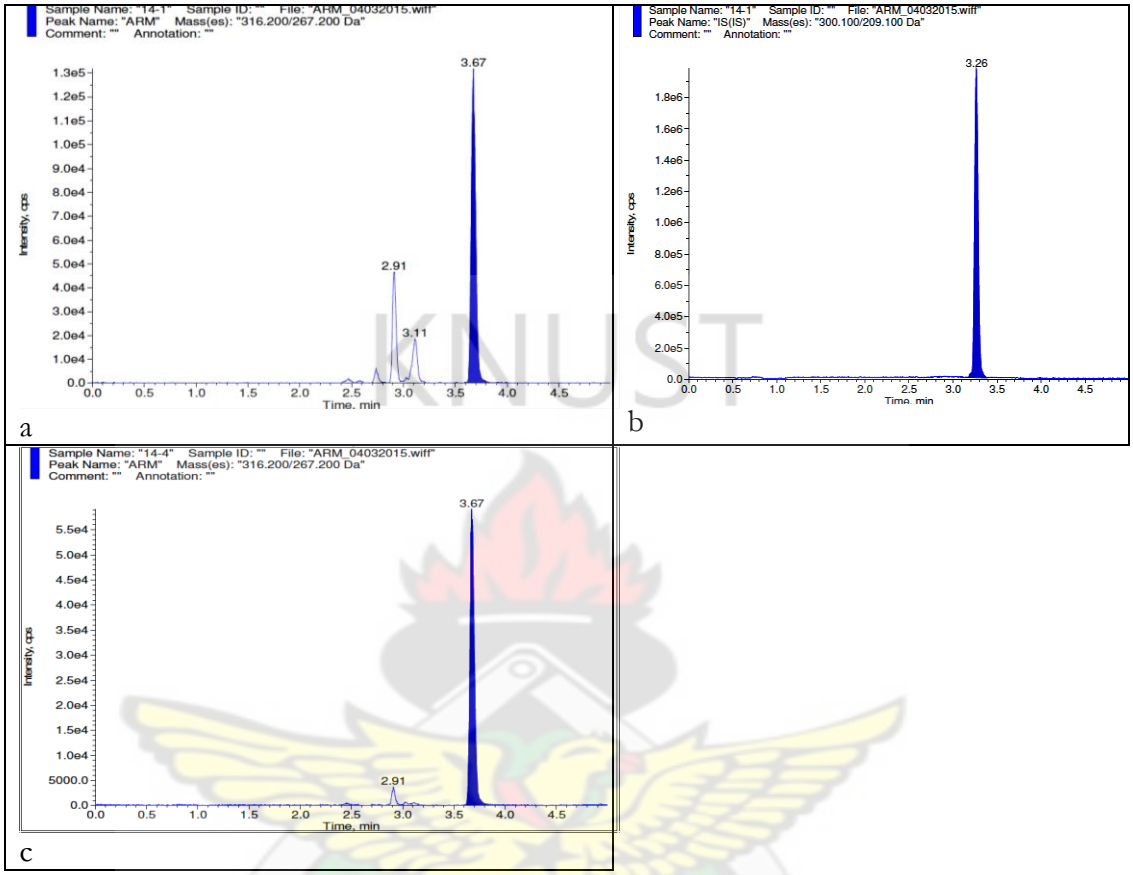

Figure 4.69 Chromatograms Artemether multiple injections (conventional) group (a) Artemether and dihydroartemisinin (b) Artemisinin (IS) one hour plasma sample and (c) presence of artemether and dihydroartemisinin in day 7 plasma sample

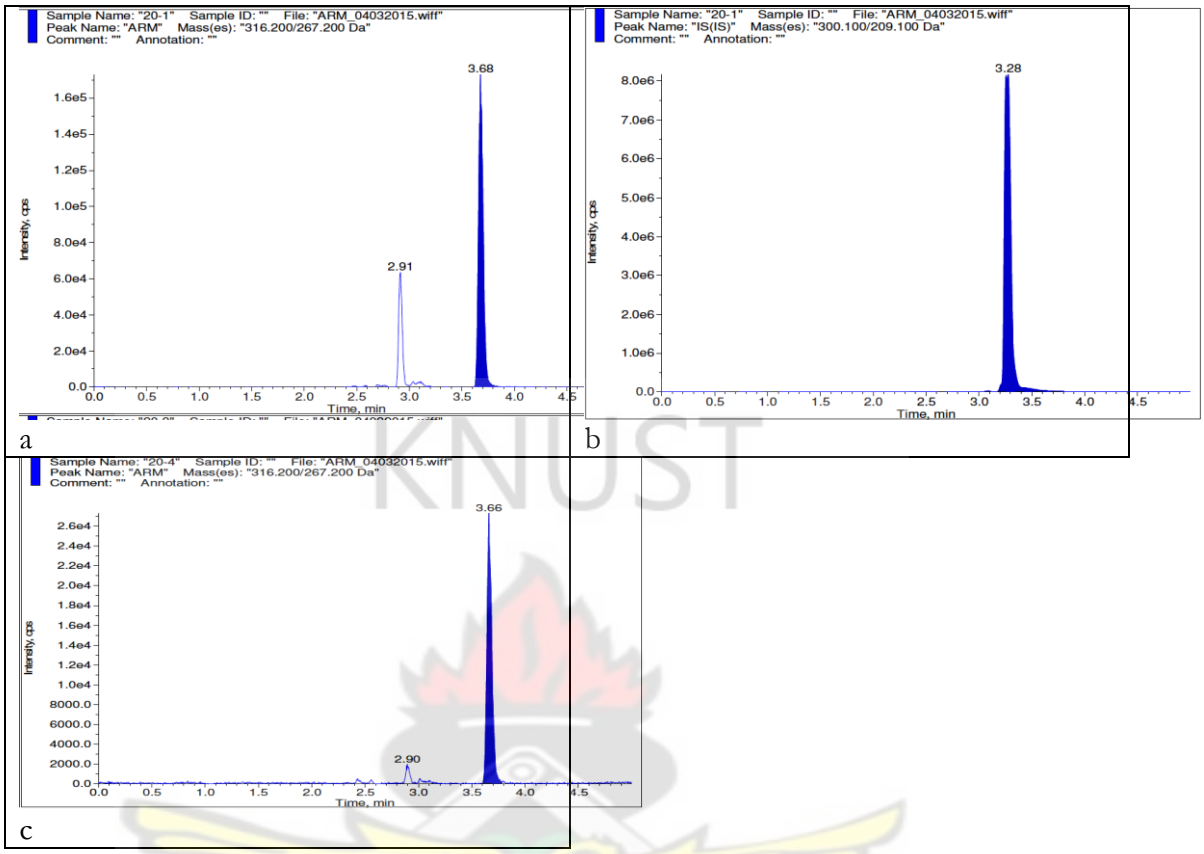

Figure 4.70 Chromatograms for Artemether single injections group (a) Artemether and dihydroartemisinin (b) Artemisinin (IS) one hour plasma sample and (c) presence of artemether and dihydroartemisinin in day 7 plasma sample

Chapter 5

DISCUSSIONS, CONCLUSIONS AND RECOMMENDATIONS

5.1 DISCUSSIONS

Severe malaria has increasingly been a cause of morbidity and mortality among children under five especially those living in sub-Saharan Africa. The current use of intramuscular artemether IM injections for the treatment of severe malaria has many limitations. Although artemether has a quick onset of action, which makes it suitable for initial and substantial reduction of *plasmodium* parasite load, its short half-life necessitates multiple injections which are also associated with many undesirable effects as well as poor patient compliance.

A number of formulations have been prepared with artemether over the years with the aim of improving the treatment outcomes of severe malaria through better delivery of artemether. These formulations include self-microemulsifying suppositories, intranasal nanostructured lipid carriers (NLC) and microemulsions. The limitations of these formulations range from low drug loading and encapsulation efficiencies and inability to control the release of artemether thus requiring multiple administrations to patient acceptability problems, just to mention a few (Joshi *et al*., 2008; Tayade *et al*., 2010, Gugulothu *et al*., 2010; Jain *et al*., 2015).

The formulation of a controlled release dosage form with artemether with a high encapsulation efficiency using an easily reproducible technique that can be scaled up with ease will help to improve the treatment of severe malaria substantially by overcoming the limitations of the current available formulations.

Since children under five are the most affected by the disease, a formulation targeted to this population group can help to drastically reduce the incidence of malaria mortality significantly.

The total dose required to be incorporated in a single IM injection for six months old infant with a body weight of 5 kilogrammes was calculated as 64 mg. The use of artemether in children below six months is prohibited (Standard Treatment Guidelines, 2010). The total mass of microspheres that can be given by a single IM injection is 250 mg. The percentage drug loading obtained for RG502H and RG503H formulations were 20 % and 25 % respectively. Hence for the RG502H and RG503H formulations, 50 mg and 63 mg of artemether can be incorporated respectively. The RG503H formulation can successfully be administered as a single injection. To achieve same for the RG502H formulation, the formulation parameters may be manipulated to obtain higher drug loading. Alternatively, 2 injections may be administered to replace the multiple injections.

The single emulsion solvent evaporation method was used in the formulation of the artemether-loaded microspheres. The use of vortex mixing initially in the formation of the emulsion yielded microspheres with sizes above 90 μm and light microscopy imaging of the formulated microspheres showed that the individual particles were clumped together as depicted in Figure 4.1. The clumps formed could possibly cause aggregation and uneven loading of artemether in the microspheres. Homogenization was therefore introduced to obtain well-formed microspheres with no clumps or aggregates and less than 90 μm in diameter (Figures 4.2 and 4.3).

The choice of the single emulsion solvent evaporation method of formulation of microspheres yielded well-formed microspheres with a method that was simple, easy to scale up and required less organic solvent as compared to other methods such as phase separation, spray drying and other supercritical fluid methods (Nahata and Saini, 2008).

The speeds and times of homogenization that yielded the highest amounts of artemether-loaded microspheres differed for the different molecular weights of PLGA used. The size range of artemether-loaded microspheres chosen for the intramuscular injection formulation was 45-90 μm. This microparticle size range is small enough for IM injection and large enough not to be engulfed by cells at the site of injection. This falls within, the size range that is most applicable to IM and subcutaneous administration, ~ 5 to 150 μm (Berkland *et al*., 2003). Microspheres which are injected intramuscularly may be engulfed by surrounding cells in phagocytosis. Anderson and Shive (2012) reported that microspheres larger than 10 μm in diameter were too large for phagocytosis. The formulations chosen for further analysis for both RG503H and RG502H respectively were those that produced the highest yield of microspheres of the size range 45-90 μm shown in Figures 4.6 and 4.7.

The method of formulation of the microspheres, which involves the emulsification process, in this case determines the size and size distribution of the microspheres produced. The size of the microspheres in terms of their diameters may also affect the rate of drug release, syringeability, drug loading and loading efficiency as well as the ability of phagocytic cells to engulf the microspheres. The biodistribution of the microspheres after IM injection may also be affected by the size of the microspheres (Berkland *et al*., 2002). Thus, any method and series of procedures employed to

formulate microspheres must yield microspheres of the desired size range for ease of clinical application and effectiveness. Thus the single emulsion solvent evaporation method was successfully used to formulate artemether-loaded PLGA microspheres.

In the dissolution testing of drugs, the maintenance of sink conditions is a requirement for hydrophobic drugs with low water solubility. This is because sink conditions increases the *in vitro* dissolution rate of hydrophobic drugs (Liu *et al*., 2013). Artemether is a hydrophobic drug with a log octanol-water partition coefficient (log P) of 3.51 and a water solubility of 0.16 mg/ ml, which is very slightly soluble. A log P value of greater than zero characterizes hydrophobic substances soluble in the lipid phase. The use of 50 ml of PBST release medium in the *in vitro* release study was intended to maintain sink conditions. This volume (50 ml) was large enough to completely dissolve the expected amount of artemether (2-2.5 mg) in the 10 mg of microspheres. The use of PBST instead of phosphate buffer solution (PBS) was meant to improve the wetting of the microspheres. This is because tween 80, which is a surfactant and a component of PBST, improves the wettability of the microspheres and prevents agglomeration of the microspheres which reduces the surface-area-to-volume ratio of the microspheres in solution (Wischke and Schwendeman, 2008).

The coefficient of correlation values of 0.9979 and 0.79469 shown in Figures 4.8 and 4.9 respectively show that artemether was more soluble in 60 % acetonitrile in water than in the PBST buffer. This further informed the decision to measure the amount of artemether released by calculating from the amount loaded although sink conditions were ensured. The amount of artemether in the release media would otherwise have been difficult to quantify accurately.

The percentage drug loading and corresponding encapsulation efficiencies of artemether were high for both the low and high molecular weight PLGA microsphere formulations, but were higher with the higher molecular weight RG503H PLGA. The high values obtained for both formulations may be the result of the use of the relatively hydrophilic PLGA that possesses free carboxylic end groups.

Yeo and Park (2004) reported that PLGA with free carboxylic end groups RG503H and RG502H produce higher encapsulation efficiencies than end-capped polymers such as RG502 and RG503. The relatively hydrophilic PLGA, which carries free carboxylic end groups precipitates faster than the end-capped polymer since its solubility is less in methylene chloride. Moreover, the stability of the primary emulsion formed by the more hydrophilic PLGA, which promotes higher encapsulation efficiency, is conferred by its high hydrophilic nature. The choice of methylene chloride as organic solvent also contributed to the high encapsulation efficiency. This confirms the findings of Bodmeier and McGinity (1987) who compared the encapsulation efficiency obtained when methylene chloride was used as solvent compared to chloroform or benzene. They reported that poly lactic acid (PLA) was more soluble in methylene chloride and the encapsulation efficiency produced was higher (Bodmeier and McGinity, 1988).

Comparatively, the higher molecular weight RG503H showed higher drug loading and encapsulation efficiency than the lower molecular weight RG502H. Figures 4.12 and 4.13 show the particle size distribution of the PGLA microspheres. The particle sizes of the microspheres of the two polymer formulations were normally distributed, which is a good indication of the polydisperse nature of the microspheres formulated.

Figures 4.14 and 4.15 present the SEM images of blank and artemether-loaded PLGA microspheres of the two resomers. In general, the microspheres were spherical in shape. The microspheres had smooth non-porous surfaces. The particle size range obtained from the SEM analysis corresponded with the size range obtained from the particle size analysis. The spherical shape of the particles observed under light microscopy (Figures 4.1 – 4.3) also corresponded with the shape observed in the SEM analysis. Thus, well-formed, spherical microspheres with smooth unbroken surfaces were formulated. The initial burst release observed was due to desorption of artemether adsorbed on the surface of the microspheres. Figures 4.14 and 4.15 show that there was no difference in particle size and particle morphology between the blank microspheres and the artemether-loaded microspheres. This could be due to the efficient encapsulation and uniform distribution of artemether in the microspheres.

Generally, the release pattern of drugs from PLGA microspheres may be dependent on diffusion, erosion, osmotic-mediated events or a combination of all three mechanisms (Shenderova *et al*., 1997). The erosion mechanisms are based on the characteristics of the polymer and the drug. The type of polymer and the degradation profile of the polymer affect drug release from polymer microspheres. With respect to the degradation profile of the polymer, they may be classified as surface-eroding or bulk-eroding polymers based on the rate of hydrolysis of their functional groups (Tamada & Langer, 1993; Bozdag *et al*., 2001; Kumar *et al*., 2002).

PLGA polymers are bulk-eroding polymers because permeation of water into the polymer matrix is achieved with degradation throughout the entire microsphere matrix (Saltzman, 2001). Figure 4.23 presents the molecular weight profiles of the RG503H

and RG502H formulations. The molecular weight of the RG503H formulation, remained steady from Day 0 to Day 1 after which it declined markedly to Day 14 with corresponding water uptake of 30 % (Figure 4.24). The RG502H formulation exhibited continuous decline in molecular weight over 14 days with corresponding elevated water uptake levels (57 %). The degradation profiles of the two polymer formulations show that bulk erosion of the polymers occurred. These degradation profiles of the two formulations also further confirm the report of von Burkersroda *et al*, (2002) that, at acidic and neutral pH PLGA matrices exhibit bulk-erosion.

The formulated microspheres were incubated in PBST release buffer at a neutral pH of 7.4. According to O'Donnell and McGinity, (1997), bulk-eroding polymer-microspheres are often characterized by a burst release of drug. They stated that about 50 % of the total drug loaded could be released within the first few hours of incubation of the microspheres in the release media. They reported that this initial burst release was followed by a slow diffusion controlled release and later a degradation release third phase as a result of rapid degradation of the polymer matrix. This triphasic drug release has also been reported by Makino *et al*. (2000). The release curves shown in Figures 4.17, 4.19 and 4.20 for RG503H and RG502H formulations show a semblance of triphasic and diphasic release of artemether respectively. For the RG502H there was a burst release within the first three days followed by a slower release up to day 14 whereas RG503H showed a burst release on day one and slowed on day 3. There was a rapid release from the RG503H formulation from day 3 to day 7 which became almost constant from day 7 to 21. The amount of drug released from day 3 to day 7 was however markedly higher with the RG502H formulation (72.9 %) than the RG503H formulation (66.3 %).

In general, the RG503H microsphere formulation exhibited a greater control of the release of artemether than the RG502H formulation. The mass loss of the microspheres (Figure 4.21) also conformed to the release patterns and generally showed an increase in mass loss with time. Polymer degradation studies such as mass loss and molecular weight declining profiles are used to explain the *in vitro* drug release mechanisms of microsphere formulations (Wada *et al*, 1995). Although the molecular weights recorded for the two formulations for Day 14 were not significantly different ($p>0.05$), the release of artemether for both formulations differed significantly ($p<0.01$) on Day 14 with a corresponding significant difference ($p<0.0001$) in water uptake. However, there was no significant difference in mass loss on Day 14, comparing the two formulations. Thus it may be deduced that release of artemether from the two polymer microsphere formulations on Day 14 were as a result of diffusion and not polymer degradation.

From literature, the release models commonly used to describe drug release in general include the zero order, first order, Higuchi, Hixson Crowell and the Korsemeyer-Peppas models. The correlation coefficients (R^2) shown in Table 4.9 show how well the experimental data fit the proposed mechanisms. The relatively higher R^2 values shown by the Higuchi and Korsemeyer Peppas models respectively may imply that the mechanism of drug release from the microspheres followed these models. The highest R^2 value obtained for RG502H corresponded to the Higuchi model. Thus the RG502H formulation may be said to release the artemether via fickian diffusion. The Higuchi model has been used to describe drug release from several types of modified release pharmaceutical dosage forms. The highest R^2 value obtained for the RG503H

formulation corresponded to the Korsemeyer-Peppas model. This model describes drug release from a polymeric system. The release exponent obtained was 0.6854, which demonstrated that the mechanism of drug release from the formulated artemether-loaded RG503H microspheres was by non-fickian transport/diffusion.

The kinetics of diffusion mediated drug release is enhanced by the degradation of the polymer matrix, which is characterized by erosion. This makes it very difficult to describe the kinetics of drug release from biodegradable polymers. Since matrix degradation plays an important role in the drug release kinetics, the drug release mechanism cannot be characterized by diffusion alone (Wada *et al*, 1995). The degradation profiles of the two polymers shown by the mass loss (Figure 4.21) and declining molecular weight profiles (Figure 4.23) over time depict the involvement of degradation of the RG503H and RG502H microspheres in the release of artemether respectively.

The *in vivo* release study was conducted to determine whether artemether was released from the formulated microspheres in experimental rats and if the release could occur in a controlled manner. The pilot study carried out with three rats treated as shown in Table 4.10 was to determine if the chosen method of analysis LC-MS/MS could detect artemether in plasma samples. Table 4.10 shows that artemether was detected in the plasma sample of rats and thus the main *in vivo* study was carried out subsequently.

The choice of needle for parenteral injections affects the delivery of the formulation. The length of the needle and the needle gauge (diameter) are two important parameters considered in choosing a needle for parenteral injections. The higher the gauge number the smaller the diameter of the needle. For IM injections, longer needles with wider

diameters (23 G-18 G) and 2.5 to 7.5 cm long are used. Smaller needles are used for subcutaneous injections (25 G-23 G) and 1.5 to 2 cm long (Gill and Prausnitz, 2007; Buchholz and Henke, 2008). The use of a 23-gauge (23 G) needle for the subcutaneous injection of the rats in this study was in line with the recommended needle size for use in subcutaneous administrations.

The LC-MS/MS method was employed to simultaneously determine ARM and its metabolite DHA in rat plasma. The method involved the use of electrospray ionization (ESI) and multiple reactions monitoring (MRM) as quantification mode. These quantitation methods have been previously used to quantify artemether in human plasma (Xing *et al*., 2007; Huang *et al*., 2009; Lee *et al*., 2010).

Identification of primary ion species for artemether and artemisinin (IS) seen on the chromatograms indicate that the precursor-product ion pairs for artemether and artemisinin (IS) were m/z 316.200 /267.200 and m/z 300.100 / 209.100 respectively. Detector response was specific and linear for ARM (r = 0.7256) and DHA (r = 0.7400) at a concentration range of 10 -1000 ng/ml.

Artemether and its metabolite dihydroartemisinin were detected in plasma samples with the mean concentrations of artemether shown in the plasma-concentration time curves in Figure 4.66. The cumulative concentrations of artemether measured in plasma of the various groups of rats demonstrated that artemether was released under controlled conditions from the microsphere formulations (Groups 2 and 3). The other groups showed no increase in artemether release over time. The maximum concentration (C_{max}) and the times at which they occurred (T_{max}) as well as the area under the curve from zero to the last observed time are shown in Table 4.12. The relatively high C_{max} and $AUC_{(0-504)}$ values obtained for rats injected with 12.5 mg/kg

artemether loaded microspheres possibly means that the fraction of artemether absorbed and available for antimalarial activity is highest for that formulation compared to the others. The relatively lower AUC $_{(0\text{-}504)}$ (6.8215 μg.h/ml) of the 25 mg/kg injection as compared to that of the 12.5 mg/kg injection (1815 μg.h/ml) may have probably been as a result of dose dumping at the site of injection of the higher concentration of artemether microspheres. The difference in AUC values observed may also have been as a result of the likelihood of the release of lipid soluble artemether being impeded due to the fatty nature of the subcutaneous site of injection.

5.2 CONCLUSIONS

In the current study, well-formed spherical artemether-loaded PLGA microspheres with smooth surfaces were successfully formulated using the single emulsion solvent evaporation method. Different conditions of homogenization speeds and durations for the two different polymers used, yielded the desired particle size range of 45-90 μm. Both formulations yielded high drug loading and encapsulation efficiencies although the higher molecular weight RG503H formulation yielded higher values. The controlled release of artemether from the microspheres in simulated physiological conditions occurred over a 21-day period. Mathematical modeling of the release kinetics showed that artemether was released from the RG502H and RG503H microspheres through fickian diffusion and non-fickian diffusion, respectively. The *in vitro* release of artemether from the formulations may be by both diffusion and polymer erosion. The marked degradation of the polymers as well as the uptake of water by the particles provides evidence for this. The *in vivo* pharmacokinetic study with male Sprague-Dawley rats depicted that artemether was released from the microspheres *in vivo*. Quantification of artemether in plasma samples was successfully

done using LC-MS/MS and some pharmacokinetic parameters (C_{max}, T_{max} and AUC) were successfully determined.

5.3 RECOMMENDATIONS

The following are recommended for future work in order to achieve an artemether-loaded microsphere formulation for use in children for the treatment of severe malaria:

A higher molecular weight PLGA polymer RG504H should be used for formulation of artemether-loaded microspheres to determine whether a better loading and loading efficiency can be obtained which would make large-scale production more cost effective.

The *in vivo* study should be conducted using a lager number of experimental rats (n > 4 per group) and the quantification of DHA should be investigated in order to establish the rate of conversion of artemether to DHA its active metabolite. This will give a clearer picture of the pharmacokinetics of artemether released from microspheres in rat plasma.

The clearance of IM artemether in experimental rats should be investigated in order to make a good extrapolation or comparison for dose calculations for administration in experimental rats.

REFERENCES

Aditya N.P., Vathsala P.G., Vieira V, Murthy R. S. R., Souto E. B. 2013. Advances in nanomedicines for malaria treatment. *Advances in Colloid Interface Science*, (201-202): 1-17.

Aditya N.P., Patankar S., Madhusudhan B., Murthy R.S.R. 2010. Artemether loaded lipid nanoparticles produced by modified thin-film hydration: pharmacokinetics, toxicological and *in vivo* anti-malarial activity. *European Journal of Pharmaceutical Sciences* 40:448-455.

Alam M.I., Baboota S., Ahuja A., Ali M, Ali J., Sahni K. 2013. Intranasal infusion of nanostructured lipid carriers (NLC) containing CNS acting drug and estimation in brain and blood. *Drug Delivery*, 20(6): 247-251.

Alin, M.H., Björkman, A. and Ashton, M. 1990. *In vitro* activity of artemisinin, its derivatives, and pyronaridine against different strains of Plasmodium falciparum. *Transactions of the Royal Society of Tropical Medicine and Hygiene*, *84*(5): 635-637.

Allen, L.V., and Ansel, H.C. 2013. *Ansel's Pharmaceutical Dosage Forms and Drug Delivery Systems*. Lippincott Williams & Wilkins. 10: 508-515.

Anderson, J.M. and Shive, M.S. 2012. Biodegradation and biocompatibility of PLA and PLGA microspheres. *Advanced Drug Delivery Reviews*, *64*: 72-82.

Anderson J.M., Shive M.S. 1997. Biodegradation and biocompatibility of PLA and PLGA microspheres, *Advanced Drug Deliver Reviews* 28 (1): 5–24.

Ansah, E.K., Reynolds, J., Akanpigbiam, S., Whitty, C.J. and Chandler, C.I. 2013. “Even if the test result is negative, they should be able to tell us

what is wrong with us": a qualitative study of patient expectations of rapid diagnostic tests for malaria. *Malaria Journal*, *12*(258): 10-1186.

Antimalaria policy for Ghana. WHO. 2009. Ministry of Health, Ghana

Antimalarials, C.C.R.G.o.Q.a.I.D.a. 1972. Chemical studies on qinghaosu (artemisinine). *Journal of Traditional Chinese Medicine,* 2: 3–8.

Arshady R. 1991. Preparation of biodegradable microspheres and microcapsules: 2. Polylactides and related polyesters. *Journal of Control Release,* 17:1–21.

Ashley, E.A., McGready, R., Hutagalung, R., Phaiphun, L., Slight, T., Proux, S., Thwai, K.L., Barends, M., Looareesuwan, S., White, N.J. and Nosten, F. 2005. A randomized, controlled study of a simple, once-daily regimen of dihydroartemisinin-piperaquine for the treatment of uncomplicated, multidrug-resistant falciparum malaria. *Clinical Infectious Diseases*, *41*(4): 425-432.

Ashton M., Hai T.N., Sy N.D., Huong D.X., van Huong N., Nieu N.T., Cong L. D. 1998. Artemisinin pharmacokinetics is time dependent during repeated oral administration in healthy male adults. *Drug Metabolism and Disposition*, 26: 25-7.

Atkinson J., Bobogare A., Fitzgerald L., Boaz L., Appleyard B., Toaliu H., Vallely A. 2009. A qualitative study on the acceptability and preference of three types of long-lasting insecticide-treated bed nets in Solomon Islands: implications for malaria elimination. *Malaria Journal,* 8:119 DOI: 10.1186/1475-2875-8-119.

Aulton, M.E., and Taylor, K.M. 2013. *Aulton's Pharmaceutics: The Design and Manufacture of Medicines*. Elsevier Health Sciences. 4:623-627, 795-

796.

Baker, J.K., McChesney, J.D., and Chi, H.T. 1993. Decomposition of arteether in simulated stomach acid yielding compounds retaining antimalarial activity. *Pharmaceutical Research*, *10*(5): 662-666.

Barnes, K.I., Chanda, P., and Barnabas, G. 2009. Impact of the large-scale deployment of artemether/lumefantrine on the malaria disease burden in Africa: case studies of South Africa, Zambia and Ethiopia. *Malaria Journal*, *8*(1): 1.

Bazile, D.V., Ropert, C., Huve, P., Verrecchia, T., Mariard, M., Frydman, A., Veillard, M. and Spenlehauer, G. 1992. Body distribution of fully biodegradable [14 C]-poly (lactic acid) nanoparticles coated with albumin after parenteral administration to rats. *Biomaterials*, *13*(15): 1093-1102.

Berkland, C., Kim, K.K., and Pack, D.W. 2003. PLG microsphere size controls drug release rate through several competing factors. *Pharmaceutical Research*, *20*(7): 1055-1062.

Berkland, C., King, M., Cox, A., Kim, K.K. and Pack, D.W. 2002. Precise control of PLG microsphere size provides enhanced control of drug release rate. *Journal of Controlled Release*, *82*(1): 137-147.

Bhattarai, A., Ali, A.S., Kachur, S.P., Mårtensson, A., Abbas, A.K., Khatib, R., Al-Mafazy, A.W., Ramsan, M., Rotllant, G., Gerstenmaier, J.F. and Molteni, F. 2007. Impact of artemisinin-based combination therapy and insecticide-treated nets on malaria burden in Zanzibar. *PLOS Medicine*, *4*(11): 309.

Binns, F., and Wallace, T.W. 1989. An unsuccessful approach to the framework

of the antimalarial, arteether. *Tetrahedron Letters*, *30*(9): 1125-1128.

Biritwum, R.B., Welbeck, J. and Barnish, G. 2000. Incidence and management of malaria in two communities of different socio–economic level, in Accra, Ghana. *Annals of Tropical Medicine and Parasitology*, *94*(8): 71-778.

Birnbaum, D.T., Kosmala, J.D., Henthorn, D.B., Brannon-Peppas, L. 2000. Controlled release of estradiol from PLGA microspheres: the effect of organic phase solvent on encapsulation and release. *Journal of Controlled Release*, 65: 375–387.

Bodmeier, R., McGinity, J.W. 1988. Solvent selection in the preparation of poly (dl-lactide) microspheres prepared by the solvent evaporation method. International. *Journal of Pharmaceutical Sciences*, 43: 179–186.

Bodmeier, R., and McGinity J., M. 1987. The preparation and evaluation of drug containing poly(dl-Lactide) microspheres formed by the solvent evaporation method. *Pharmaceutical Research*, 4: 465-471.

Bozdağ, S., Calis, S., Kas, H.S., Ercan, M.T., Peksoy, I., Hincal, A.A. 2001. *In vitro* evaluation and intra-articular administration of biodegradable microspheres containing naproxen sodium. *Journal of Microencapsulation*, 18(4): 443–456.

Brewer, T.G., Peggins, J.O., Grate, S.J., Petras, J.M., Levine, B.S., Weina, P.J., Swearengen, J., Heiffer, M.H. and Schuster, B.G. 1994. Neurotoxicity in animals due to arteether and artemether. *Transactions of the Royal Society of Tropical Medicine and Hygiene*, *88*(1): 33-36.

Brossi, A., Venugopalan, B., Dominguez Gerpe, L., Yeh, H.J.C., Flippen-Anderson, J.L., Buchs, P., Luo, X.D., Milhous, W. and Peters, W. 1988.

Arteether, a new antimalarial drug: synthesis and antimalarial properties. *Journal of Medicinal Chemistry*, *31*(3): 645-650.

Bruce-Chwatt, L.J. 1984. DNA probes for malaria diagnosis. *The Lancet*, *323*(8380): 795.

Buchholz, S. and Henke, G. 2008. *Henke's Med-math: Dosage Calculation, Preparation and Administration*. Lippincott Williams & Wilkins.

Chaisri W., Hennink W. E., Okonogi S. 2009. Preparation and characterization of cephalexin loaded PLGA microspheres. *Current Drug Delivery*, 6:69–75.

Chan, V.O., Colville, J., Persaud, T., Buckley, O., Hamilton, S. and Torreggiani, W.C. 2006. Intramuscular injections into the buttocks: are they truly intramuscular? *European Journal of Radiology*, *58*(3): 480-484.

Chandramohan, D., Jaffar, S., and Greenwood, B. 2002. Use of clinical algorithms for diagnosing malaria. *Tropical Medicine & International Health*, *7*(1): 45-52.

Chen, L., Qu, F.Y., and Zhou, Y.C. 1982. Field observations on the antimalarial piperaquine. *Chinese Medical Journal*, *95*(4): 281-286.

China Cooperative Research Group on Qinghaosu and Its Derivatives as Antimalarials. 1982. Metabolism and pharmacokinetics of qinghaosu and its derivatives. *Journal of Traditional Chinese Medicine,* 2: 25-30.

Churchill, F.C., Patchen, L.C., Campbell, C.C., Schwartz, I.K., Nguyen-Dinh, P., and Dickinson, C.M. 1985. Amodiaquine as a prodrug: importance of metabolite(s) in the antimalarial effect of amodiaquine in humans. *Life Sciences*, *36*(1): 53-62.

Cohen S., Yoshioka T., Lucarelli M., Hwang L.H., and Langer R. 1991. Controlled

delivery systems for proteins based on poly (Lactic/Glycolic Acid) microspheres. *Pharmaceutical Research*, 8(6): 713–720.

Crotts, G., and Park, T.G. 1998. Protein delivery from poly (lactic-co-glycolic acid) biodegradable microspheres: release kinetics and stability issues. *Journal of Microencapsulation*, *15*(6): 699-713.

D'Acremont, V., Kahama-Maro, J., Swai, N., Mtasiwa, D., Genton, B. and Lengeler, C. 2011. Reduction of anti-malarial consumption after rapid diagnostic tests implementation in Dar es Salaam: a before-after and cluster randomized controlled study. *Malaria Journal*, *10*(1):107.

Danhier, F., Ansorena, E., Silva, J.M., Coco, R., Le Breton, A. and Préat, V., 2012. PLGA-based nanoparticles: an overview of biomedical applications. *Journal of Controlled Release*, *161*(2): 505-522.

Dash, S., Murthy, P.N., Nath, L., and Chowdhury, P. 2010. Kinetic modeling on drug release from controlled drug delivery systems. *Acta Poloniae Pharmaceutica*, *67*(3): 217-23.

Davidson, D.E. 1994. Role of arteether in the treatment of malaria and plans for further development. *Transactions of the Royal Society of Tropical Medicine and Hygiene*, *88*(1): 51-52.

de Vries P. J., Dien T. K. 1996. Clinical pharmacology and therapeutic potential of artemisinin and its derivatives in the treatment of malaria. *Drugs*, 52 (6): 818-36.

Denis, M.B., Davis, T.M., Hewitt, S., Incardona, S., Nimol, K., Fandeur, T., Poravuth, Y., Lim, C. and Socheat, D. 2002. Efficacy and safety of dihydroartemisinin-piperaquine (Artekin) in Cambodian children and adults with uncomplicated falciparum malaria. *Clinical Infectious*

Diseases, *35*(12): 1469-1476.

Doolan, D.L., Dobaño, C., and Baird, J.K. 2009. Acquired immunity to malaria. *Clinical Microbiology Reviews*, *22*(1): 13-36.

Dowling, M.A.C., and Shute, G.T., 1966. A comparative study of thick and thin blood films in the diagnosis of scanty malaria parasitaemia. *Bulletin of the World health Organization*, *34*(2): 249.

Druilhe, P., Daubersies, P., Patarapotikul, J., Gentil, C., Chene, L., Chongsuphajaisiddhi, T., Mellouk, S. and Langsley, G. 1998. A primary malarial infection is composed of a very wide range of genetically diverse but related parasites. *Journal of Clinical Investigation*, *101*(9): 2008.

Dwivedi, P., Khatik, R., Khandelwal, K., Taneja, I., Raju, K.S.R., Paliwal, S.K., Dwivedi, A.K. and Mishra, P.R. 2014. Pharmacokinetics study of arteether loaded solid lipid nanoparticles: an improved oral bioavailability in rats. *International Journal of Pharmaceutics*, *466*(1): 321-327.

English, M., Esamai, F., Wasunna, A., Were, F., Ogutu, B., Wamae, A., Snow, R.W., Peshu, N. 2004. Assessment of in-patient paediatric care in first referral level hospitals in 13 districts in Kenya. *Lancet* 363(9425): 1948–1953.

Ertl, B., Platzer, P., Wirth, M., Gabor, F., 1999. Poly (d,l-lactic-co-glycolic acid) microspheres for sustained delivery and stabilization of camptothecin. *Journal of Controlled Release*, 61: 305–317.

Esmaeili F., Ghahremani MH, Esmaeili B, Khoshayand M.R., Atyabi F., Dinarvand R. 2008. PLGA nanoparticles of different surface properties: Preparation and evaluation of their body distribution. *International*

Journal of Pharmaceutics, 349:249–255.

Fleischer, B. 2004. Editorial: 100 years ago: Giemsa's solution for staining of plasmodia. *Tropical Medicine & International Health*, *9*(7): 755-756.

Gibaldi, M., Feldman, S. 1967. Establishment of sink conditions in dissolution rate determinations – theoretical considerations and application to nondisintegrating dosage forms. *Journal of Pharmaceutical Sciences,* 56: 1238–1242.

Gill, H.S., and Prausnitz, M.R. 2007. Does needle size matter? *Journal of Diabetes Science and Technology*, *1*(5): 725-729.

Gilles, H.M., Warrell, D.A. 1993. Clinical features of malaria. *Bruce-Chwatt's Essential Malariology. London, Boston, Melbourne, Auckland: Edward Arnold*, 5-49.

Greenwood B. M., Bojang K., Whitty C. J., Targett G. A. 2005. Malaria. *Lancet*, 365:1487–98.

Gugulothu, D., Pathak, S., Suryavanshi, S., Sharma, S. and Patravale, V. 2010. Self-microemulsifiyng suppository formulation of β-artemether. *AAPS PharmSciTech, 11*(3):1179-1184.

Guillet, P., N'guessan, R., Darriet, F., Traore-Lamizana, M., Chandre, F. and Carnevale, P. 2001. Combined pyrethroid and carbamate 'two-in-one' treated mosquito nets: field efficacy against pyrethroid-resistant *Anopheles gambiae* and *Culex quinquefasciatus*. *Medical and Veterinary Entomology*, *15*(1): 105-112.

Hadjiioannou T.P., Christian G.D., Koupparis M.A. 1993. Quantitative calculations in pharmaceutical practice and research. Eds. VCH Publishers Inc., New York.

Hans, M.L. and Lowman, A.M., 2002. Biodegradable nanoparticles for drug delivery and targeting. *Current Opinion in Solid State and Materials Science*, *6*(4): 319-327.

Hänscheid, T. 1999. Diagnosis of malaria: a review of alternatives to conventional microscopy. *Clinical & Laboratory Haematology*, *21*(4): 235-245.

Haque, F., Shu, D., Shu, Y., Shlyakhtenko, L.S., Rychahou, P.G., Evers, B.M. and Guo, P. 2012. Ultrastable synergistic tetravalent RNA nanoparticles for targeting to cancers. *Nano today*, *7*(4): 245-257.

Hassan Alin, M., Ashton, M., Kihamia, C.M., Mtey, G.J.B. and Björkman, A. 1996. Clinical efficacy and pharmacokinetics of artemisinin monotherapy and in combination with mefloquine in patients with falciparum malaria. *British Journal of Clinical Pharmacology*, *41*(6): 587-592.

Herrmann, J., and Bodmeier, R. 1998. Biodegradable, somatostatin acetate containing microspheres prepared by various aqueous and non-aqueous solvent evaporation methods. *European Journal of Pharmaceutics and Biopharmaceutics*, *45*(1): 75-82.

Hien, T.T., and White, N.J. 1993. Qinghaosu. *The Lancet*, *341*(8845): 603-608.

Hien, T.T., Dolecek, C., Mai, P.P., Dung, N.T., Truong, N.T., An, D.T.H., Thanh, T.T., Stepniewska, K., White, N.J. and Farrar, J. 2004. Dihydroartemisinin-piperaquine against multidrug-resistant Plasmodium falciparum malaria in Vietnam: randomised clinical trial. *The Lancet*, *363*(9402): 18-22.

Higuchi, T. 1963. Mechanism of sustained action medication: theoretical analysis

of rate of release of solid drugs dispersed in solid matrices. *Journal of Pharmaceutical Sciences,* 52: 1145–1148.

Hixson, A.W., Crowell, J.H. 1931. Dependence of reaction velocity upon surface and agitation: theoretical considerations. *Industrial and Engineering Chemistry,* 23: 923–931.

Holland, S.J., Tighe, B.J. and Gould, P.L. 1986. Polymers for biodegradable medical devices. The potential of polyesters as controlled macromolecular release systems. *Journal of Controlled Release*, *4*(3): 155-180.

Houchin, M.L., and Topp, E.M. 2009. Physical properties of PLGA films during polymer degradation. *Journal of Applied polymer Science*, *114*(5): 2848-2854.

Houwen, B. 2002. Blood film preparation and staining procedures. *Clinics in Laboratory Medicine*, *22*(1): 1-14.

Huang, L., Jayewardene, A.L., Li, X., Marzan, F., Lizak, P.S. and Aweeka, F.T. 2009. Development and validation of a high-performance liquid chromatography/tandem mass spectrometry method for the determination of artemether and its active metabolite dihydroartemisinin in human plasma. *Journal of Pharmaceutical and Biomedical Analysis*, *50*(5): 959-965.

Hudson, D., and Margaritis, A. 2014. Biopolymer nanoparticle production for controlled release of biopharmaceuticals. *Critical Reviews in Biotechnology*, *34*(2): 161-179.

Jain, K., Sood, S., and Gowthamarajan, K. 2015. Optimization of artemether-loaded NLC for intranasal delivery using central composite design.

Drug Delivery, *22*(7): 940-954.

Jalil, R., Nixon, J.R. 1990a. Microencapsulation using poly (l-lactic acid) II: preparative variables affecting microcapsule properties. *Journal of Microencapsulation*, 7: 25–39.

Jalil, R., Nixon, J.R. 1990b. Microencapsulation using poly (l-lactic acid) III: effect of the polymer molecular weight on the microcapsule properties. *Journal of Microencapsulation*, 7: 41–52.

Jalil, R., Nixon, J.R. 1990c. Microencapsulation using poly (l-lactic acid) IV: release properties of microcapsule containing phenobarbitone. *Journal of Microencapsulation*, 7: 53–66.

Kager, P.A., Schultz, M.J., Zijlstra, E.E., van Berg, B., van Boxtel, J. 1994. Arteether administration in humans: preliminary studies of pharmacokinetics, safety and tolerance. *Transactions of the Royal Society of Tropical Medicine and Hygiene*, 88 (1): 53-54.

Kahook, M.Y., Kimura, A.E., Wong, L.J., Ammar, D.A., Maycotte, M.A. and Mandava, N. 2009. Sustained elevation in intraocular pressure associated with intravitreal bevacizumab injections. *Ophthalmic Surgical Lasers Imaging*, *40*(3): 293-295.

Karbwang, J., Na-Bangchang, K., Thanavibul, A. and Molunto, P. 1998. Plasma concentrations of artemether and its major plasma metabolite, dihydroartemisinin, following a 5-day regimen of oral artemether, in patients with uncomplicated malaria falciparum. *Annals of Tropical Medicine and Parasitology*, *92*(1): 31-36.

Kent, J.S., Lewis, D.H., Sanders, L.M. and Tice, T.R. 1987. Syntex (USA) Inc., *Microencapsulation of Water Soluble Active Polypeptides*. U.S. Patent

4,675,189.

Kilian, A.H.D., Metzger, W.G., Mutschelknauss, E.J., Kabagambe, G., Langi, P., Korte, R. and Sonnenburg, F.V. 2000. Reliability of malaria microscopy in epidemiological studies: results of quality control. *Tropical Medicine & International Health*, *5*(1): 3-8.

Kim K.K., Daniel W. 2006 Chapter: Microspheres for Drug Delivery. BioMEMS and Biomedical Nanotechnology 19-50.

King, T.W., and Patrick, C.W. 2000. Development and *in vitro* characterization of vascular endothelial growth factor (VEGF)-loaded poly (DL-lactic-co-glycolic acid)/poly (ethylene glycol) microspheres using a solid encapsulation/single emulsion/solvent extraction technique. *Journal of Biomedical Materials Research*, *51*(3): 383-390.

Klayman, D.L., Lin, A.J., Acton, N., Scovill, J.P., Hoch, J.M., Milhous, W.K., Theoharides, A.D. and Dobek, A.S. 1984. Isolation of artemisinin (qinghaosu) from Artemisia annua growing in the United States. *Journal of Natural Products*, *47*(4): 715-717.

Klayman D.L. 1985. Qinghaosu (artemisinin). An antimalarial drug from China. *Science*, 228: 1049-55.

Korsmeyer, R.W., Gurny, R., Doelker, E., Buri, P., Peppas, N.A. 1983. Mechanism of solute release from porous hydrophilic polymers. *International Journal of Pharmaceutics*, 15: 25–35.

Krishna, A.K., and Flanagan, D.R. 1989. Micellar solubilization of a new antimalarial drug, β-arteether. *Journal of Pharmaceutical Sciences*, *78*(7): 574-576.

Kumar N.L., Robert S., and Abraham J.D. 2002. Polyanhydrides: an overview.

Advanced Drug Delivery Reviews, 54(7): 889–910.

Kumar, V.V., Chandrasekar, D., Ramakrishna, S., Kishan, V., Rao, Y.M. and Diwan, P.V. 2007. Development and evaluation of nitrendipine loaded solid lipid nanoparticles: influence of wax and glyceride lipids on plasma pharmacokinetics. *International Journal of Pharmaceutics, 335*(1): 167-175.

Kumari A., Yadav S.K., Yadav S.C. 2010. Biodegradable polymeric nanoparticles based drug delivery systems, *Colloids and Surfaces B: Biointerfaces,* 75 (1): 1–18.

Lai, P., Daear, W., Löbenberg, R. and Prenner, E.J. 2014. Overview of the preparation of organic polymeric nanoparticles for drug delivery based on gelatine, chitosan, poly (d, l-lactide-co-glycolic acid) and polyalkylcyanoacrylate. *Colloids and Surfaces B: Biointerfaces, 118*: 154-163.

Langer, R.S., and Peppas, N.A. 1981. Present and future applications of biomaterials in controlled drug delivery systems. *Biomaterials, 2*(4): 201-214.

Lavelle, W., Lavelle, E.D. and Lavelle, L. 2007. Intra-articular Injections. *Anesthesiology Clinics, 25*(4): 853-862.

Laxmi, M., Bhardwaj, A., Mehta, S. and Mehta, A. 2015. Development and characterization of nanoemulsion as carrier for the enhancement of bioavailability of artemether. *Artificial Cells, Nanomedicine, and Biotechnology, 43*(5): 334-344.

Lefèvre, G., Looareesuwan, S., Treeprasertsuk, S., Krudsood, S., Silachamroon, U., Gathmann, I., Mull, R., Bakshi, R. 2001. A clinical and

pharmacokinetic trial of six doses of artemether-lumefantrine for multidrug-resistant *Plasmodium falciparum* malaria in Thailand. *The American Journal of Tropical Medicine and Hygiene*, 64(5-6): 247–256.

Li, G.Q., Guo, X.B., Fu, L.C., Jian, H.X. and Wang, X.H. 1994. Clinical trials of artemisinin and its derivatives in the treatment of malaria in China. *Transactions of the Royal Society of Tropical Medicine and Hygiene, 88*: 5-6.

Li, W. H., Shu, H. L., Xu, G. Y., & Zeng, Y. L. 1982. The binding of qinghaosu (artemisinin) and its derivatives to plasma protein. *Acta Pharmacologica Sinica* 17: 783–786.

Li, M., Rouaud, O., and Poncelet, D. 2008. Microencapsulation by solvent evaporation: State of the art for process engineering approaches. *International Journal of Pharmaceutics*, *363*(1): 26-39.

Li, Q.G., Peggins, J.O., Fleckenstein, L.L., Masonic, K., Heiffer, M.H. and Brewer, T.G. 1998. The pharmacokinetics and bioavailability of dihydroartemisinin, arteether, artemether, artesunic acid and artelinic acid in rats. *Journal of Pharmacy and Pharmacology*, *50*(2): 173-182.

Lin, A. J., Klayman, D. L., Milhous, W. K. 1987. Antimalarial activity of new water-soluble dihydroartemisinin derivatives. *Journal of Medicinal Chemistry* 30: 2147-2150.

Lines, J. 1996. Mosquito nets and insecticides for net treatment: a discussion of existing and potential distribution systems in Africa. *Tropical Medicine & International Health*, 1(5): 16-632.

Liu, P., De Wulf, O., Laru, J., Heikkila, T., van Veen, B., Kiesvaara, J., Hirvonen, J., Peltonen, L., Laaksonen, T. 2013. Dissolution studies of poorly soluble

nanosuspensions in non-sink conditions. *AAPS PharmSciTech*, 14(2): 748-756. DOI: 10. 1208/s12249-013-9960-2.

Maguire, J.D., Lederman, E.R., Barcus, M.J., AP O'Meara, W., Jordon, R.G., Duong, S., Muth, S., Sismadi, P., Bangs, M.J., Prescott, W.R. and Baird, J.K. 2006. Production and validation of durable, high quality standardized malaria microscopy slides for teaching, testing and quality assurance during an era of declining diagnostic proficiency. *Malaria Journal*, *5*(1): 92.

Mahmood I. 2010. Prediction of drug clearance in children 3 months and younger: an allometric approach. *Drug Metabolism and Drug Interactions*, 25(1-4): 25–34

Makadia, H.K. and Siegel, S.J. 2011. Poly lactic-co-glycolic acid (PLGA) as biodegradable controlled drug delivery carrier. *Polymers*, *3*(3): 1377-1397.

Makanga, M., Krudsood, S. 2009. The clinical efficacy of artemether/lumefantrine (Coartem®). *Malaria Journal*, 8(1): S5. DOI: 10.1186/1475-2875-8-S1-S5.

Makino, K., Mogi, T., Ohtake, N., Yoshida, M., Ando, S., Nakajima, T., Ohshima, H. 2000. Pulsatile drug release from poly (lactide-co-glycolide) microspheres: how does the composition of the polymer matrices affect the time interval between the initial burst and the pulsatile release of drugs? Colloids and Surfaces B: *Biointerfaces* 19(2): 173–179. DOI:10.1016/S0927-7765(00)00148-X.

Mandawgade, S.D., Sharma, S., Pathak, S. and Patravale, V.B. 2008.

Development of SMEDDS using natural lipophile: application to β-artemether delivery. *International Journal of Pharmaceutics, 362*(1): 179-183.

Mao S., Xu J., Cai C., Germershaus O., Schaper A., Kissel T. 2007. Effect of WOW process parameters on morphology and burst release of FITC-dextran loaded PLGA microspheres. *International Journal of Pharmaceutics*, 334:137–148.

McKenzie, F.E., Prudhomme, W.A., Magill, A.J., Forney, J.R., Permpanich, B., Lucas, C., Gasser, R.A. and Wongsrichanalai, C. 2005. White blood cell counts and malaria. *Journal of Infectious Diseases, 192*(2): 323-330.

McLennan, D.N., Porter, C.J., and Charman, S.A. 2005. Subcutaneous drug delivery and the role of the lymphatics. *Drug Discovery Today: Technologies*, *2*(1): 89-96.

Medana, I.M., and Turner, G.D. 2006. Human cerebral malaria and the blood–brain barrier. *International Journal for Parasitology*, *36*(5): 555-568.

Miller, L.H., and Su, X. 2011. Artemisinin: discovery from the Chinese herbal garden. *Cell*, *146*(6): 855-858.

Milne, L.M., Kyi, M.S., Chiodini, P.L. and Warhurst, D.C. 1994. Accuracy of routine laboratory diagnosis of malaria in the United Kingdom. *Journal of Clinical Pathology*, *47*(8): 740-742.

Mogi, T., Ohtake, N., Yoshida, M., Chimura, R., Kamaga, Y., Ando, S., Tsukamoto, T., Nakajima, T., Uenodan, H., Otsuka, M. and Matsuda, Y. 2000. Sustained release of 17β-estradiol from poly (lactide-co-glycolide) microspheres *in vitro* and *in vivo*. *Colloids and Surfaces B: Biointerfaces*, *17*(3): 153-165.

Moody A. 2002. Rapid diagnostic tests for malaria parasites. *Clinical Microbiology Reviews,* 15(1): 66–78. DOI: 10.1128/CMR.15.1.66-78.2002.

Mulholland, E.K., Adegbola, R.A., 2005. Bacterial infections–a major cause of death among children in Africa. *New England Journal of Medicine*, 352(1): 75–77.

Murambiwa, P., Masola, B., Govender, T., Mukaratirwa, S. and Musabayane, C.T. 2011. Anti-malarial drug formulations and novel delivery systems: a review. *Acta Tropica*, *118*(2): 71-79.

Murray, C.J.L., Rosenfeld, L.C., Lim, S.S., Andrews, K.G., Foreman, K.J., Haring, D., Fullman, N., Naghavi, M., Lozano, R., Lopez, A.D. 2012. Global malaria mortality between 1980 and 2010: a systematic analysis. *Lancet* 379: 413–431.

Na-Bangchang, K., Congpuong, K., Hung, L.N., Molunto, P. and Karbwang, J. 1998. Simple high-performance liquid chromatographic method with electrochemical detection for the simultaneous determination of artesunate and dihydroartemisinin in biological fluids. *Journal of Chromatography B: Biomedical Sciences and Applications*, *708*(1): 201-207.

Nahata, T., and Saini, T.R. 2008. Optimization of formulation variables for the development of long acting microsphere based depot injection of olanzapine. *Journal of Microencapsulation*, *25*(6): 426-433.

Nair L.S., Laurencin C.T. 2007. Biodegradable polymers as biomaterials. *Progress in Polymer Science,* 32:762–798.

Narayani, R., and Rao, K.P. 1994. Controlled release of anticancer drug

methotrexate from biodegradable gelatin microspheres. *Journal of Microencapsulation*, *11*(1): 69-77.

National Institute of Allergy and Infectious Diseases. 2016. Life Cycle of Malaria Parasite. https://www.niaid.nih.gov/topics/**Malaria**/Pages/**lifecycle**.aspx

Nolan, T., Angos, P., Cunha, A.J., Muhe, L., Qazi, S., Simoes, E.A., Tamburlini, G., Weber, M., Pierce, N.F. 2001. Quality of hospital care for seriously ill children in less-developed countries. *Lancet* 357(9250): 106–110.

O'donnell, P.B., Iwata, M. and McGinity, J.W. 1995. Properties of multiphase microspheres of poly (D, L-lactic-co-glycolic acid) prepared by a potentiometric dispersion technique. *Journal of Microencapsulation*, *12*(2): 155-163.

O'Donnell, P.B., McGinity, J.W. 1997. Preparation of microspheres by the solvent evaporation technique. *Advanced Drug Delivery Reviews*, 28(1): 25–42. DOI:10.1016/S0169-409X(97)00049-5.

Ockenhouse, C.F., Sun, P.F., Lanar, D.E., Wellde, B.T., Hall, B.T., Kester, K., Stoute, J.A., Magill, A., Krzych, U., Farley, L. and Wirtz, R.A. 1998. Phase I/IIa safety, immunogenicity, and efficacy trial of NYVAC-Pf7, a pox-vectored, multiantigen, multistage vaccine candidate for *Plasmodium falciparu*m malaria. *Journal of Infectious Diseases*, *177*(6): 1664-1673.

Okochi, H., and Nakano, M. 2000. Preparation and evaluation of w/o/w type emulsions containing vancomycin. *Advanced Drug Delivery Reviews*, *45*(1): 5-26.

Panagi, Z., Beletsi, A., Evangelatos, G., Livaniou, E., Ithakissios, D.S. and

Avgoustakis, K. 2001. Effect of dose on the biodistribution and pharmacokinetics of PLGA and PLGA–mPEG nanoparticles. *International Journal of Pharmaceutics*, *221*(1): 143-152.

Park, J., Ye, M. and Park, K. 2005. Biodegradable polymers for microencapsulation of drugs. *Molecules*, *10*(1): 146-161.

Passerini, N., and Craig, D.Q.M. 2001. An investigation into the effects of residual water on the glass transition temperature of polylactide microspheres using modulated temperature DSC. *Journal of Controlled Release*, *73*(1): 111-115.

Peniche H., and Peniche C., (2011) Chitosan nanoparticles: a contribution to nanomedicine. *Polymer International*, 60 (6): 883–889.

Pussard, E., Verdier, F., Faurisson, F., Scherrmann, J.M., Le Bras, J. and Blayo, M.C. 1987. Disposition of monodesethylamodiaquine after a single oral dose of amodiaquine and three regimens for prophylaxis against *Plasmodium falciparum* malaria. *European Journal of Clinical Pharmacology*, *33*(4): 409-414.

Quinghaosu Antimalarial Coordinating Research Group. 1979. Antimalaria studies on qinghaosu. *Chinese Medical Journal*, 92: 811–816.

Ramchandani, M., and Robinson, D. 1998. *In vitro* and *in vivo* release of ciprofloxacin from PLGA 50: 50 implants. *Journal of Controlled Release*, *54*(2): 167-175.

Rosca, I.,D., Watari F., Uo M. 2004. Microparticle formation and its mechanism in single and double emulsion solvent evaporation. *Journal of Controlled Release*, 99:271–280.

Ruebush, T.K., Kern, M.K., Campbell, C.C. and Oloo, A.J. 1995. Self-treatment

of malaria in a rural area of western Kenya. *Bulletin of the World Health Organization, 73*(2): 229.

Ruscoe, J.E., Tingle, M.D., O'Neill, P.M., Ward, S.A. and Park, B.K. 1998. Effect of disposition of mannich antimalarial agents on their pharmacology and toxicology. *Antimicrobial Agents and Chemotherapy, 42*(9): 2410-2416.

Sah, H., 1997. Microencapsulation techniques using ethyl acetate as a dispersed solvent: effect of its extraction rate on the characteristics of PLGA microspheres. *Journal of Controlled Release* 47: 233–245.

Salman, S., Bendel, D., Lee, T.C., Templeton, D. and Davis, T.M. 2015. Pharmacokinetics of a novel sublingual spray formulation of the antimalarial drug artemether in African children with malaria. *Antimicrobial Agents and Chemotherapy*, *59*(6): 3208-3215.

Saltzman, W.M. 2001. Drug Delivery: Engineering Principles for Drug Therapy. Oxford University Press, New York.

Schwendeman, S.P., Shah, R.B., Bailey, B.A. and Schwendeman, A.S., 2014. Injectable controlled release depots for large molecules. *Journal of Controlled Release*, *190*: 240-253.

Seju U, Kumar A, Sawant KK. 2011. Development and evaluation of olanzapine-loaded PLGA nanoparticles for nose-to-brain delivery: *in vitro* and *in vivo* studies. *Acta Biomaterialia* 7:4169–76.

Shenderova A., Burke T.G., and Schwendeman S.P. 1999. The acidic microclimate in poly (lactide-co-glycolide) microspheres stabilizes camptothecins. *Pharmaceutical Research,* 16(2): 241–248.

Shenderova A., Burke, T.G., Schwendeman, S.P., 1997. Stabilization of 10-hydroxycamptothecin in poly (lactide-co-glycolide) microsphere delivery vehicles. *Pharmaceutical Research*, 14(10): 1406-1414.

Siegel, S.J., Kahn, J.B., Metzger, K., Winey, K.I., Werner, K. and Dan, N. 2006. Effect of drug type on the degradation rate of PLGA matrices. *European Journal of Pharmaceutics and Biopharmaceutics*, *64*(3): 287-293.

Singhvi, G., and Singh, M. 2011. Review: *in-vitro* drug release characterization models. *International Journal of Pharmaceutical Studies and Research, 2*(1): 77-84.

Sinha, V.R., and Trehan, A. 2003. Biodegradable microspheres for protein delivery. *Journal of Controlled Release*, *90*(3): 261-280.

Smithuis, F., Kyaw, M.K., Phe, O., Aye, K.Z., Htet, L., Barends, M., Lindegardh, N., Singtoroj, T., Ashley, E., Lwin, S. and Stepniewska, K.,2006. Efficacy and effectiveness of dihydroartemisinin-piperaquine versus artesunate-mefloquine in falciparum malaria: an open-label randomised comparison. *The Lancet*, *367*(9528): 2075-2085.

Snounou, G., Pinheiro, L., Gonçalves, A., Fonseca, L., Dias, F., Brown, K.N. and do Rosario, V.E. 1993. The importance of sensitive detection of malaria parasites in the human and insect hosts in epidemiological studies, as shown by the analysis of field samples from Guinea Bissau. *Transactions of the Royal Society of Tropical Medicine and Hygiene*, *87*(6): 649-653.

Snow R. W., Guerra C. A., Noor A. M., Myint H. Y., Hay S. I. 2005. The global distribution of clinical episodes of Plasmodium falciparum malaria. *Nature,* 434:214–7.

Standard Treatment Guidelines. 2010. Sixth Edition. Ministry of Health, Ghana, 365-374.

Streatfield, R.K., Khan, W.A., Bhuiya, A., Hanifi, S.M.A., Alam, N., Diboulo, E., et al., 2014. Malaria mortality in Africa and Asia: evidence from INDEPTH health and demographic surveillance system sites. Global Health Action. DOI: 10.3402/gha.v7.25369

Sulzer, A.J., Wilson, M. and Hall, E.C. 1969. Indirect fluorescent-antibody tests for parasitic diseases. Y. An evaluation of a thick-smear antigen in the IFA test for malaria antibodies. *American Journal of Tropical Medicine and Hygiene*, *18*(2): 199-205.

Svensson, U.S., Ashton, M., Hai, T.N., Bertilsson, L., Huong, D.X., Van Huong, N., Niêu, N.T., Sy, N.D., Lykkesfeldt, J. and Công, L.D. 1998. Artemisinin induces omeprazole metabolism in human beings. *Clinical Pharmacology & Therapeutics*, *64*(2): 60-167.

Tamada, J.A., Langer, R. 1993. Erosion kinetics of hydrolytically degradable polymers. *Proceedings of the National Academy of Sciences of the USA*, 90(2): 552–556.

Tayade, N.G., and Nagarsenker, M.S. 2010. Development and evaluation of artemether parenteral microemulsion. *Indian Journal of Pharmaceutical Sciences*, *72*(5): 637.

Trape, J.F., Snow, R.W., and Marsh, K. 2001. The past, present and future of childhood malaria mortality in Africa. *Trends in Parasitology*, *17*(12): 593-597.

Trape, J.F., Pison, G., Spiegel, A., Enel, C. and Rogier, C. 2002. Combating malaria in Africa. *Trends in parasitology*, *18*(5): 224-230.

Uhrich K. E., Cannizzaro S. M., Langer R.S., Shakesheff K. M. 1999. Polymeric systems for controlled drug release. *Chemical Reviews,* 99:3181–3198.

UN Millenium Project. 2005. Coming to Grips with Malaria in the New Millenium Task Force on HIV/AIDS, Malaria, TB and access to essential medicines, Working Group on Malaria. Sterling, VA: Earthscan.

van Agtmael M. A., Cheng-Qi S., Qing J. X., Mull R., van Boxtel C. J. 1999. Multiple dose pharmacokinetics of artemether in Chinese patients with uncomplicated falciparum malaria. *International Journal of Antimicrobial Agents,* 12:151-8.

van Vianen, P.H., van Engen, A., Thaithong, S., van der Keur, M., Tanke, H.J., van der Kaay, H.J., Mons, B. and Janse, C.J. 1993. Flow cytometric screening of blood samples for malaria parasites. *Cytometry*, *14*(3): 276-280.

Varelas, C.G., Dixon, D.G., Steiner, C. 1995. Zero-order release from biphasic polymer hydrogels. *Journal of Controlled Release,* 34: 185–192.

von Burkersroda, F., Schedl, L., Göpferich, A. 2002. Why degradable polymers undergo surface erosion or bulk erosion. *Biomaterials* 23(21): 4221–4231

Wada, R., Hyon, S.H., Ikada, Y. 1990. Lactic acid oligomer microspheres containing hydrophilic drugs. *Journal of Pharmaceutical Sciences,* 79: 919–924.

Wada, S., Suzuki, T., Noma, T. 1995. The effect of the particle sizes and the correlational sizes of dipoles introduced by the lattice defects on the crystal structure of barium titanate fine particles. *Japanese Journal of Applied Physics,* 34(1,9B): 5368–5379. DOI: 10.1143/JJAP.34.5368

Wagner, J.G. 1969. Interpretation of percent dissolved-time plots derived from *in vitro* testing of conventional tablets and capsules. *Journal of Pharmaceutical Sciences*, 58: 1253–1257.

Wang, G. and Uludag, H. 2008. Recent developments in nanoparticle-based drug delivery and targeting systems with emphasis on protein-based nanoparticles. *Expert Opinion on Drug Delivery*, *5*(5): 499-515.

Wang, S.H., Zhang, L.C., Lin, F., Sa, X.Y., Zuo, J.B., Shao, Q.X., Chen, G.S., Zeng, S. 2005. Controlled release of levonorgestrel from biodegradable poly (d,l-lactide co-glycolide) microspheres: *in vitro* and *in vivo* studies. *International Journal of Pharmaceutics*, 31: 217–225.

Warhurst, D.C., 1999. Drug resistance in Plasmodium falciparum malaria. *Infection*, *27*(2): S55-S58.

Wesche D. L., Decoster, M. A., Tortella F. C., and Brewer T. G. 1994 Neurotoxicity of artemisinin analogs in vitro. *Antimalarial Agents & Chemotherapy* 38 1813-1819.

White NJ, van Vugt M, Ezzet F. 1999. Clinical pharmacokinetics and pharmacodynamics of artemether-lumefantrine. *Clinical Pharmacokinetics*, 37 (2): 105-25.

White, N.J., 1994. Artemisinin: current status. *Transactions of the Royal Society of Tropical Medicine and Hygiene*, *88*(1): 3-4.

WHO, 1995. WHO Model Prescribing Information: Drugs used in Parasitic Diseases, 2nd Edition. 152. http://apps.who.int/medicinedocs/en/d/Jh2922e/2.5.10.html Accessed on 6th November, 2015.

World Health Organization and WHO Expert Committee on Malaria, 2000. WHO Expert Committee on Malaria: twentieth report.

WHO, 2013. Global malaria programme. World Malaria Report. WHO, Geneva. http://www.who.int/malaria/publications/world_malaria_report_2013/en/.

WHO, 2015. World Malaria Report. WHO, Geneva. http://www.who.int/**malaria**/publications/world-malaria-report-2015/report/en/.

Wischke, C., Schwendeman, S.P. 2008. Principles of encapsulating hydrophobic drugs in PLA/PLGA microspheres. *International Journal of Pharmaceutics*, 364(2): 298–327. DOI: 10.1016/j.ijpharm.2008.04.042

Wischke, C., Zhang, Y., Mittal, S., Schwendeman, S.P. 2010. Development of PLGA-based injectable delivery systems for hydrophobic fenretinide. *Pharmaceutical Research*, 27(10): 2063–2074. DOI: 10.1007/s11095-010-0202-y.

Woerdenbag, H.J., Pras, N., Bos, R., Visser, J.F., Hendriks, H. and Malingré, T.M. 1991. Analysis of artemisinin and related sesquiterpenoids from *Artemisia annua* L. by combined gas chromatography/mass spectrometry. *Phytochemical Analysis*, *2*(5): 215-219.

Wongsrichanalai, C., Barcus, M.J., Muth, S., Sutamihardja, A. and Wernsdorfer, W.H., 2007. A review of malaria diagnostic tools: microscopy and rapid diagnostic test (RDT). *The American Journal of Tropical Medicine and Hygiene*, *77*(6): 119-127.

World Health Organization and WHO Expert Committee on Malaria, 2000. WHO Expert Committee on Malaria: twentieth report.

World Health Organization, 2002. *The world health report 2002: reducing risks, promoting healthy life*. World Health Organization.

World Health Organization, 2008. *World malaria report. Geneva: World Health Organization*. WHO/HTM/GMP.

World Health Organization, 2011. World Malaria Report (World Health Organization, Geneva).

World Health Organization, 2013. Malaria entomology and vector control.

World Health Organization. 2010. Guidelines for the treatment of malaria, second edition. *World Health Organization* http://whqlibdoc.who.int/publications/2010/9789241547925_eng.pdf.

World Health Organization. World malaria report. 2012. *World Health Organization* http://www.who.int/malaria/publications/world_malaria_report_2012/wmr2012_full_report.pdf (2012).

Wu, X.S. and Wang, N. 2001. Synthesis, characterization, biodegradation, and drug delivery application of biodegradable lactic/glycolic acid polymers. Part II: biodegradation. *Journal of Biomaterials Science, Polymer Edition*, *12*(1): 21-34.

Xing, J., Xie, C. and Lou, H. 2007. Recent applications of liquid chromatography–mass spectrometry in natural products bioanalysis. *Journal of Pharmaceutical and Biomedical Analysis*, *44*(2): 368-378.

Yamamoto, M., Takada, S. and Ogawa, Y., Takeda Chemical Industries, Ltd., 1994. *Sustained release microcapsule*. U.S. Patent 5,330,767.

Yang, Y.Y., Chung, T.S. and Ng, N.P. 2001. Morphology, drug distribution, and *in vitro* release profiles of biodegradable polymeric microspheres

containing protein fabricated by double-emulsion solvent extraction/evaporation method. *Biomaterials, 22*(3): 231-241.

Yeo, Y., Park, K., 2004. Control of encapsulation efficiency and initial burst in polymeric microparticle systems. *Archives of Pharmaceutical Research*, 27(1): 1–12.

Youyou T. (2011). The discovery of artemisinin (qinghaosu) and gifts from Chinese medicine. *Nature Medicine*, 17:19-22.

APPENDIX

A1 Particle size distribution of artemether-loaded RG503H PLGA microspheres

Particle Name: PLGA	**Accessory Name:** Hydro 2000S (A)	**Analysis model:** General purpose	**Sensitivity:** Normal
Particle RI: 1.590	**Absorption:** 0.01	**Size range:** 0.020 to 2000.000 um	**Obscuration:** 2.52 %
Dispersant Name: Water	**Dispersant RI:** 1.330	**Weighted Residual:** 1.523 %	**Result Emulation:** Off
Concentration: 0.0238 %Vol	**Span :** 0.680	**Uniformity:** 0.215	**Result units:** Volume
Specific Surface Area: 0.0899 m²/g	**Surface Weighted Mean D[3,2]:** 66.764 um	**Vol. Weighted Mean D[4,3]:** 71.375 um	

d(0.1): 49.403 um d(0.5): 69.057 um d(0.9): 96.380 um

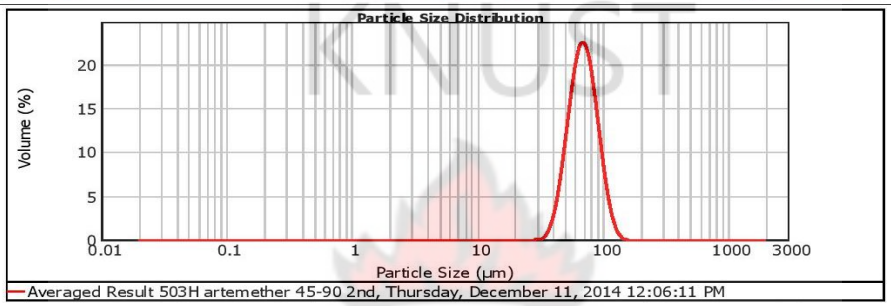

A2 Particle size distribution of artemether-loaded RG503H PLGA microspheres

Particle Name: PLGA	**Accessory Name:** Hydro 2000S (A)	**Analysis model:** General purpose	**Sensitivity:** Normal
Particle RI: 1.590	**Absorption:** 0.01	**Size range:** 0.020 to 2000.000 um	**Obscuration:** 1.76 %
Dispersant Name: Water	**Dispersant RI:** 1.330	**Weighted Residual:** 1.373 %	**Result Emulation:** Off
Concentration: 0.0168 %Vol	**Span :** 0.760	**Uniformity:** 0.24	**Result units:** Volume
Specific Surface Area: 0.0887 m²/g	**Surface Weighted Mean D[3,2]:** 67.611 um	**Vol. Weighted Mean D[4,3]:** 73.342 um	

d(0.1): 48.608 um d(0.5): 70.406 um d(0.9): 102.133 um

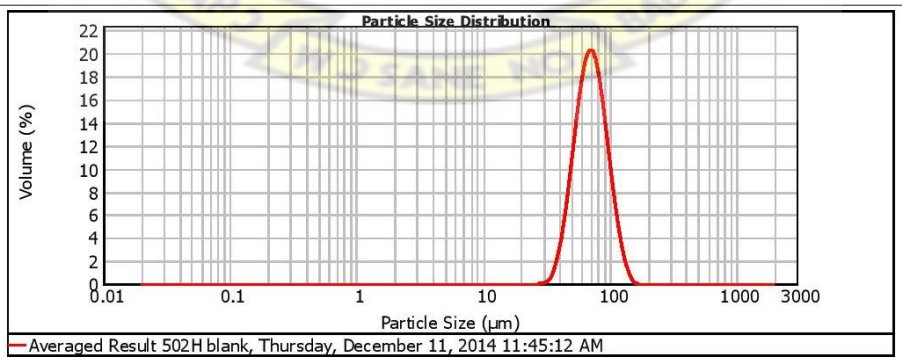

B1 Parameters for calculation of release of artemether from RG503H polymer microspheres

	Peak area of artemether	**mg/ml**	**mg/10 ml**	**%loading 1**	**Mass of artemether released**	**% release 1**
Day 0	116503	0.247739247	2.477392473	24.77392473	0	0
Day 1	102449	0.21840165	2.1840165	21.840165	2.933759738	11.84212744
Day 3	98766	0.210713421	2.107134209	21.07134209	3.702582644	14.94548273
Day7	36391	0.080506175	0.805061748	8.05061748	16.72330725	67.50366538
Day 14	37735	0.083311763	0.833117626	8.331176259	16.44274847	66.37118927
Day 21	36294	0.080303688	0.803036882	8.030368818	16.74355592	67.58539915

B2 Parameters for calculation of release of artemether from RG503H polymer microspheres

	Peak area of artemether	**mg/ml**	**mg/10 ml**	**%loading 2**	**Mass of artemether released**	**% RELEASE 2**
Day 0	116503	0.247739247	2.477392473	24.77392473	0	0
Day 1	104633	0.22296073	2.229607301	22.29607301	2.477851721	10.00185376
Day 3	93974	0.200710164	2.007101644	20.07101644	4.702908292	18.98329935
Day 7	39188	0.086344887	0.863448869	8.63448869	16.13943604	65.146868
Day 14	31177	0.069621997	0.696219971	6.962199714	17.81172502	71.89706601
Day 21	34637	0.076844716	0.768447157	7.684471573	17.08945316	68.98161412

mg/ml = (peak area+2175)/479044)

% loading = (Mass in 10 ml/10 mg) *100

mg/10 ml = Mass of artemether in 10 ml

mass of artemether released = day 0 loading – loading of specific day

% release = (mass of artemether released /day 0 loading) * 100

B3 Parameters used to obtain calibration curve for release of artemether from RG502H polymer microspheres

Concentration of artemether (mg/ml)	Peak Area of artemether 1	Peak Area of artemether 2	Peak Area of artemether 3	Peak Area (Average)
0.5	3.942785883	4.22547244	4.045755288	4.07133787
0.3	2.383035629	2.371963019	2.39444622	2.383148289
0.1	0.691576906	0.784588566	0.89887663	0.791680701
0.05	0.424303233	0.393426714	0.074498975	0.297409641
0.03	0.252726831	0.193617274	0.43100216	0.292448755
0.02	0.122056704	0.139744021	0.127792723	0.129864483
0.01	0.047537985	0.047547296	0.047398668	0.04749465

B4 Parameters for calculation of release of artemether from RG503H polymer microspheres

	Peak Area	mg/ml	mg/10 ml	% loading	Average %loading	% Release
Day 0	95410	0.205771095	2.057710953	20.57710953	19.6	0
Day 0	90309	0.194872803	1.948728034	19.48728034		
Day 0	87322	0.188491075	1.884910748	18.84910748		
Day 1	75117	0.162415079	1.624150794	16.24150794	15.6	20.5
Day 1	72907	0.157693412	1.576934121	15.76934121		
Day 1	68454	0.148179573	1.481795729	14.81795729		
Day 3	39101	0.085466858	0.854668575	8.546685753	8.6	56.1
Day 3	37891	0.082881691	0.828816913	8.288169125		
Day 3	41110	0.089759088	0.897590881	8.975908814		
Day 7	23848	0.052878807	0.52878807	5.287880698	5.2	73.0
Day 7	16044	0.036205553	0.362055528	3.620555277		
Day 7	31743	0.069746483	0.697464828	6.974648279		
Day 14	15247	0.034502761	0.345027614	3.450276143	3.6	81.7
Day 14	18451	0.041348111	0.413481108	4.13481108		
Day 14	14053	0.031951779	0.319517792	3.195177917		
Day 21	29606	0.06518078	0.6518078	6.518078004	6.7	66.5
Day 21	33442	0.073376398	0.733763981	7.337639807		
Day 21	29172	0.064253539	0.642535386	6.425353858		

B5 Release of artemether from RG503H and RG502H polymer microspheres

Time (days)	Average % Drug Release for RG502H polymer microspheres	Average % Drug Release For RG502H polymer microspheres
0	**0** ± 0	**0** ± 0
1	**11** ± 1.3012	**20.5** ± 1.2510
3	**17** ± 2.8552	**56.1** ±3.2638
7	**66** ± 1.6665	**72.9** ±9.2906
14	**69** ± 3.9074	**81.7** ± 2.5181
21	**68** ± 0.9873	**65.5** ± 3.0070

B6 Mass loss of artemether-loaded PLGA microspheres

	Mass loss (%)	
	RG502H formulation	RG503H formulation
Day 0	20.78 ± 0	15.48 ± 2.2698
Day 1	14.72 ± 0	22.31 ± 1.7819
Day 7	24.81 ± 2.0718	11.20 ± 4.8649
Day 14	46.47 ± 0.1556	35.36 ± 5.0205

B7 Parameters for determination of molecular weight profiles of artemether loaded PLGA microspheres

	Mw	Average Retention time (min)	V-V0	KD	LOG Mw	V-V0
STD 1	476.8	10.17	-16.2987	0.615772592	2.678336247	-16.2987
STD 2	183.3	10.504	-15.9647	0.603153914	2.263162465	-15.9647
STD 3	101.3	10.723	-15.7457	0.59487999	2.005609445	-15.7457
STD 4	48.1	10.957	-15.5117	0.58603936	1.682145076	-15.5117
STD 5	18	11.345	-15.1237	0.571380536	1.255272505	-15.1237
STD 6	4.13	12.258	-14.2107	0.536886965	0.615950052	-14.2107
STD 7	0.79	13.414	-13.0547	0.493212738	-0.102372909	-13.0547

V=6

VT = 26.4687

B8 Parameters for determination of molecular weight profiles of artemether loaded PLGA microspheres

Sample no.	Retention time 1 (min)	Retention time 2 (min)	Average Retention (min)	V-V0	K_D	Log Mw	Sample label
1	12.117	12.117	12.117	-14.352	0.542214011	6.47	RG502H
2	11.983	12	11.9915	-14.4772	0.546955461	8.31	RG502H
3	12.05	12.033	12.0415	-14.4272	0.545066437	7.52	RG503H
4	12.083	12.05	12.0665	-14.4022	0.544121925	7.15	RG503H
5	11.85	11.866	11.858	-14.6107	0.551999154	10.85	D0-1
6	11.861	11.85	11.8555	-14.6132	0.552093605	10.90	D0-2
7	11.5	11.467	11.4835	-14.9852	0.566147941	22.91	D0-3
8	11.492	11.491	11.4915	-14.9772	0.565845697	22.55	D0-4
9	11.958	11.946	11.952	-14.5167	0.548447789	8.99	D1-1
10	11.983	11.971	11.977	-14.4917	0.547503277	8.55	D1-2
11	11.481	11.508	11.4945	-14.9742	0.565732356	22.42	D1-3
12	11.455	11.46	11.4575	-15.0112	0.567130233	24.14	D1-4
13	12.55	12.667	12.6085	-13.8602	0.523644909	2.42	D7-1
14	12.367	12.383	12.375	-14.0937	0.532466649	3.86	D7-2
15	11.783	11.817	11.8	-14.6687	0.554190421	12.18	D7-3
16	11.789	11.768	11.7785	-14.6902	0.555002701	12.71	D7-4
17	12.417	12.471	12.444	-14.0247	0.529859797	3.37	D14-1
18	12.483	12.417	12.45	-14.0187	0.529633114	3.33	D14-2
19	12.467	12.45	12.4585	-14.0102	0.52931198	3.27	D14-3
20	12.587	12.584	12.5855	-13.8832	0.52451386	2.54	D14-4

B9 Key to parameters for determination of molecular weight profiles of artemether loaded PLGA microspheres (appendices 4 & 5)

Key	**Description**
1,2	RG502H formulations
3,4	RG503H formulations
D0	Day 0
D1	Day 1
D 7	Day 7
D 14	Day 14
K_D	Distribution coefficient

B10 Molecular weight profiles of artemether-loaded PLGA microspheres

Formulation type	Day 0	Day 1	Day 7	Day 14
RG502H microspheres	10.87 ± 0.038	8.77 ± 0.310	3.14 ± 1.018	3.35 ± 0.028
RG503H microspheres	22.73 ± 0.257	23.28 ± 1.216	12.45 ± 0.378	2.90 ± 0.518

A3 Calibration curve for LC-MS/MS quantification of artemether extracted from rat plasma

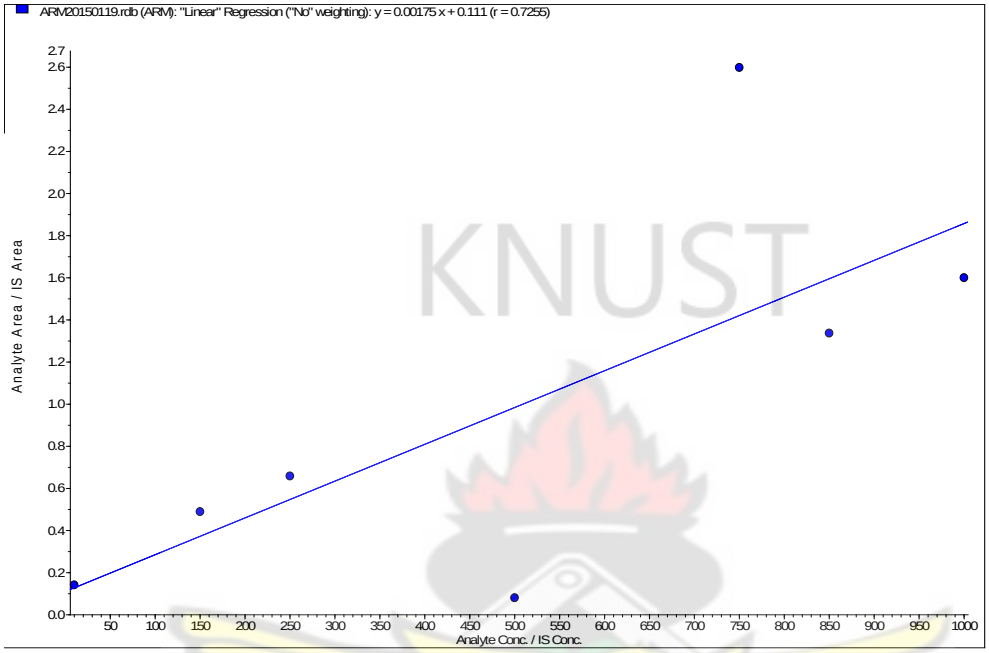

A4 Calibration curve for LC-MS/MS quantification of dihydroartemisinin extracted from rat plasma

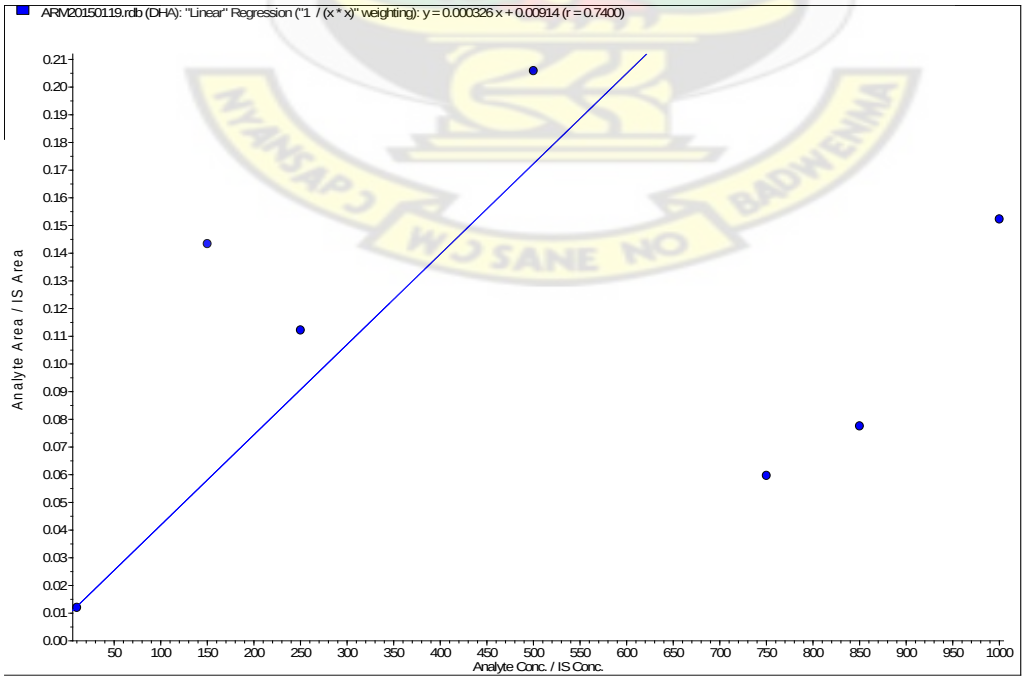

‘

A 5 Chromatograms of extracted artemether, dihydroartemisinin and artemisinin from rat plasma in pilot *in vivo* study

Acq. File: ARM LCMS.dam,..

Sample Name: 10ng/mL
Sample Number: Sample 1 of 21

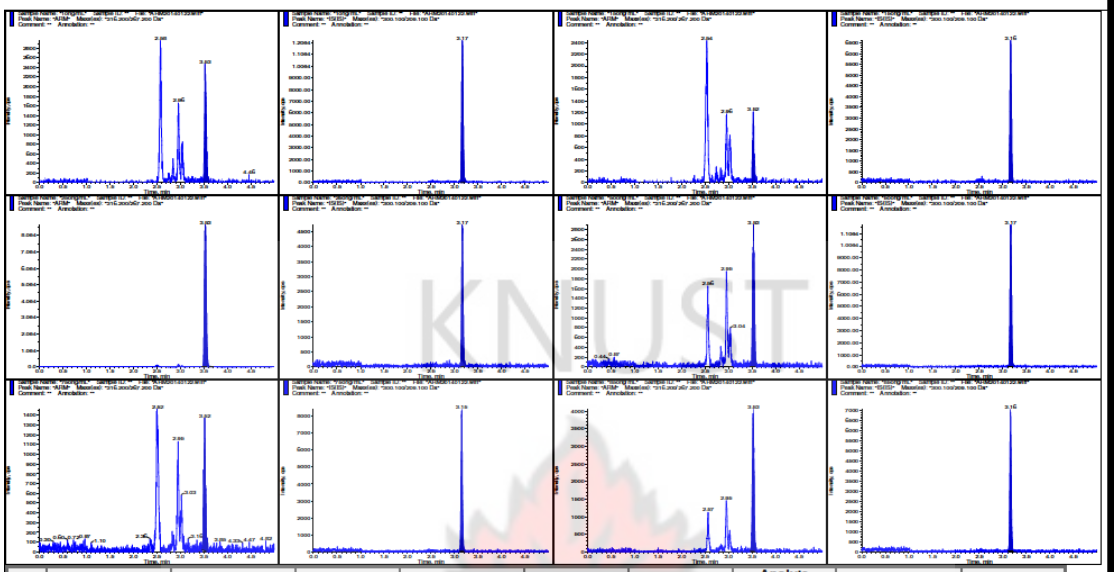

	Sample Name	Sample ID	Sample Type	File Name	Analyte Peak Area (counts)	Analyte Peak Height (cps)	Analyte Concentration (ng/mL)	Standard Query Status	IS Peak Area (counts)
1	10ng/mL		Standard	ARM20140122.wiff	5.87e+003	2.46e+003	10.0	N/A	2.46e+004
2	150ng/mL		Standard	ARM20140122.wiff	2.32e+003	1.20e+003	150.	N/A	1.26e+004
3	250ng/mL		Standard	ARM20140122.wiff	2.20e+005	8.64e+004	250.	N/A	9.08e+003
4	500ng/mL		Standard	ARM20140122.wiff	6.88e+003	2.89e+003	500.	N/A	2.32e+004

Acq. File: ARM LCMS.dam,..

Sample Name: 1000ng/mL
Sample Number: Sample 1 of 21

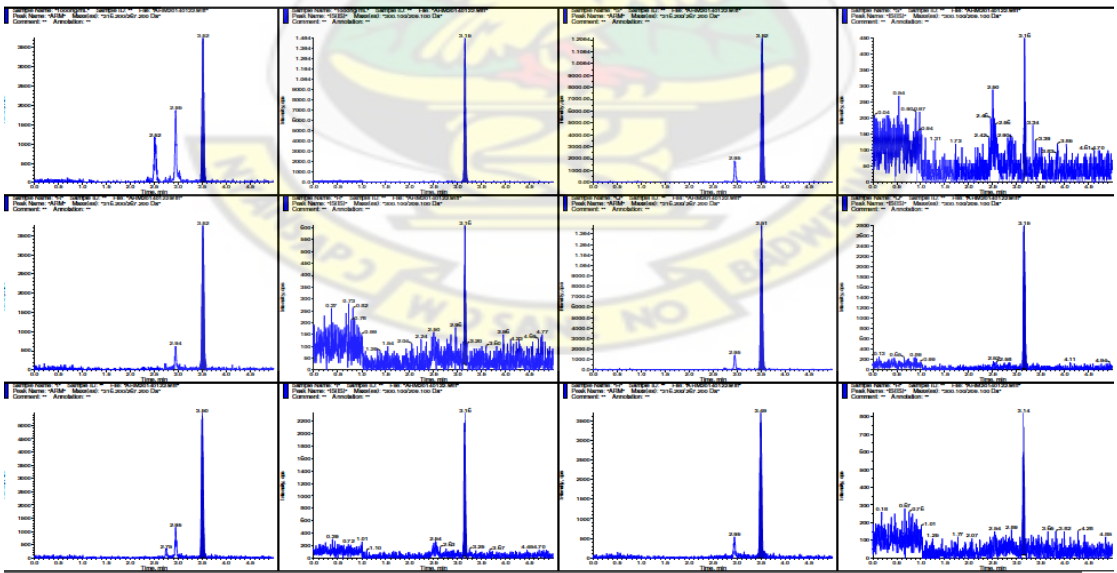

	Sample Name	Sample ID	Sample Type	File Name	Analyte Peak Area (counts)	Analyte Peak Height (cps)	Analyte Concentration (ng/mL)	Standard Query Status	IS Peak Area (counts)
7	1000ng/mL		Standard	ARM20140122.wiff	8.83e+003	3.79e+003	1000.	N/A	2.73e+004
8	S		Unknown	ARM20140122.wiff	3.01e+004	1.21e+004	N/A	N/A	5.60e+002
9	R		Unknown	ARM20140122.wiff	9.53e+003	3.76e+003	N/A	N/A	9.05e+002
10	Q		Unknown	ARM20140122.wiff	3.41e+004	1.38e+004	N/A	N/A	5.75e+003

cq. File: ARM LCMS.dam,..

Sample Name: 10ng/mL
Sample Number: Sample 1 of 21

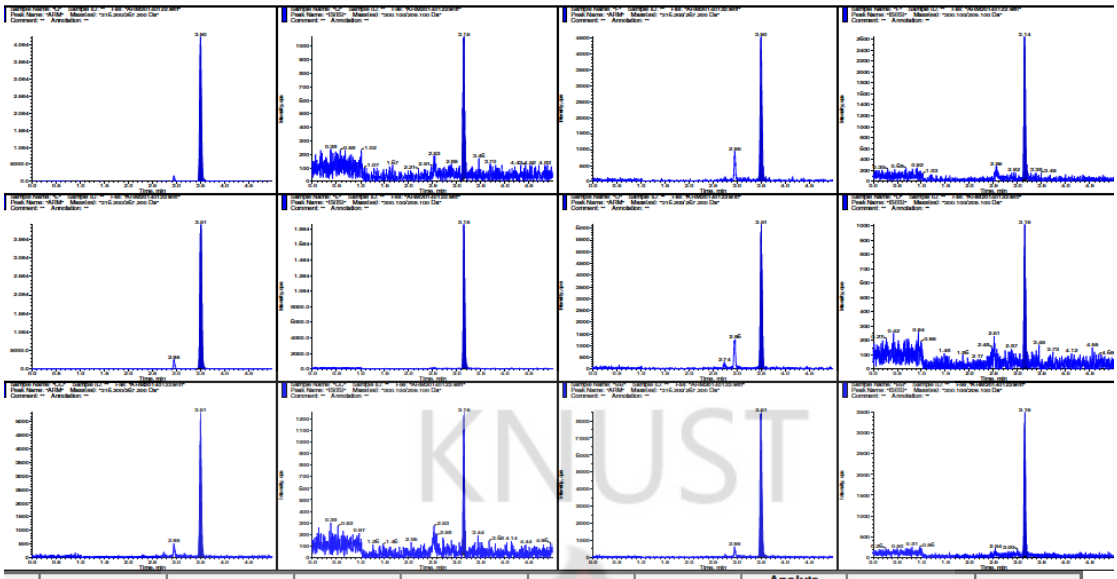

	Sample Name	Sample ID	Sample Type	File Name	Analyte Peak Area (counts)	Analyte Peak Height (cps)	Analyte Concentration (ng/mL)	Standard Query Status	IS Peak Area (counts)
13	G		Unknown	ARM20140122.wiff	1.09e+005	4.25e+004	N/A	N/A	2.19e+003
14	F		Unknown	ARM20140122.wiff	1.14e+004	4.63e+003	N/A	N/A	5.09e+003
15	E		Unknown	ARM20140122.wiff	9.99e+004	3.93e+004	N/A	N/A	3.48e+004
16	D		Unknown	ARM20140122.wiff	1.40e+004	6.17e+003	N/A	N/A	1.93e+003

cq. File: ARM LCMS.dam,..

Sample Name: 10ng/mL
Sample Number: Sample 1 of 21

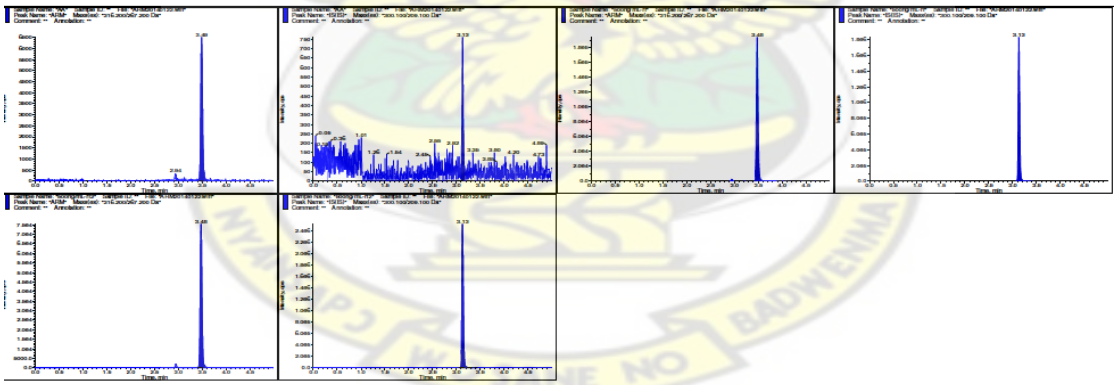

	Sample Name	Sample ID	Sample Type	File Name	Analyte Peak Area (counts)	Analyte Peak Height (cps)	Analyte Concentration (ng/mL)	Standard Query Status	IS Peak Area (counts)
19	AA		Unknown	ARM20140122.wiff	1.60e+004	6.55e+003	N/A	N/A	1.32e+003
20	500ng/mL-rf		Quality Control	ARM20140122.wiff	4.83e+005	1.94e+005	500.	N/A	3.84e+006
21	500ng/mL-rf2		Quality Control	ARM20140122.wiff	1.87e+005	7.57e+004	500.	N/A	5.42e+006

A6 Chromatograms of extracted artemether, dihydroartemisinin and artemisinin from rat plasma in main *in vivo* study

Acq. File: ARM LCMS.dam,..

Sample Name: Ung/mL
Sample Number: Sample 1 of 88

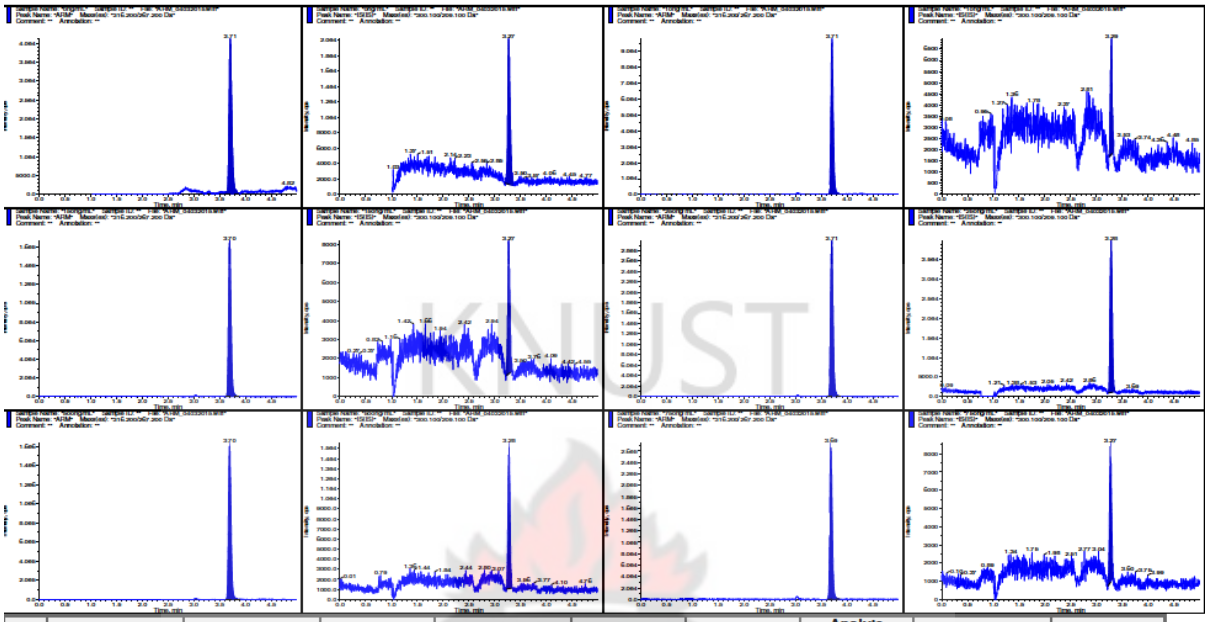

	Sample Name	Sample ID	Sample Type	File Name	Analyte Peak Area (counts)	Analyte Peak Height (cps)	Analyte Concentration (ng/mL)	Standard Query Status	IS Peak Area (counts)
1	0ng/mL		Unknown	ARM_04032015.wif	1.47e+005	4.09e+004	N/A	N/A	5.62e+004
2	10ng/mL		Standard	ARM_04032015.wif	3.06e+005	9.77e+004	10.0	N/A	1.07e+004
3	150ng/mL		Standard	ARM_04032015.wif	5.16e+005	1.70e+005	150.	N/A	1.72e+004
4	250ng/mL		Standard	ARM_04032015.wif	9.64e+005	3.00e+005	250.	N/A	1.04e+005

Acq. File: ARM LLMs.dam,..

Sample Name: 0ng/mL
Sample Number: Sample 1 of 88

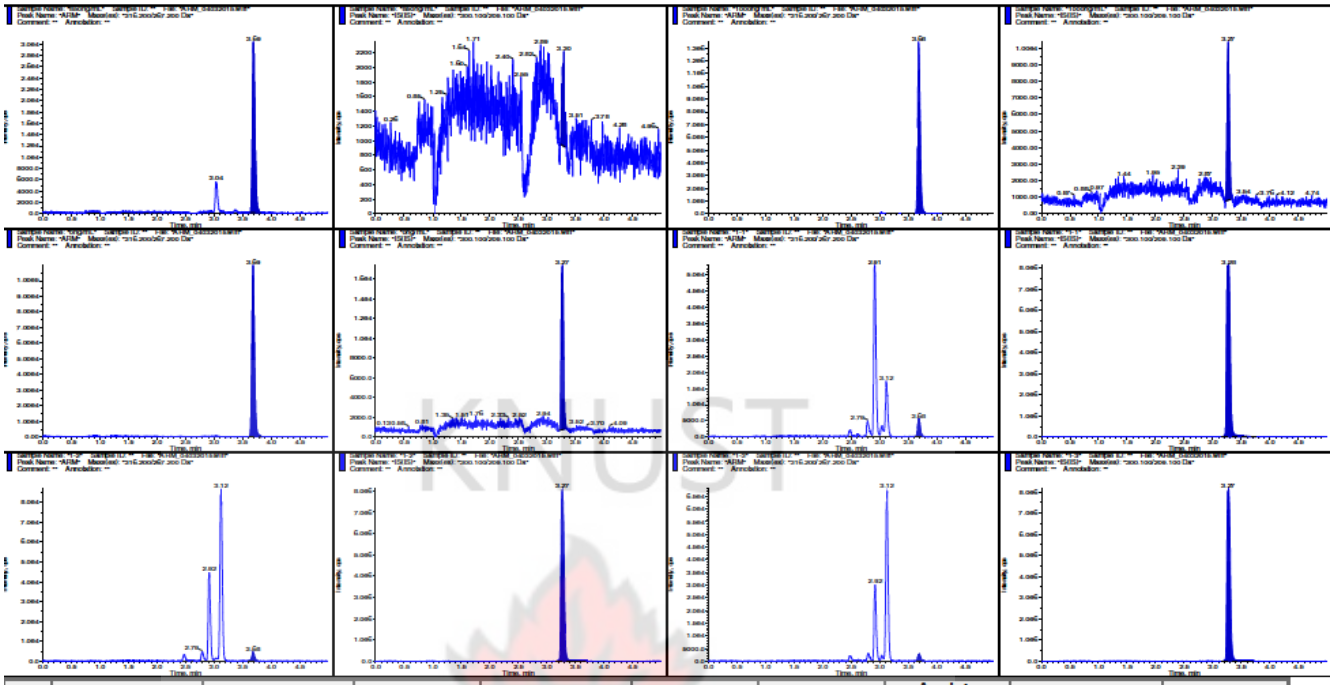

	Sample Name	Sample ID	Sample Type	File Name	Analyte Peak Area (counts)	Analyte Peak Height (cps)	Analyte Concentration (ng/mL)	Standard Query Status	IS Peak Area (counts)
7	850ng/mL		Standard	ARM_04032015.wif	9.03e+004	3.03e+004	850.	N/A	2.92e+003
8	1000ng/mL		Standard	ARM_04032015.wif	4.11e+006	1.37e+006	1000.	N/A	2.45e+004
9	0ng/mL		Unknown	ARM_04032015.wif	3.20e+005	1.10e+005	N/A	N/A	4.60e+004
10	1-1		Unknown	ARM_04032015.wif	1.66e+004	5.54e+003	N/A	N/A	3.44e+007

Acq. File: ARM LCMS.dam,..

Sample Name: Ung/mL
Sample Number: Sample 1 of 88

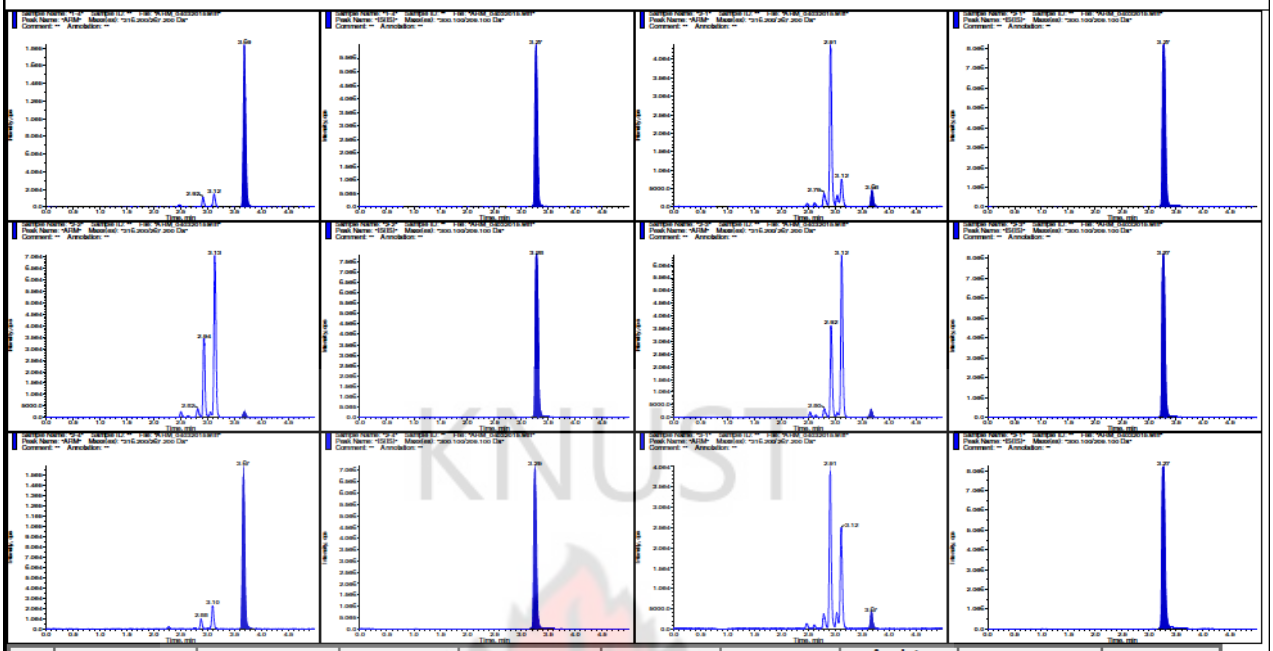

	Sample Name	Sample ID	Sample Type	File Name	Analyte Peak Area (counts)	Analyte Peak Height (cps)	Analyte Concentration (ng/mL)	Standard Query Status	IS Peak Area (counts)
13	1-4		Unknown	ARM_04032015.wif	5.36e+005	1.84e+005	N/A	N/A	2.08e+007
14	2-1		Unknown	ARM_04032015.wif	1.26e+004	4.31e+003	N/A	N/A	3.43e+007
15	2-2		Unknown	ARM_04032015.wif	7.19e+003	2.51e+003	N/A	N/A	2.86e+007
16	2-3		Unknown	ARM_04032015.wif	8.70e+003	3.02e+003	N/A	N/A	3.05e+007

Acq. File: ARM LCMS.dam,..

Sample Name: 0ng/mL
Sample Number: Sample 1 of 88

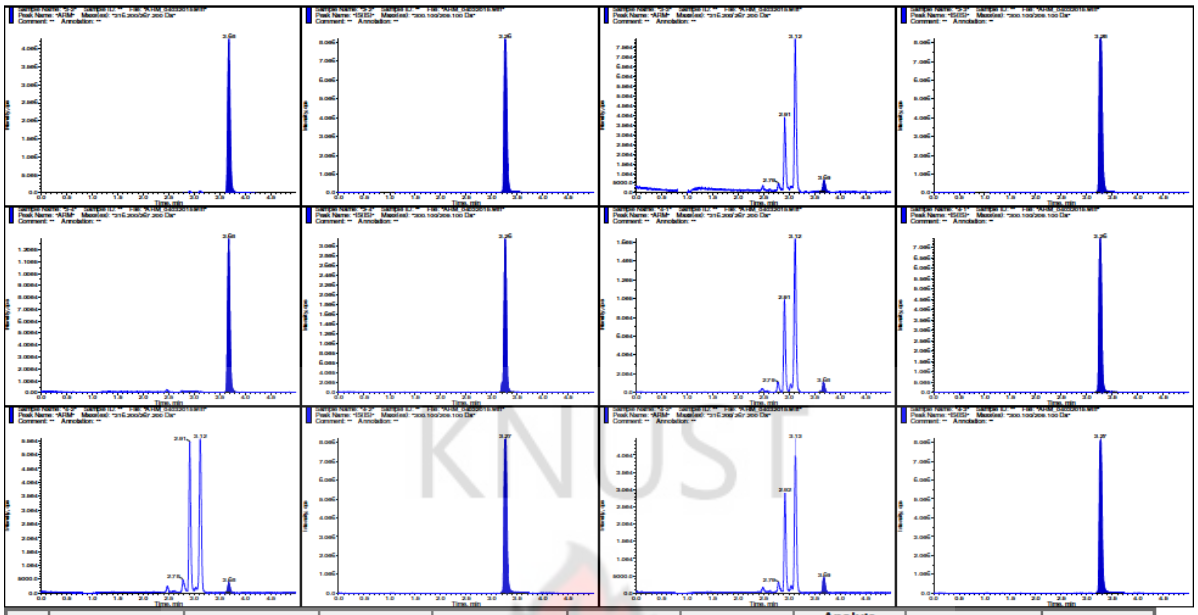

	Sample Name	Sample ID	Sample Type	File Name	Analyte Peak Area (counts)	Analyte Peak Height (cps)	Analyte Concentration (ng/mL)	Standard Query Status	IS Peak Area (counts)
19	3-2		Unknown	ARM_04032015.wif	1.42e+007	4.35e+006	N/A	N/A	3.27e+007
20	3-3		Unknown	ARM_04032015.wif	1.80e+004	5.85e+003	N/A	N/A	3.30e+007
21	3-4		Unknown	ARM_04032015.wif	3.78e+005	1.29e+005	N/A	N/A	9.85e+006
22	4-1		Unknown	ARM_04032015.wif	3.12e+004	1.04e+004	N/A	N/A	2.64e+007

Acq. File: ARM LCMS.dam,..

Sample Name: 0ng/mL
Sample Number: Sample 1 of 88

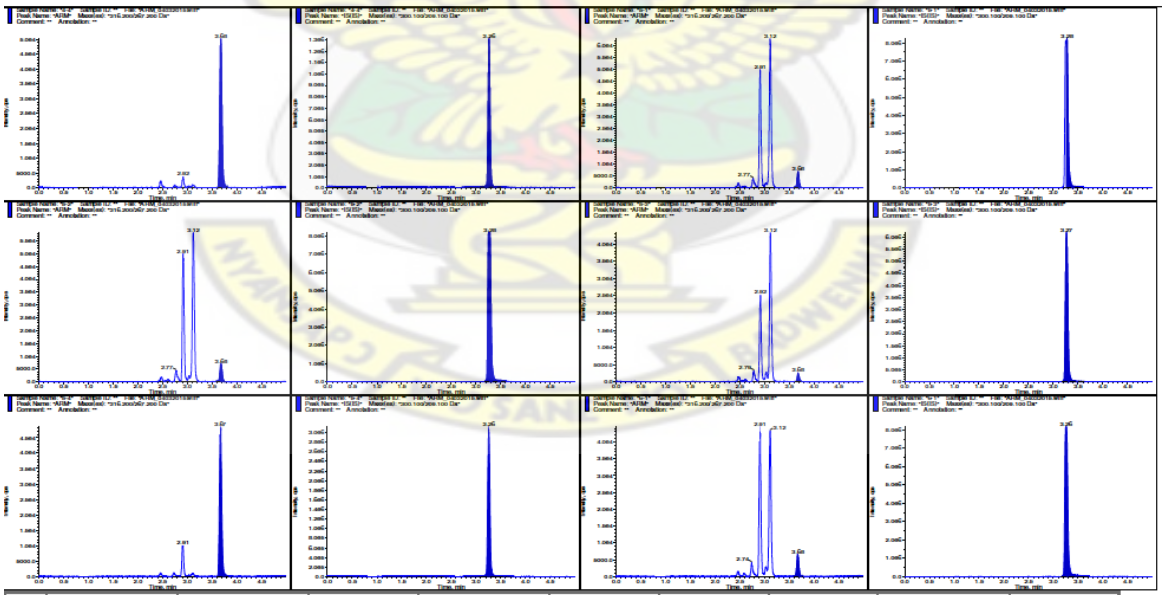

	Sample Name	Sample ID	Sample Type	File Name	Analyte Peak Area (counts)	Analyte Peak Height (cps)	Analyte Concentration (ng/mL)	Standard Query Status	IS Peak Area (counts)
25	4-4		Unknown	ARM_04032015.wif	1.53e+005	5.05e+004	N/A	N/A	3.66e+006
26	5-1		Unknown	ARM_04032015.wif	2.05e+004	6.84e+003	N/A	N/A	2.01e+007
27	5-2		Unknown	ARM_04032015.wif	2.08e+004	7.01e+003	N/A	N/A	3.68e+007
28	5-3		Unknown	ARM_04032015.wif	6.47e+003	2.50e+003	N/A	N/A	2.14e+007

Acq. File: AKM LLMs.dam,..

Sample Name: 0ng/mL
Sample Number: Sample 1 of 88

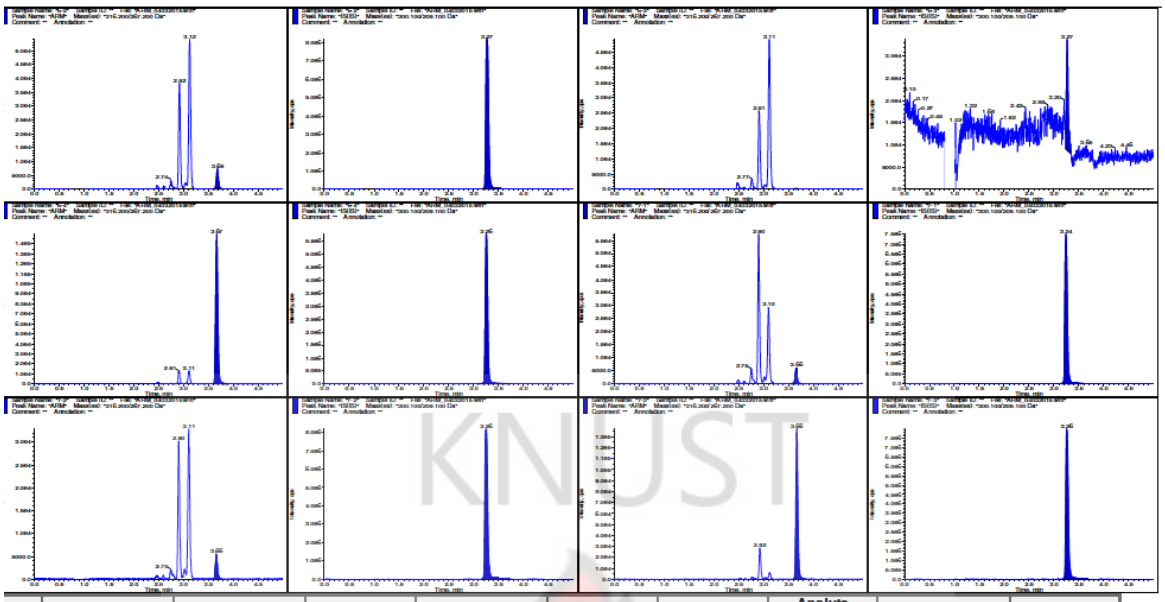

	Sample Name	Sample ID	Sample Type	File Name	Analyte Peak Area (counts)	Analyte Peak Height (cps)	Analyte Concentration (ng/mL)	Standard Query Status	IS Peak Area (counts)
31	6-2		Unknown	ARM_04032015.wif	2.08e+004	7.25e+003	N/A	N/A	3.20e+007
32	6-3		Unknown	ARM_04032015.wif	3.23e+002	2.03e+002	N/A	N/A	6.09e+004
33	6-4		Unknown	ARM_04032015.wif	4.58e+005	1.50e+005	N/A	N/A	1.94e+007
34	7-1		Unknown	ARM_04032015.wif	1.75e+004	6.13e+003	N/A	N/A	2.63e+007

Acq. File: AKM LLMs.dam,..

Sample Name: 0ng/mL
Sample Number: Sample 1 of 88

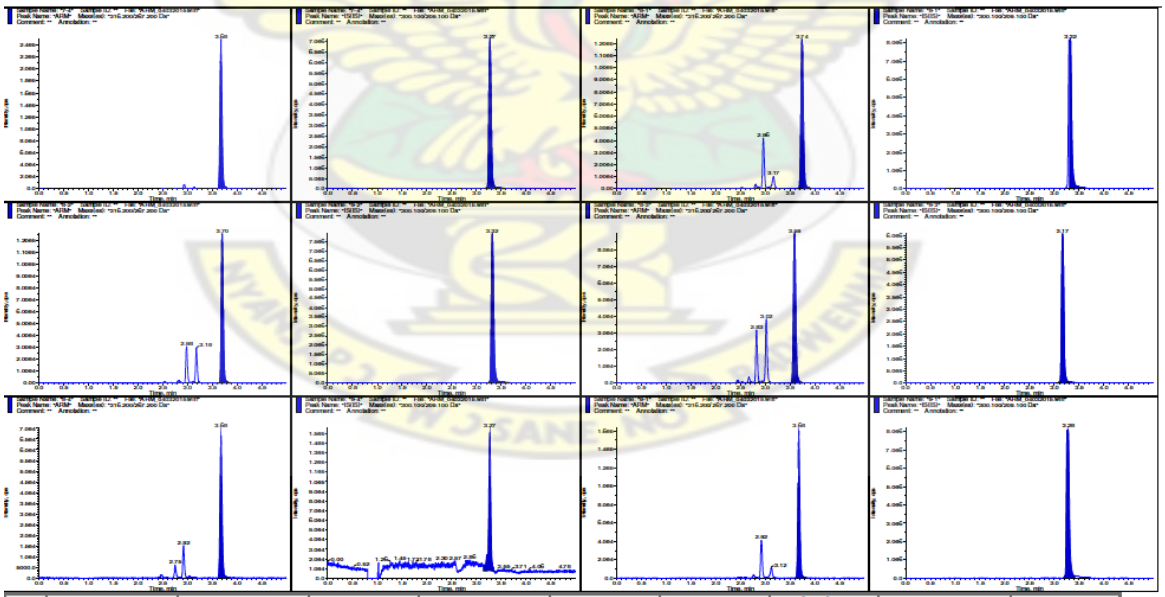

	Sample Name	Sample ID	Sample Type	File Name	Analyte Peak Area (counts)	Analyte Peak Height (cps)	Analyte Concentration (ng/mL)	Standard Query Status	IS Peak Area (counts)
37	7-4		Unknown	ARM_04032015.wif	7.38e+005	2.51e+005	N/A	N/A	2.44e+007
38	8-1		Unknown	ARM_04032015.wif	4.11e+005	1.23e+005	N/A	N/A	2.30e+007
39	8-2		Unknown	ARM_04032015.wif	3.55e+005	1.26e+005	N/A	N/A	2.88e+007
40	8-3		Unknown	ARM_04032015.wif	2.97e+005	9.04e+004	N/A	N/A	2.03e+007

Sample Number: Sample 1 of 88

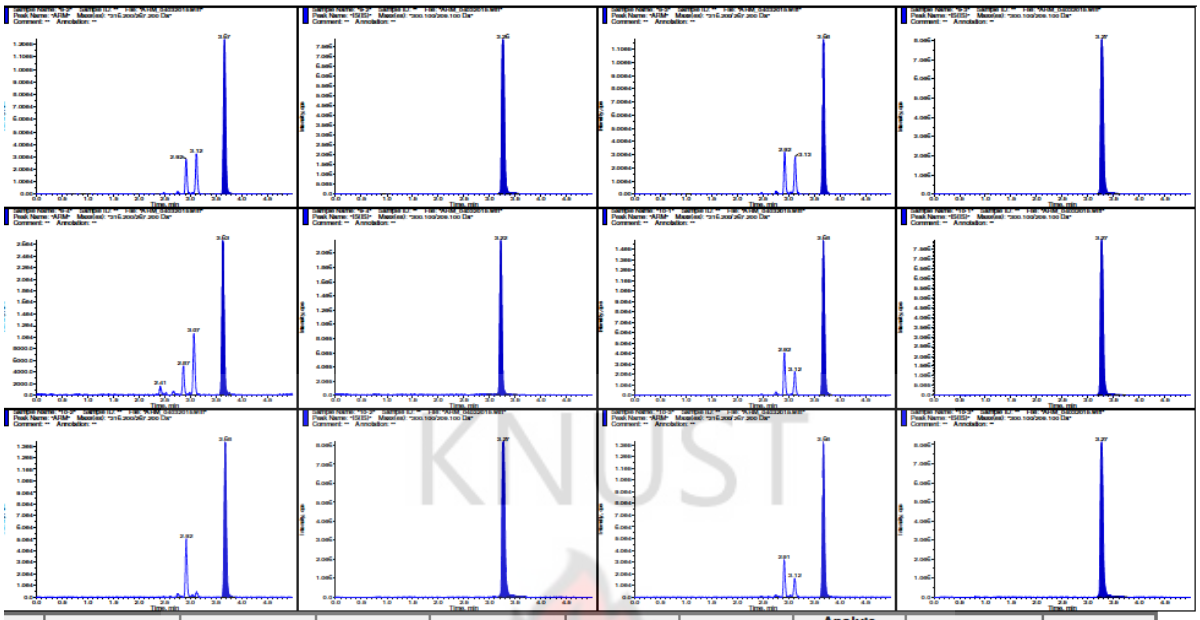

	Sample Name	Sample ID	Sample Type	File Name	Analyte Peak Area (counts)	Analyte Peak Height (cps)	Analyte Concentration (ng/mL)	Standard Query Status	IS Peak Area (counts)
43	9-2		Unknown	ARM_04032015.wif	3.75e+005	1.25e+005	N/A	N/A	2.89e+007
44	9-3		Unknown	ARM_04032015.wif	3.53e+005	1.18e+005	N/A	N/A	2.93e+007
45	9-4		Unknown	ARM_04032015.wif	8.00e+004	2.66e+004	N/A	N/A	6.09e+006
46	10-1		Unknown	ARM_04032015.wif	4.22e+005	1.49e+005	N/A	N/A	2.94e+007

Acq. File: ARM LCMS.dam,..

Sample Name: Ung/mL
Sample Number: Sample 1 of 88

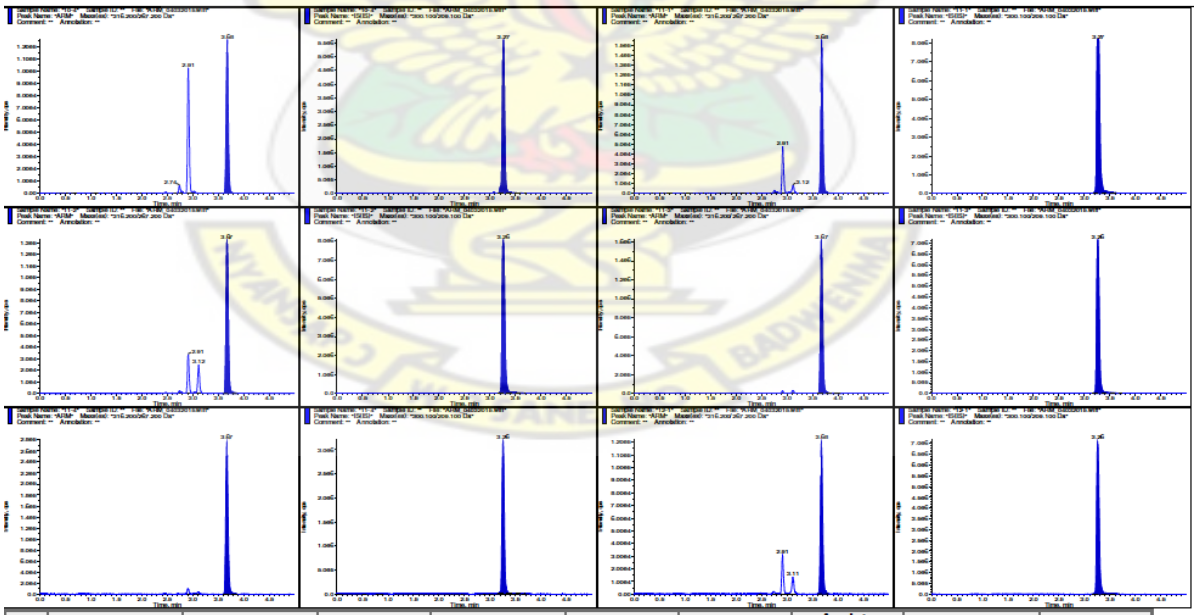

	Sample Name	Sample ID	Sample Type	File Name	Analyte Peak Area (counts)	Analyte Peak Height (cps)	Analyte Concentration (ng/mL)	Standard Query Status	IS Peak Area (counts)
49	10-4		Unknown	ARM_04032015.wif	3.56e+005	1.26e+005	N/A	N/A	1.77e+007
50	11-1		Unknown	ARM_04032015.wif	4.44e+005	1.56e+005	N/A	N/A	3.50e+007
51	11-2		Unknown	ARM_04032015.wif	3.93e+005	1.33e+005	N/A	N/A	3.00e+007
52	11-3		Unknown	ARM_04032015.wif	4.91e+006	1.63e+006	N/A	N/A	2.45e+007

Acq. File: ARM LCMS.dam,..
Sample Name: Ung/mL
Sample Number: Sample 1 of 88

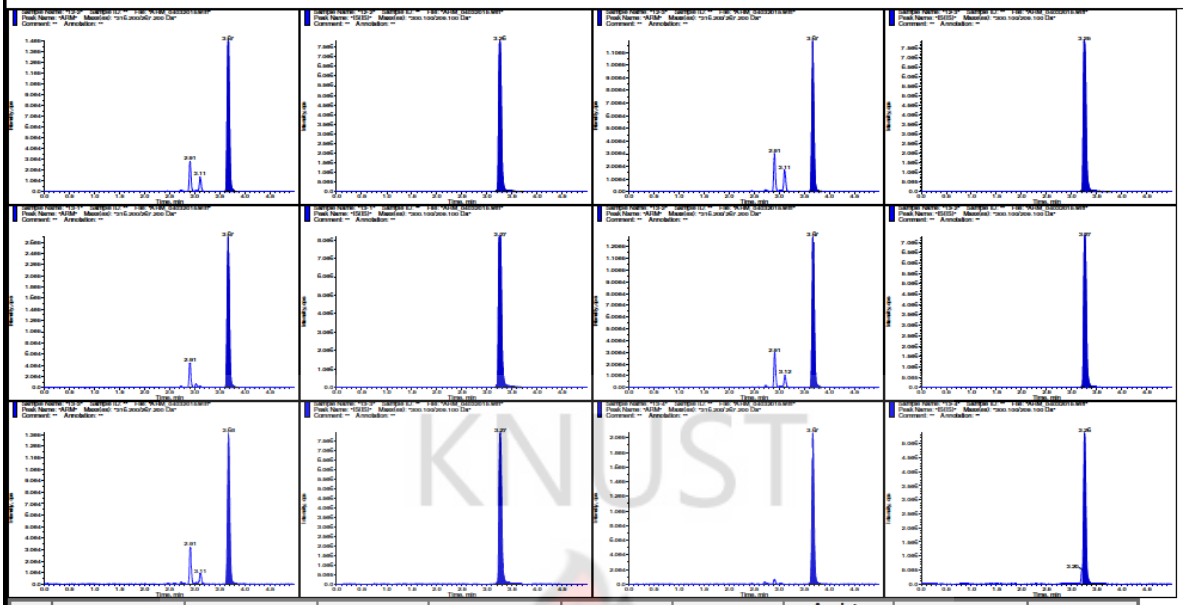

	Sample Name	Sample ID	Sample Type	File Name	Analyte Peak Area (counts)	Analyte Peak Height (cps)	Analyte Concentration (ng/mL)	Standard Query Status	IS Peak Area (counts)
55	12-2		Unknown	ARM_04032015.wif	4.41e+005	1.40e+005	N/A	N/A	2.93e+007
56	12-3		Unknown	ARM_04032015.wif	3.47e+005	1.19e+005	N/A	N/A	2.97e+007
57	13-1		Unknown	ARM_04032015.wif	8.10e+005	2.71e+005	N/A	N/A	3.53e+007
58	13-2		Unknown	ARM_04032015.wif	3.98e+005	1.29e+005	N/A	N/A	2.62e+007

Sample Number: Sample 1 of 88

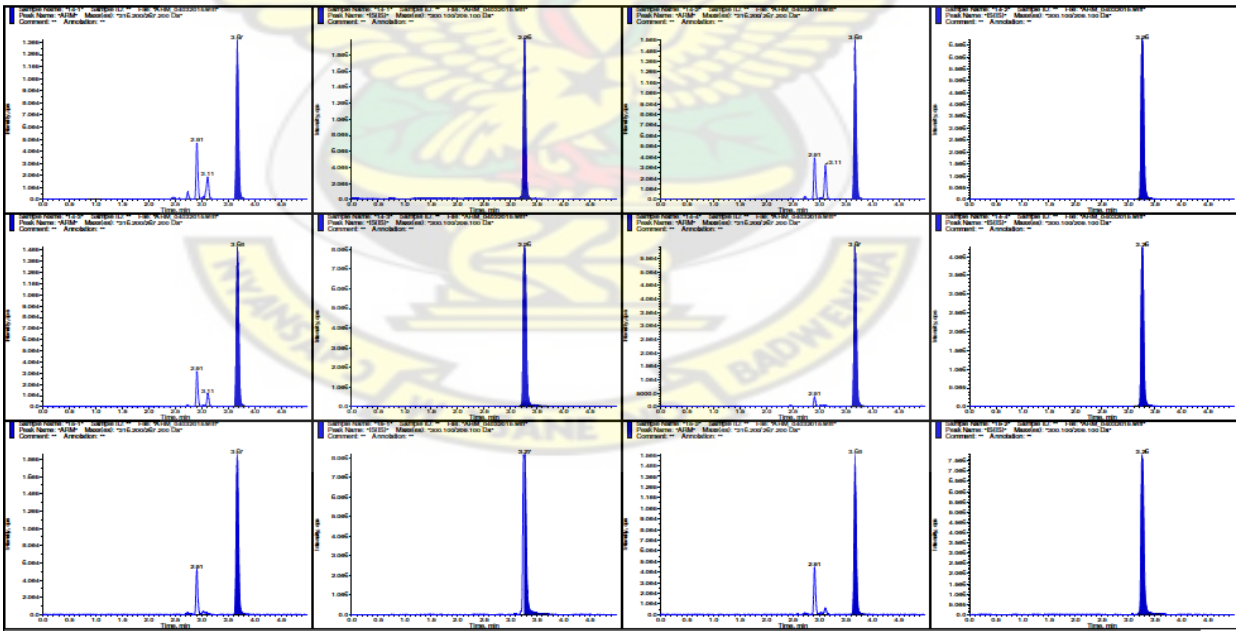

	Sample Name	Sample ID	Sample Type	File Name	Analyte Peak Area (counts)	Analyte Peak Height (cps)	Analyte Concentration (ng/mL)	Standard Query Status	IS Peak Area (counts)
61	14-1		Unknown	ARM_04032015.wif	3.78e+005	1.32e+005	N/A	N/A	5.57e+006
62	14-2		Unknown	ARM_04032015.wif	4.34e+005	1.50e+005	N/A	N/A	2.29e+007
63	14-3		Unknown	ARM_04032015.wif	4.19e+005	1.43e+005	N/A	N/A	3.15e+007
64	14-4		Unknown	ARM_04032015.wif	1.85e+005	5.97e+004	N/A	N/A	1.32e+007

Acq. File: AKM LLMs.dam,..

Sample Name: Ung/mL
Sample Number: Sample 1 of 88

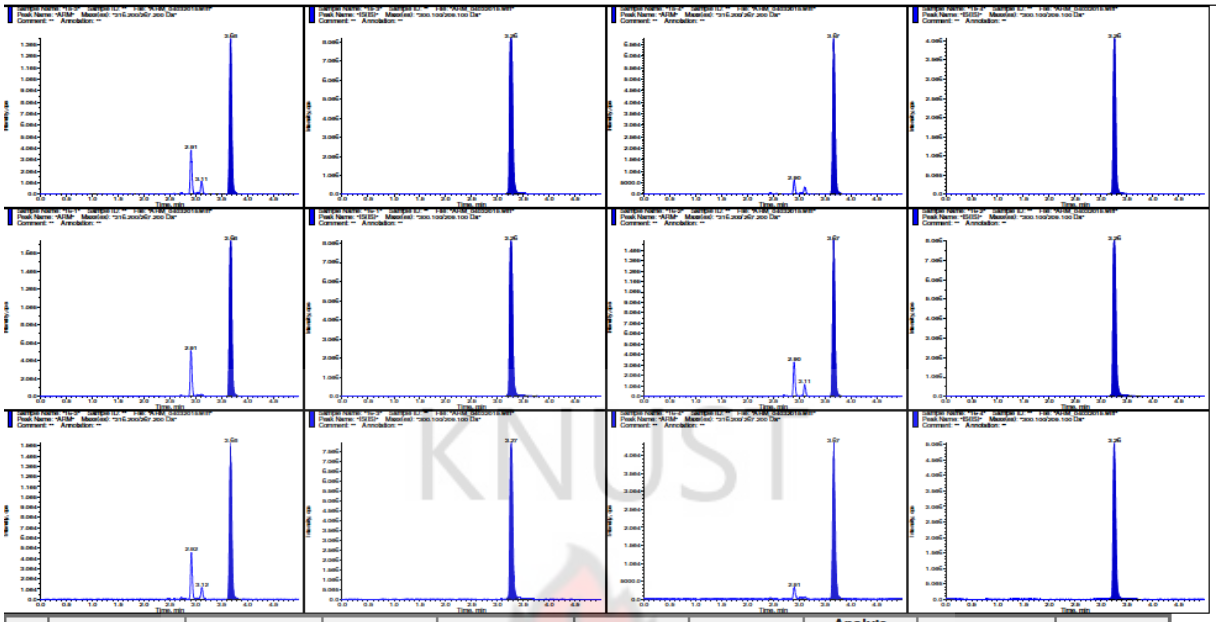

	Sample Name	Sample ID	Sample Type	File Name	Analyte Peak Area (counts)	Analyte Peak Height (cps)	Analyte Concentration (ng/mL)	Standard Query Status	IS Peak Area (counts)
67	15-3		Unknown	ARM_04032015.wif	4.05e+005	1.35e+005	N/A	N/A	3.25e+007
68	15-4		Unknown	ARM_04032015.wif	2.03e+005	6.76e+004	N/A	N/A	1.26e+007
69	16-1		Unknown	ARM_04032015.wif	5.27e+005	1.74e+005	N/A	N/A	3.11e+007
70	16-2		Unknown	ARM_04032015.wif	4.50e+005	1.51e+005	N/A	N/A	3.09e+007

Acq. File: AKM LLMs.dam,..

Sample Name: Ung/mL
Sample Number: Sample 1 of 88

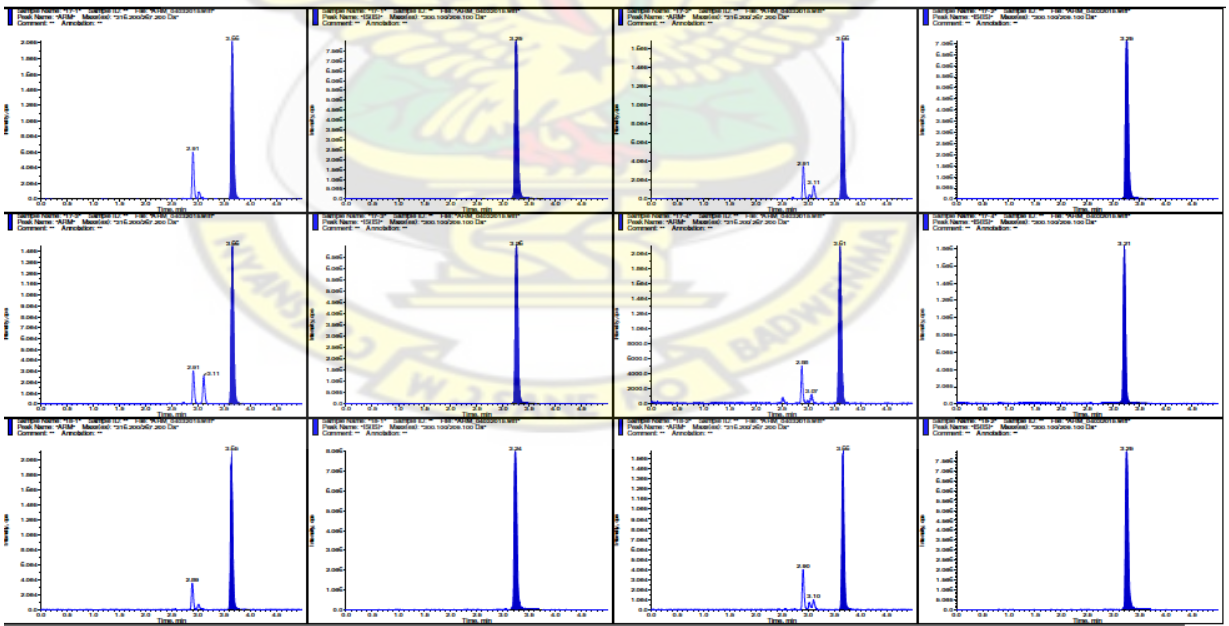

	Sample Name	Sample ID	Sample Type	File Name	Analyte Peak Area (counts)	Analyte Peak Height (cps)	Analyte Concentration (ng/mL)	Standard Query Status	IS Peak Area (counts)
73	17-1		Unknown	ARM_04032015.wif	6.41e+005	2.02e+005	N/A	N/A	3.17e+007
74	17-2		Unknown	ARM_04032015.wif	5.26e+005	1.68e+005	N/A	N/A	2.63e+007
75	17-3		Unknown	ARM_04032015.wif	4.45e+005	1.45e+005	N/A	N/A	2.49e+007
76	17-4		Unknown	ARM_04032015.wif	6.65e+004	2.09e+004	N/A	N/A	5.41e+006

Acq. File: ARM LCMS.dam,..

Sample Name: 0ng/mL
Sample Number: Sample 1 of 88

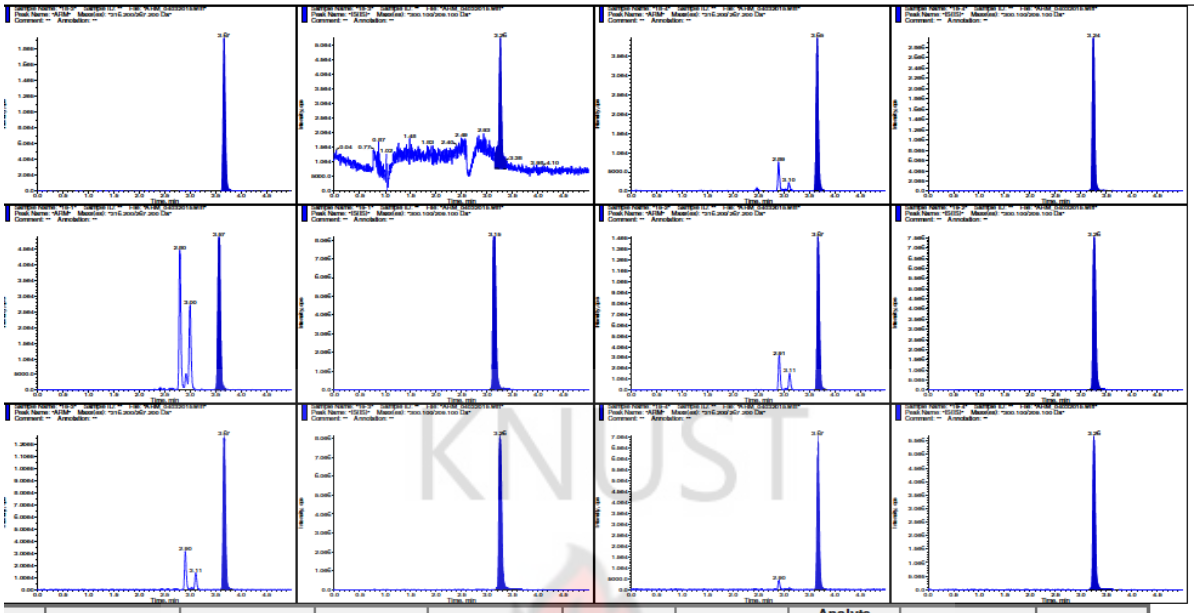

	Sample Name	Sample ID	Sample Type	File Name	Analyte Peak Area (counts)	Analyte Peak Height (cps)	Analyte Concentration (ng/mL)	Standard Query Status	IS Peak Area (counts)
79	18-3		Unknown	ARM_04032015.wif	5.77e+005	1.94e+005	N/A	N/A	1.45e+005
80	18-4		Unknown	ARM_04032015.wif	1.17e+005	3.97e+004	N/A	N/A	8.79e+006
81	19-1		Unknown	ARM_04032015.wif	1.62e+005	4.88e+004	N/A	N/A	3.37e+007
82	19-2		Unknown	ARM_04032015.wif	4.33e+005	1.41e+005	N/A	N/A	2.72e+007

Acq. File: ARM LCMS.dam,..

Sample Name: 0ng/mL
Sample Number: Sample 1 of 88

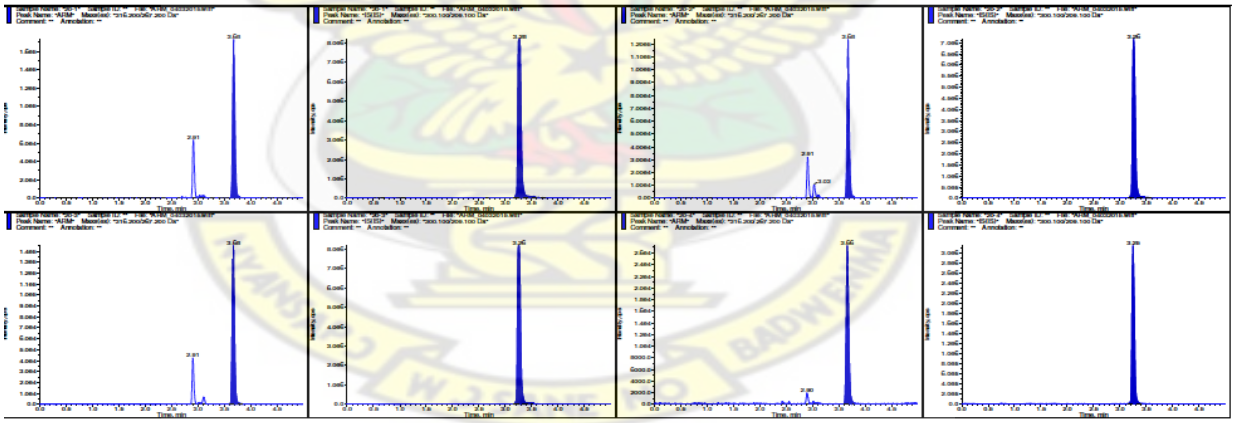

	Sample Name	Sample ID	Sample Type	File Name	Analyte Peak Area (counts)	Analyte Peak Height (cps)	Analyte Concentration (ng/mL)	Standard Query Status	IS Peak Area (counts)
85	20-1		Unknown	ARM_04032015.wif	5.19e+005	1.73e+005	N/A	N/A	3.60e+007
86	20-2		Unknown	ARM_04032015.wif	3.69e+005	1.24e+005	N/A	N/A	2.62e+007
87	20-3		Unknown	ARM_04032015.wif	4.29e+005	1.45e+005	N/A	N/A	3.34e+007
88	20-4		Unknown	ARM_04032015.wif	8.90e+004	2.72e+004	N/A	N/A	9.90e+006

B11 Concentrations of artemether (ng/ml) extracted from rat plasma

Time (h)	Group 1 Mean Conc. (ng/ml)	SD	Group 2 Mean Conc. (ng/ml)	SD	Group 3 Mean Conc. (ng/ml)	SD
1	0	0	13	0	13	0
24	0	0	13	0	13.75	0.75
72	0	0.25	13	0	13	0
120	0	0.25	13.75	0.75	13	0
168	-39.75	268.3342	-281	110.6413	-436.75	35.59348
336	-411.75	72.47572	4824.25	5198.115	-214.5	126.6639
504	-423	95.26979	12011.25	7757.161	955	1480.828

Time (h)	Group 4 Mean Conc. (ng/ml)	SD	Group 5 Mean Conc. (ng/ml)	SD
1	13	0	13	0
24	13	0	13	0
72	19	6	13	0
120	13	0	13	0
168	-251	286.5382	-305.5	137.8867
336	219.75	344.1275	82.25	201.2889
504	-479.25	35.66599	-392.5	66.87115